TM94-2080
Copy 1

NUWC-NPT Technical Memorandum 942080

Naval Undersea Warfare Center Division
Newport, Rhode Island

942080   001N

PROCEEDINGS OF THE NUWC DIVISION NEWPORT SEMINAR SERIES ON

SWIMMING AND FLYING IN NATURE

Promode R. Bandyopadhyay
Weapons Technology and Undersea Systems Department

16 August 1994

ABSTRACT

This memorandum records the proceedings of a two-part seminar series sponsored by the Naval Undersea Warfare Center (NUWC) Division, Newport, RI during 1994. The first part of the seminar series dealt with the *hydrodynamics and aerodynamics of swimming and flying in nature*; the second part dealt with several aspects of *theoretical turbulence*.

ADMINISTRATIVE INFORMATION

ACKNOWLEDGMENTS

TABLE OF CONTENTS

Section   **Page**

Part 1:   Swimming and Flying in Nature

Part 2:   Theoretical Turbulence

FOREWORD

The Naval Undersea Warfare Center (NUWC) Division, Newport, RI, sponsored a two-part seminar series in 1994 entitled "Swimming and Flying in Nature." The theme originated from a desire to find out *what can be learned from the hydrodynamics of the biological world that can be applied to engineering vehicles.* This series follows one held in 1992, entitled "Turbulence and Its Control", and another in 1993, titled "Microfabrication and Turbulence." The proceedings of these preceding series appear, respectively, in the NUWC-NPT TM 922089 and 932089.

The first part of the 1994 series, *Swimming and Flying in Nature,* comprised four seminars devoted to the hydrodynamics of swimming and the aerodynamics of flying in nature; the second part comprised two seminars that dealt with several theoretical aspects of turbulence. The seminars held in January, February, March, April and May were an activity of NUWC Newport's *Hydrodynamics Sphere of Excellence*, which is one of NUWC's leadership areas. The presentation materials used during the seminars, consisting mainly of viewgraphs, are reproduced in this report in their original form, with only minor reformatting having been done.

In the first seminar, Professor Kashin gave the highlights of his lifelong experimental research on the biological aspects of fish locomotion, conducted in Russia and Sweden. He made many interesting connections between the physiology of a fish and its hydrodynamics. Most importantly, Professor Kashin examined the neural origin for the generation of locomotion. He closed his presentation with the videophotograph of a transected eel, the lower part of whose body was performing continuous swimming movements when the interneural network was appropriately excited.

In the second seminar, Professor Newman gave a glimpse of his long association with the aerodynamics of flight in nature, particularly of the flights of dragonfly and nocturnal owl. He brought attention to the many features of the leading edges and of the topology of the wing surface of these flying animals, which have no counterpart in engineering aerodynamics. Clearly, animals in flight adapt purposefully to their environment in ways that defy conventional engineering. It follows from Professor Newman's experimental studies that there are many ill-understood mysteries in nature that are of interest to hydrodynamics and acoustics.

Professor Wu, in the third seminar, visited the so called Gray's Paradox on the energetics of fish locomotion. After equating thrust to drag, which is mostly the pressure drag for a fish, Professor Wu used potential flow analysis to conclude that the drag of a live undulating fish is significantly lower than that of a freshly dead fish, or the drag of a rigid fish model. Professor Wu proposed that the origin of this economical locomotion in a fish lies in unsteady hydrodynamics. It is tempting to think that the study of the unsteady hydrodynamics of aquatic animals might lead to the development of new concepts on the locomotion of engineering vehicles.

The fourth seminar by Professor Lumley, unfortunately, was canceled due to the sudden illness of his wife.

The second part of the seminar series was brief, consisting of only two lectures. In the first, Professor Walker dealt with the transport of turbulence vorticity away from a solid surface. He used inviscid vortex analysis to argue the existence of very thin shear layers that are normal to the wall in a turbulent boundary layer. Professor Walker's work suggests that, in a time-dependent viscous computation, very fine grid resolution is needed to capture any intermittent outward eruptions of vorticity from the wall.

In the second seminar on theoretical turbulence, Professor Sreenivasan showed how one can build the synthetic time series of any turbulence variable that has the "right" statistical properties. He has distilled the knowledge of the fractal nature of turbulence to invent this method of creating a synthetic time series. The utility of his invention seems to lie in the time savings that might be derived from its use as the initial condition for generating a turbulence data base using the so-called Direct Numerical Simulation method.

Part 1:

Swimming and Flying in Nature

1.1 Fish Swimming

Sergei Kashin
Northeastern University
(Formerly of Moscow State University)

SEMINAR NOTICE

FISH SWIMMING:

KINEMATICS, NEURAL AND MUSCULAR CONTROL

Dr. Sergei Kashin
Department of Biology and Marine Science Center
Northeastern University
(formerly with Moscow State University)

20 000 fish species show great diversity in modes of swimming. The most common mode is the undulation of the body or/and fins. The wave of undulations travels along the body and usually low speed is controlled by the amplitudes of undulations whereas high speed is controlled by frequency of undulations. The fish musculature is divided onto a number of segments along the body. The number of segments is exactly equal to the number of vertebra and each segment or myotome is supplied with its own pair of sensory (dorsal) and motor ventral) nerve roots from spinal cord. The structural and functional organization to decrease the number of degrees of freedom of system is discussed. The nervous commands to the muscular system were investigated in fish. The functioning of "locomotor center" in fish brain is described as well as its relation to the spinal generators of rhythm. The behavior of molecular units of contraction (sarcomeres) was studied in intact fish with laser.

Some applications to the understanding the hunting behavior as well as some problems in engineering a fish-like robot are discussed.

Thursday, the 27th January 1994
Conference Room, Bldg. 679 First Floor
Time: 10:30 AM

POC: Dr. Promode R. Bandyopadhyay (Code: 8233; Bldg. 108/2) NPT x2588

Movements of the body to produce swimming

Muscle architecture

How muscle work to produce movements

Nervous control of movements

Molecular contractile activity in vivo

Fish-like robots

panded, is followed here. Examples of fish displaying these modes are shown in Fig. 1. As Breder stated, the suffix "-form" (e.g., in anguilliform) refers to the types of movement and not to the body forms, and is therefore not strictly parallel to words such as "fusiform." Indeed,
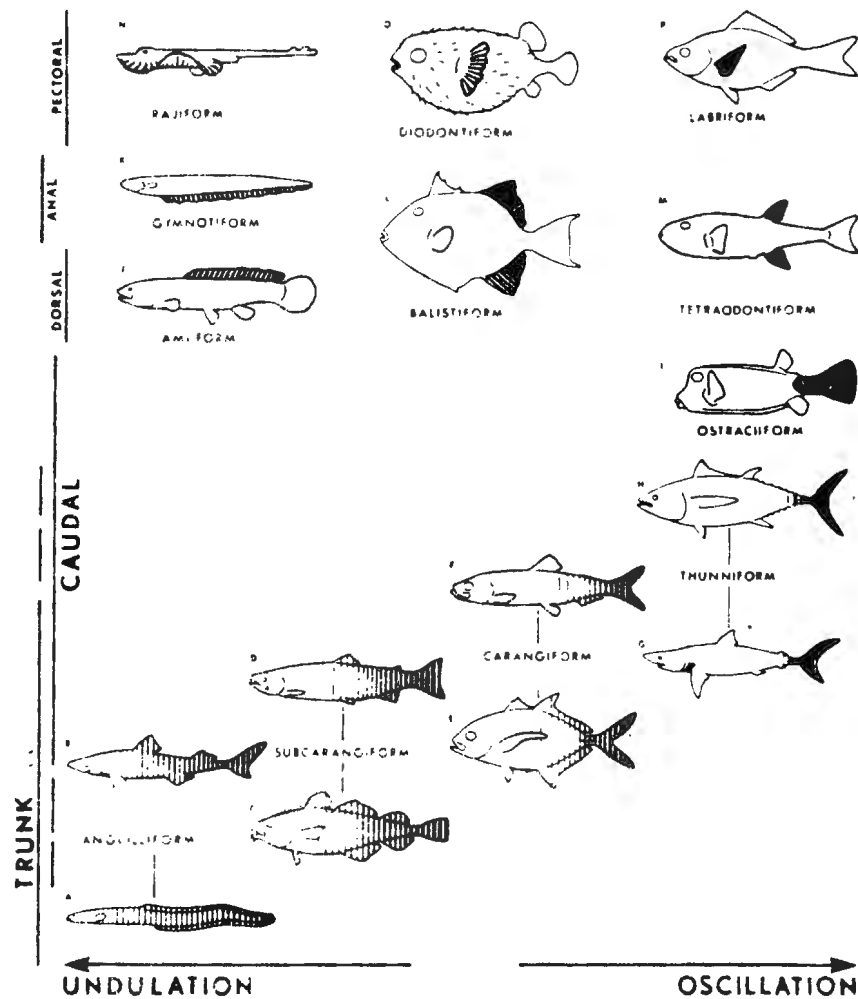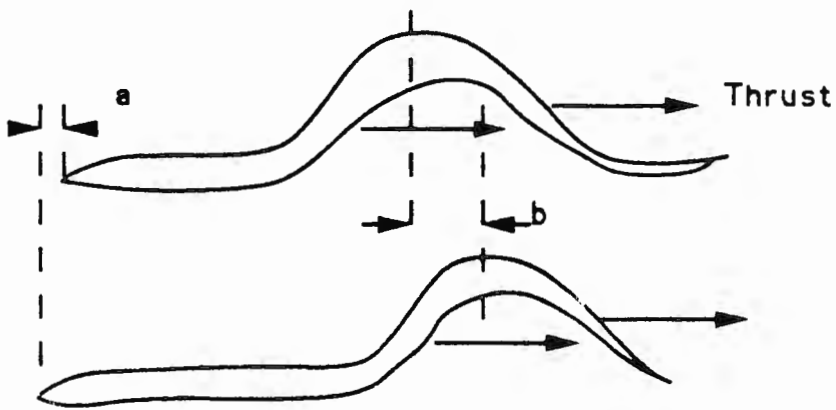

Fig. 1. Modes of forward swimming in fish, arranged along the vertical axis according to the propulsive contributions of body and fins (indicated by density of shading), and along the horizontal axis according to a scale running from serpentine undulation (more than one wavelength present) to an illu...
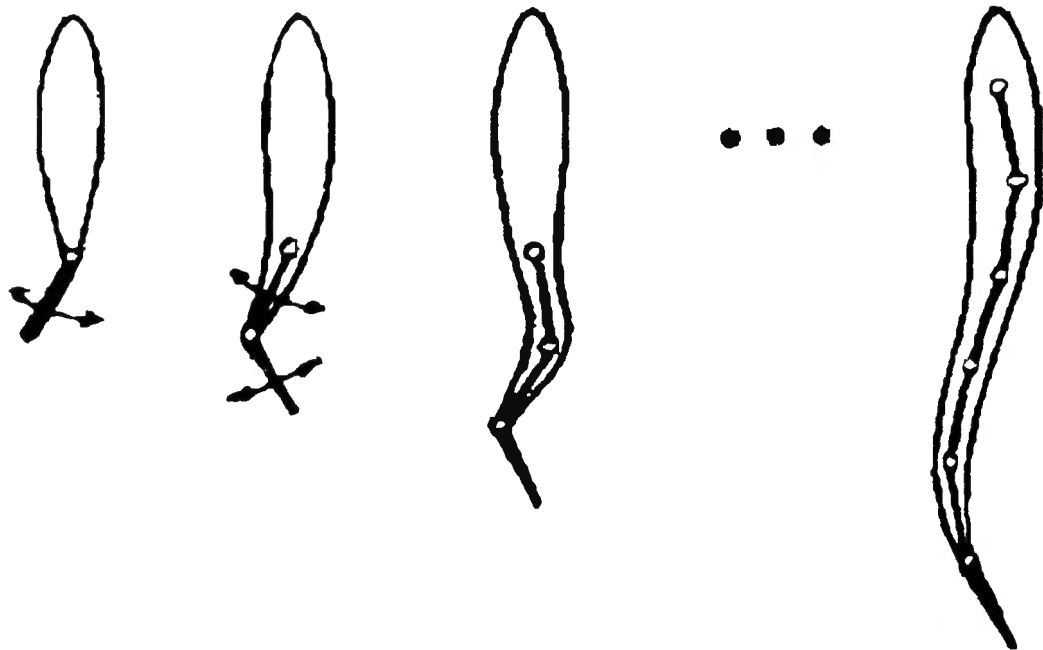
Thrust

a – movement of aniomal
    forward

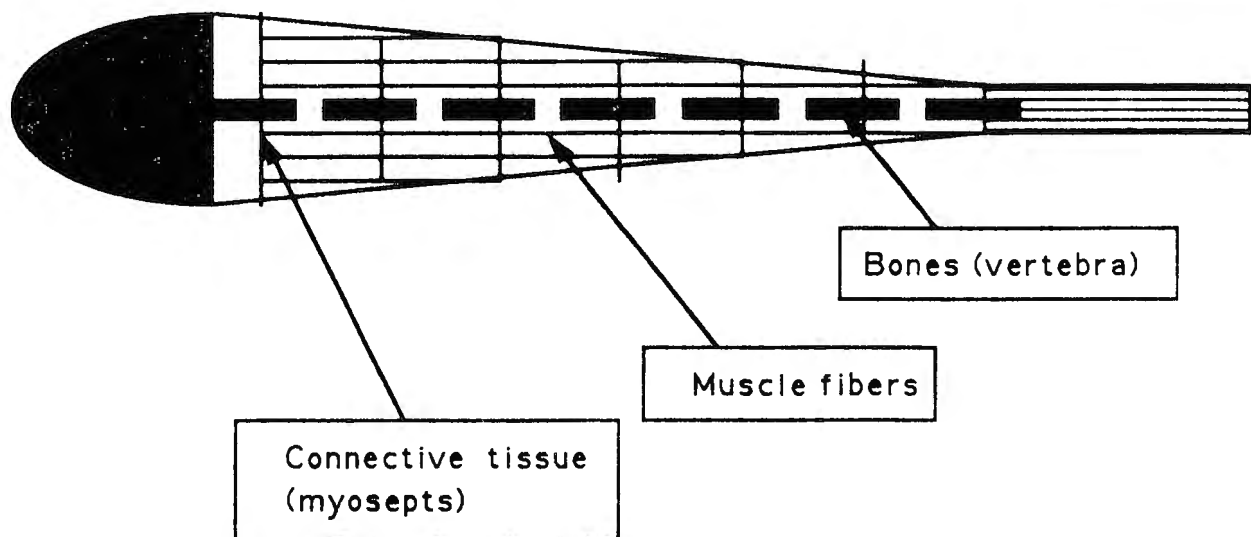b – movement of bending
    backward

3

ANGUILLIFORM MODE

Thrust
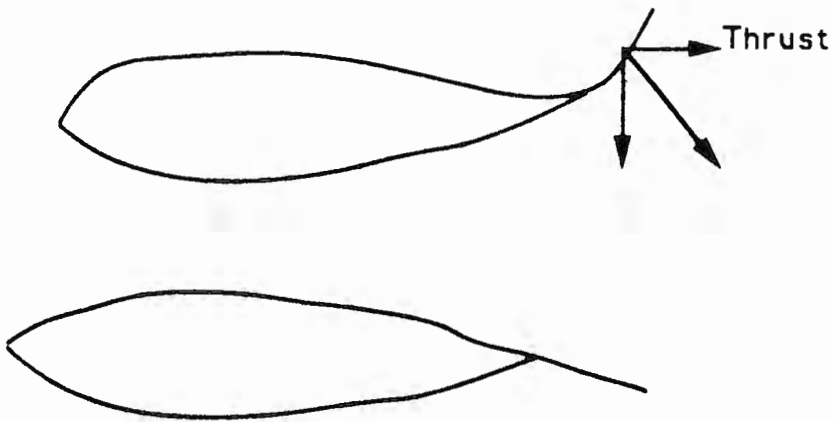
CARANGIFORM MODE

The evolution of locomotor system of fish could be considered as a process of multipliction of a number of joints (the degrees of freedom) or ...
as reduction of it.

Connective tissue
(myosepts)

Muscle fibers

Bones (vertebra)

5

__Myotome__ (*myomere*) — all musle fibers between
two neghboring myosepts. Each myotome has its own
innervation from spinal cord — two dorsal and two
ventral spinal nerves.

Backbone Structure

- **Dimensions (l).** Scaled to the bodylength (L).For mackerel or perch type $l=0.66L/N$, where N is number of vertebras. And $l= L/N$ for long fish like lamprey or eel.

- **Number. Equal to:**
  - **24-30** for bass and perch
  - **30-40** for mackerel type (tuna-39)
  - **40-60** for cod, herring, salmon etc.
  - **>100** for lamprey and eel

- **Shape.** Short cylinders $(d/l=1)$ with attached processes and arcs. In vertical plane - neural and hemal arches and processes. Processes are used as levers for rotarion. Horisontal - ribs - are also used for muscle attachment. Zygapophysis processes restricting rotation.

- **Material.** Bone consists of polysaccharide and protein matrices where calcium phosphate is deposited.

DORSAL

Dorsal
cone

Central
cone

Tail

Head
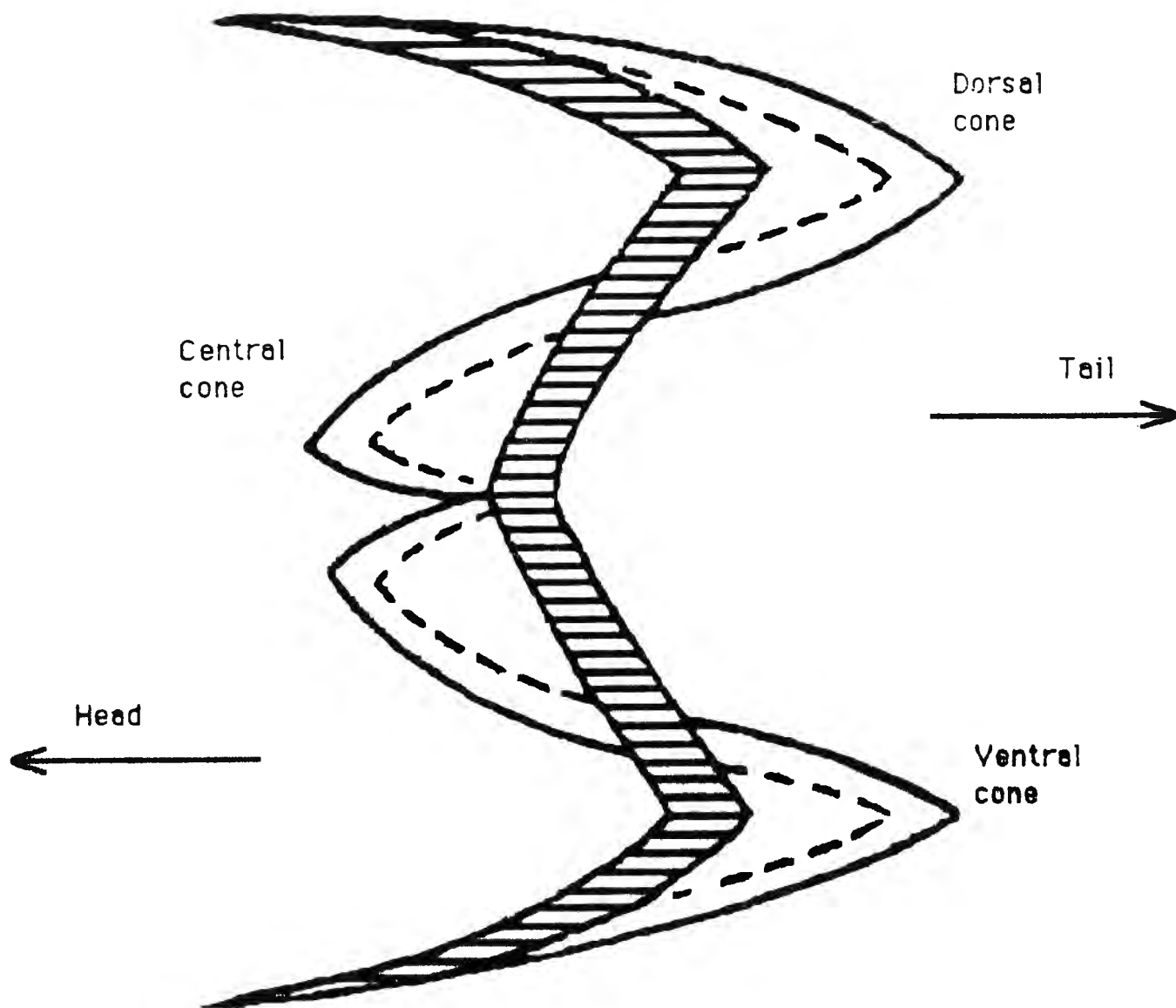
Ventral
cone

VENTRAL
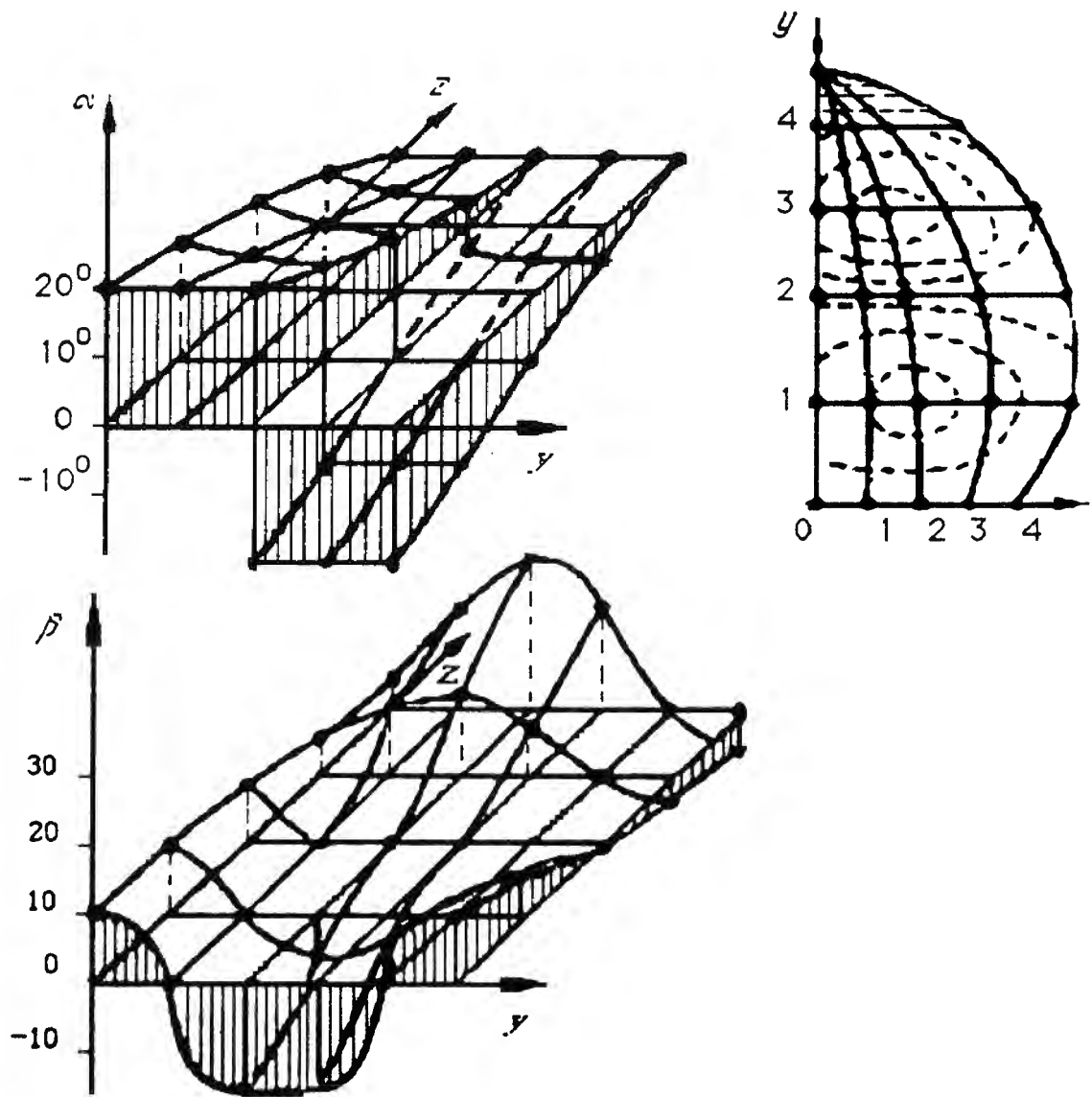
Angles of muscle fibers witn the main axes of the body as a function of
the cross-sectional co-ordinates (upper right).
Projections on the horizontal plane (upper left)
Projection on the vertical plane (below)

Dorsal

Muscle trajectory

Post

Medial
septa

Ant

vertebra

horizontal septa

Ventral
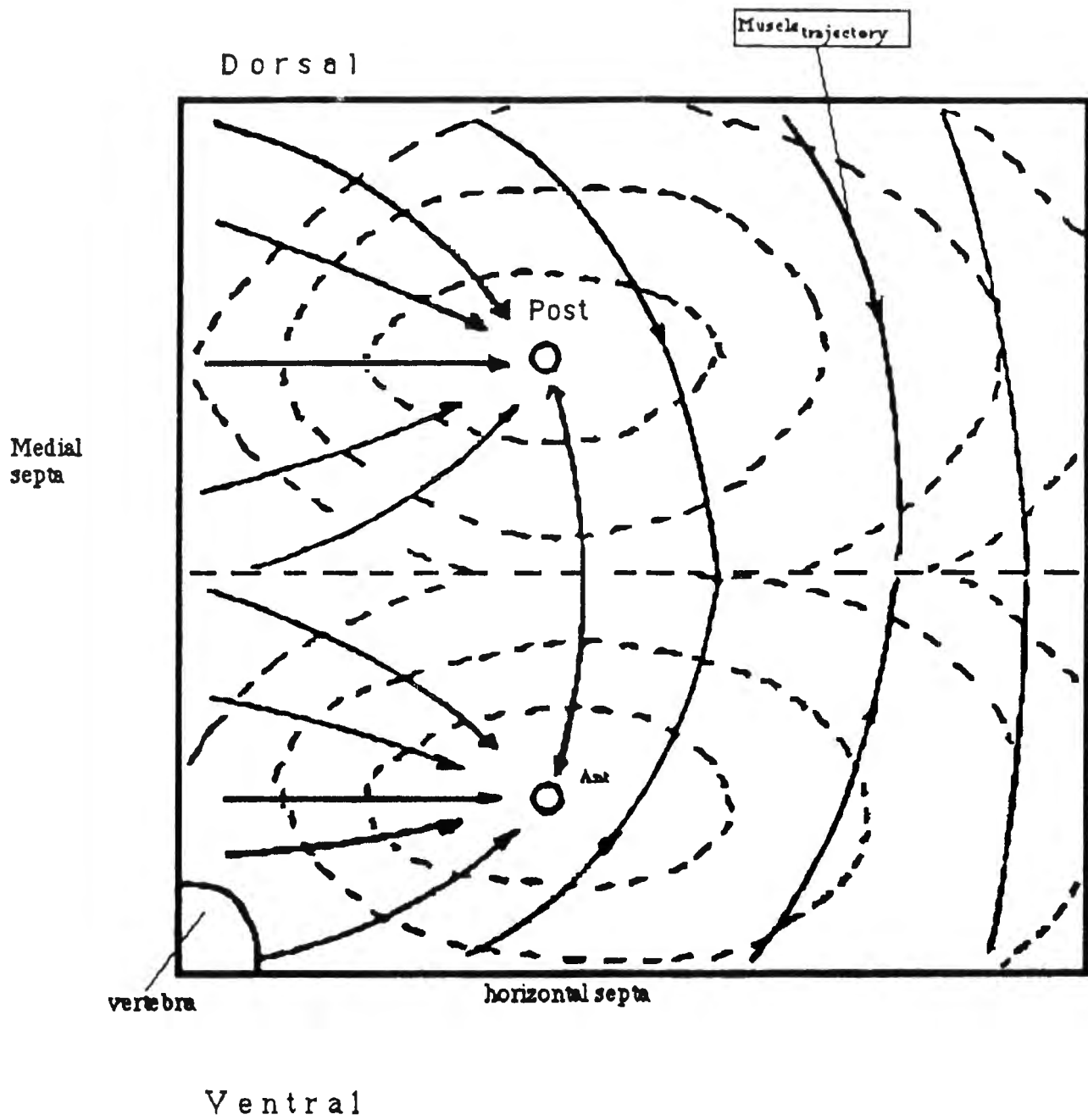
Diagram of the projections of the muscle trajectories
on the cross-sectional plane

view from above

0.15 m

0.70 m
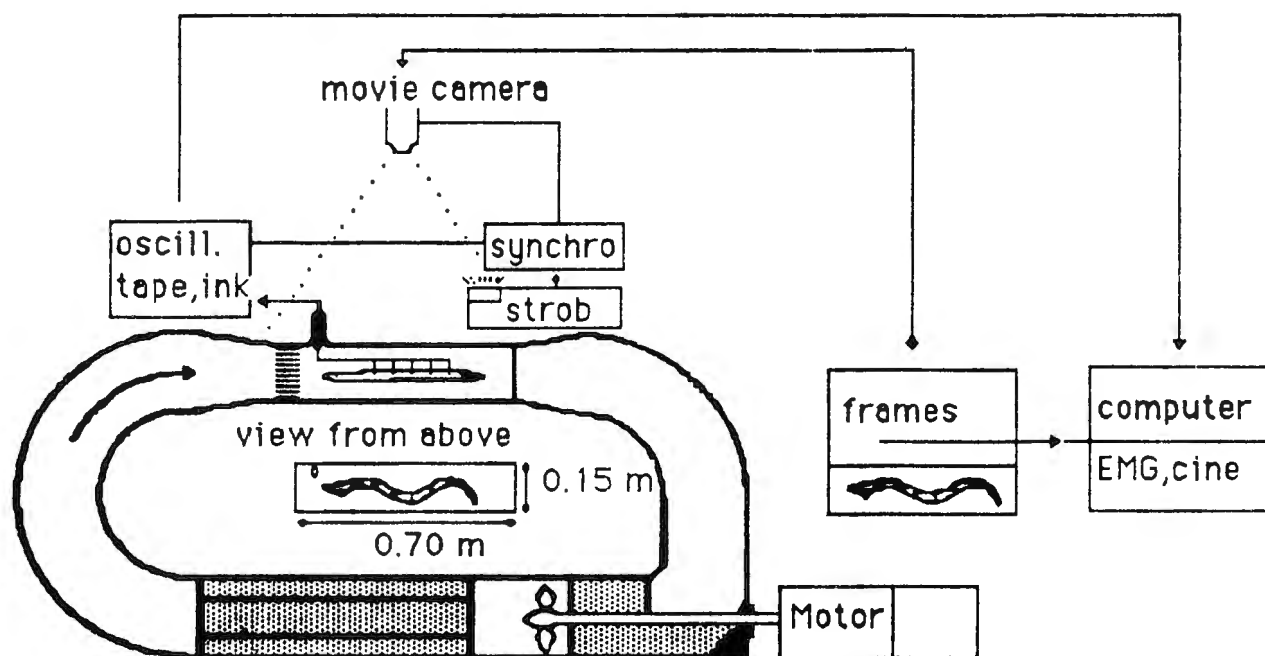
Experimental design
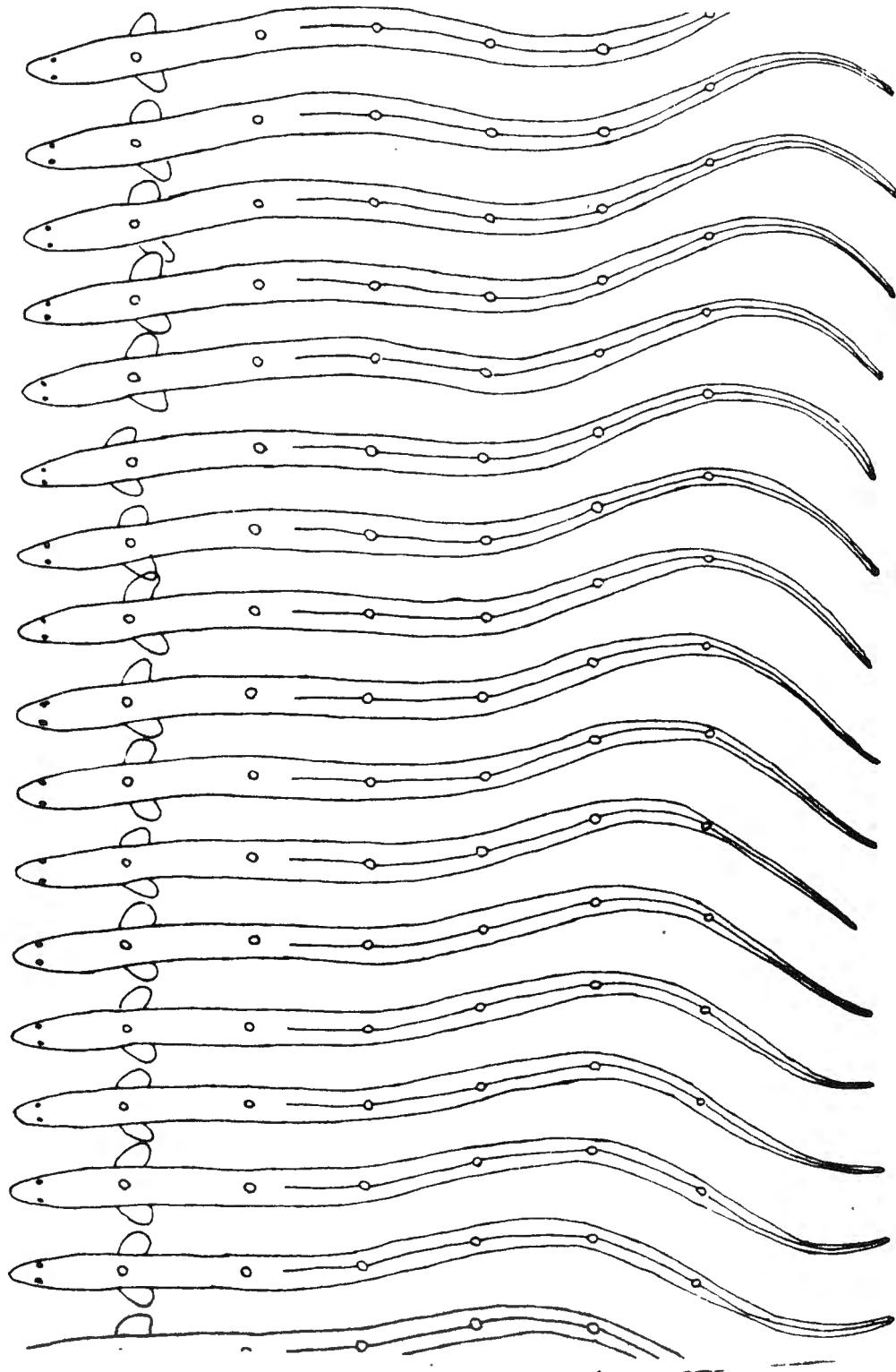
Kinogram of the swimming eel (bodylength 35.8 cm). Speed of flow 32 cm/s. 100 frames pes second
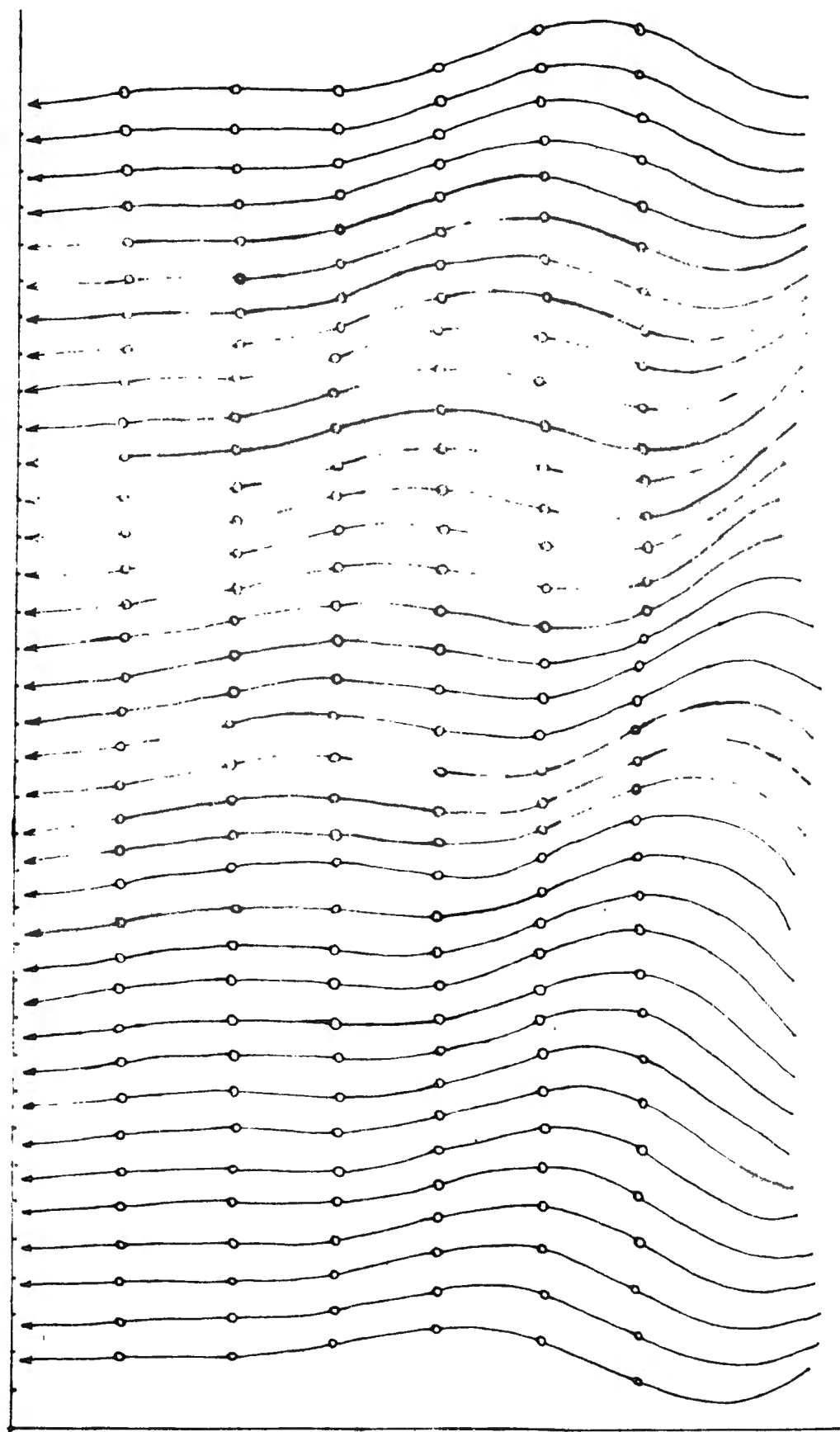
Рис. 4. Положение точек средней линии тела в последовательных фазах движения угря. Тот же проплыв, что и на рис. 4.
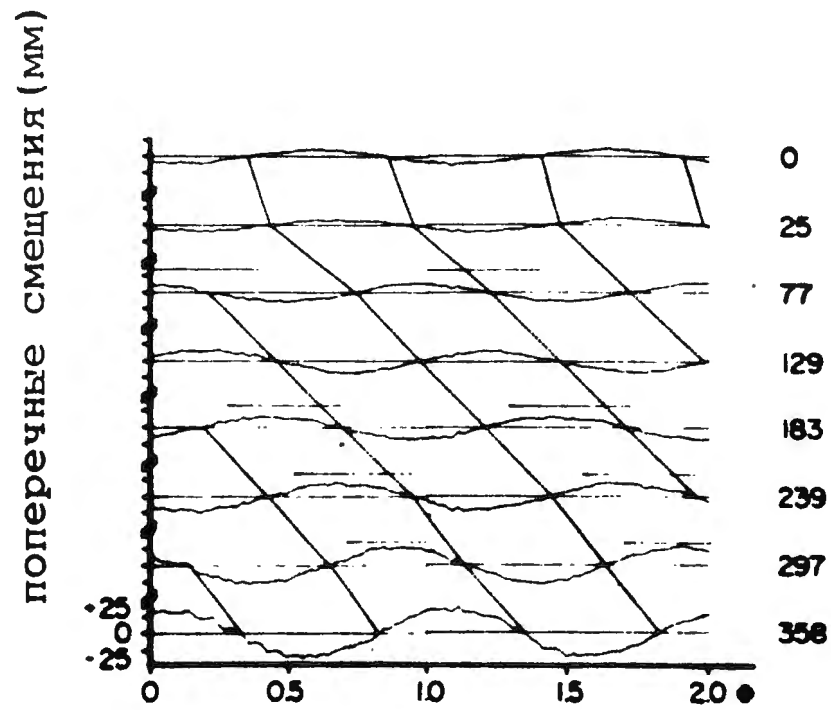
Lateral displacement of different parts of the body of the eel.
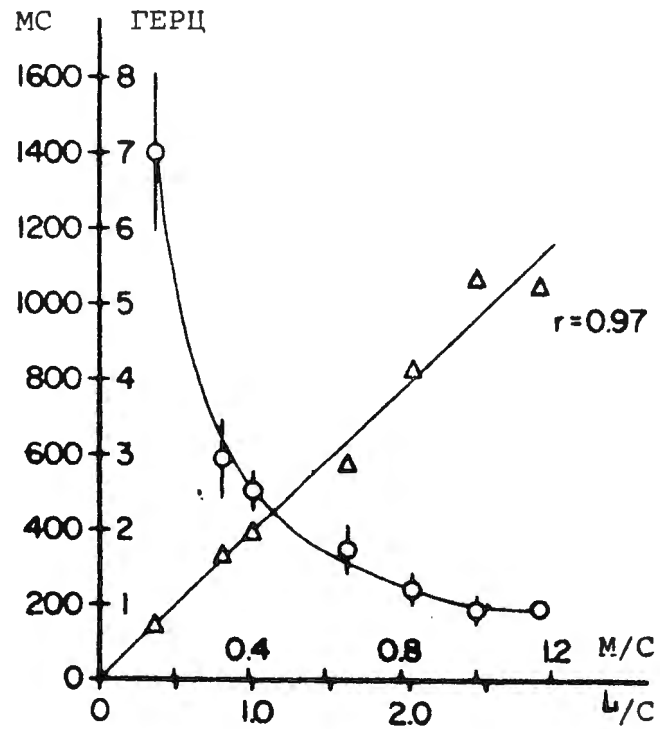
Speed of swimmind vs frequency and periodlength
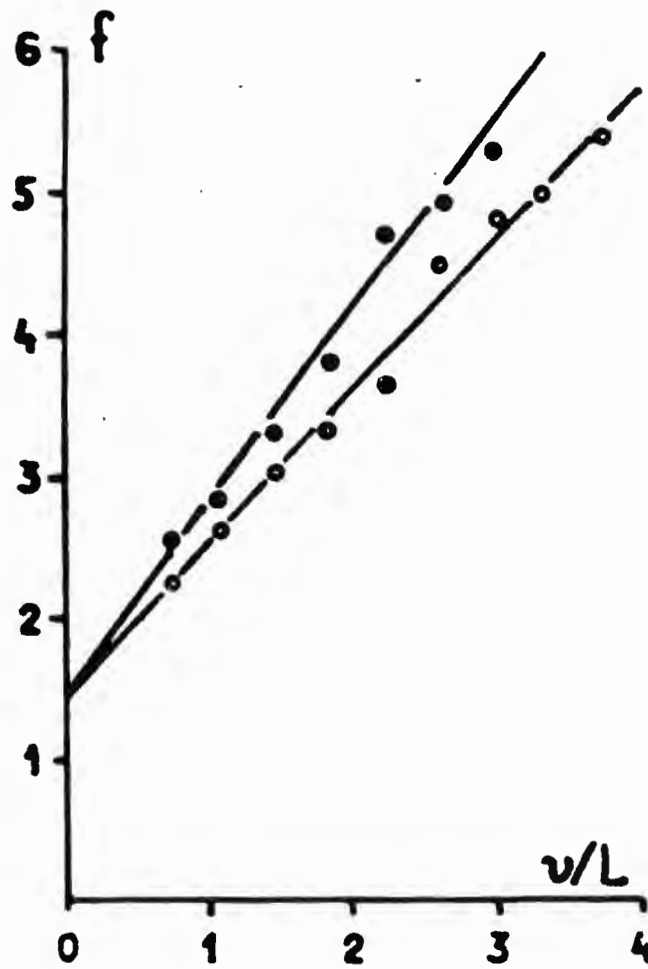
Frequency of undulations vs speed of swimming

1.1-19
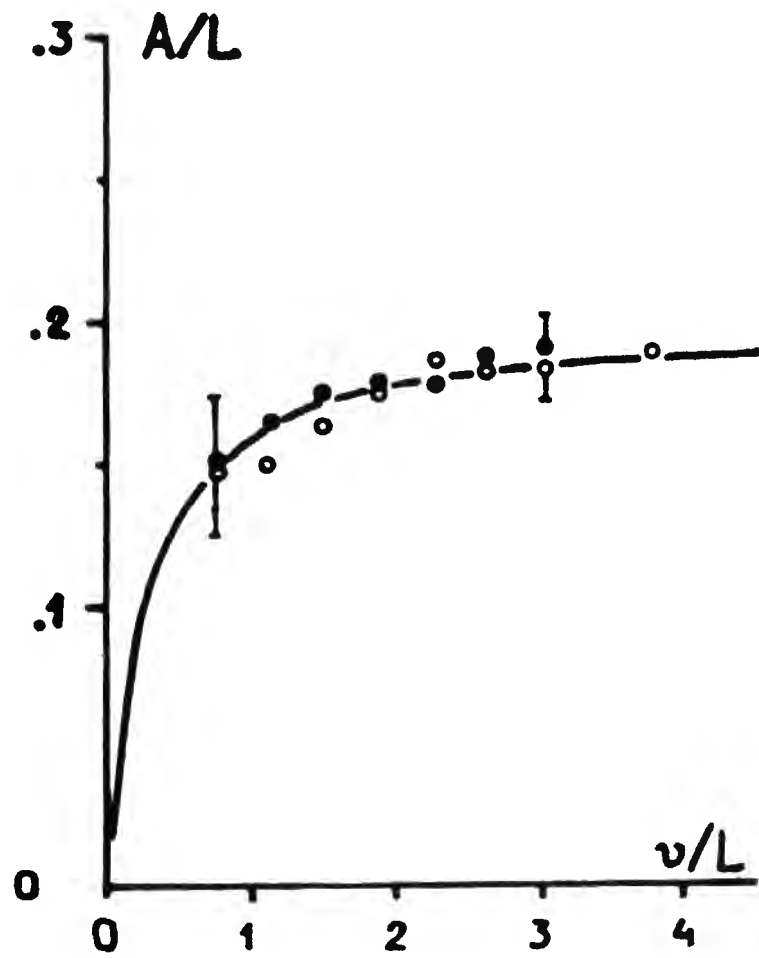
The tailfin ampl swimming speed
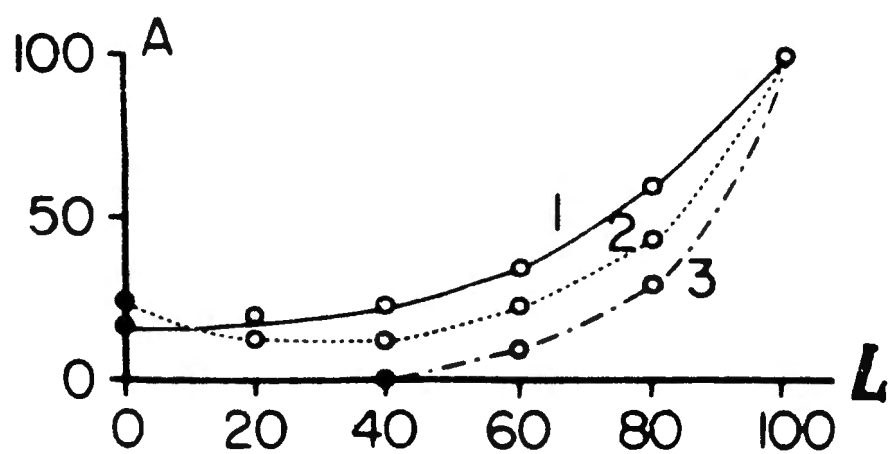
Three types of the distribution od amplitudes along the fish body (1 - eel, 2 - trout, 3 - sculpin)
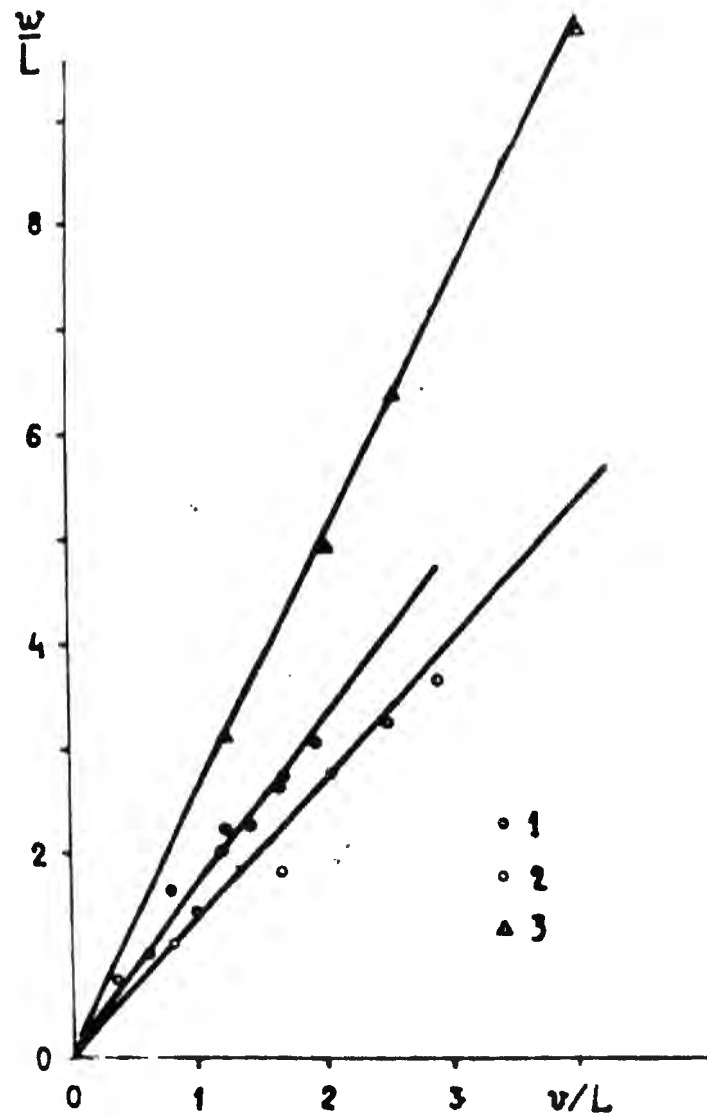
Velocity of bending wave along the body vs speed of
swimming for three species (goldfish, eel and trout)

1.1-22
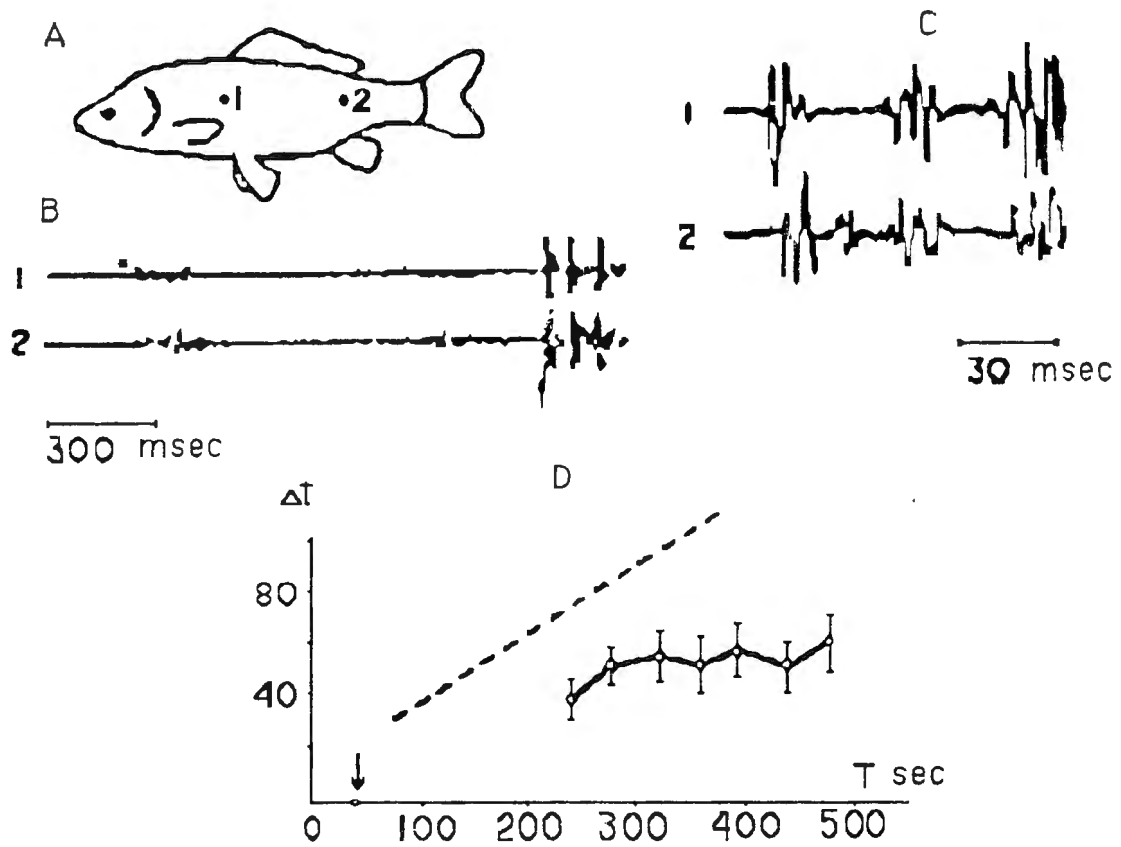
Electromyography of the Ciprinus carpio
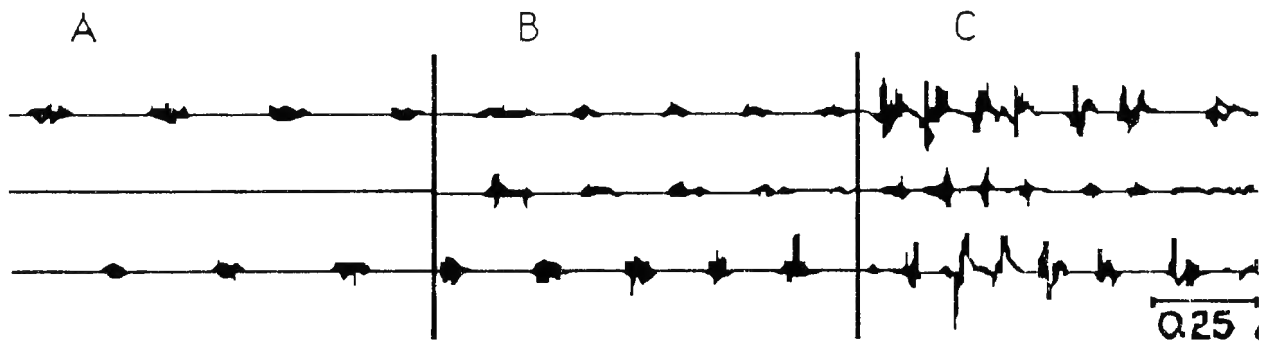
Electromyography of trout for three speeds of swimming. Midline - white muscles

A 0.15 M/c

B 0.41 M/c

C 063 M/c

D 117 M/c
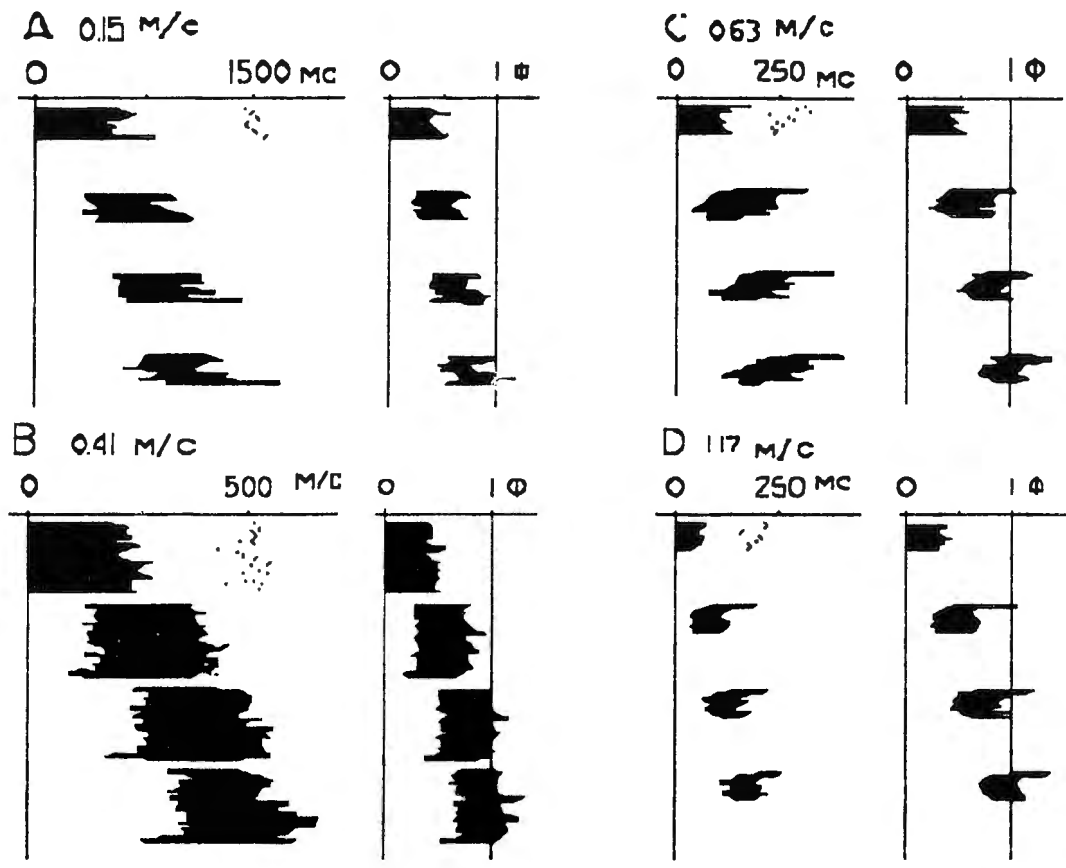
For graphs represents the EMGs recorded from eel swimming with four different speeds.

Bars on the left side of each graph represent the duration of EMG (Dots show the cycle duration).

The faster fish swims the shorter the delays along the bodylength. However the phase is constant as it is seen on the right side of each graph.

EMG   undul.

EMG

50
sec

1 sec

4 sec
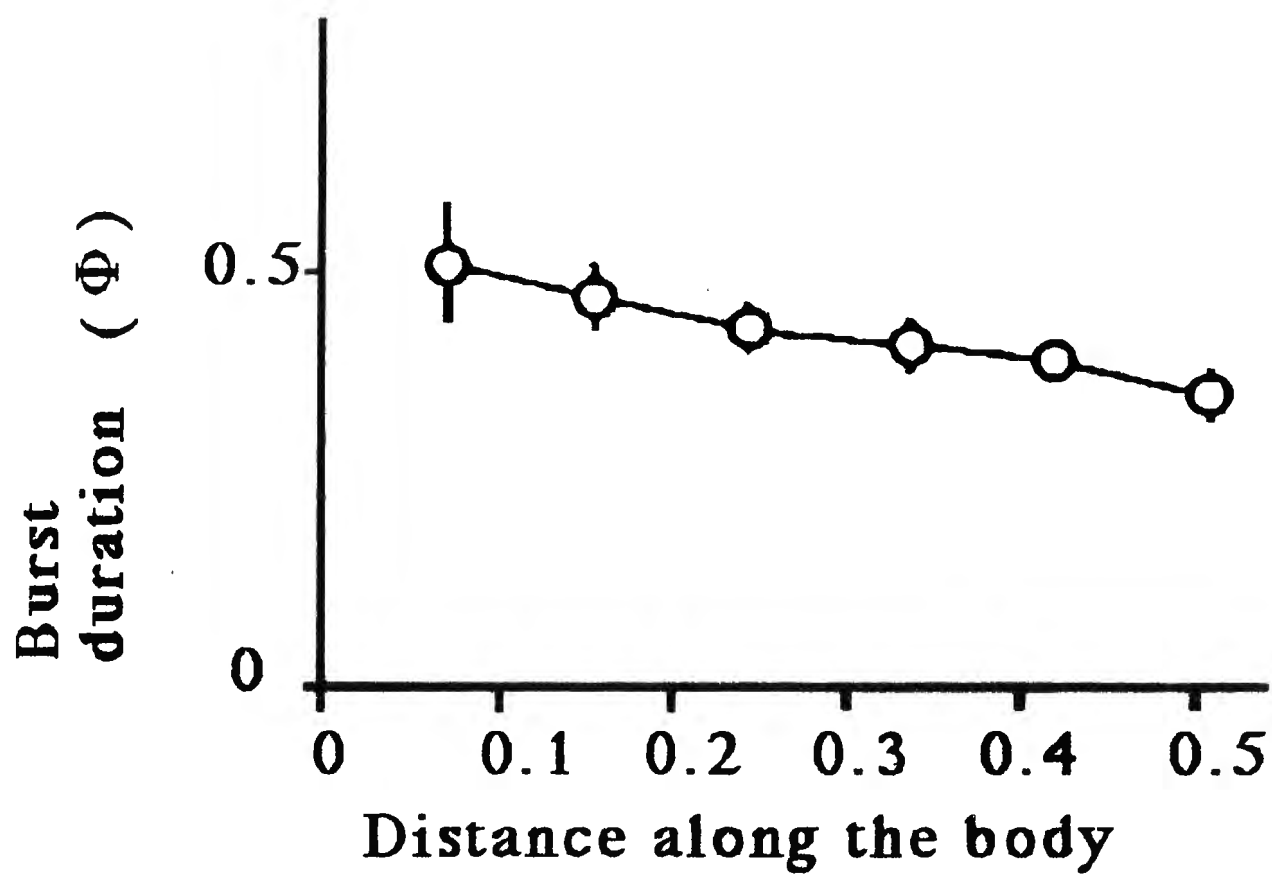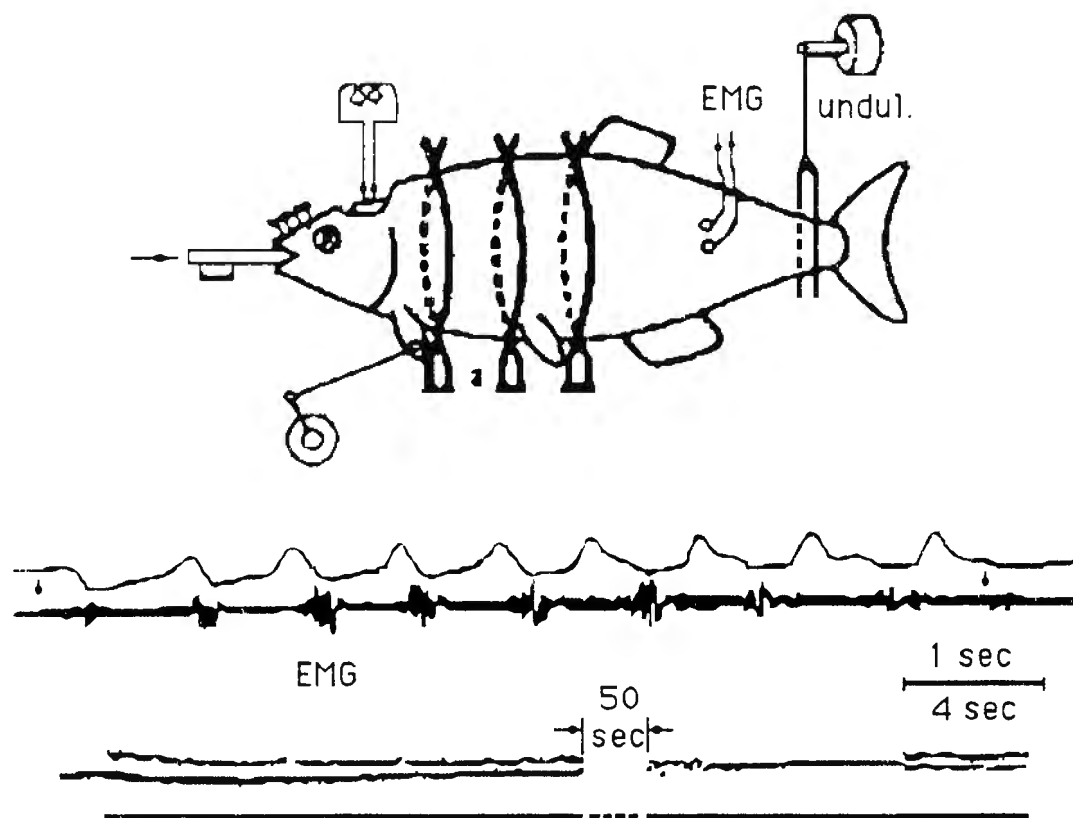
Stimulation of the locomotor center in the midbrain.
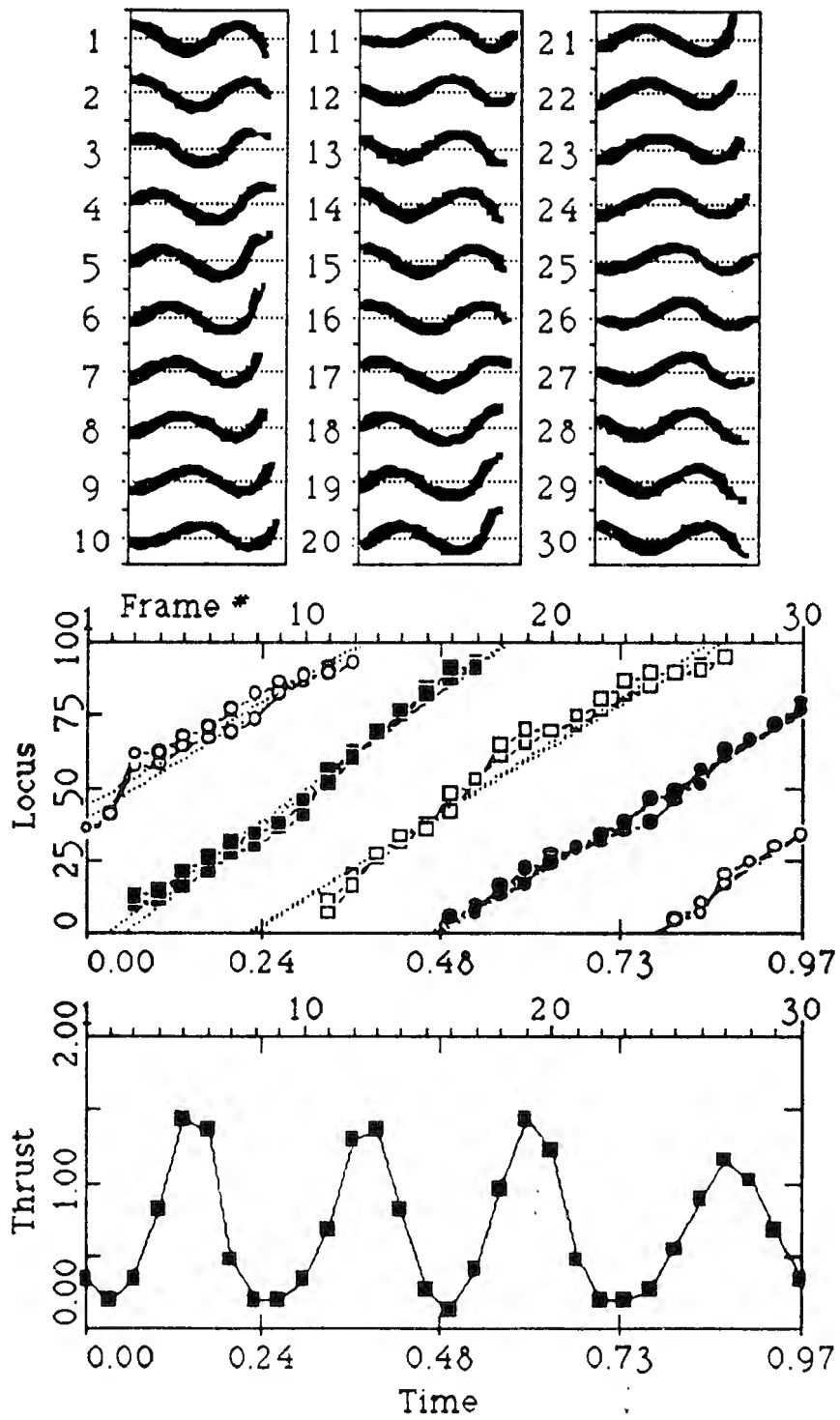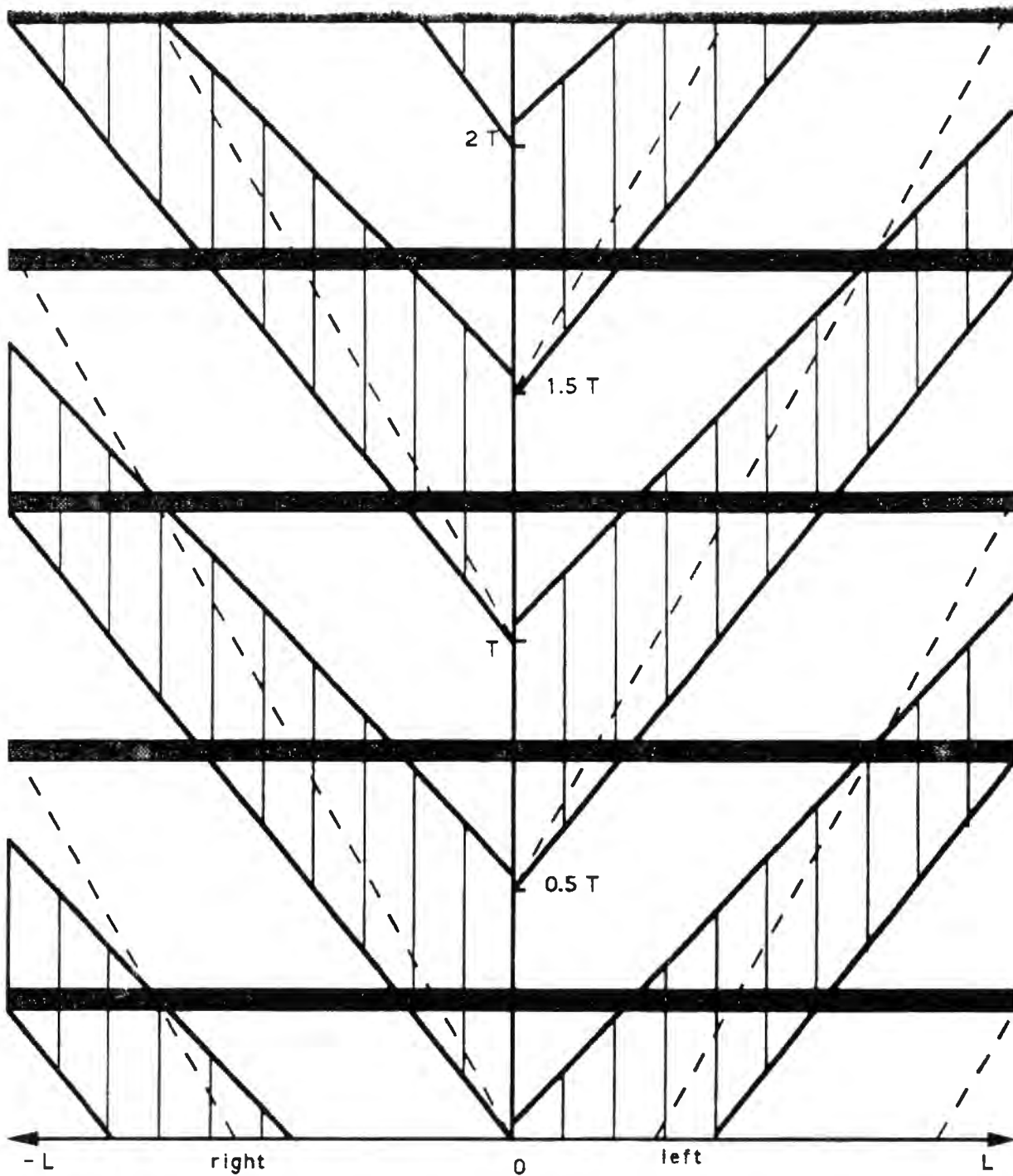
Fig. 2. Propagation of EMG waves along the body of lamprey. Based on Williams et al., 1989. All temporal and linear parameters are normalized to the bodylength (L) and the periodlength (T).

UNDULATING ROBOT PROGRAM

BIOLOGICAL RELATIONSHIPS IMPORTANT TO ENGINEERING MODEL DESIGN

- Time delay between activation of segments is always a fixed percentage of cycle time.

- Frequency of oscillation is linearly related to speed.

- Increasing stiffness is required to increase frequency hence speed.

- Left and right sides of system are alternately activated.

- Duration of excitation does not exceed 1/2 of cycle time.

- Different muscles are used for slow and fast speed

- Thrust is in form of pulses at twice the frequency.

- Amplitudes of undulation are directly correlated to basic structure. ie Mass, cross section area, and areas of lateral projection.

NORTHEASTERN UNIVERSITY
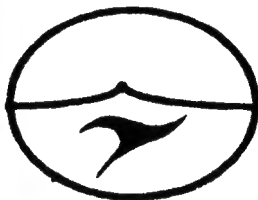
UNDULATING ROBOT PROGRAM

ROBOT VS FISH PROPULSION

- **ROBOT:**

  Local flexures propagate from front to rear pushing water back and thus produces thrust.

  Movement of tail from side to side also produces thrust

  It will have 2 basic frequencies: 1 hz for slow swimming and 10 hz for fast swimming.

- **FISH:**

  Bending waves propagate along body from front to rear generating thrust. In good swimmers fish moves about 0.8 bodylength in 1 cycle.

  The frequency of undulation varies smoothly from 0.5 to 20 hz (25 cm fish). Larger fish have lower maximum frequency.

  The amplitude of the trailing edge of the tail is maximal and equal to 0.2 bodylengths for all species and almost all ranges of speed.

NORTHEASTERN UNIVERSITY
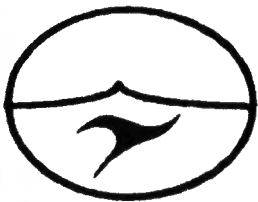
BIOLOGICALLY BASED UNDULATORY AUTONOMOUS UNDERWATER VEHICLE

FISH VERSUS ROBOT MUSCLE ANALOGY

Parameter:	Fish	Nitinol
Muscle Contraction	.2%	3% - 5%
Frequency	0.5 - 20hz	0.1 - 10 hz
Nominal efficiency	30%	5%
Muscle Types	slow/fast	slow/fast variable sizes
Force-velocity rel.	inverse	inverse
Max. Cycles	lifetime	several million

SOME MAJOR ENGINEERING ISSUES

* Optimize number of segments to achieve smooth motion

* Minimize size and number of SMA wires to minimize energy needs

* Control and coordination of multiple elements: maneuverability, rigidity, speed, and buoyancy

* Control of temperature (heating & cooling) to maximize frequency response

* Mechanical design & fabrication of skeleton, mass distribution system, & mechanism to transfer internal motive forces to external interface with water column

NORTHEASTERN UNIVERSITY

- Complicated muscular morphology results from the necessity to bend the body in any particular point
- Red muscle system functions in hydrostatic skeleton, whereas white muscle belongs to the lever type
- Cinematically low speed is controlled by the tail amplitude and high speed by the frequency of undulations
- Basic synergies are constant in phase. Only period length is controlled by the brain locomotor center. Recruitment (stiffness of the body?) and intersegmental phase lag are controlled by the frequencies perhaps on spinal level
- All that simplifies the problem of designing the fish-like robot

1.2 Aerodynamics of Bird Flight

Barry G. Newman
McGill University

LOW-SPEED AERODYNAMICS: ANIMAL FLIGHT AND SKIN FRICTION

Professor B. G. Newman
Canadair Professor of Aerodynamics
McGill University, Montreal, Canada

As suggested by Dr. Bandyopadhyay, three studies will be discussed:

1. Large Dragonflies have a wingspan of 90 mm and an unusual wing section consisting of pleats near the leading edge. Hand-launched gliders with this section were tested at $Re \approx 5 \times 10^4$ and showed that the maximum lift to drag ratio was about 10, slightly better than that for arc aerofoils often used on model aircraft at this Reynolds number. The separation and reattachment of the flow in the pleats generates a turbulent boundary layer which increases the maximum lift.

   Other aspects of wing geometry will be mentioned.

2. Nocturnal owls have wings with at least three unusual features that are thought to contribute to their quiet flight. Two of these are leading-edge combs and downy surfaces.

   The combs are formed by a curved extension of the barbs on the exposed leading edges of primary feathers. They probably produce trailing vortices which inhibit separation near the leading edge (the common Alula also does this but on a larger scale). Smoke tunnel studies show that a single primary feather has separation suppressed for about 6^0 incidence due to the presence of the comb at $Re \approx 10^4$. Suppressing the high pressure fluctuations near reattachment reduces noise propagation.

   Down (1 mm long hairs, 10 μ diameter) is found on the top of the wing. Flat plate boundary layer measurements behind downy surfaces showed that the skin friction coefficient C_f was <u>increased</u> by about 85% : however the downy surface was rough but never fully rough. In contrast the longitudinal turbulence was reduced very close to the surface and with it the surface pressure fluctuations. Thus down is an unusual type of roughness, not bluff and turbulent, but streamlined and laminar.

3. An instrument has been developed for measuring skin friction on a "rough" surface. Three pitot tubes are used to measure the velocity gradient $\dfrac{dU}{dy}$ at two places within the wall-low region where $\dfrac{y}{\left(\frac{\tau_w}{\rho}\right)^{\frac{1}{2}}} \dfrac{\partial U}{\partial y} = \dfrac{1}{K}$ a constant, independent of viscosity and the geometry of the roughness. The origin for the wall distance y is uncertain, which explains why three pitot tubes are required.

   The final formula for the skin friction τ_w is precise and the instrument does not require any calibration. Measurements have been compared with a Dickinson skin friction balance.

   It could be used for ribletted surfaces as well as those with marine growth.

Thursday, the 10th February 1994
Conference Room, Newport Bldg. 679 First Floor
Time: 10:30 AM

1.2-3/1.2-4
Reverse Blank

Dr. Bandyopadhyay has asked me to review some past and present work on animal flight and the measurement of skin friction.

I will first talk about dragonflying, the aerodynamics of anizoptera-odonata, and then describe a new robust way of measuring skin friction, which leads into the final topic, the aerodynamics of nocturnal owls. Presumably some of the "devices" which have worked (i.e. been developed on these animals) in air might be worth trying in water.

The work I am going to describe is mainly curiosity-motivated.

1. <u>Dragonfly</u>   Hertel   Structure, Form & Movement (1966)

2 Slides   →   1 overhead   Pleated aerofoil

Structure and model for smoke tunnel

$R \simeq 10^4$ very difficult to generate turbulent   b.l.
to keep the flow attached.

2 Model gliders were tested
                          Re
$\begin{cases} \text{Large} & 4 \times 10^4 \\ \text{Small} & 1 \times 10^4 \end{cases}$

plus McBride B7

$\left[\begin{array}{l} \text{40 chords travelled for every flap} \\ \quad : 25 \text{ Hz is frequency} \end{array} \right]$

27. Model Tests on a Wing Section of an Aeschna Dragonfly.

B G NEWMAN
Department of Mechanical Engineering, McGill University, Montreal, Canada

S B SAVAGE AND D SCHOUELLA
Faculty of Engineering, McGill University, Montreal, Canada

ABSTRACT

The chord Reynolds number of a dragonfly wing flying at high speed is of the order of 10^4. It is well known that aerofoils at moderate incidence experience an increase of drag coefficient and a decrease of lift coefficient as the Reynolds number is reduced below a critical value of about 5×10^4 and that this is associated with complete separation of the laminar boundary layer.

The aerofoil section of the dragonfly is unusual, as indicated by Fig. 1a which is a sketch of a photograph of the section just inboard of the nodus on the wing of *Aeschna Eremita*.

Attention is drawn to the minute saw-teeth on each web of the T section which forms the leading edge (costa), and the spurs on both sides of the matrix which supports the rear membrane. The saw-teeth very likely act as turbulators to promote transition in the separated shear layer and subsequent reattachment of the boundary layer in a turbulent state. Smoke tunnel studies of the wing section support this hypothesis. Trapped vortices are observed in the V sections at low incidence, and at high incidence (about 10°) the flow is observed to reattach to the rear cambered membrane, the leading-edge separation bubble is then greater than half a chord in length. The purpose of the spurs which are roughly the height of the viscous sub-layer for the reattached flow, is less obvious.

The average flapping frequency in forward flight (about 10 m/s⁻¹) is roughly 25 Hz (Nachtigall[12]) so that in one cycle the wing moves forward about 40 chord lengths. It is therefore postulated that the aerodynamics may be usefully studied, at least initially, on a static wing in steady flow.

Indoor free-flight tests have been made on two sizes of model glider with a similar wing section. Under stroboscopic illumination flights have been photographed using a long time exposure. With reflectors placed on the model and above the horizontal floor the flight altitude, flight-path angle and speed have been measured in steady

PRACTICAL APPLICATIONS OF TWO-DIMENSIONAL MEMBRANE RESEARCH

B.G. Newman
Professor of Aerodynamics, McGill University
Montreal, Canada

ABSTRACT

Theories, mainly inviscid, were developed several years ago for two dimensional lifting membranes. More recently experiments have shown that the predictions may be very inaccurate for medium-to-large camber ratios. Local separations of the flow are the cause of these discrepancies.

Although two-dimensional this work has some relevance to three-dimensional sails tacking obliquely into wind. For example it emphasises the importance of eliminating leading-edge separation on both head-and main-sails. Prediction of the aerodynamic forces on a three-dimensional sail with separation bubbles is very difficult and has not yet been attempted.

Sail efficiency can be improved by the judicious addition of stiffness, usually with battens. Membrane theory has been extended to cases where the stiffness may vary from leading to trailing edge, so that design for a particular pressure distribution becomes possible. Again only flattish sails give results which agree reasonably with the theory.

Luffing instability is experienced on membranes as well as sails and is shown to be a function of incidence and camber. According to linear theory it is a divergent instability and occurs just after the sail becomes S shaped at a slightly negative incidence.

For square sails and spinnakers two-dimensional membrane theory indicates how to increase drag and reduce oscillations. Flat sails are preferable although the increases in tension may be unacceptable.

NOMENCLATURE

c	length between membrane supports
C_L	lift coefficient $\dfrac{L}{\frac{1}{2}\rho U^2 c}$
C_{pb}	base pressure coefficient
C_S	leading-edge suction coefficient
C_T	tension coefficient
E	Young's modulus of elasticity
I	second moment of the cross section of a stiffened membrane
ℓ	length of membrane
n	frequency of oscillation
q	dynamic pressure of the free stream
R_e	Reynolds number $\dfrac{Uc}{\nu}$
S	suction force at the leading edge in approximately the negative x direction.
U	free stream velocity
x	along the chord
y	perpendicular to the chord
α	incidence
γ	camber ratio
ϵ	excess length ratio, $\dfrac{\ell - c}{c}$
ν	kinematic viscosity

BOOMERANGS

by Barry G. Newman, FRAeS
Professor of Aerodynamics
McGill University, Montreal

Photo: The Australian Information Service, London.

Dr Barry G. Newman was educated at Manchester Grammar School and Cambridge University. He completed his PhD at Sydney University in 1952. He has been the Canadair Professor of Aerodynamics at McGill University since 1959. Previously he was Lecturer in Aeronautics at Cambridge University and before that he undertook flight research with both the Royal Australian Air Force and the National Aeronautical Establishment, Canada. He has broad research interests in aerodynamics ranging from turbulent shear flows, wakes, jets and vortices, boundary layers and boundary-layer control, Coanda effect and the aerodynamics of animal flight, air-cushion vehicles, wind turbines and large-scale flexible membranes such as sails, parachutes and inflated buildings. He is currently a consultant to Pratt & Whitney Canada Ltd and the Pulp & Paper Research Institute of Canada. He is a Fellow of the Canadian Aeronautics and Space Institute, the Royal Aeronautical Society and the Royal Society of Canada.

Returning boomerangs are used by certain tribes of aborigines in Australia and appear to have been invented by them. In this paper both aboriginal and "modern" aerodynamic boomerangs are described. The flight dynamics of returning boomerangs is qualitatively explained with particular reference to the work of Walker, Lanchester and Hess. The non-dimensional parameters which determine the main features of each part of the motion are identified, and simplified analyses are presented. The predicted behaviour is compared with boomerang flights. The predictions include the connection between boomerang inclination and advance ratio at launch and the effect of scale and density on range and on the final hovering mode.

Aboriginal Boomerangs

There are three main types of Australian boomerang: the non-returning killer or war boomerang which is usually asymmetrical with arms of different length, the returning boomerang which is usually lighter, and the ceremonial boomerang which is not thrown. Non-returning boomerangs are not peculiar to Australia and they are traditionally found on at least three other continents. Sometimes these non-Australian weapons are made of metal in the form of throwing knives and pictures of them may be found in Ref 1. Although some of these weapons do have a tendency to return, the fully returning boomerang appears to have been an invention of the Australian aborigine.[2,3]

Two examples of asymmetrical non-returning Australian boomerangs are shown among the author's collection, Nos 1 and 2 in Fig 1. Sometimes a hook is added to the short end of the boomerang

DRAGON FLY EXPERIMENT
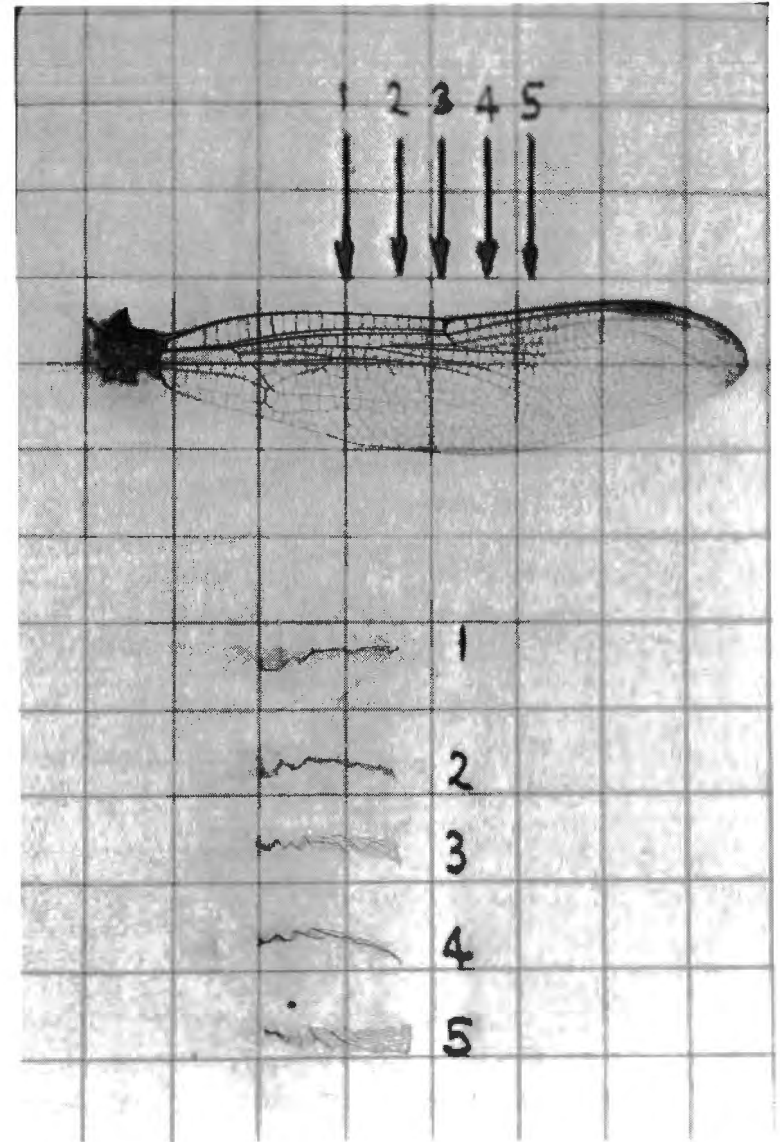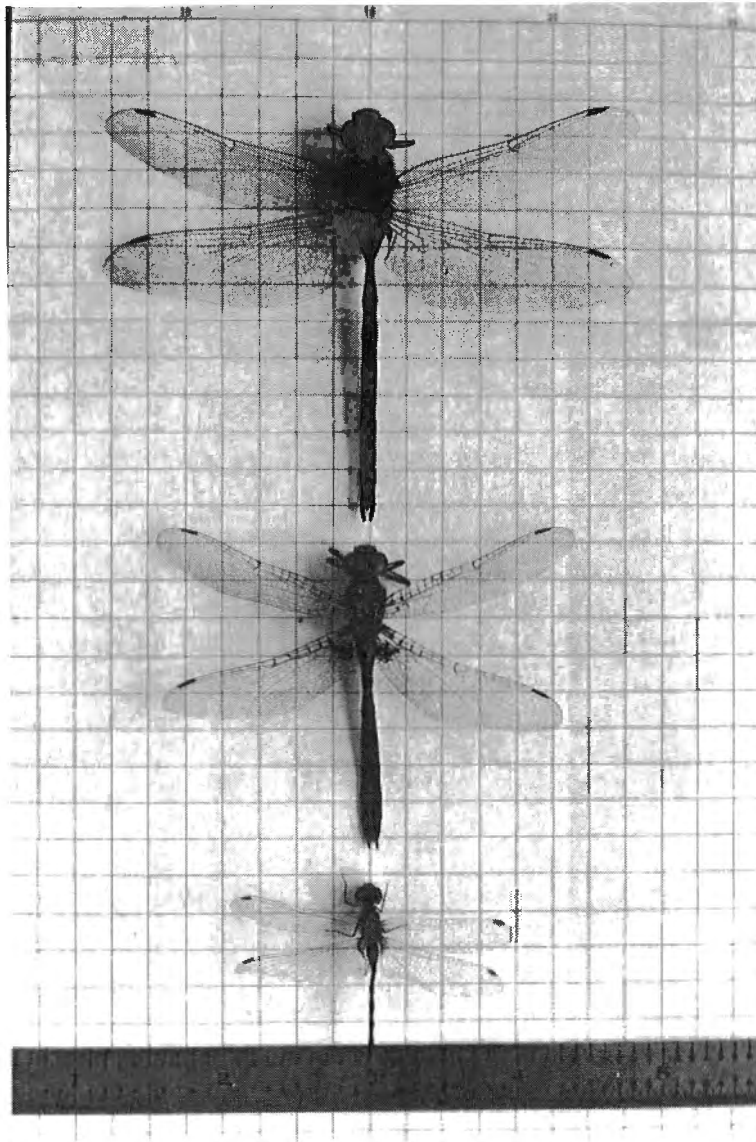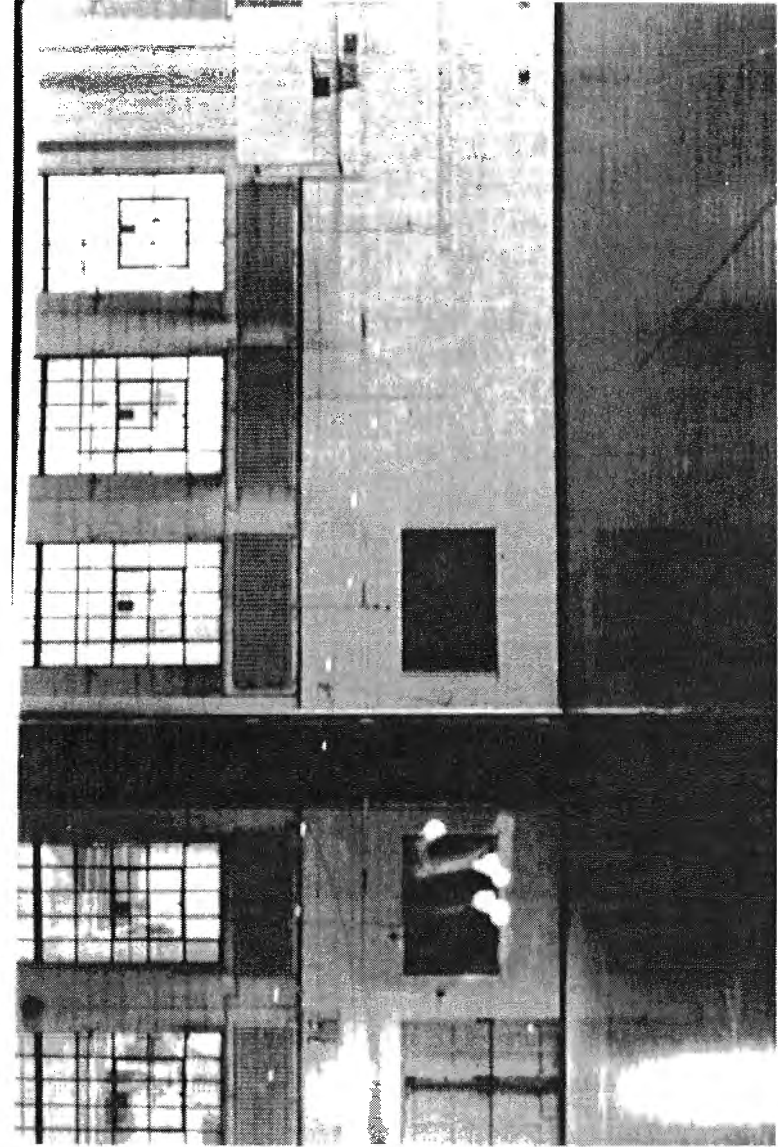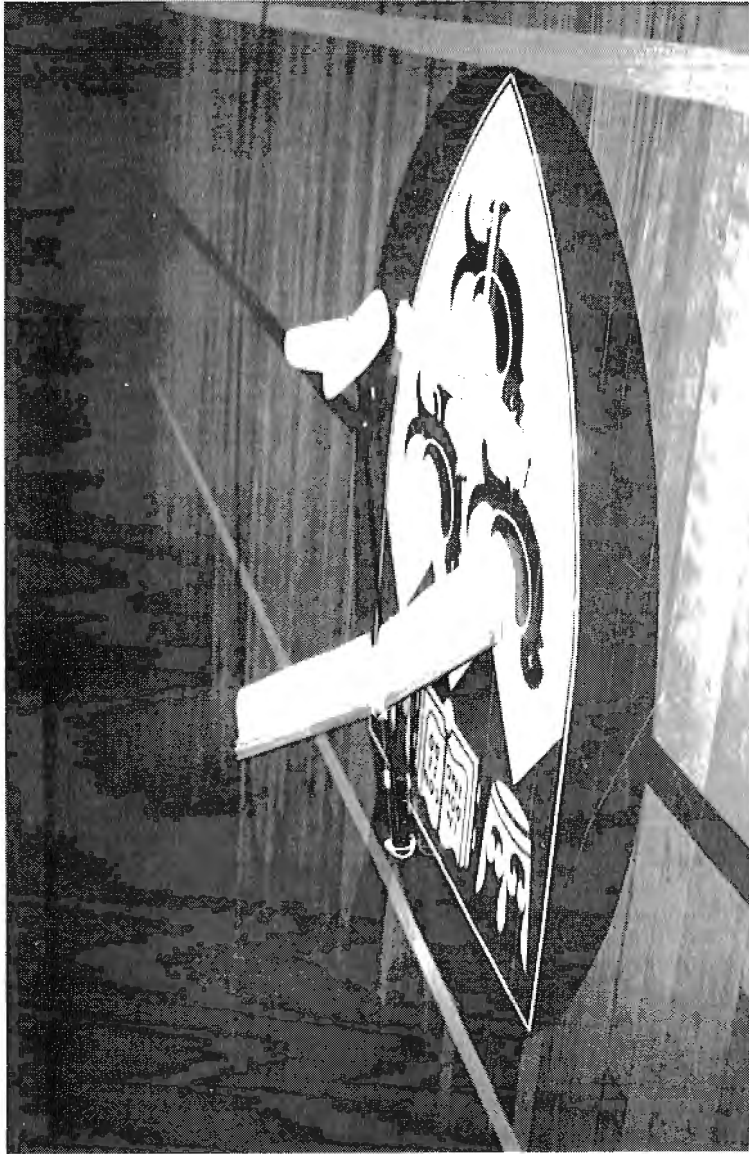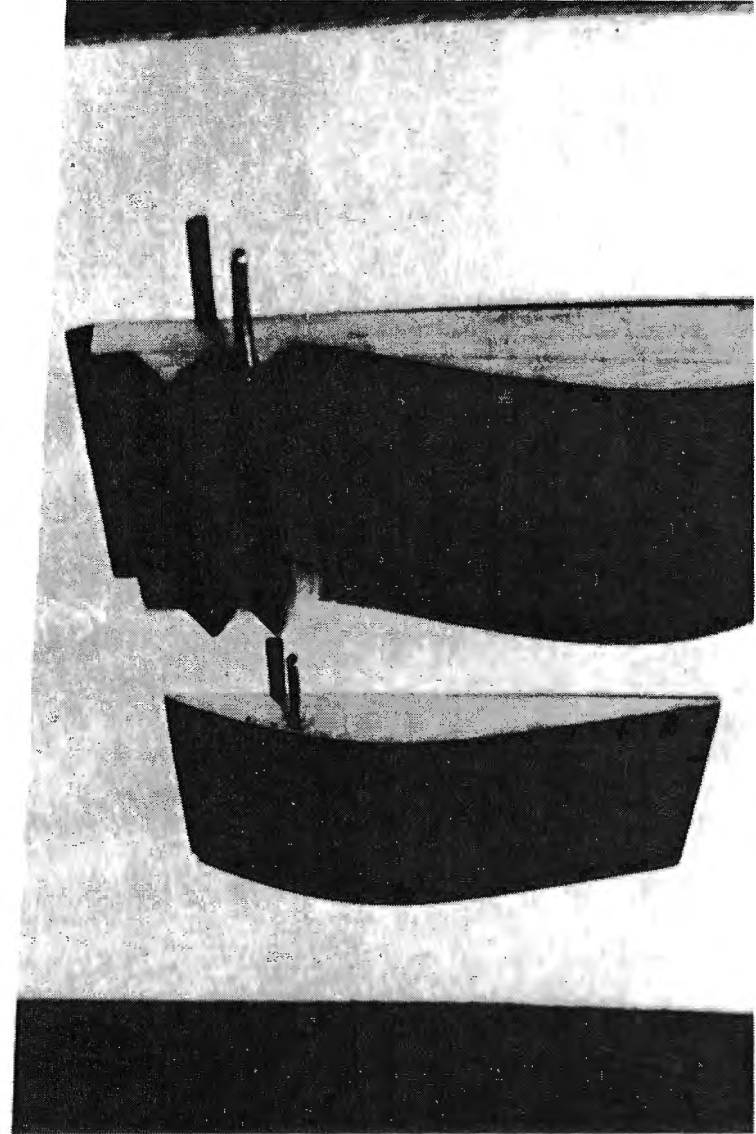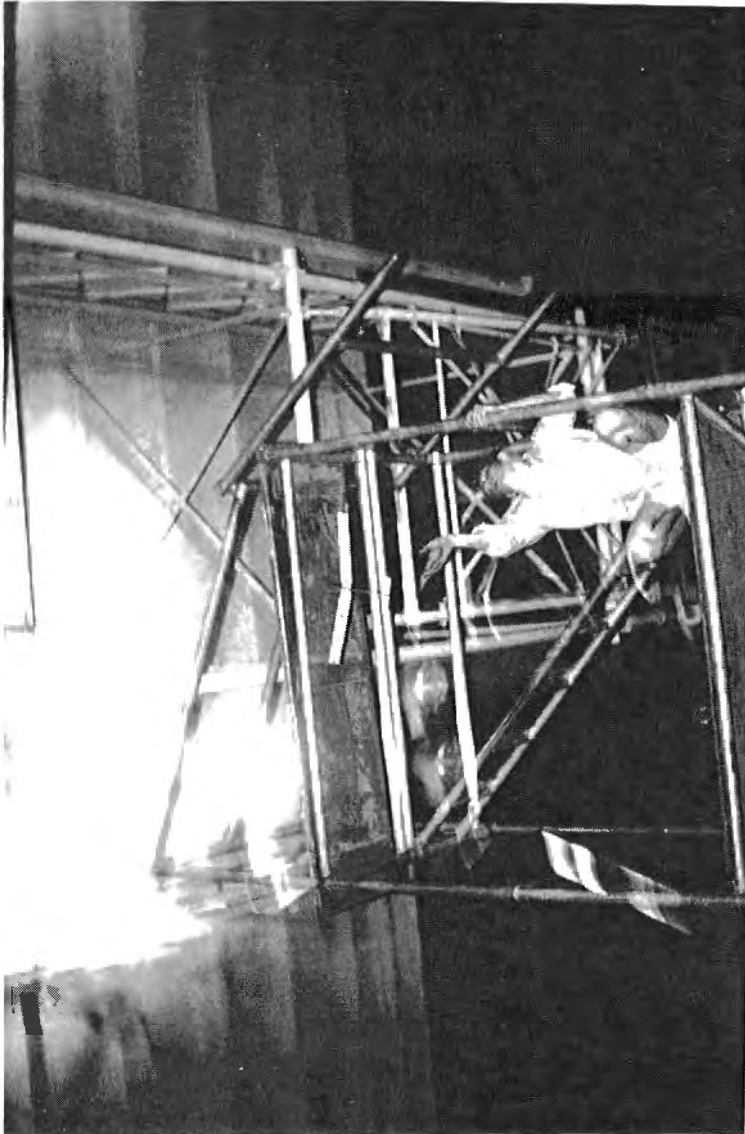
DRAGON FLY EXPERIMENT
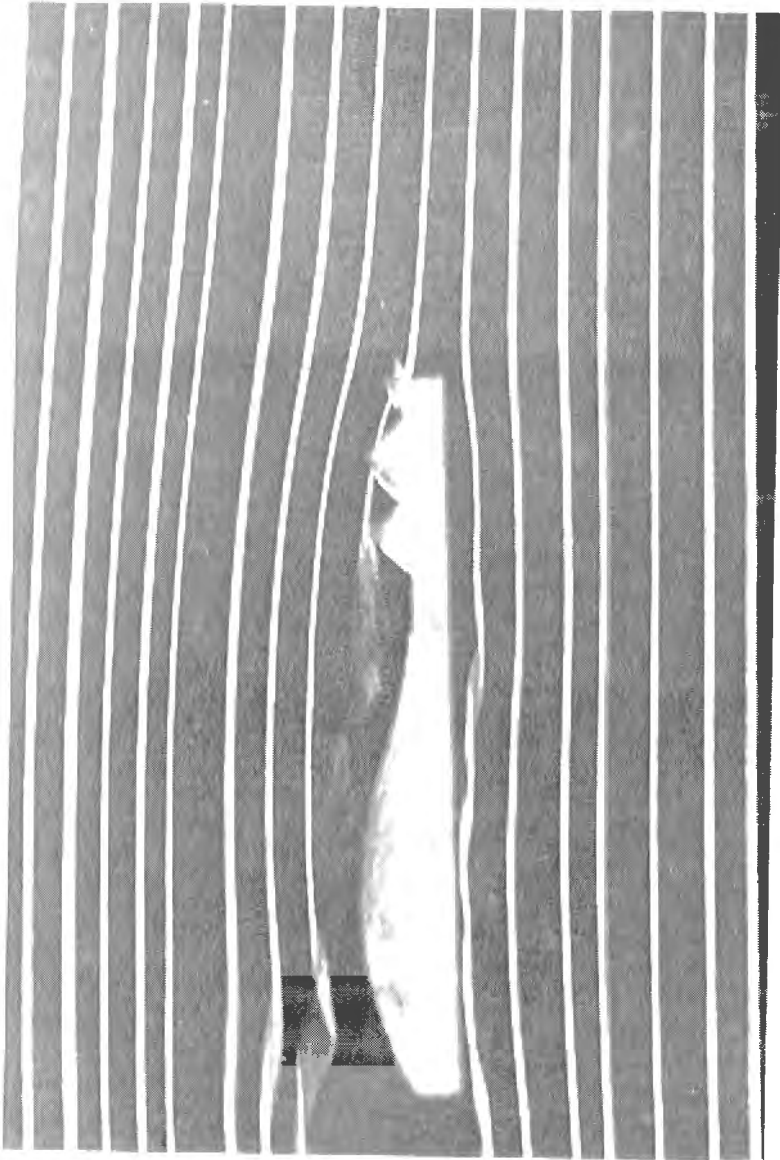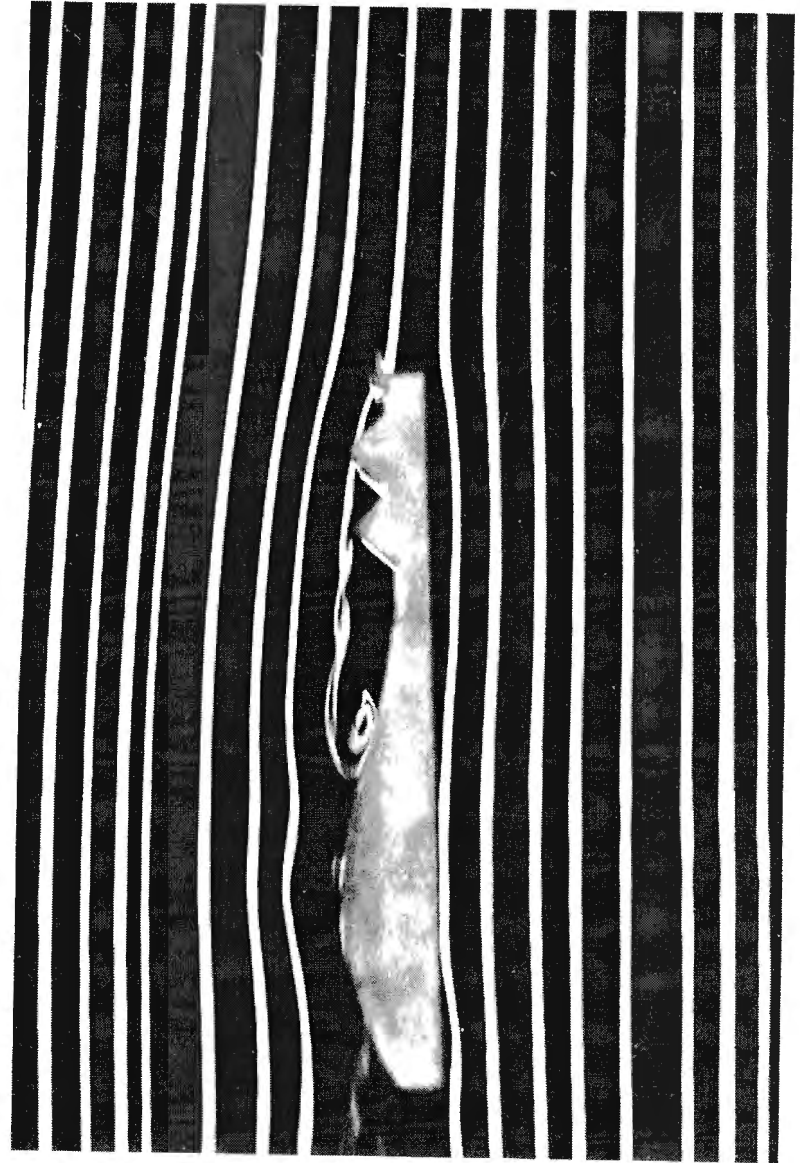
DRAGON FLY EXPERIMENT
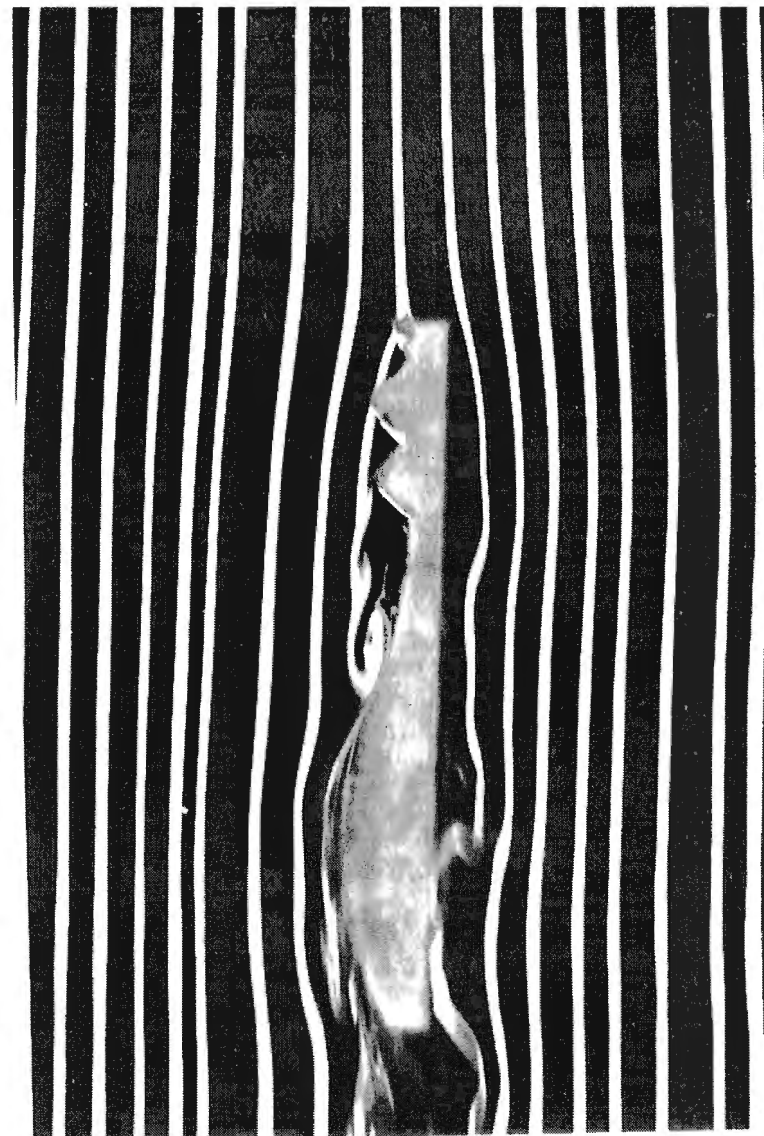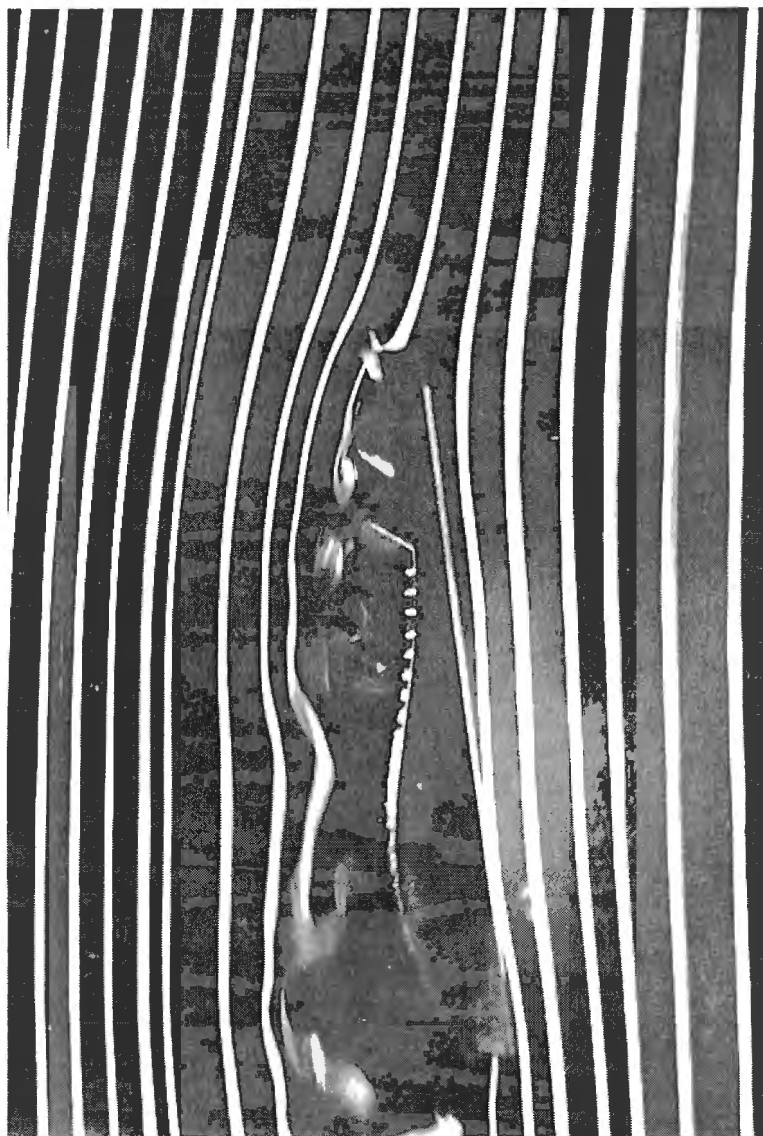
DRAGON FLY EXPERIMENT
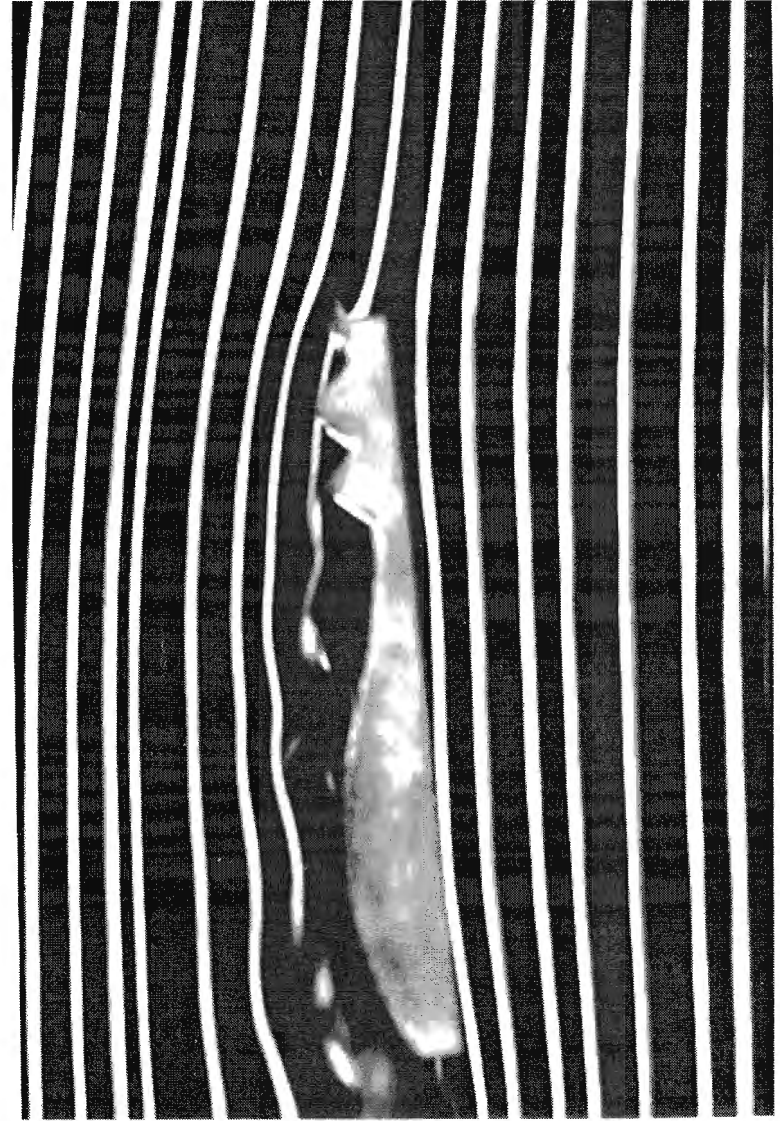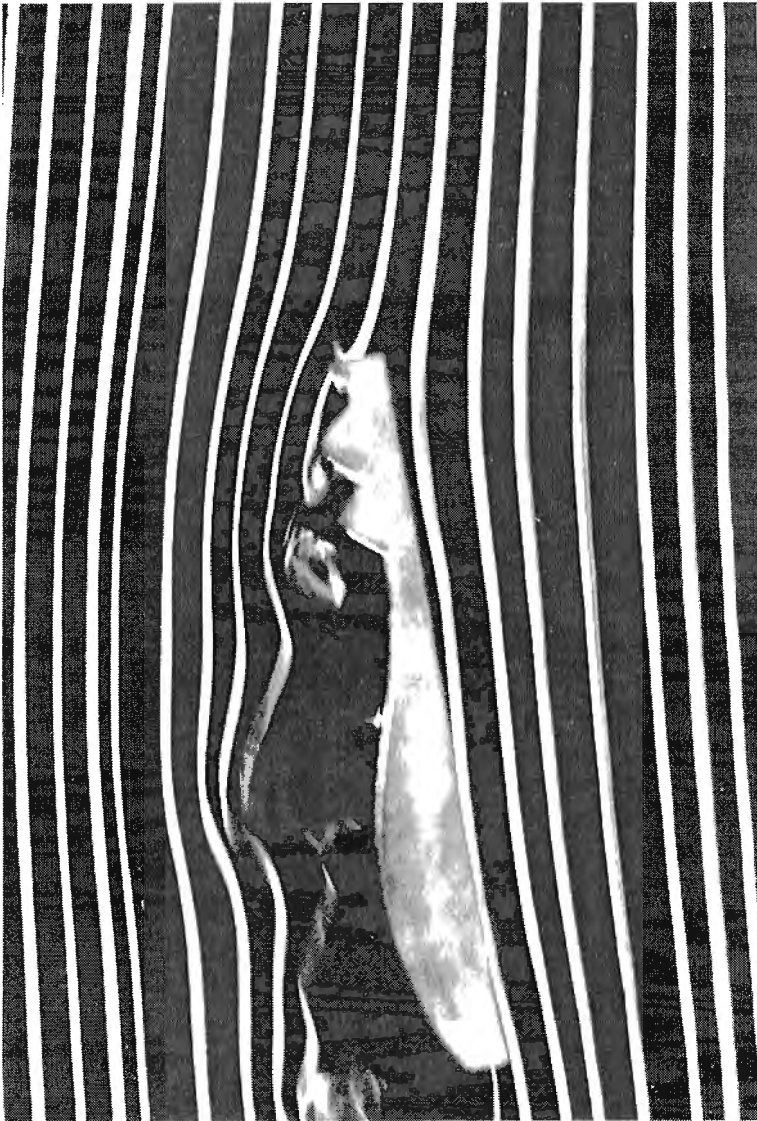
DRAGON FLY EXPERIMENT
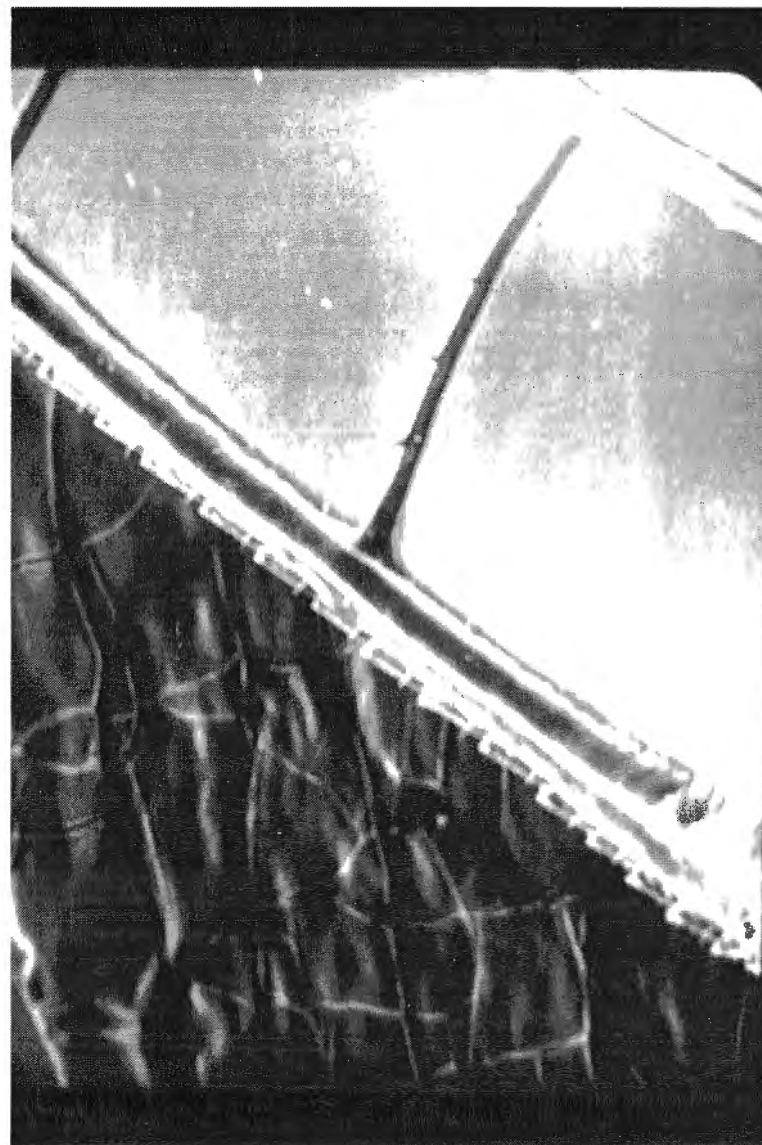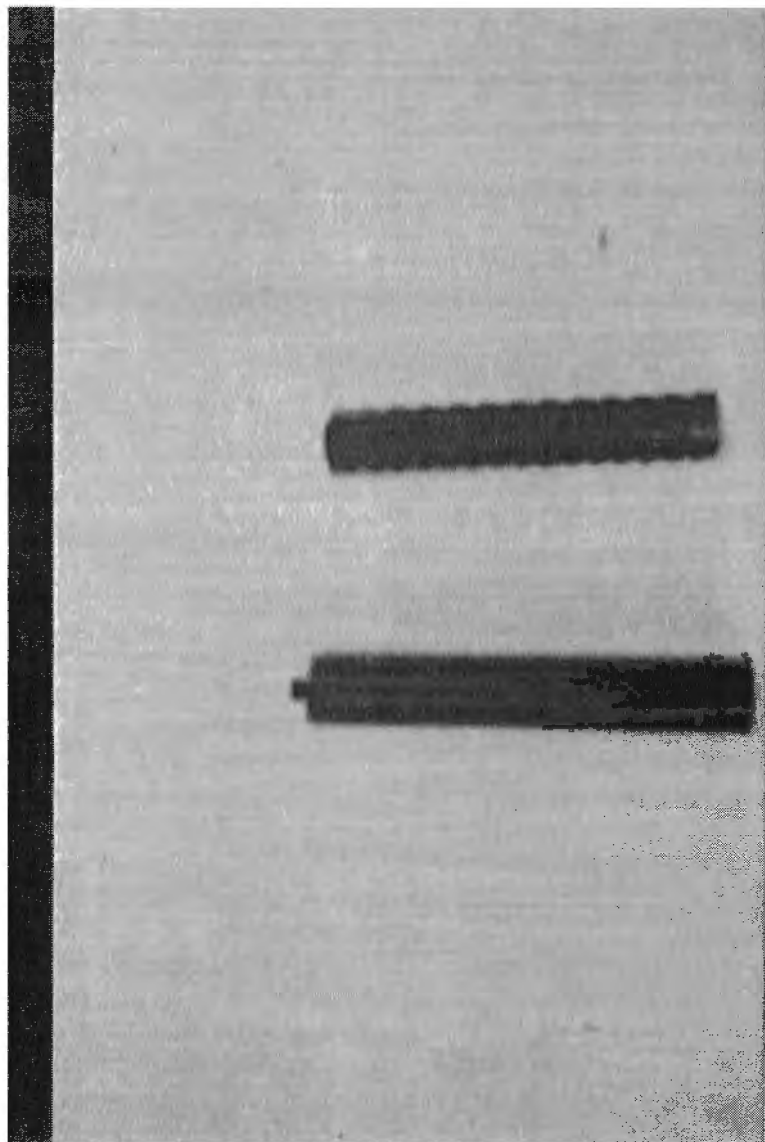
DRAGON FLY EXPERIMENT
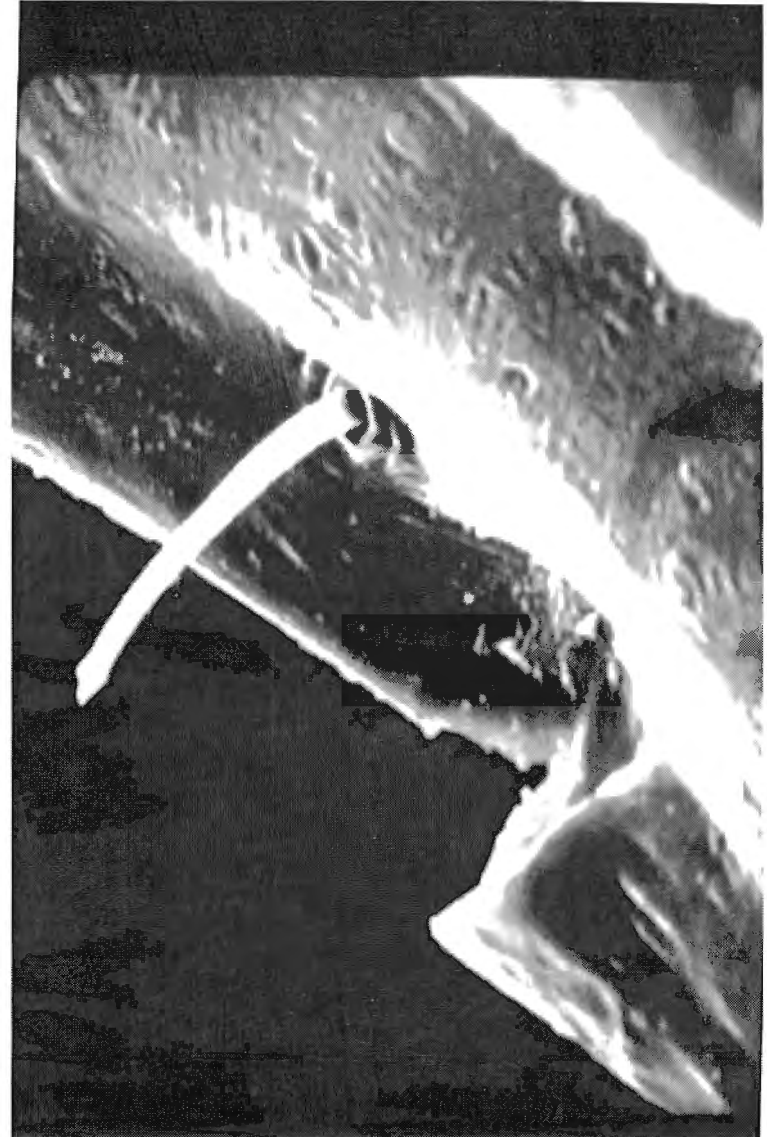
DRAGON FLY EXPERIMENT
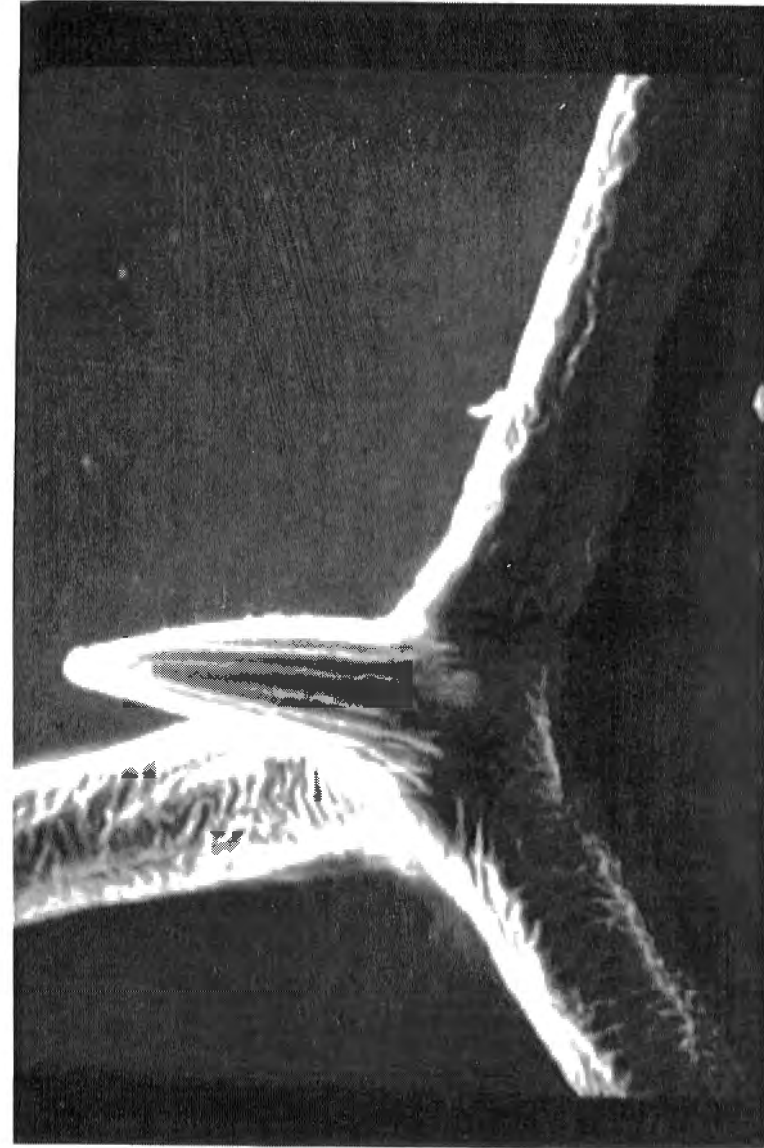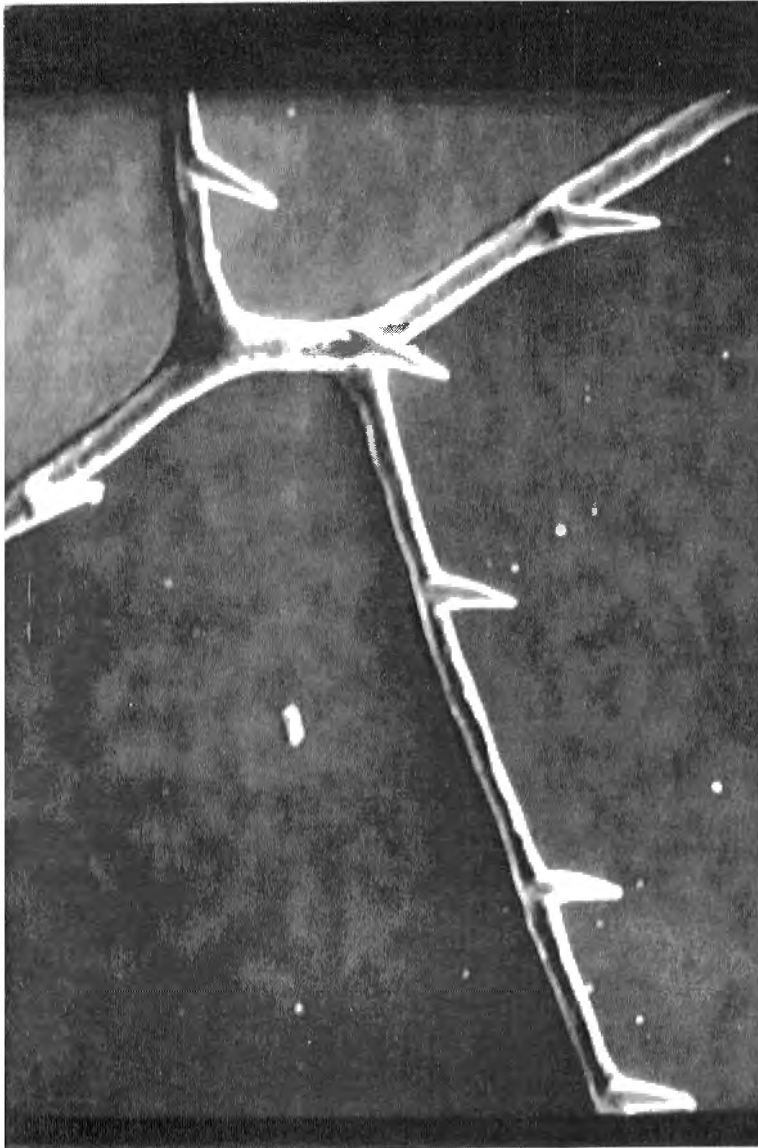
DRAGON FLY EXPERIMENT

DRAGONFLY   WING   SECTION
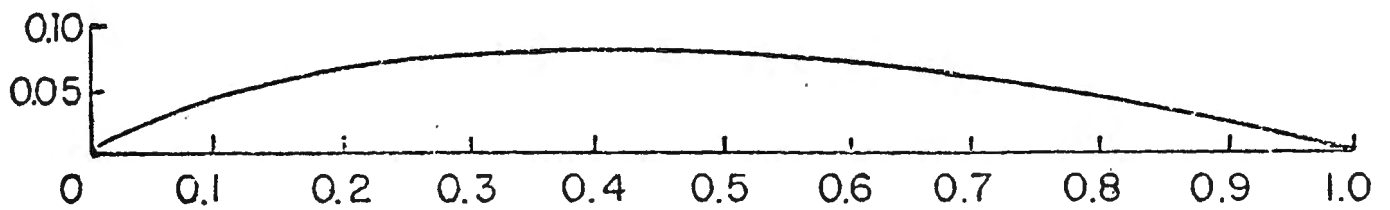
McBRIDE   B-7

% CHORD	0	5	10	20	30	40	50	60	70	80	90	100
% CAMBER	0	2.35	4.40	6.70	7.80	8.30	7.90	6.90	5.60	3.90	2.00	0

DRAGONFLY

WITH TURBULATOR

DRAGONFLY WITH
TURBULATOR &
ENDPLATES

C_{L_W}

C_{L_W}

CURVED
PLATE

PLAIN
DRAGONFLY
SECTION

LARGE MODELS
$Re \approx 3.5 \times 10^4 - 6 \times 10^4$

C_L

α (DEGREES)

1.2-24

PLAIN DRAGONFLY
SECTION (LARGE MODEL)

$C_{D_{GLIDER}}$

$C_{D_{WING}}$

C_{D_O}

C_D

α (DEGREES)

1.2-25

LARGE MODEL
$(Re \approx 3.5 \times 10^4 - 6 \times 10^4)$

SMALL MODEL
$(Re \approx 1.2 \times 10^4 - 2.5 \times 10^4)$

DRAGONFLY SECTION
(NO TURBULATORS)

c_{L_W}

c_{D_O}
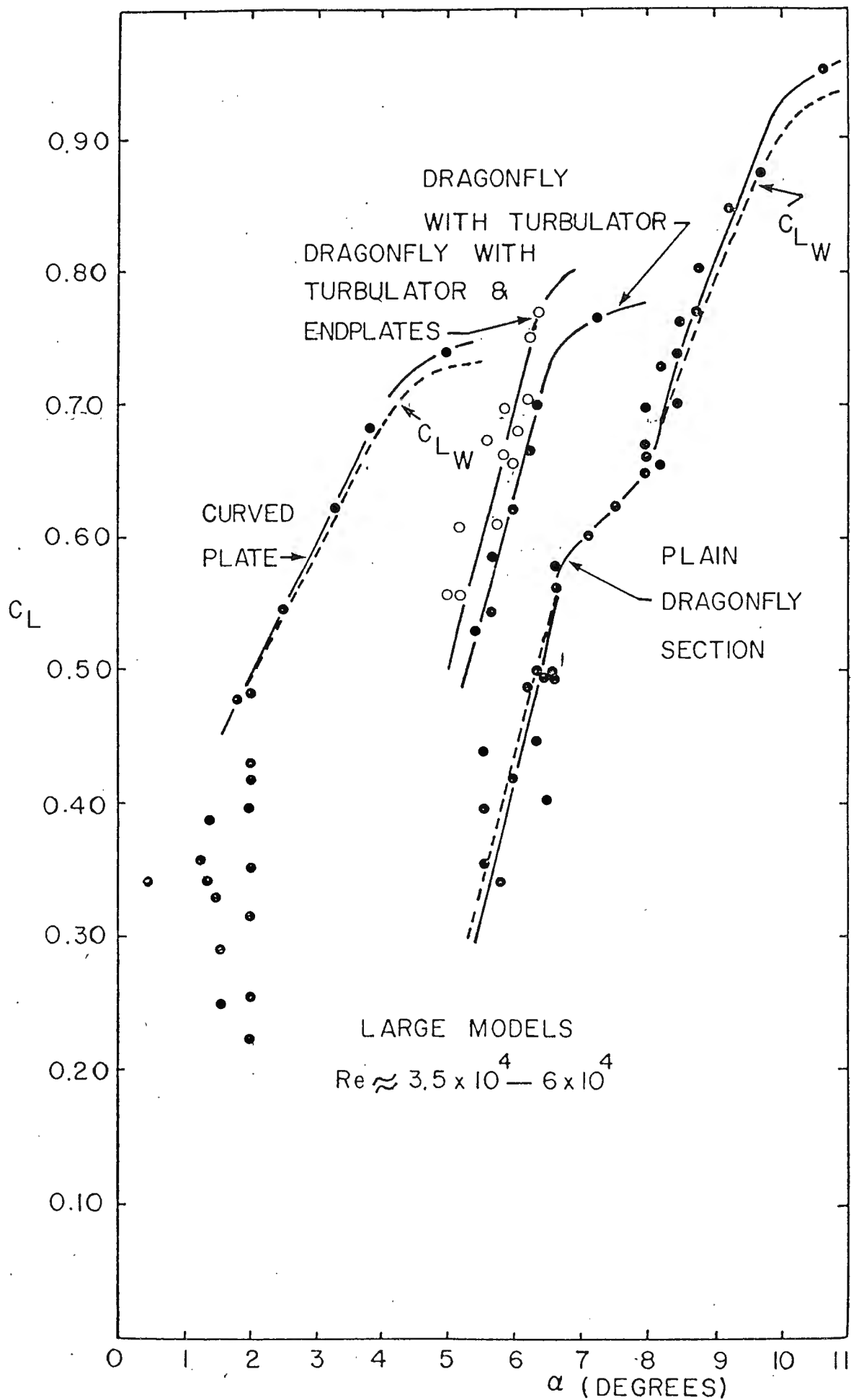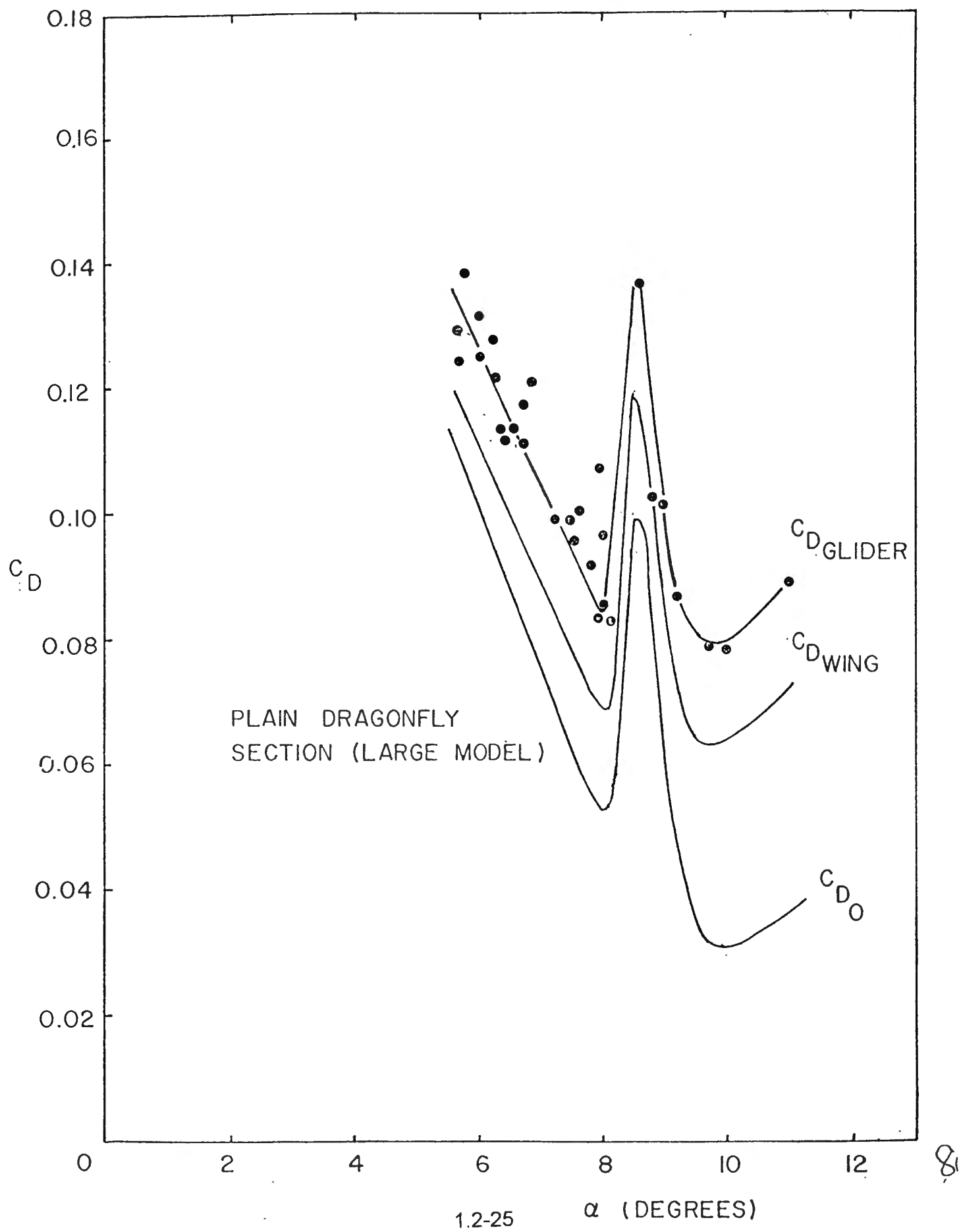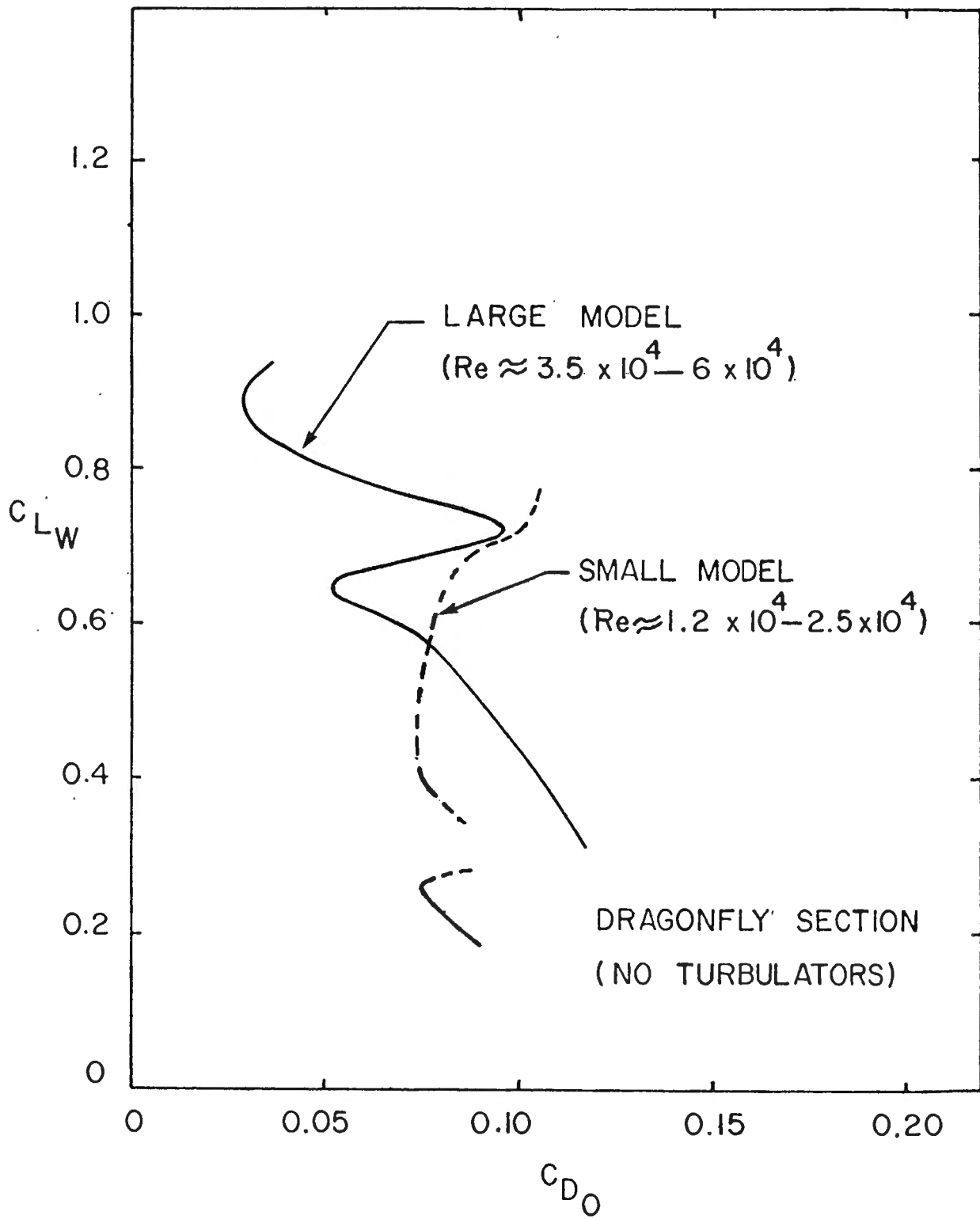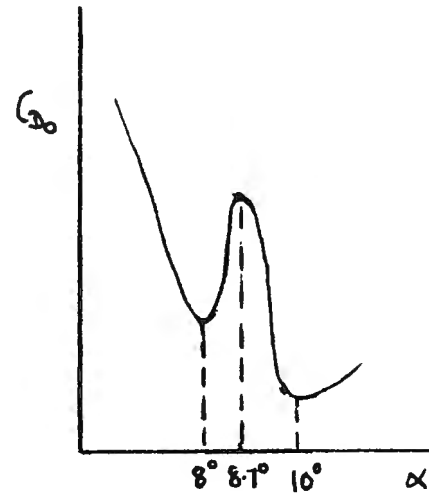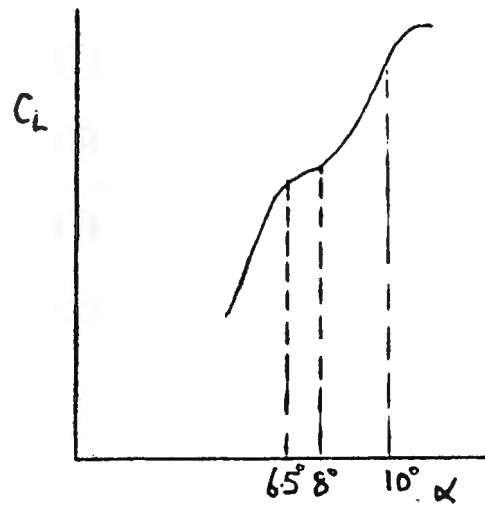
The unusual pleated aerofoil has a good aerodynamic performance at Reynolds numbers of around 10^4 10,000. Our tests on a glider having a constant chord pleated section typical of the dragonfly just inboard of the nodus compared well with a high performance low Reynolds number conventional aerofoil fitted with an upstream turbulator. It is ~~extremely~~ probable that the actual dragonfly wing, which contains several features not present on the test models, has an even higher performance

Other possibilities

Leading edge serrations produce small trailing vortices which help to destabilize the separated laminar shear layer & promote transition and reattachment This is commonly done on model aircraft for Reynolds numbers between 10^4 and 10^5.

The rows of hairlets on the three arms of the leading edge at the base of each serration may serve not only to detect foreign objects but also the airflow direction so that the position of the leading edge stagnation points may be controlled. Likewise the trailing edge hairlets may be used to ensure that the flow leaves the trailing edge smoothly

It is abundantly clear that from the aerodynamic viewpoint the ancient dragonfly is a complex and highly efficient flying machine which for... depends it's ...
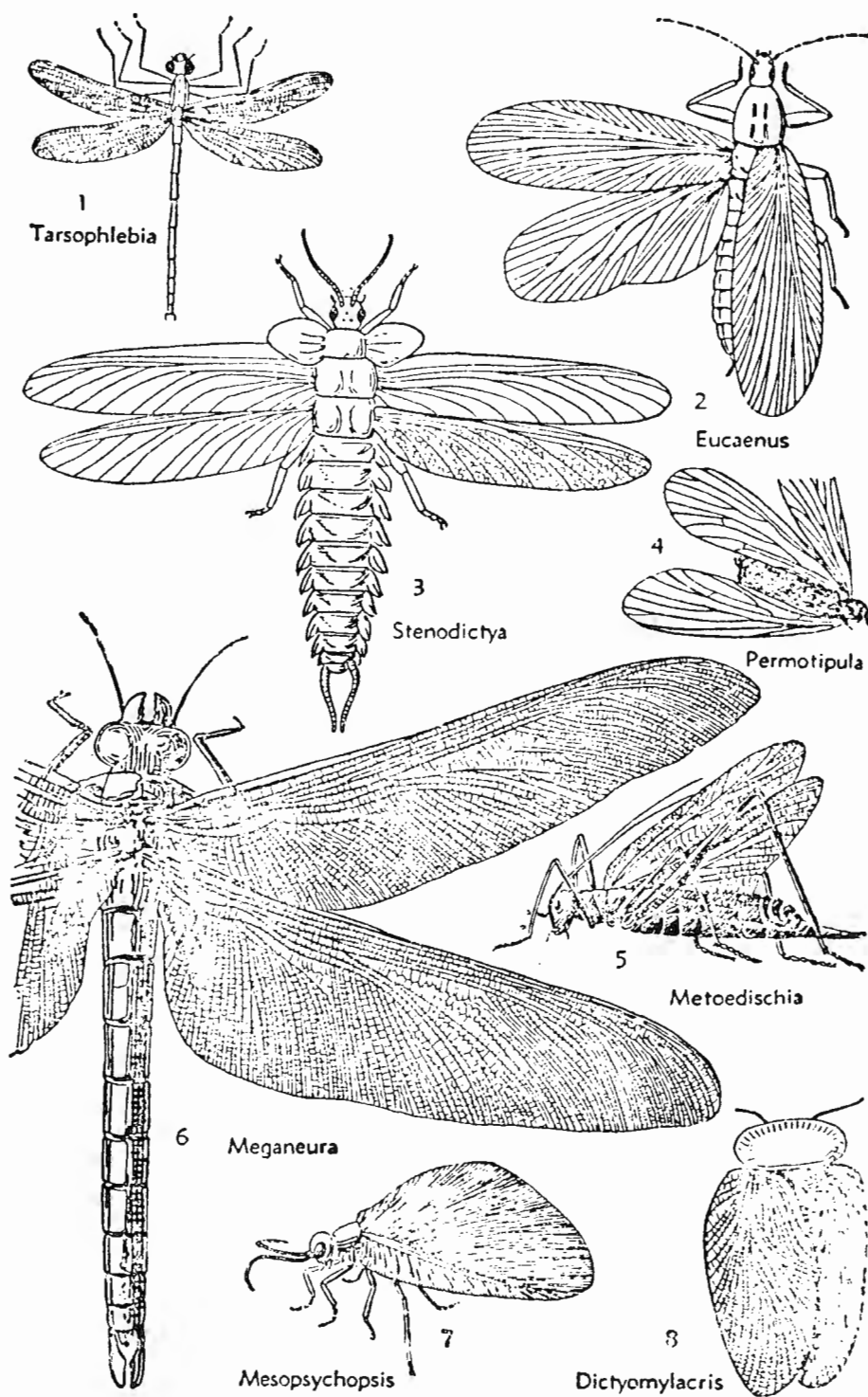
1
Tarsophlebia

2
Eucaenus

3
Stenodictya

4
Permotipula

5
Metoedischia

6   Meganeura

7
Mesopsychopsis

8
Dictyomylacris

Fig. 15-11.

Incompressible flow past a flat plate aerofoil with leading edge separation bubble

B. G. NEWMAN and M-C. TSE
Department of Mechanical Engineering McGill University, Montreal

<u>Nocturnal Owls</u>

as distinct from, say Snowy Owls

Hunt by diving on rodents at night.

Silent flight is usually attributed to

(a) Downy surface on TOP and biggest near trailing edge of the downstream primary feather.

(b) Shawl-like trailing edge.

(c) Comb at exposed leading edge of the primaries.

FIGURE 2 (*right*): Primary feather of a Great Horned Owl

1 cm
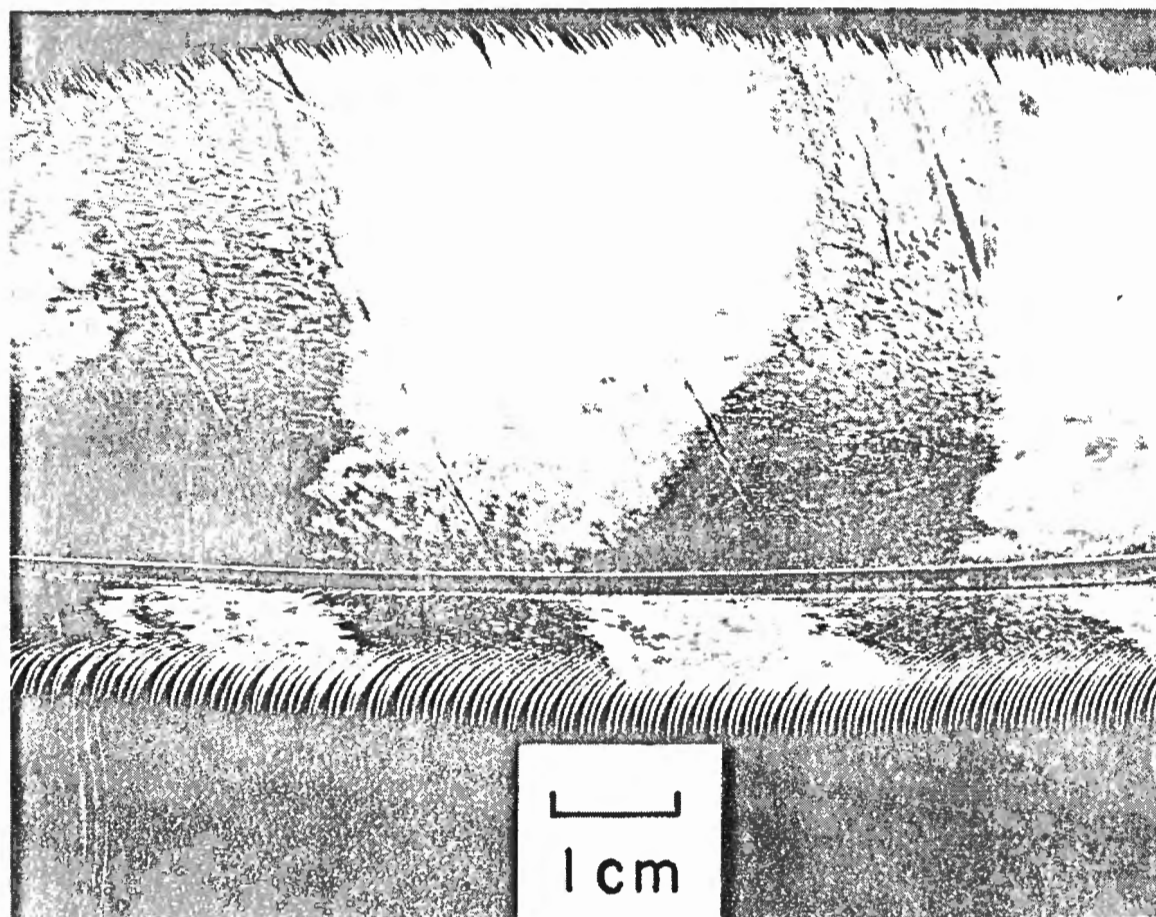
Flat plate measurements

downy surfaces surrounded by silk velvet (Figs. 2 ~~and~~ 2 1/2).

Pitot and hot wire traverses.

$$\frac{U}{U_\tau} \Big/ log_{10} \frac{yU_\tau}{\nu} = 5.6 + - - - \qquad\qquad \text{Figs. 3-5.}$$

$$U_\tau \rightarrow C_f$$

Down increases C_f by about 85%, but not independent of $\frac{\ell U_\tau}{\nu}$, i.e. not "fully rough".

O.K. for steep descent.

Longitudinal turbulence (Fig.6), downy surface has reduced turbulence for $\frac{yU_\tau}{\nu} < 100$. Similar to surface pressure fluctuations.

Down 'rough' due to laminar flow over the down in contrast to conventional roughness.

Spectra shows a shift to higher frequencies. $10 \times$ about. Fig. 7.

This could then be attenuated by long grass and low shrubs.

<u>Leading-edge comb.</u>

The leading edge of all exposed leading edges of primary feathers has a comb which is an extension of the barbs.

We compared leading-separation bubble for such a feather with flat plate in a smoke tunnel. Slightly dependent on Reynolds number (based on feather chord). Fig. ⁇

Comb on feather suppresses the bubble by $\Delta \alpha = 6°$.

$\left(\text{note} \quad \dfrac{x_R}{c} \quad \text{increases only slightly with roughness}\right)$

No comb $\quad \dfrac{p_{rms}}{\frac{1}{2}\rho U_\infty^2} = 0.12$ at reattachment cf 0.03 no separation.

0.09 at reattachment if downy.

Position of time mean reattachment zone (fully smooth surface)

13 Static pressure taps at 20 mm. Intervals

9 Static pressure taps at 124.5 mm. Intervals

203

89.5   406   267   406

Far downstream measurement station X = 1092

152

140

Y

Traverse rod

1.2-37

X

Insert 1   Insert 2

Z

Flap

705

30°

12.7

4.5°

176

Tunnel floor

1121

914

1248

1.2-38
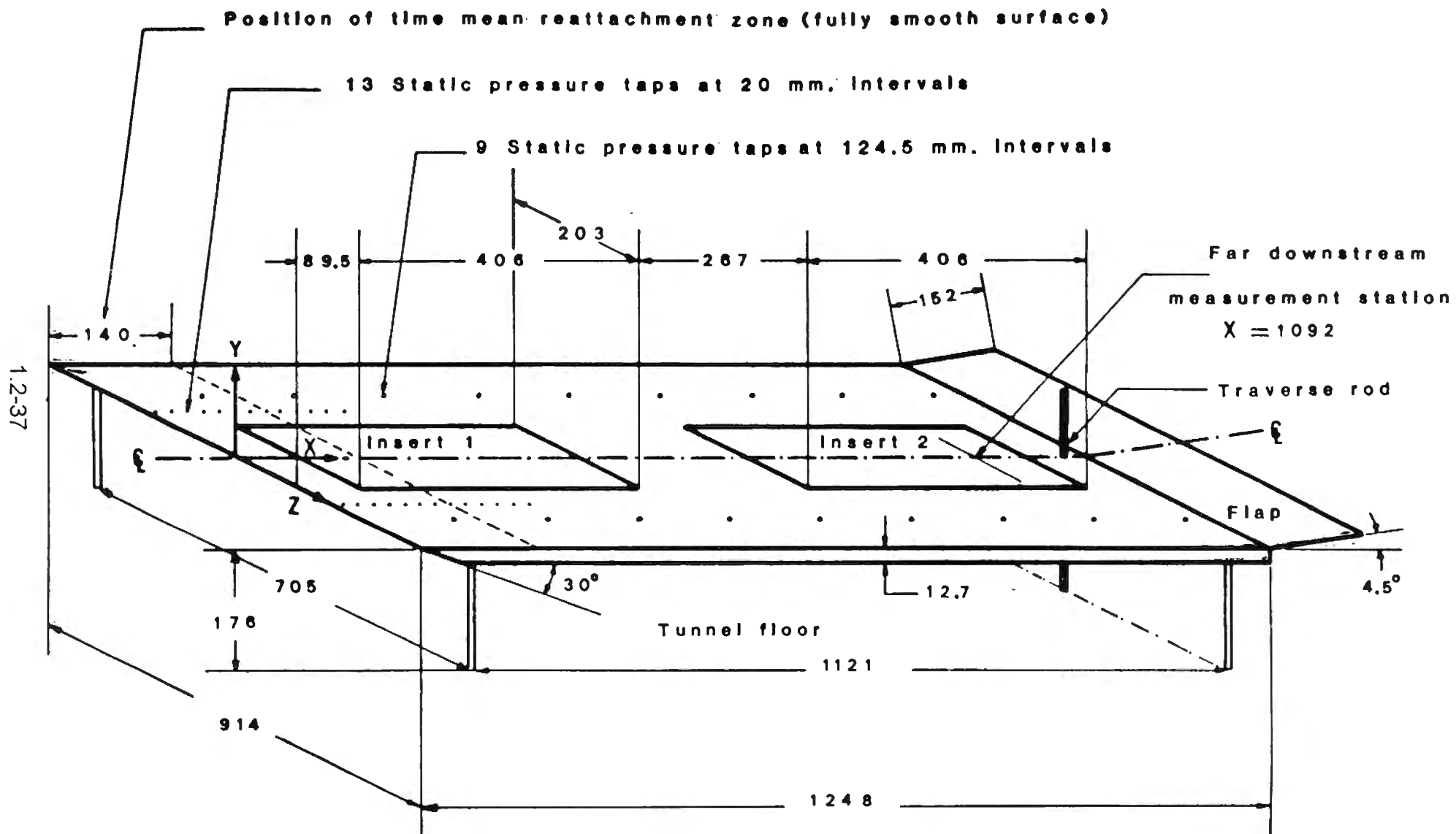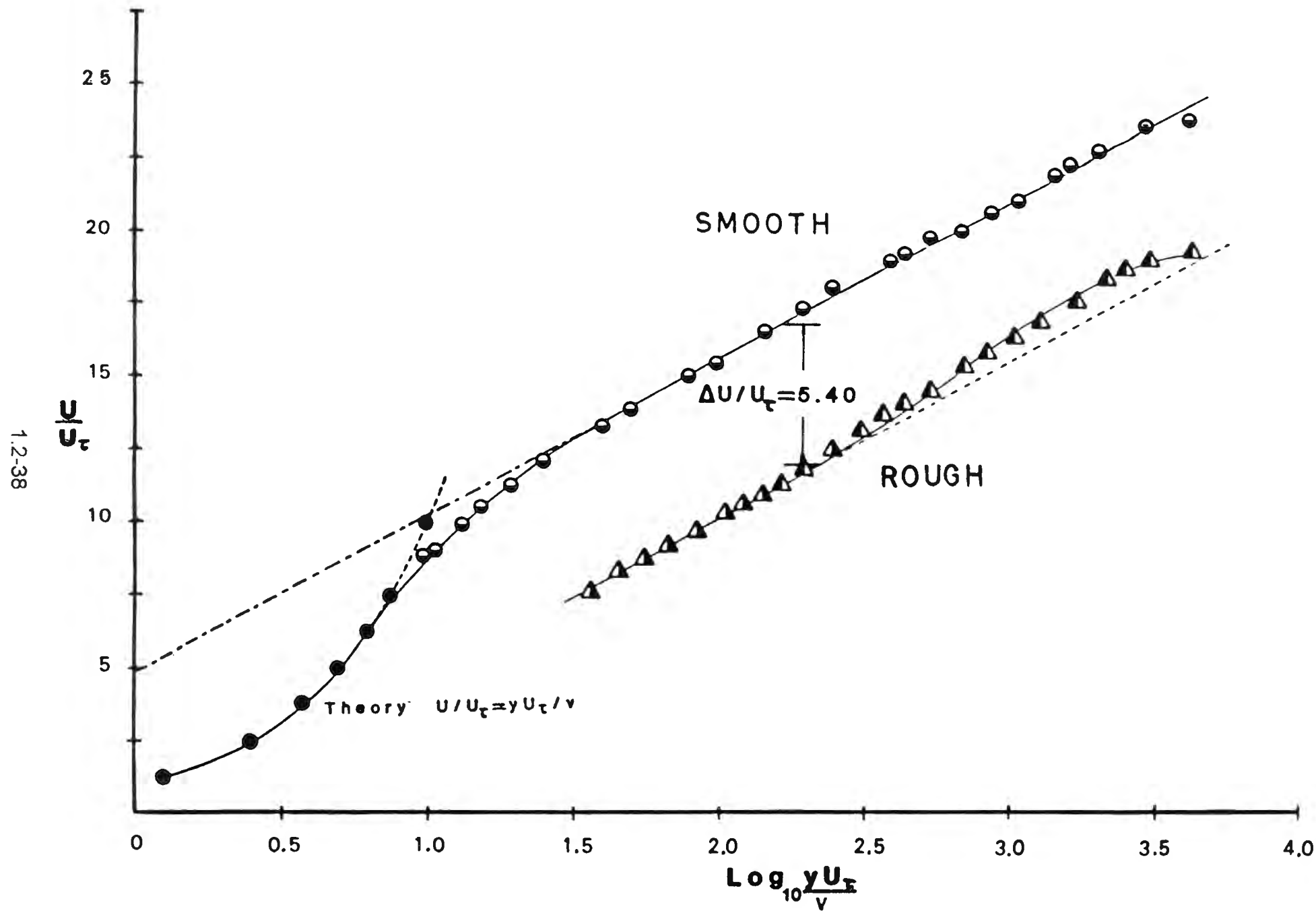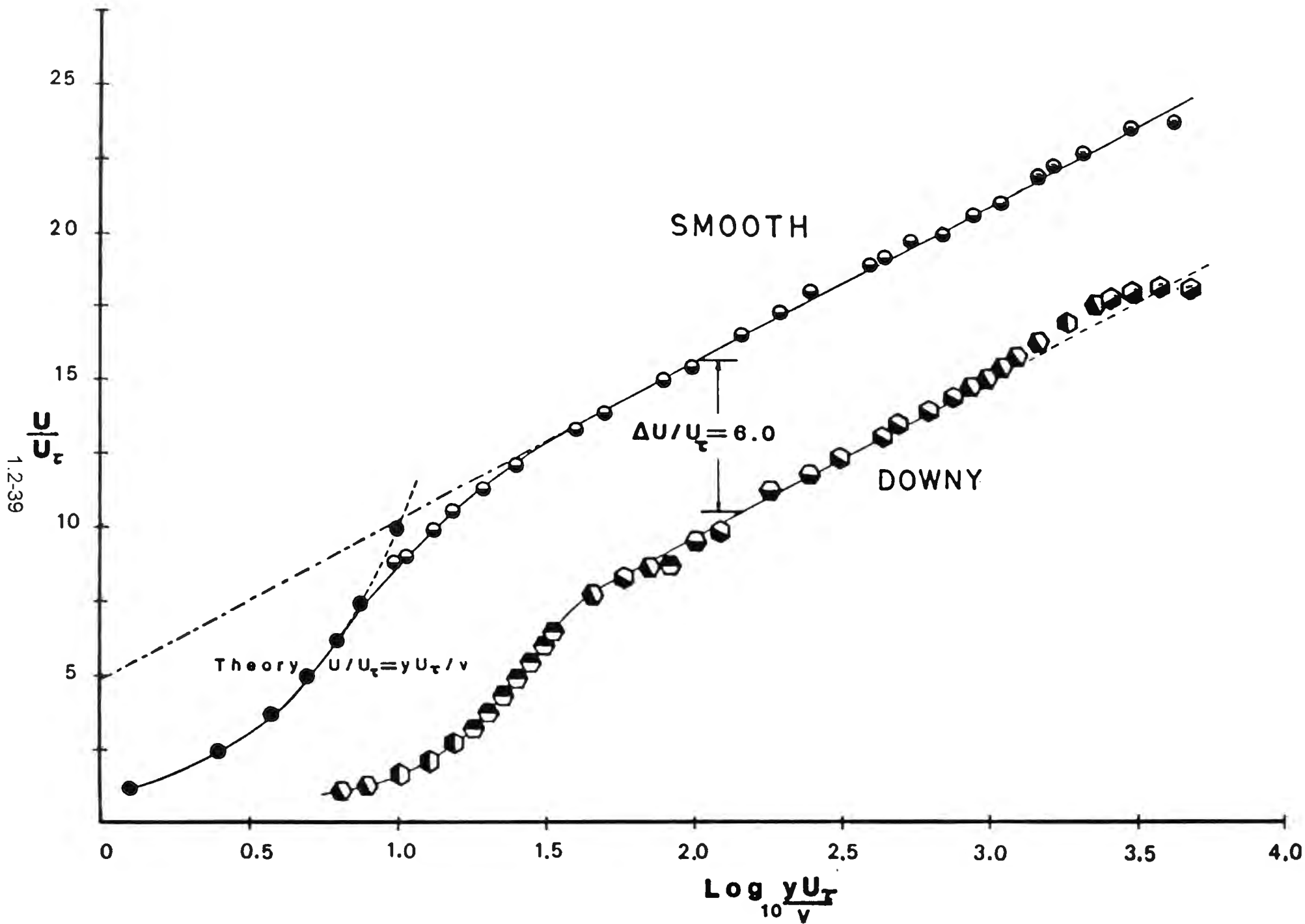
Turbulent Boundary Layer
near a Downy Wall

$$\tau_w = \rho U_\tau^2$$
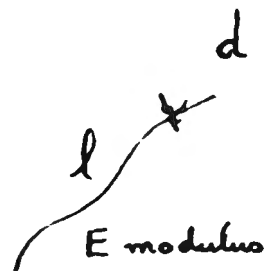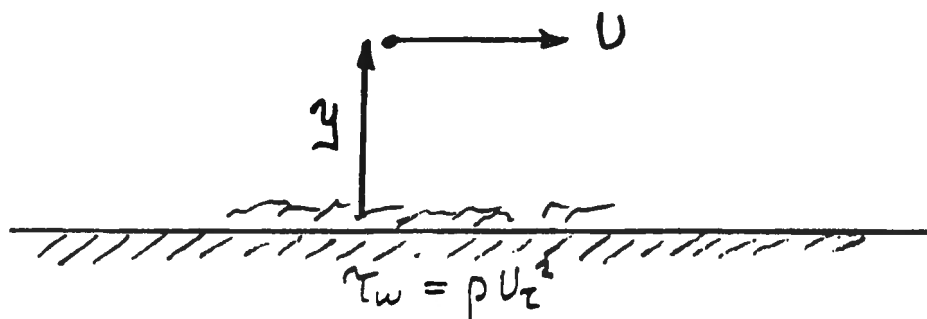
$$\frac{y}{U_\tau} \frac{\partial U}{\partial y} = \frac{1}{K}$$

$$\frac{U}{U_\tau} = \frac{1}{K} \ln \frac{y U_\tau}{\nu} + f\left(\frac{\rho' U_\tau^2}{E}, \underbrace{n l^2, \frac{\ell}{d}}_{geometry}, \frac{\ell U_\tau}{\nu} \right)$$

$\underline{y}$ is adjusted to give a straight line on log plot

U_τ is adjusted to give the von Karman slope $\frac{1}{K}$.

$\frac{\rho U_\tau^2}{E}$ is unimportant if it is less than 1.5×10^{-10}

— estimated —

Table 1. Boundary layers on the large flat plate.

SURFACE	U_∞ m/s	δ^x mm	c_f	$\dfrac{U_\tau}{U_\infty}$	$\dfrac{\Delta U}{U\tau}$	k_s mm Equivalent Sand Roughness	$\dfrac{k_s U_\tau}{\nu}$	k mm Measured Roughness
SMOOTH	13.4	8.24	.0035	.042	-			
	27.8	7.00	.0030	.039	-			
ROUGH	13.3	9.85	.0053	.051	5.40	.810	37	.57
	27.1	9.58	.0052	.051	8.00	1.120	75	.57
DOWNY	13.7	9.08	.0059	.054	6.00			.9
	30.4	8.52	.0058	.054	8.35			.9
SILK VELVET	14.0	9.23	.0056	.053	5.35			.7
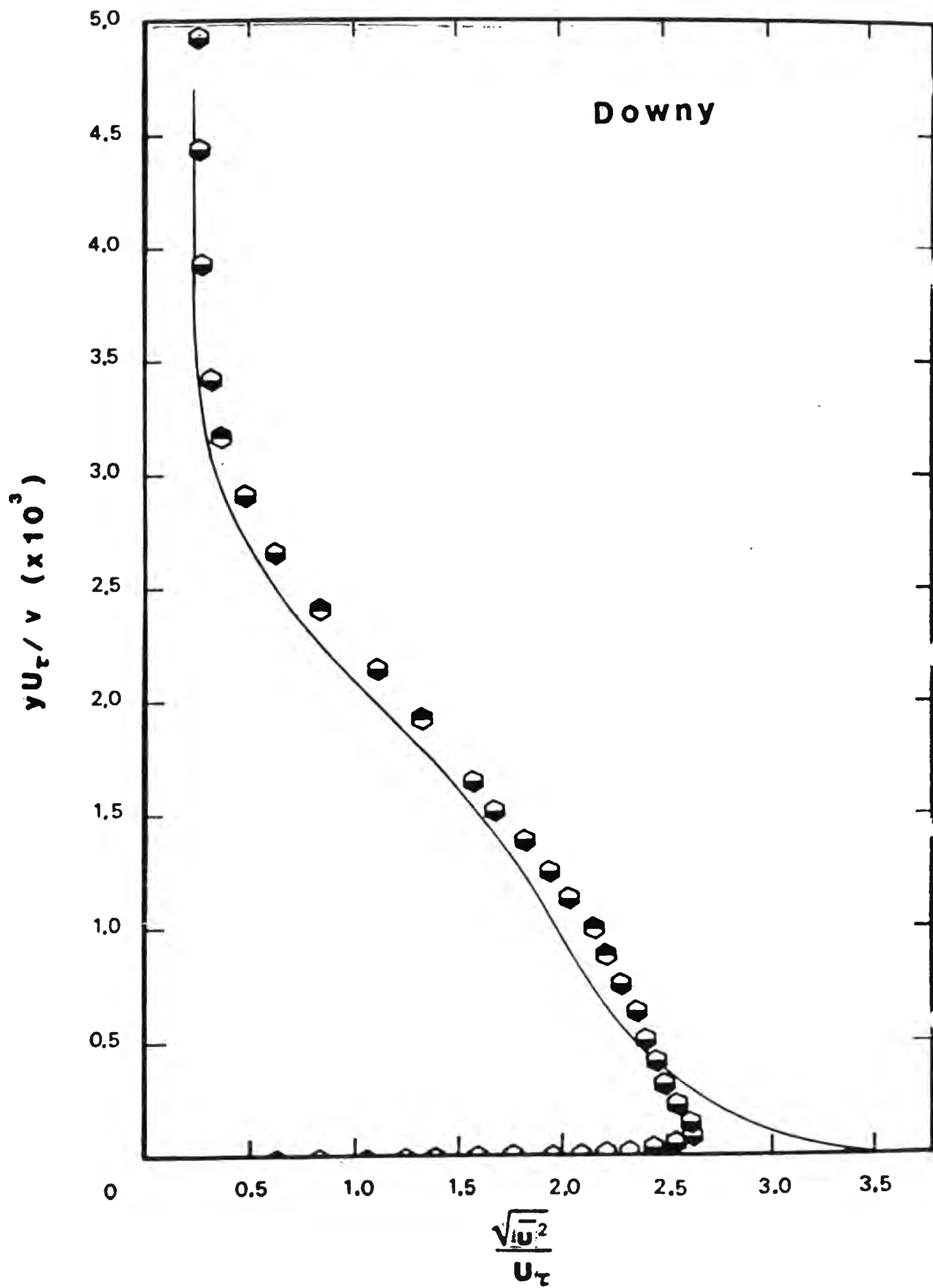
Downy
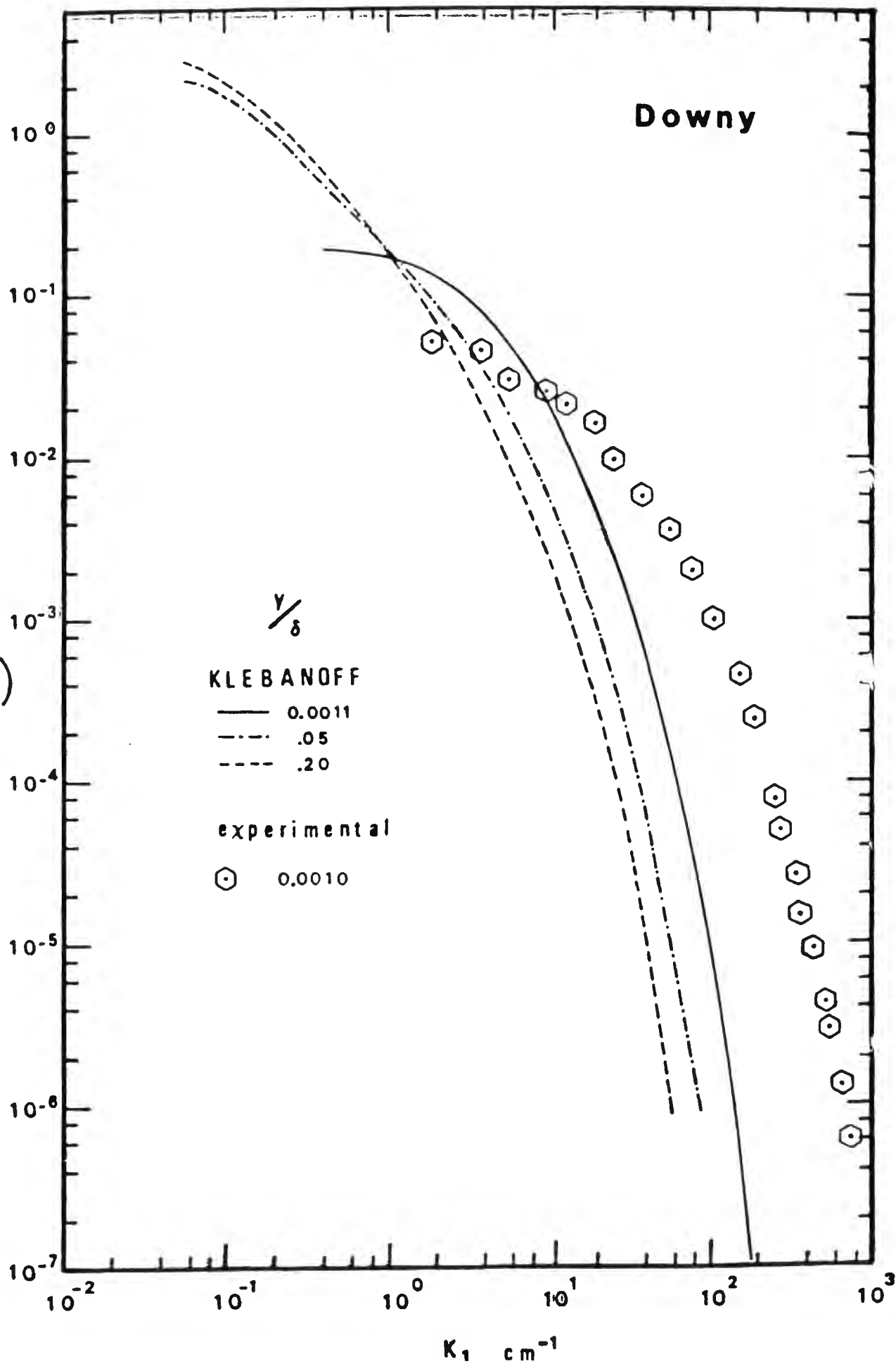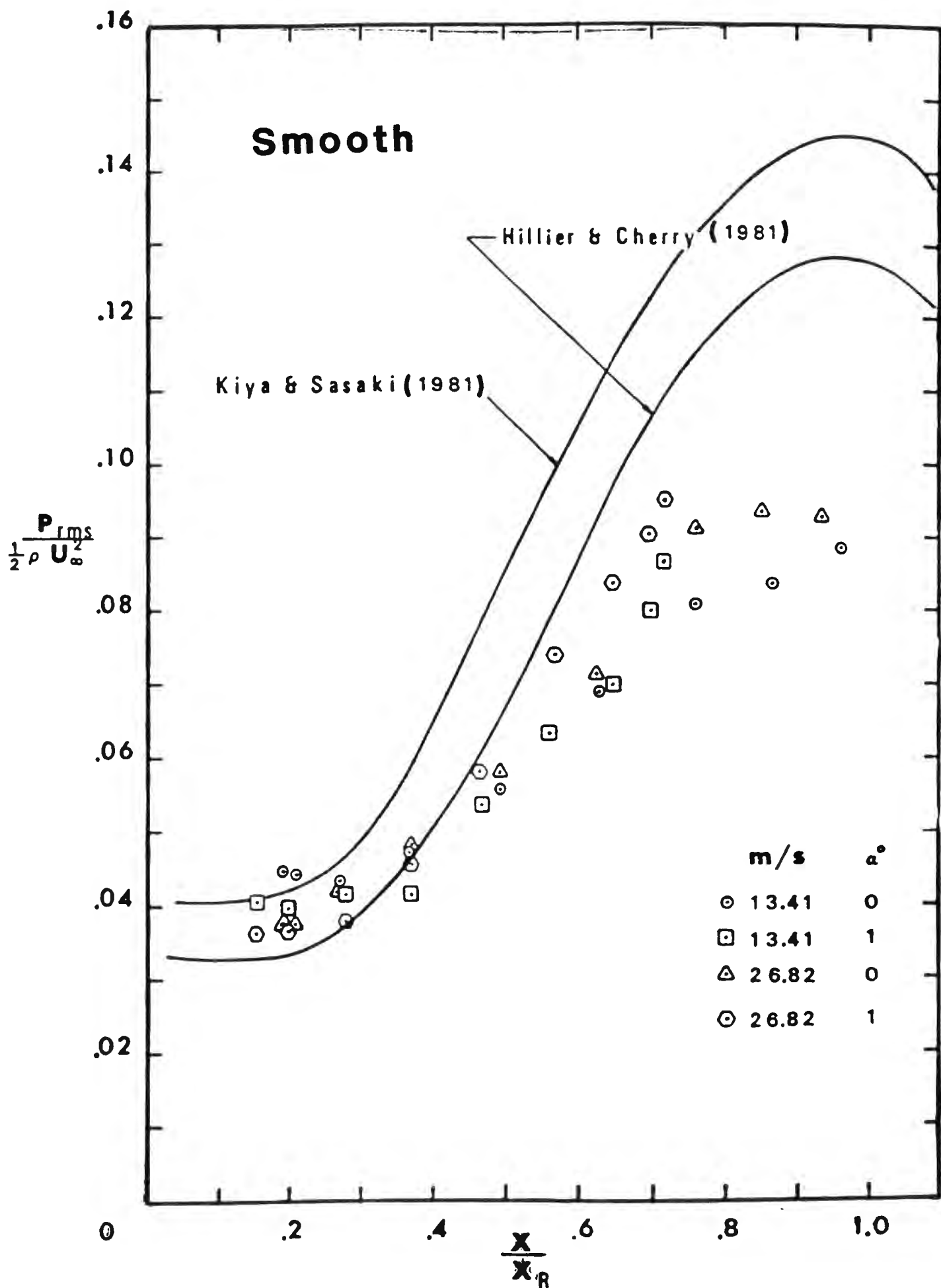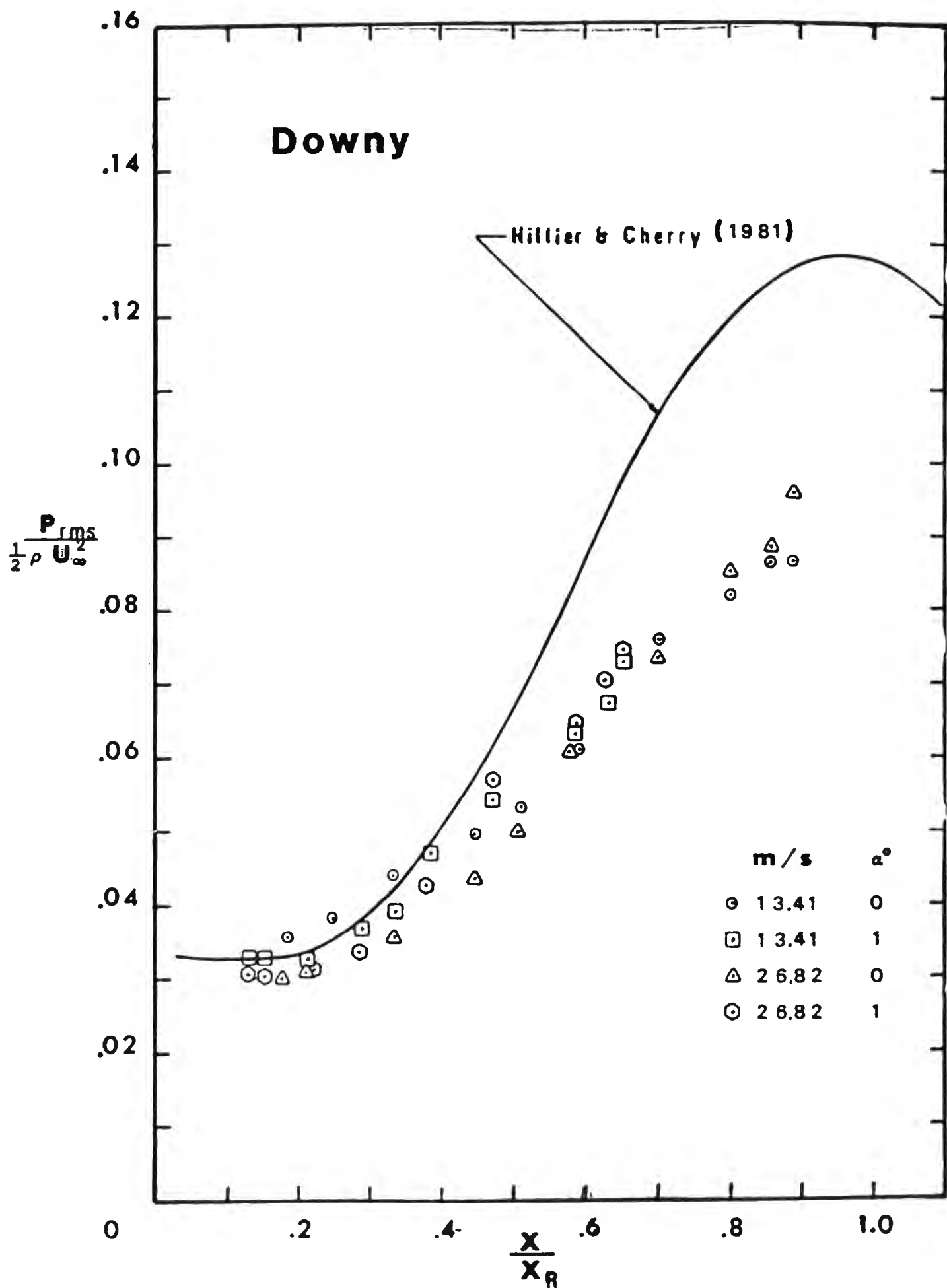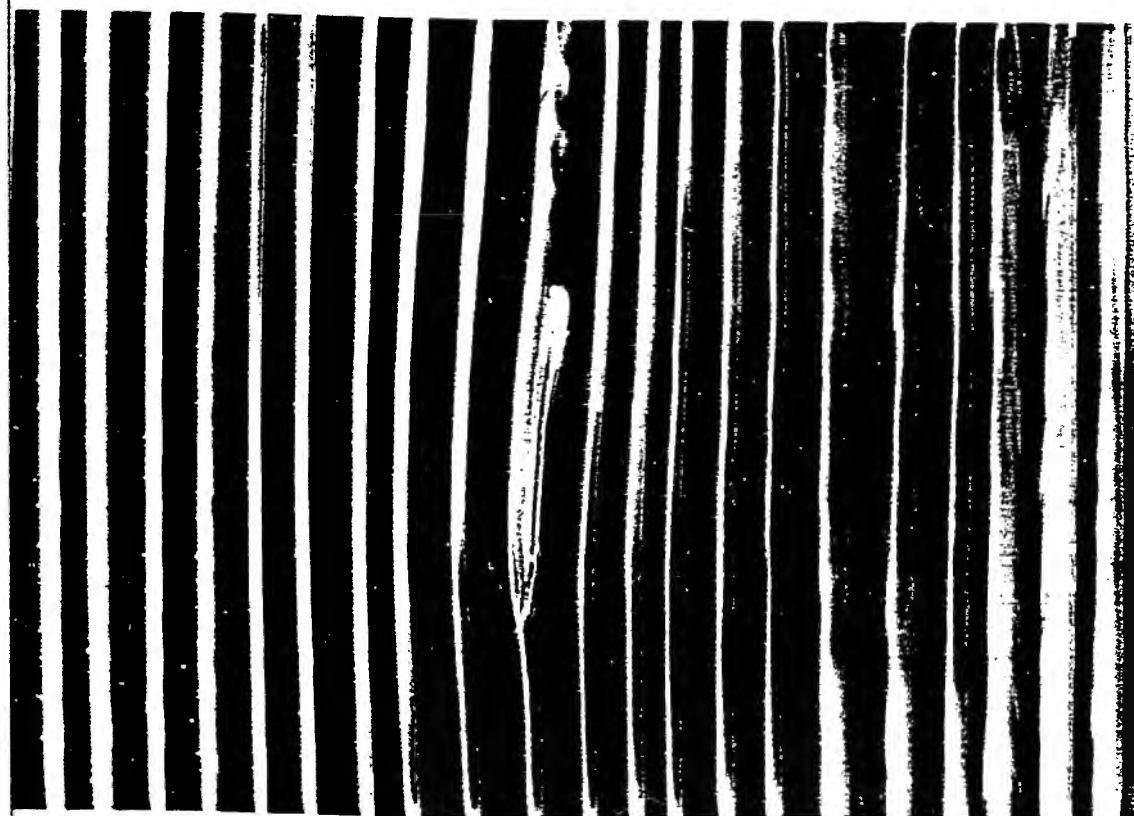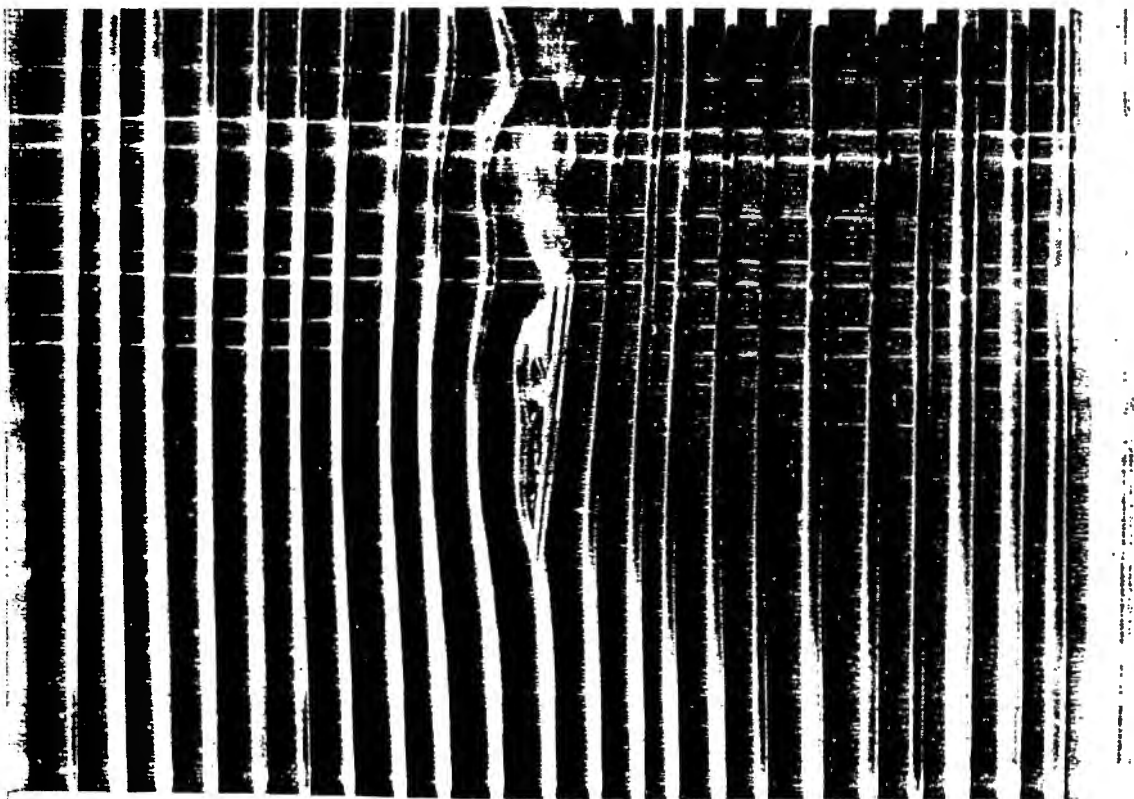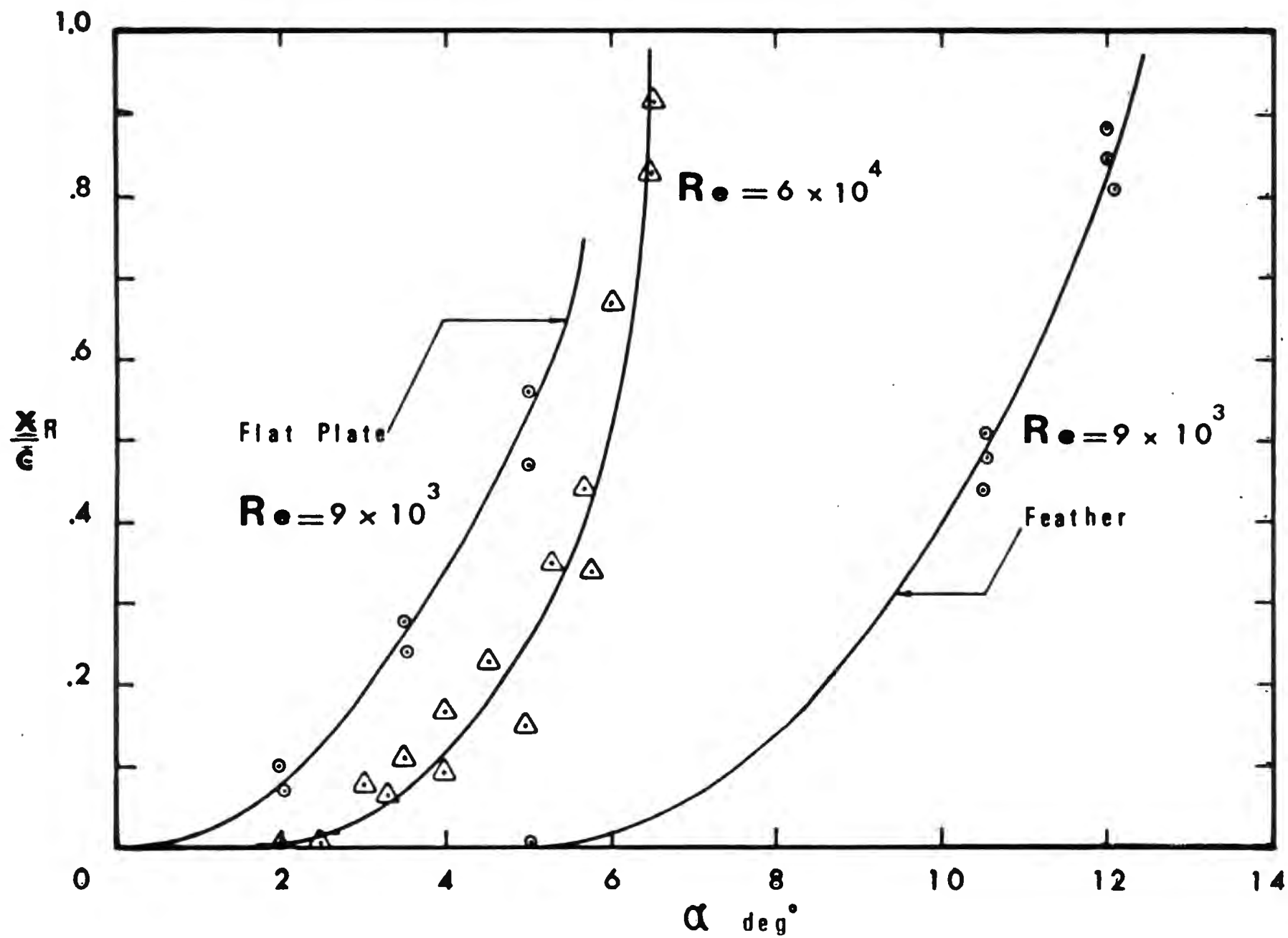
1.2-42

Downy

$F_u(\kappa_1)$

y/δ

KLEBANOFF
——— 0.0011
—·—· .05
– – – .20

experimental
⊙ 0.0010

K_1 cm^{-1}

1.2-43

Smooth

Hillier & Cherry (1981)

Kiya & Sasaki (1981)

$\dfrac{P_{rms}}{\frac{1}{2}\rho\, U_\infty^2}$

	m/s	$a°$
⊙	13.41	0
⊡	13.41	1
△	26.82	0
⊙	26.82	1

$\dfrac{X}{X_R}$

1.2-44

Downy

1.2-45

1.2-46

A pressure instrument to measure skin friction in turbulent boundary layers on smooth and non-smooth walls

P. V. Storm and B.G. Newman
Department of Mechanical Engineering, McGill University
Montreal, Quebec, Canada

3. Measurement of Skin Friction

An instrument consisting of 3 pitot tubes mounted in the wall law region of a turbulent B.L. can be used to obtain the skin friction for both smooth and non smooth walls. It is a sort of extension of Preston's method.

Rotta

$$U_T = \sqrt{\frac{\tau_w}{\rho}} \quad : \quad \frac{y}{U_\tau} \frac{\partial U}{\partial y} = \frac{1}{k}$$

ind. of viscosity and all aspects of the roughness, geometry, size, if not too big.

Number pitots

1-2
$$\frac{y_1 + y_2}{2U_\tau} \left(\frac{U_1 - U_2}{y_1 - y_2} \right) = \frac{1}{k}$$

and 2 - 3
$$y_1 - y_2 = a_{12}, \quad U_1 - U_2 = \frac{2}{\rho(U_1 + U_2)} (P_1 - P_2) = \frac{2}{\rho(U_1 + U_2)} \Delta_{12}$$

$$\frac{1}{U_\tau} = \text{formula in terms of } \Delta_{12}, \ \Delta_{23} \ \& \ a_{23}$$

Checked for smooth walls

and #40 and #24 sandpaper roughness.

Pitots project sufficiently ahead of support, and static tube is mounted to the side. Compared with skin friction measured on a floating element balance

Null - LVDT   linear voltage differential transducer

i.e. variable reluctance transducer

Possible error a_{ij} O.K.   3D analysis using sources | unimportant

Pressure difference Δ_{ij} Low Re Dynamic | 8, 10, 11, 13

Gaussian smoothing Barocel 590   Capacity   type

Fig. 10

$\pm \cdot 1 Pa \ \rightarrow \ < 1 Hz$ sequential readings

Possible use   Hull roughness due to marine growth.

Figure 2: Three Tube Instrument
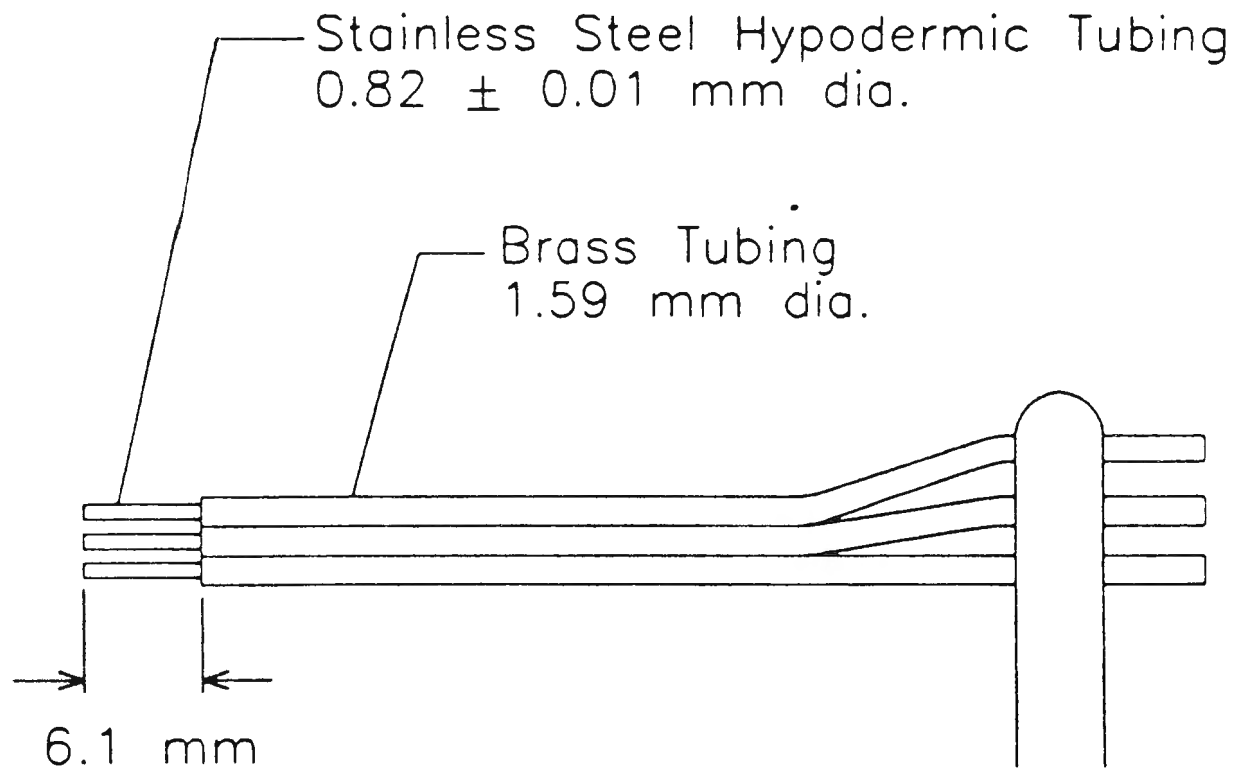
$$a_{12} = 1.57 \pm 0.01 \ mm$$
$$a_{23} = 1.62 \pm 0.01 \ mm$$

following Rotta (1962), if the surface roughness is not too large,

$$\frac{y}{U_\tau}\frac{\partial U}{\partial y} = \frac{1}{\kappa},\qquad(2)$$

where $U_\tau \equiv (\tau_w/\rho)^{\frac{1}{2}}$ is the skin friction velocity and $\kappa \approx 0.41$ is the von Kármán constant. Approximating the velocity gradient at the midpoint between tubes 1 and 2 by a linear interpolation of the velocity,

$$\frac{y_1 + y_2}{2U_\tau}\left(\frac{U_1 - U_2}{y_1 - y_2}\right) = \frac{1}{\kappa}\qquad(3)$$

provided $y_1 - y_2 \ll y_1$. Similarly, for tubes 2 and 3,

$$\frac{y_2 + y_3}{2U_\tau}\left(\frac{U_2 - U_3}{y_2 - y_3}\right) = \frac{1}{\kappa},\qquad(4)$$

provided $y_2 - y_3 \ll y_2$. The origin for the y-coordinate is difficult to establish for a rough surface and therefore y is eliminated by taking the difference of these two equations. This leads to the expression

$$\frac{1}{U_\tau} = \frac{2}{\kappa(a_{12} + a_{23})}\left(\frac{a_{12}}{U_1 - U_2} - \frac{a_{23}}{U_2 - U_3}\right),\qquad(5)$$

where $a_{12} \equiv y_1 - y_2$ and $a_{23} \equiv y_2 - y_3$.

Since pressures rather than velocities are measured, the velocities are expressed as

$$U_2 = \left[\frac{2}{\rho}(P_2 - p)\right]^{1/2}\qquad(6)$$
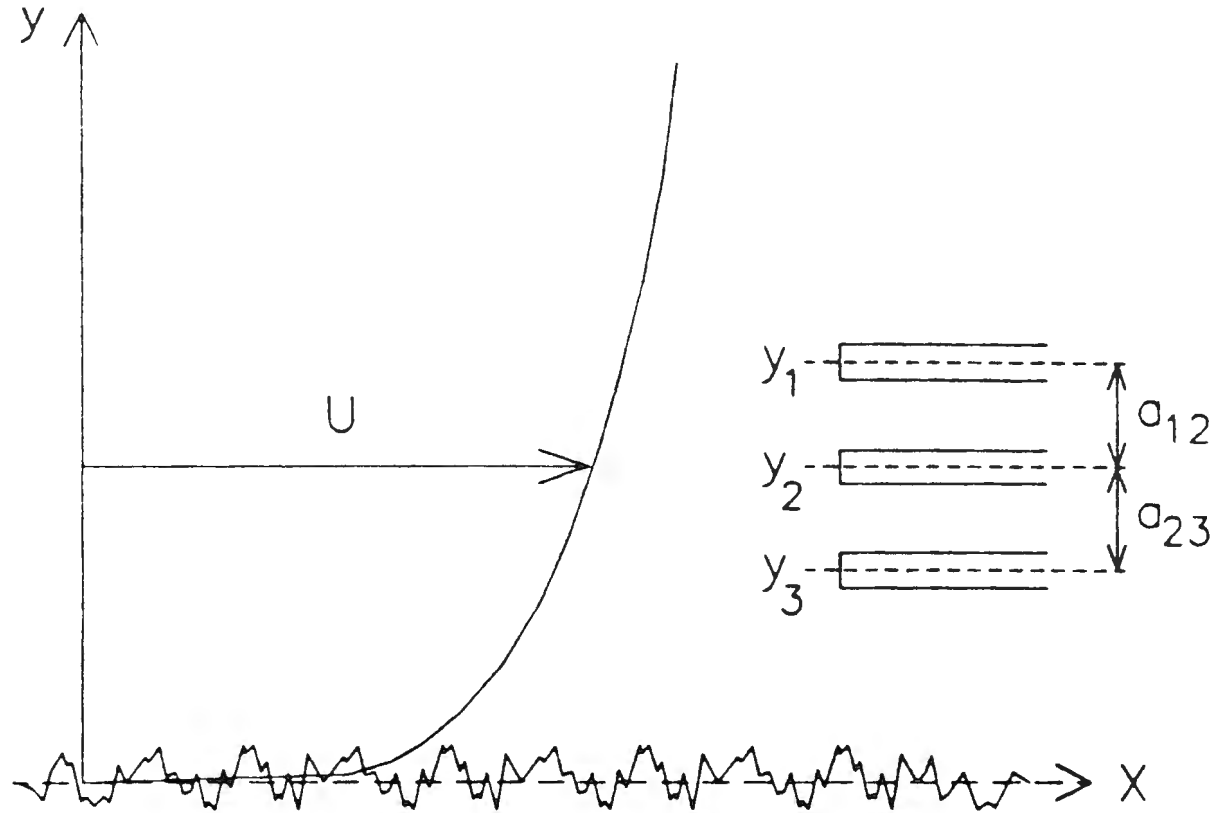
Figure 1: Three Pitot Tubes in the Logarithmic Region

Expanding the velocities to second order in $\Delta_{ij}/(P_2 - p)$ and substituting into Eq. 5 gives

$$\frac{1}{U_\tau} = \frac{[8\rho(P_2 - p)]^{1/2}}{\kappa(a_{12} + a_{23})} \left[\frac{a_{12}}{\Delta_{12}} - \frac{a_{23}}{\Delta_{23}} + \frac{a_{12} + a_{23}}{4(p_2 - p)} \right] \tag{10}$$
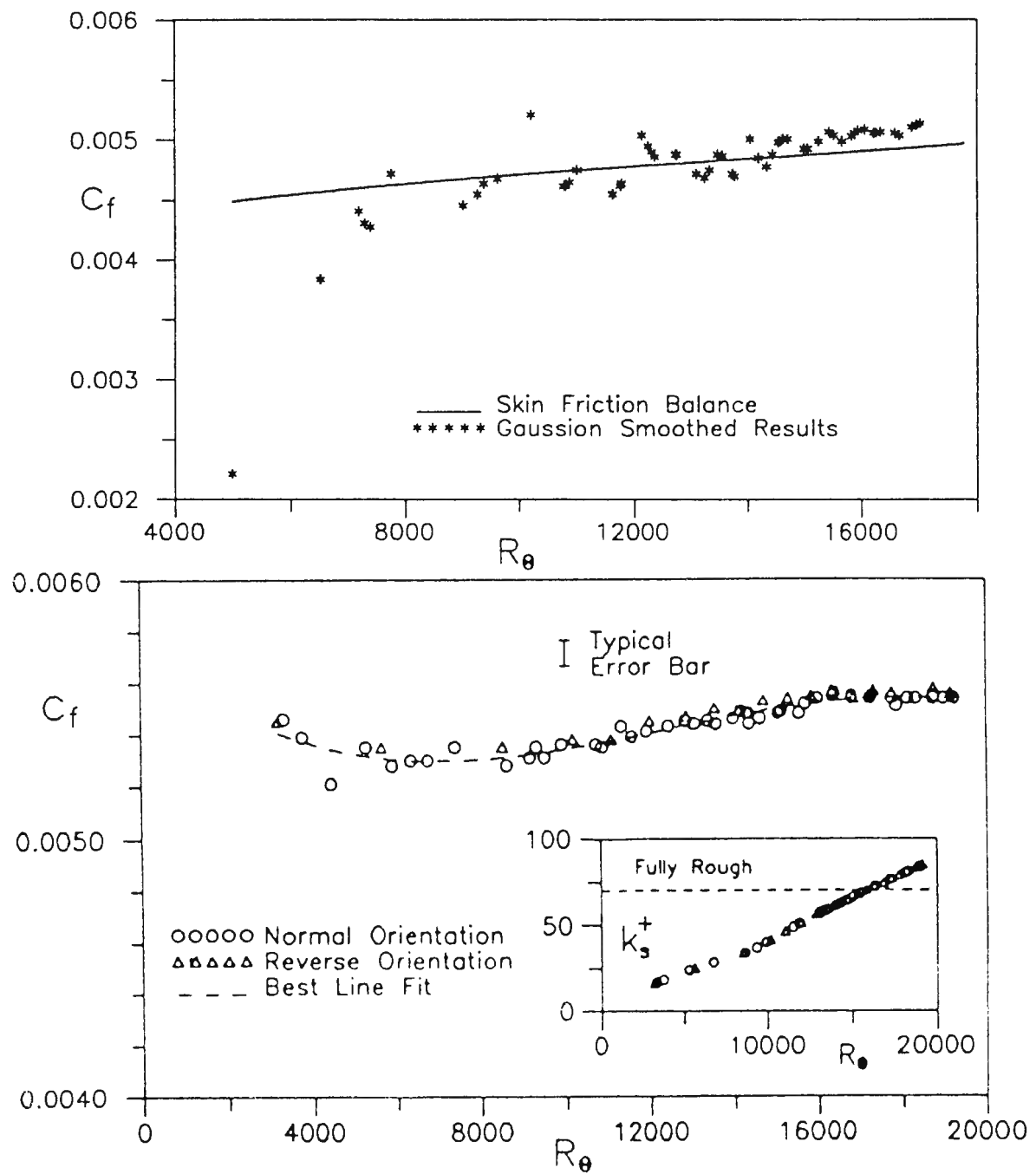
Figure 11: Sandpaper #24 c_f from Skin Friction Balance
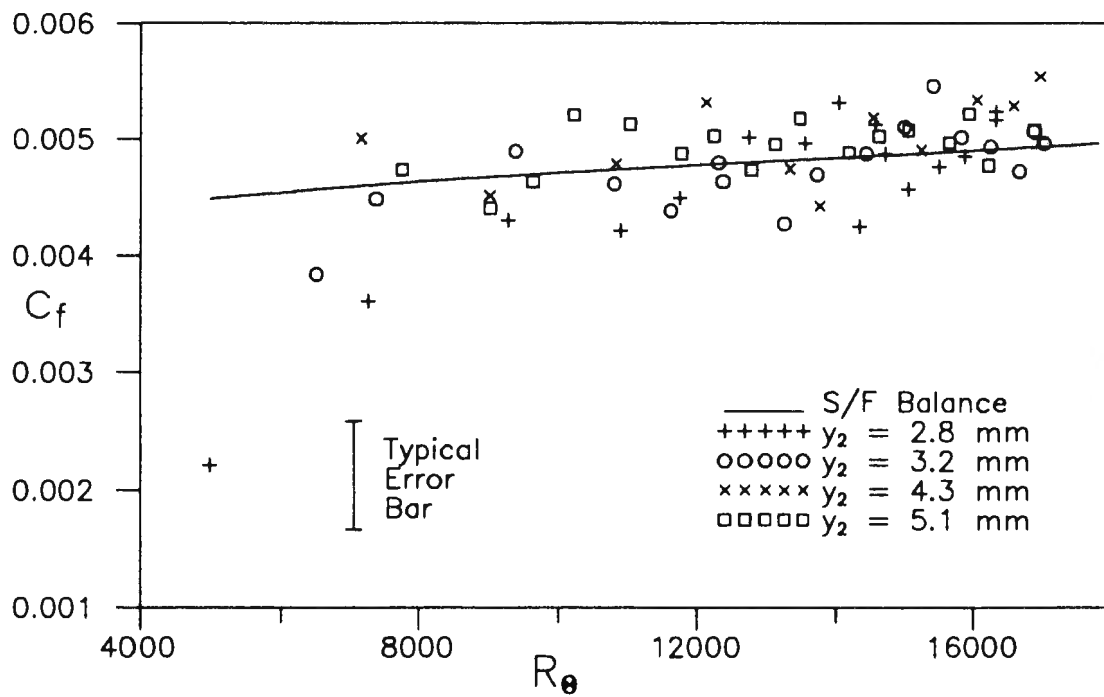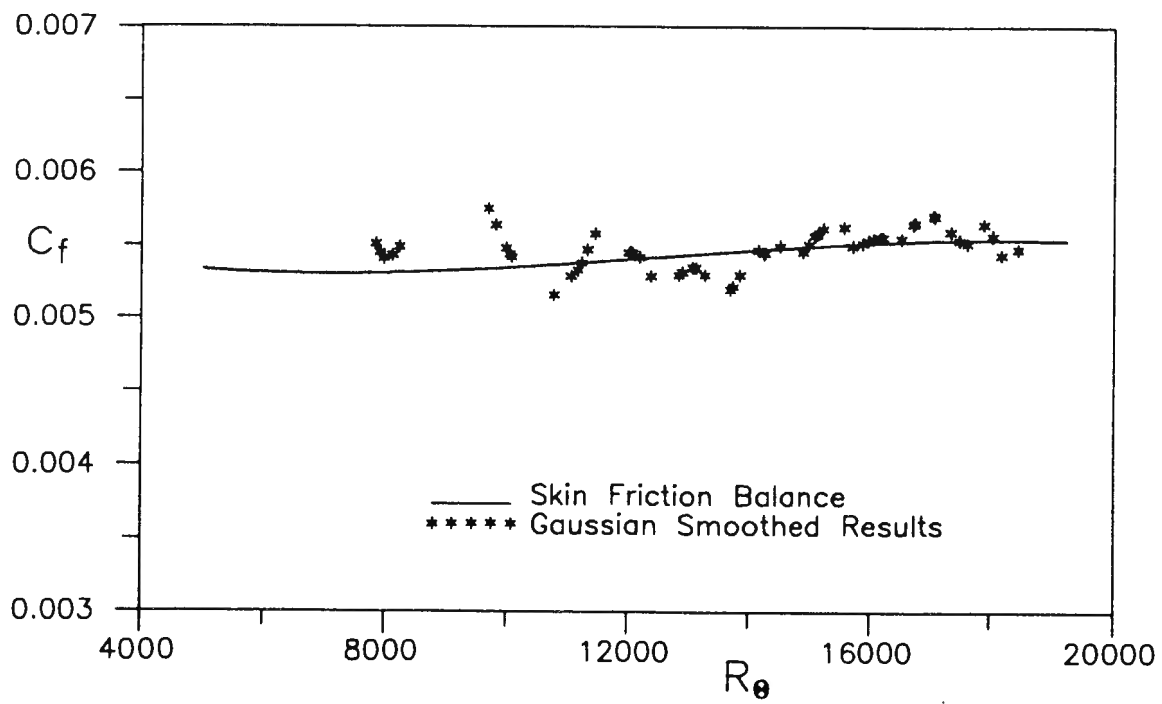
1.3 Aquatic Locomotion

Theodore Y. Wu
California Institute of Technology

BIOHYDRODYNAMICS OF AQUATIC LOCOMOTION

Professor Theodore Y. Wu

CALIFORNIA INSTITUTE OF TECHNOLOGY

Generalized slender-body theory has been fruitfully applied to the bio-hydrodynamical analysis of modes of locomotion of elongated fishes by means of body undulation. Of interest are the highly efficient modes of carangiform (employing movements of only fish's posterior end), thunniform (marked by a lunatail caudal fin), balistiform (propagating distally waves along dorsal and anal fins with body held rigid) and their derivatives. Studies of the vortex dynamics involved in these modes of swimming motion have elucidated the basic mechanism of interaction between the vortex sheets and the body-fin system, pointing out how thrust can be enhanced, loss of hydromechanical energy reduced, and biodynamic efficiency improved. Also discussed will be the problem of energetics of fish swimming from a mechanophysiological approach. From a series of comparative studies of the scale effects of fish locomotion, Gray's paradox appears to be substantially clarified.

Thursday, the 17th March 1994
* * NOTE NEW VENUE: Conference Room, Bldg. 1171 * *
Time: 10:30 AM

POC: Dr. Promode R. Bandyopadhyay (Code: 8233; Bldg. 108/2) NPT x2588

Gray's paradox on fish locomotion:

" Either fish can experience a viscous drag of water an order of magnitude smaller than the drag acting on their artificial smooth model or they can deliver muscular power in sustained swimming an order of magnitude greater than that delivered by the same mass of muscle of warm-blooded animals working at the same level of activity. "

The kingdom of aquatic animal.

mass $\qquad 10^{-10} \, gm < m < 10^{8} \, gm.$

Reynolds no. $\qquad 10^{-6} < Re < 10^{8}$

Dolphin
(Coryphaena hippurus)

Grey mullet
(Mugil cephalus)
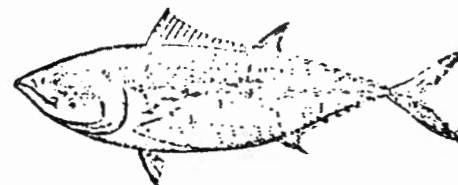
Bluefin tuna
(Thunnus thynnus)

Yellowtail
(Seriola quinqueradiata)

Barracuda
(Sphyraena pinguis)
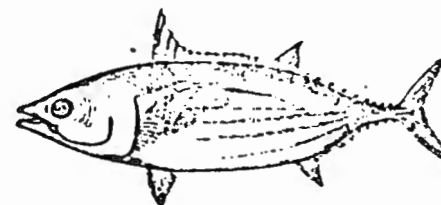
Skipjack
(Katsuwonus pelamis)
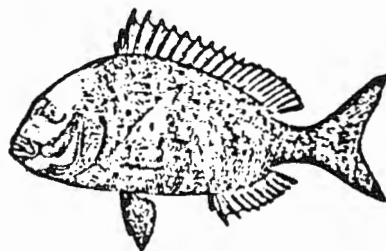
Porgy
(Pagrus major)
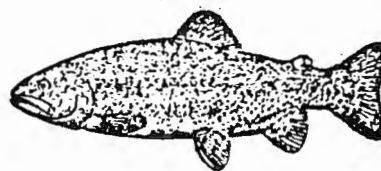
Rainbow trout
(Salmo gairdneri irideus)

Spanish mackerel
(Scomberomorus niphonius)

Atka mackerel
(Pleurogrammus asemo)
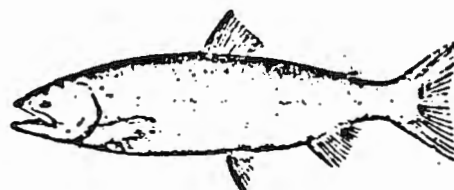
Sockeye salmon
(Oncorhynchus nerka)

Pacific saury
(Cololabis saira)
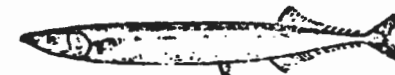
Swimming at constant velocity

momentum consideration

$$T = D$$

mean thrust   averaged drag
                     — shear friction.

                     { form drag, induced drag, wave drag,
                           all negligible }

for carangiform
    lunate-tail (thunniform) locomotion

linear theory for incompressible, inviscid flow
        of carangiform swimming.

$\Rightarrow$ hydromechanical evaluation of T.

(independent hydromechanical calculation of D ?)

Swimming of fish at various levels of activity.

Energy consideration.

$$DU = P - \dot{E}_w = \eta P$$

useful work/t Power input   energy wasted/t efficiency.

$$DU = \eta_h P_h$$

hydromechanical efficiency   hydrodyn. power

$$= \eta_h \eta_m P_m$$

biochemical efficiency   biochemical (metabolic) power.

(bio-energy → muscle power)

Hydromechanics of fish swimming

Gray, J.   1968   Animal locomotion   London: Weindenfeld.

Lighthill, M. J.   1960   J. Fluid Mech. 9,   305-317

Lighthill, M. J.   1970   JFM 44, 265
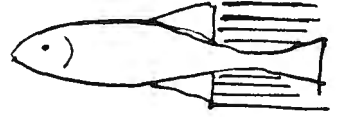
Wu, T. Y.   1961   JFM. 10, 321-344.

Wu, T. Y.   1971 a   JFM   46   545

1971 b   JFM   46   521

1971 c   JFM   46   545
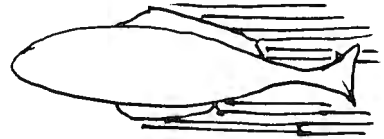
Newman, J. N. & Wu, T. Y.   1973   JFM 57, 673

Wu, T. Y. & Newman   1972   Proc. Symp. on Directional stability.   London: Inst. Mech. Engineers.
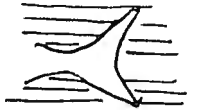
1974
Newman, J. N. & Wu, T. Y.   In " Swimming and Flying in Nat (ed. T.Y. Wu, C. J. Browkaw, C. Brennen)   Plenum Press

Wu, T. Y.   1975   Scaling of aquatic animal locomotion. In "Scaling of Animal Locomotion" (ed. T. Pedley) Acad. Pr

Wu, T. Y. & Yates, G. T.   1976   Proc. 11th ONR Symp. on Naval Hydrody.   London 517-528. Nat. Acad. Sci.
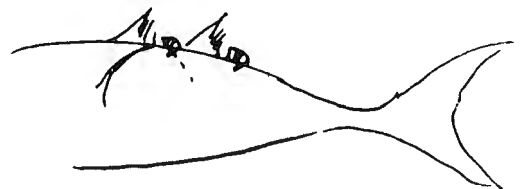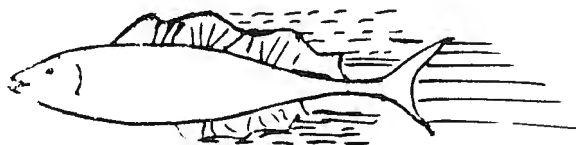
(thunniform, amiiform)

Lateral differential lift
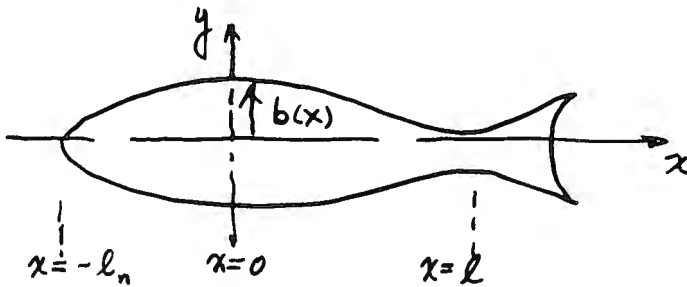
$$w(x,t) = \left(\frac{\partial}{\partial t} + U\frac{\partial}{\partial x}\right)h(x,t)$$
$$\equiv Dh \equiv V(x,t)$$
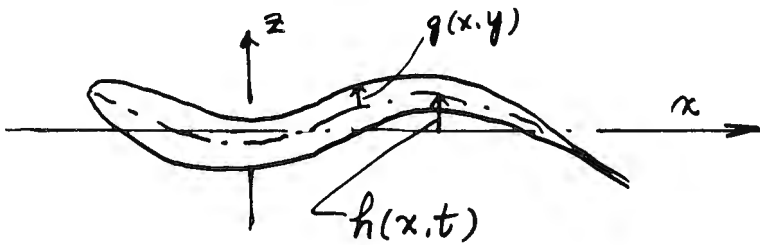
$$\mathcal{L}(x,t) = -D\left[m(x)\,V(x,t)\right]$$

(Lighthill 1960)

$m(x)$ — added mass/length
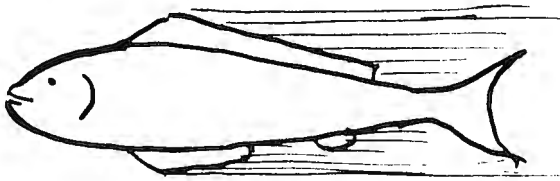
$$\mathcal{L}(x,t) = -m(x)\,D\,V(x,t)$$

(Wu, 1971) $(0<x<$
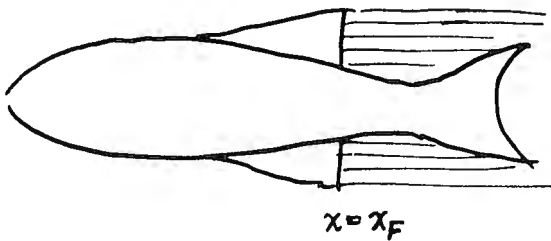
$$\mathcal{L}(x,t) = -D\left[m(x)\,V(x,t)\right]$$
$$-D\left[\tilde{m}(x)\,w(x_F,\tau_F)\right]$$

$$\tau_F = t + (x_F - x)/U$$

$(x_F < x < \ell)$

(Lighthill 1970)

Hydromechanics of fish swimming. (Wu, 1983)

Body geometry: slender. $\delta = max\ width/length = b_0/\ell_0 \ll 1$.

Renolds number

$$Re = \frac{U\ell_0}{\nu} \gg 1, \quad 10^3 - 10^9.$$

Flow model:

incompressible, and irrotational, inviscid,
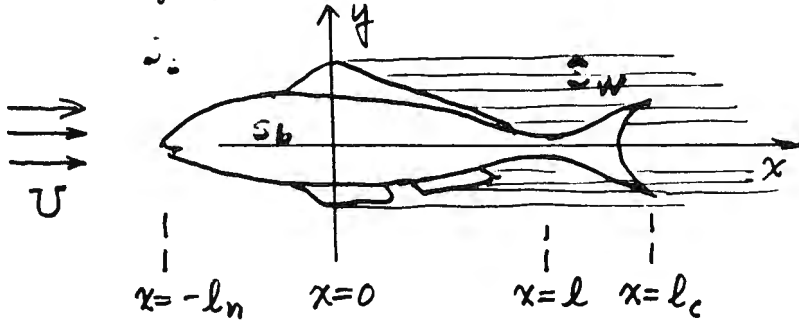
velocity $\quad \underset{\sim}{u} = (u, v, w) = \nabla\phi$

$\quad\quad\quad \nabla \cdot \underset{\sim}{u} = 0$ $\quad\Big\} \rightarrow \quad \nabla^2\phi = 0.$

Body lateral motion:

$$y = h(x,t) = h_0(x,t) \quad\quad\quad (S_b)$$
$$= h_0(x,t) + h_1(y;x,t) \quad\quad (S_f)$$

Planform regions $\quad\quad S_b$ – body, $\quad S_f$ – vortex shedding fin,

(on $z=0$) $\quad\quad\quad S_w$ – vortex wake, $\quad S_c$ – complementary.

with x scaled by ℓ_0, (y,z) by b_0,

$$\phi = U x + \phi_0(\underset{\sim}{z}) + \phi_1(\underset{\sim}{z}, t)$$

$$\quad\quad\quad\quad\quad O(\delta^2 \ln\delta) \quad O(h\delta, h^2).$$

cross-flow:

$$\frac{\partial^2\phi}{\partial y^2} + \frac{\partial^2\phi}{\partial z^2} = 0 \quad\quad (error: \ O(\delta^2\ln\delta))$$

Vortex-sheet crossing — Jean-Luc Cornet.

Cross flow

$$\zeta = y + iz, \qquad \text{complex physical plane}$$

$$f = \phi + i\psi, \qquad \text{complex velocity potential}$$

$$F = \Phi + i\Psi \qquad \text{complex acceleration potential} \quad \left(\Phi = \frac{p_\infty - i}{\rho}\right)$$

$$\vartheta = v - iw = \frac{df}{d\zeta} \qquad \text{complex velocity}.$$

Linear theory:

$$Df = F \qquad \left(D \equiv \frac{\partial}{\partial t} + U\frac{\partial}{\partial x}\right)$$

$$D\vartheta = \frac{dF}{d\zeta}$$

Boundary condition

for $f = \phi + i\psi$,	for $F = \Phi + i\Psi$,	
(i) $\underline{\phi_z^\pm} = w^\pm = Dh = \underline{V(y; x,t)}$,	(i) $\underline{\Phi_z^\pm} = D\underline{\underline{V(y; x,t)}}$	(S_b)
(ii) $D\phi^\pm = 0$,	(ii) $\Phi^\pm = 0$	(S_w)
(iii) $\phi^\pm = 0$,	(iii) $\Phi^\pm = 0$,	(S_c)
(iv) $D\phi^\pm = 0$,	(iv) $\Phi^\pm = 0$,	$(T.E.)$

$$\text{(v)} \qquad f \approx O(1/\zeta), \quad F = O\left(\tfrac{1}{\zeta}\right), \quad \vartheta = O\left(\tfrac{1}{\zeta^2}\right) \qquad \text{as } |\zeta| \rightarrow \infty.$$

$\phi = 0 \qquad (S_c)$

$D\phi = 0$

$\phi_z = V = Dh$

(S_b)

(S_w)

L

L

z

$V^\pm = \operatorname{Re}\left(\dfrac{df}{d\zeta}\right)^\pm = 0$

$V^\pm = 0$

$-b(x)$

$b(x)$

y

$w^\pm = -\operatorname{Im}\left(\dfrac{df}{d\zeta}\right)^\pm = V$

SECTION L–L $(-\ell_n < x < 0)$

$\Phi = 0 \qquad (S_c)$

$\Phi = 0$

T

$\Phi_z = DV$

(S_b)

(S_w)

T

z

$\operatorname{Re}\left(\dfrac{dF}{d\zeta}\right)^\pm = 0$

$\operatorname{Re}\left(\dfrac{dF}{d\zeta}\right)^\pm = 0$

$-b_o$

$-b(x)$

$b(x)$

b_o

y

$-\operatorname{Im}\left(\dfrac{dF}{d\zeta}\right)^\pm = DV$
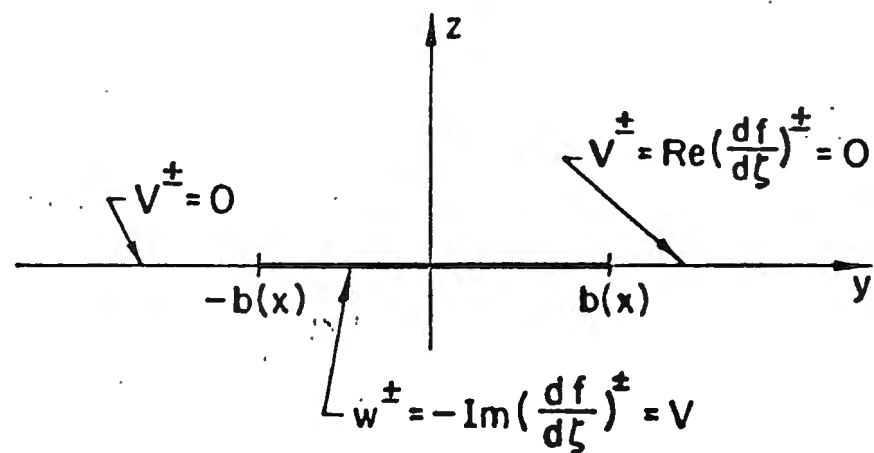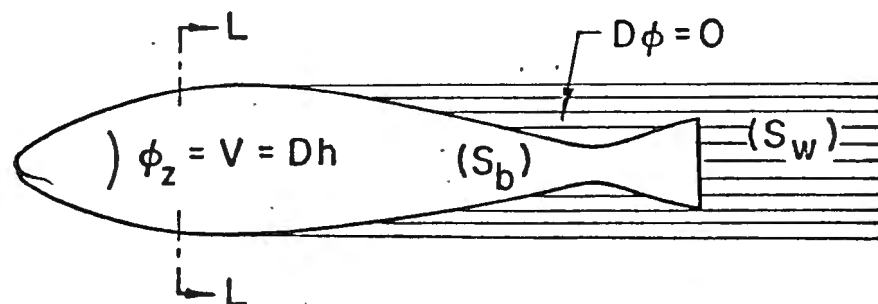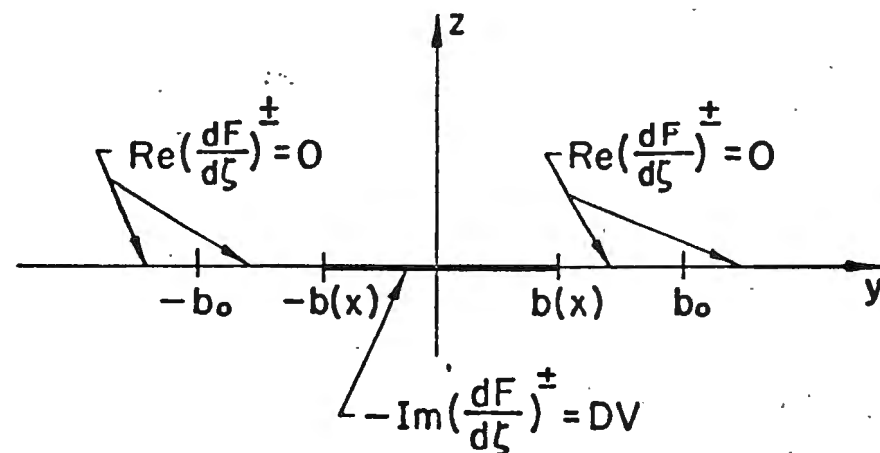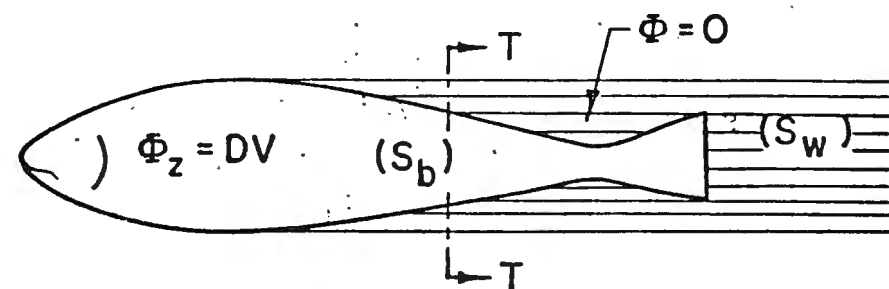
SECTION T–T $(0 < x < \ell)$

Solution

Plemelj's formula:

$$G(\zeta) = \frac{1}{2\pi i} \int_L \frac{G^+(\zeta_1) - G^-(\zeta_1)}{\zeta_1 - \zeta} d\zeta_1.$$

(I) Leading section $x_\ell < x < x_0.$ $(x_\ell < x < x_0)$

$$\frac{df}{d\zeta} = \nu = v - iw = \frac{-1}{\pi} \int_{-b}^{b} \frac{H^+(y_1; b)}{H(\zeta; b)} \frac{V(y_1; x, t)}{y_1 - \zeta} dy_1.$$

$$H(\zeta; b) = \sqrt{\zeta^2 - b^2}, \qquad H^{\pm}(y_1; b) = \pm i \sqrt{b^2 - y_1^2} \qquad (|y_1| < b)$$

(II) Trailing side-edge section $(0 < x < \ell.)$

We take $G(\zeta) = dF/d\zeta$ for this section

$$\frac{dF}{d\zeta} = -\frac{1}{\pi} \int_{-b}^{b} \frac{H^+(y_1, b)}{H(\zeta; b)} \frac{DV(y_1; x, t)}{y_1 - \zeta} dy_1.$$

$$F(\zeta; x, t) = -\frac{1}{\pi} \int_{-\infty}^{\zeta} \frac{d\zeta}{H(\zeta; b)} \int_{-b}^{b} \frac{H^+(y_1; b)}{y_1 - \zeta} DV(y_1; x, t) dy_1.$$

from $D\nu = \nu_t + U\nu_x = dF/d\zeta$, we obtain $\bar{\nu}^{\pm}(y; x, t)$

and the entire vortex system.

<u>III</u>. The caudal fin section. $(x_1 < x < x_L)$

$$w^{\pm} = {}_{,} w_c^{\pm} + {}_{,,} w_v^{\pm} \qquad (x,y, \text{ on } S_{c.f.} \text{ (fin)})$$

$$w_v^{\pm} = V_w (y; \ell. :_\ell) \qquad (|y| < b(x), \quad x > x_1)$$

$$\tau_\ell = t + (\ell - x)/U .$$

V_w — value of w given by trailing-edge section solutio

$$v_c(\zeta; x,t) = -\frac{1}{\pi} \int_{-b}^{b} \frac{H^+(y_1; b)}{H(\zeta; b)} \frac{V(y_1; x,t) - V_w(y; \ell, \tau_\ell)}{y_1 - \zeta} dy_1 .$$

Solution by complex function method.

Plemelj's formula:
$$G(\zeta) = \frac{1}{2\pi i} \int_L \frac{G^+(\zeta_1) - G^-(\zeta_1)}{\zeta_1 - \zeta} d\zeta_1.$$
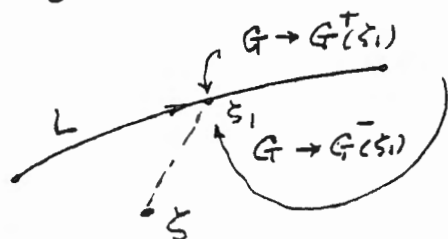
$$\text{Let} \quad G(\zeta) = \frac{1}{2\pi i} \int_L \frac{g(\zeta_1)}{\zeta_1 - \zeta} d\zeta_1$$

The left-side limit of $G(\zeta) \rightarrow G^+(\zeta_0)$,
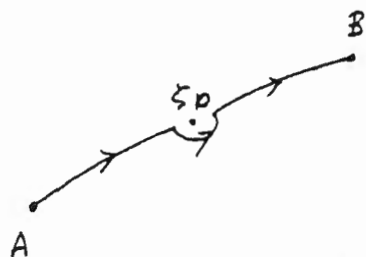
$$G^+(\zeta_0) = \frac{1}{2} g(\zeta_0) + \frac{1}{2\pi i} \oint \frac{g(\zeta_1)}{\zeta_1 - \zeta_0} d\zeta_1.$$

$$\zeta \rightarrow \zeta_0, \qquad G(\zeta) \rightarrow G^-(\zeta_0)$$

$$G^-(\zeta_0) = -\frac{1}{2} g(\zeta_0) + \frac{1}{2\pi i} \oint \frac{g(\zeta_1)}{\zeta_1 - \zeta_0} d\zeta_1.$$

$$\therefore \quad g(\zeta_0) = G^+(\zeta_0) - G^-(\zeta_0)$$
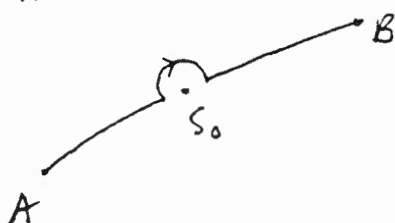
$$G^+(\zeta_0) + G^-(\zeta_0) = \frac{1}{\pi i} \oint \frac{g(\zeta_1)}{\zeta_1 - \zeta} d\zeta_1.$$

Hence the formula.

Metabolic rate depends on factors:

(1) level of activity ; (2) water temperature (disolved O_2)

(3) misc. preconditions (fasting); maturity; ~~sex~~, etc. gender.

Level of activity $\quad$ (~ the salmon & rainbow trout, Brett[1964-6.]

- sustained $\quad$ (can be maintained indefinitely)

- prolonged $\quad$ (laboring for 1-2 hr to fatigue)

- burst $\quad$ (possible to last only ~ 30 s.)

$\eta_c \propto \omega \propto V$;

metabolic power $\qquad P_m = P_0 + \alpha V^2 \qquad$ (P_0 - basal metabolic)

specific energy cost $\qquad \mathcal{E} = P_m / mg V = \frac{1}{mg}(P_0/V + \alpha V)$

$\Downarrow$

$\mathcal{E}$ reaches a min $\mathcal{E}_m$
at $V = \sqrt{P_0/\alpha}$.

Scaling of metabolic rate

$$P_m = a\, m^b.$$

$$\log P_m = \log a + b \log m.$$
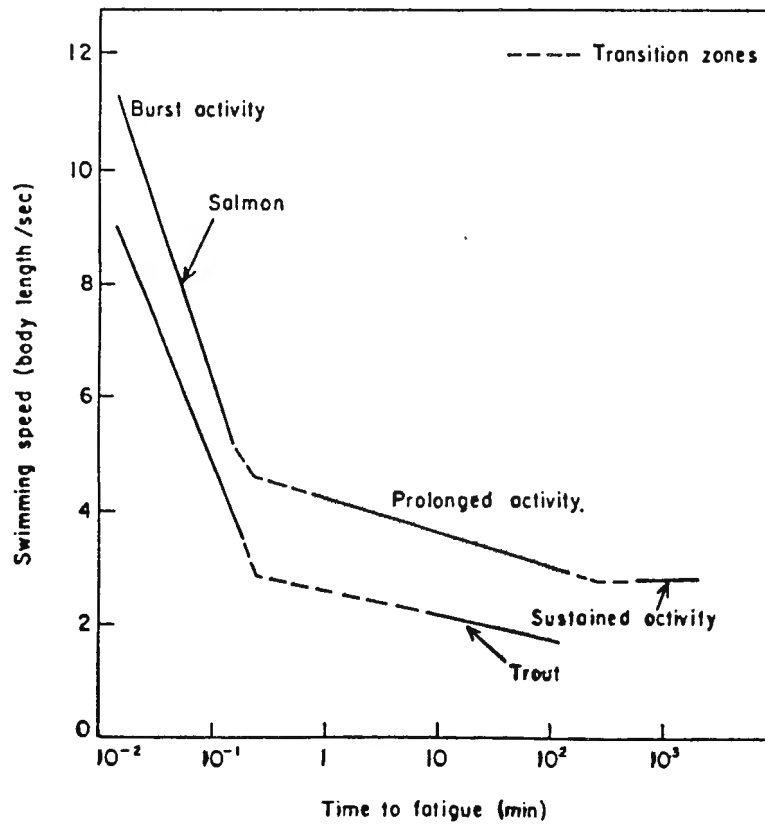
FIG. 7. Swimming endurance of sockeye salmon and rainbow trout. Transition zones between different levels of activity are shown with broken lines. (After Brett[19, 23]).
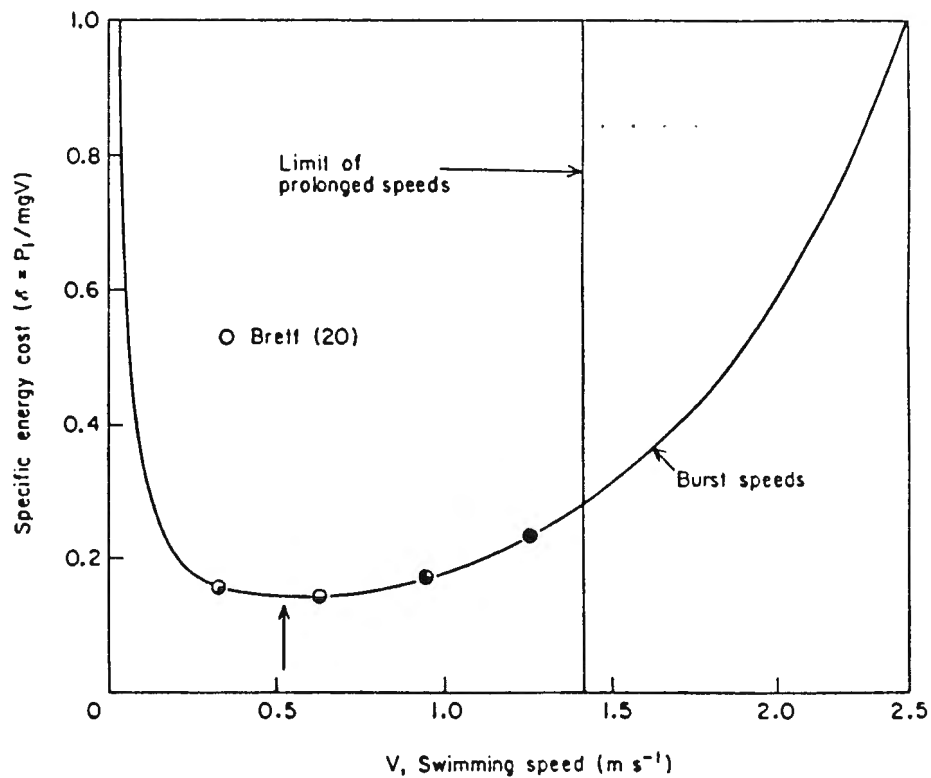
FIG. 8. Specific energy cost $\mathcal{E}$ as related to swimming speed, for adult sockeye salmon. Ocean migration occurs slightly above the speed at minimum $\mathcal{E}$ (shown with an arrow), which is about $\frac{1}{2}V_{crit}$(○), while river migration takes place nearly at V_{crit}(●). For the definition of V_{crit} see text and the caption to Fig. 9. (Adapted from Brett[21, 23]).
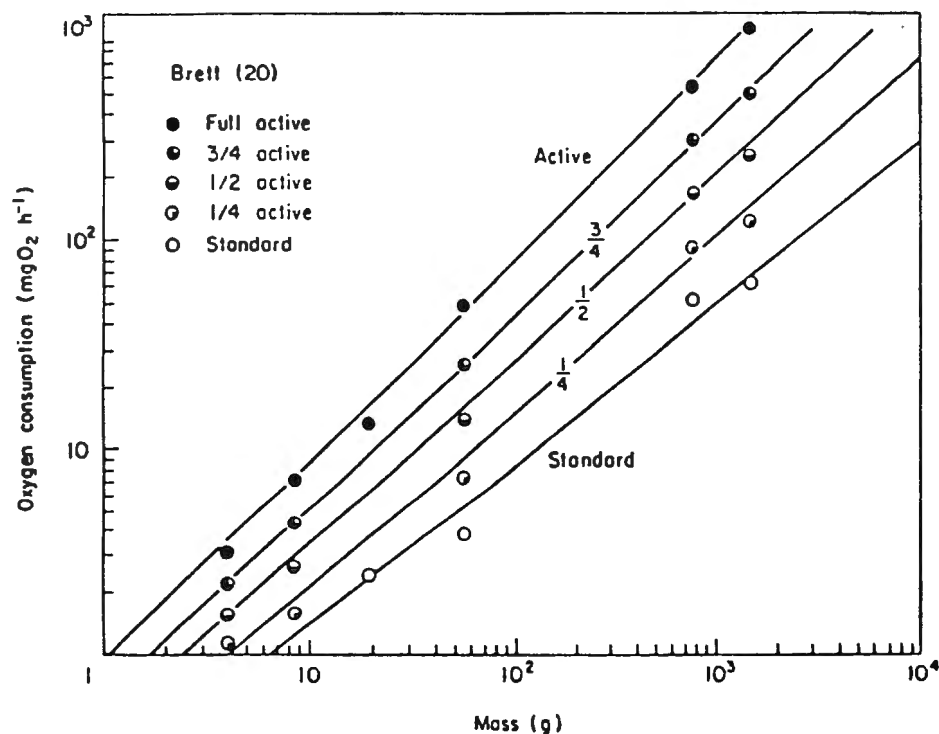
FIG. 9. Metabolic rate of sockeye salmon (*Oncorhunchus nerka*) as a function of body mass at various levels of swimming activity (15°C). The standard level was determined by extrapolation to zero swimming speed of the oxygen consumption vs. speed relation. The line at full activity corresponds to the maximum speed which could be sustained for 60 min, V_{crit}. Intermediate fraction levels correspond to swimming speeds equal to $\frac{3}{4}$, $\frac{1}{2}$, and $\frac{1}{4}$ of V_{crit} respectively.
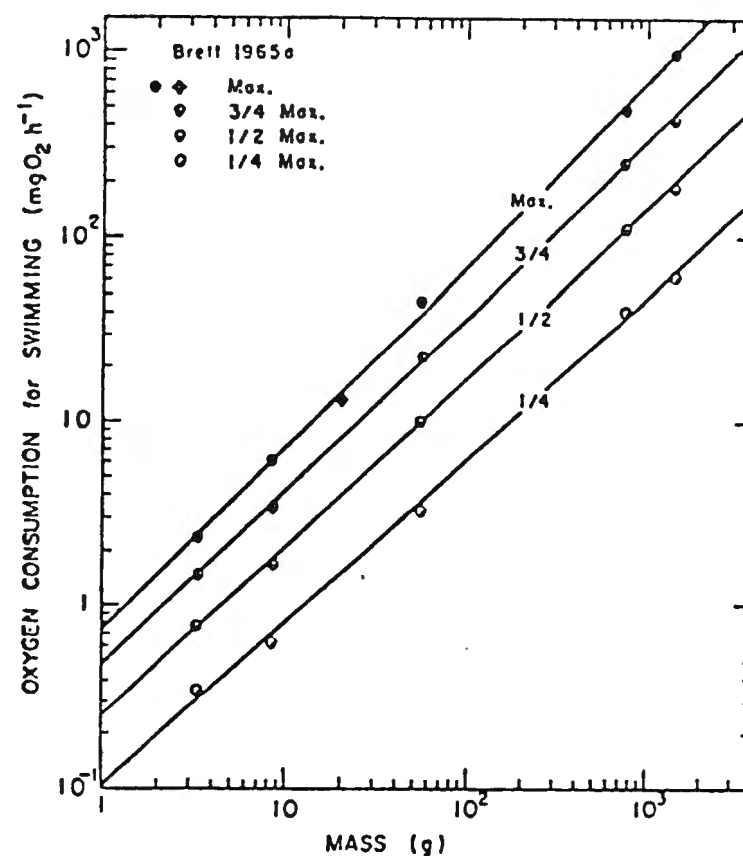
FIG. 3. The "metabolic rate for swimming," based on measured oxygen consumption less the basal rate, of sockeye salmon (Oncorhynchus nerka) as a function of body mass at various levels of activity (15°C); data adapted from Brett (1965a).

Wu, T. Y. of Yates G. (1976-)

Scaling of swimming velocity

$$D = \frac{1}{2} \rho V^2 S \, C_D$$

$$DV = \eta P = a \eta \, m^b = a \eta \, \ell^{3b}$$

$$\Big\} \rightarrow \quad V^3 \propto \ell^{3b-2} / C_D.$$

$$C_D \propto Re^{-1/2} \qquad (laminar \; flow)$$

$$\propto Re^{-1/5} \qquad (turbulent \; flow)$$

$$= const. \qquad (wake \; with \; flow \; separation)$$

$$\Downarrow$$

velocity scaling :

$$\boxed{V = const. \; \ell^{\beta}}$$

$$\beta = \frac{3}{5} (2b-1) \qquad (laminar)$$

$$= \frac{3}{14} (5b-3) \qquad (turbulent)$$

$$= b - \frac{2}{3} \qquad (C_D = const)$$

Specific energy cost :

$$\underline{\mathcal{E} = \frac{P_m}{mgV}} = \underline{const \; m^{-\gamma}}$$

$$\underline{\gamma = 1 - b + \beta/3 .}$$
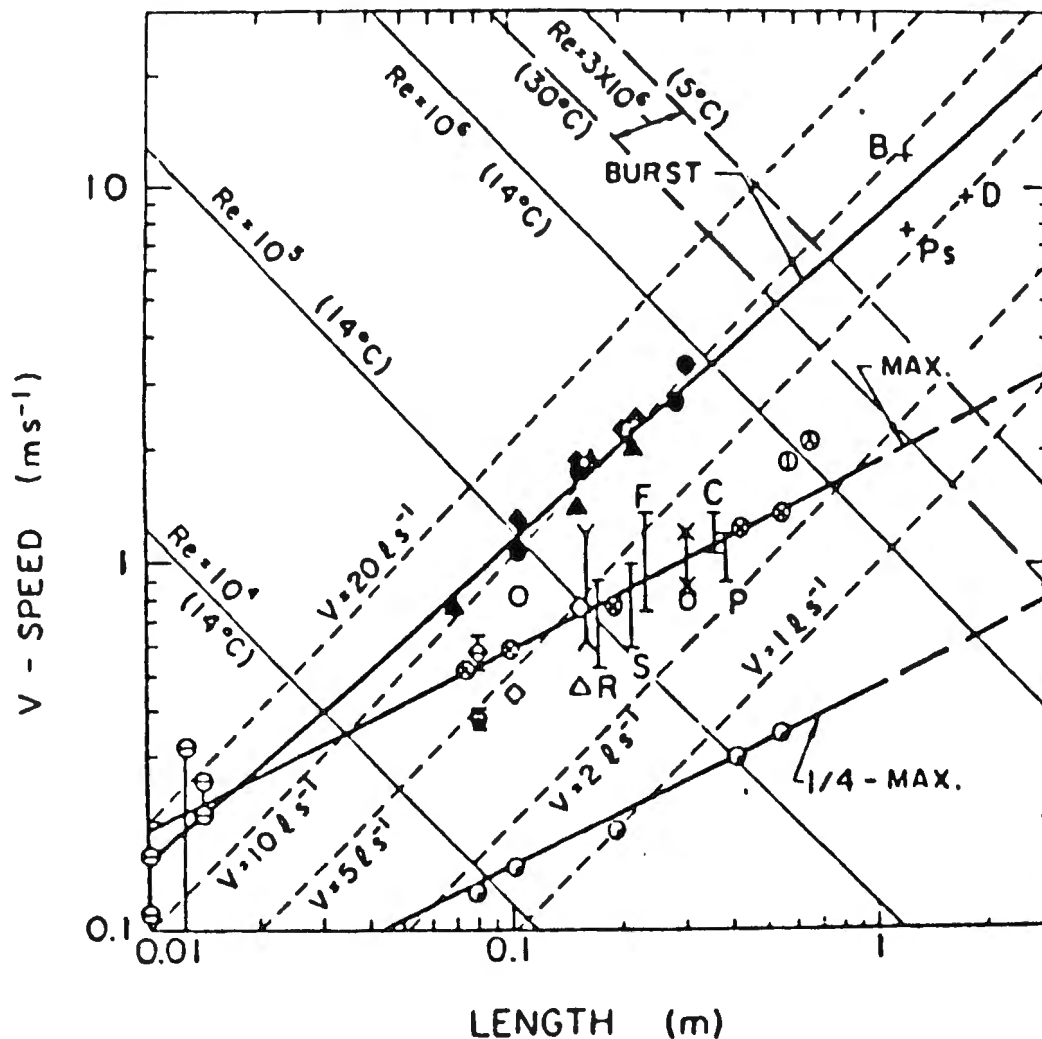
FIG. Variation of swimming speed with body length at specific levels of activity. Burst speed data: ◆ dace, ▲ goldfish, ● trout, B+ barracuda, P_s+ porpoise, D+ dolphin (Bainbridge, 1961). Full activity data: open symbols (Bainbridge, 1961); ⊗ sockeye salmon (15°C) (Brett, 1965a); ⊖ bass, ⊕ coho salmon (Dahlberg et al., 1968); ⊢——⊣, C cod, R redfish, F winter flounder, S sculpin, P pout (Beamish, 1966); ⊱——< goldfish (Smit et al., 1971); ⊖ larval anchovy (Hunter, 1972); ×——× herring (Jones, 1963); ① salmon, ② trout (Paulick and DeLacy, 1957). 1/4 - max data: ⊙ sockeye salmon at 15°C (Brett, 1965a). The lines of constant Reynolds number, Re, and lines of constant specific speed (in $l\ s^{-1}$) are indicated for reference.

Figure 4

$\sigma = \dfrac{\omega \ell}{U}$

1.3-22

$Re = \dfrac{U \ell}{\nu}$

▽ Mackerel (6.4 cm)	Hunter & Zweifel	× Goldfish
▲ Mackerel	1971	⊗ Trout
◆ Bluefish		▼ Dace
◇ Bonito (16 cm)	Pyatetskiy 1970	
○ Mullet (30 cm)		■ Trout
● Bonito	Magnuson & Prescott 1966	□ Trout (28 cm)

Bainbridge 1958

Webb 1973
Webb 1971
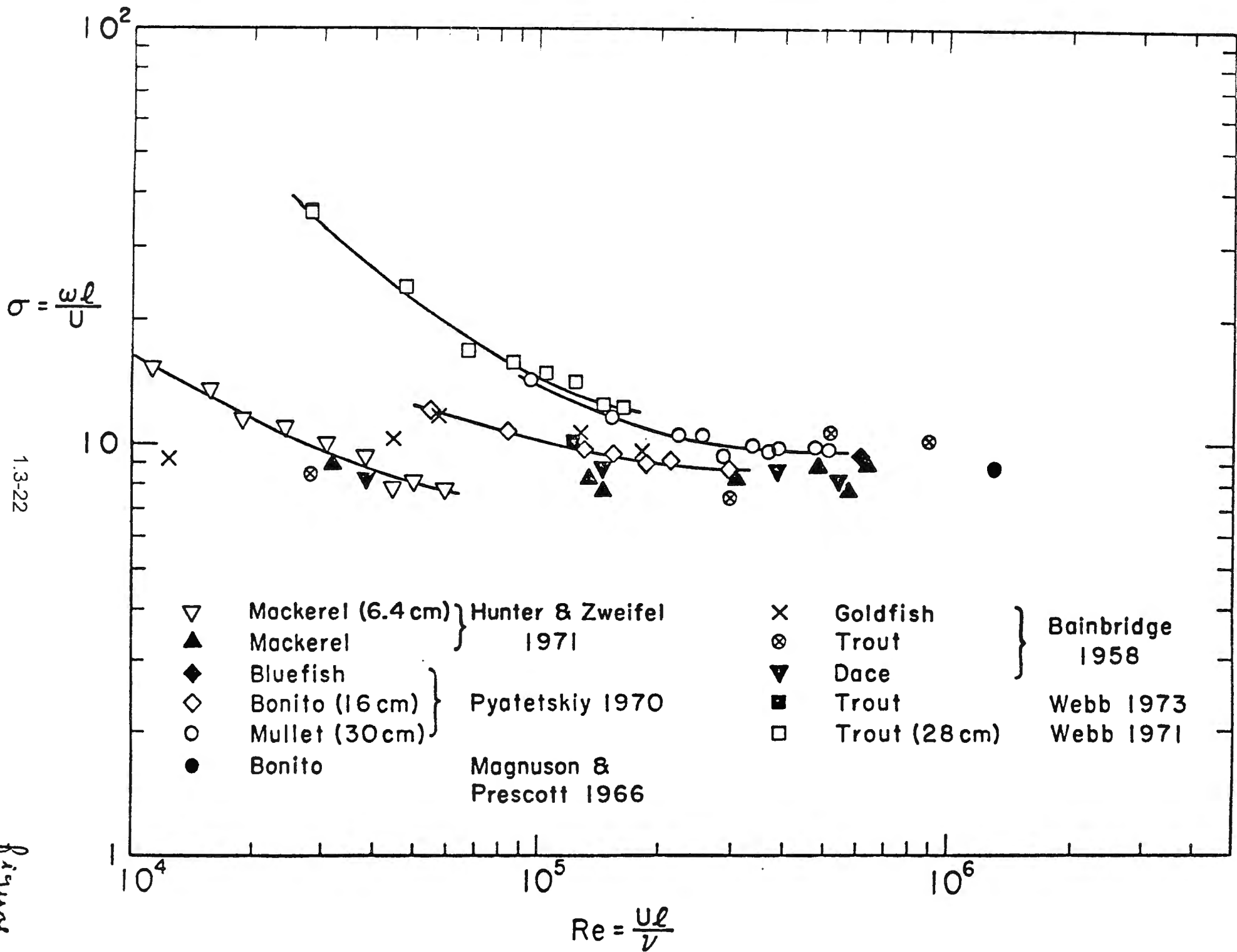
Figure 22. Selected results on the drag of rotationally-symmetric bodies (no corrections applied).
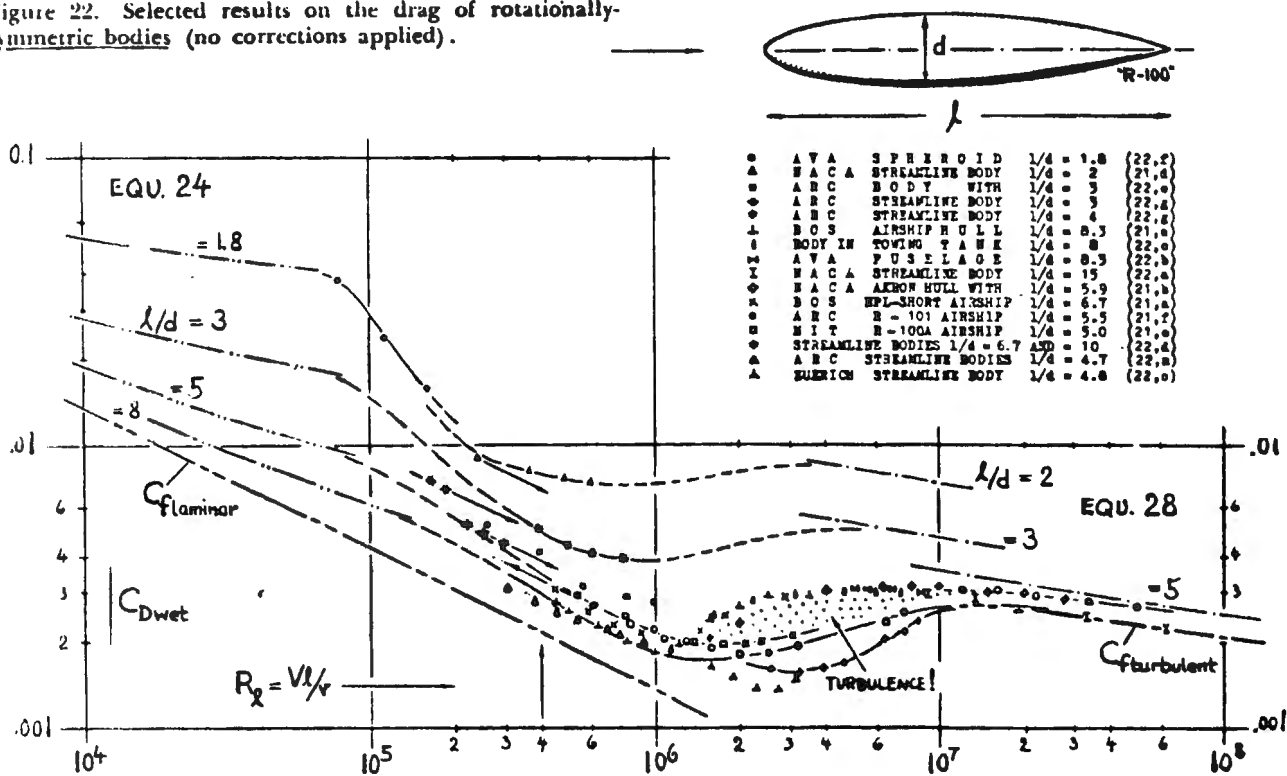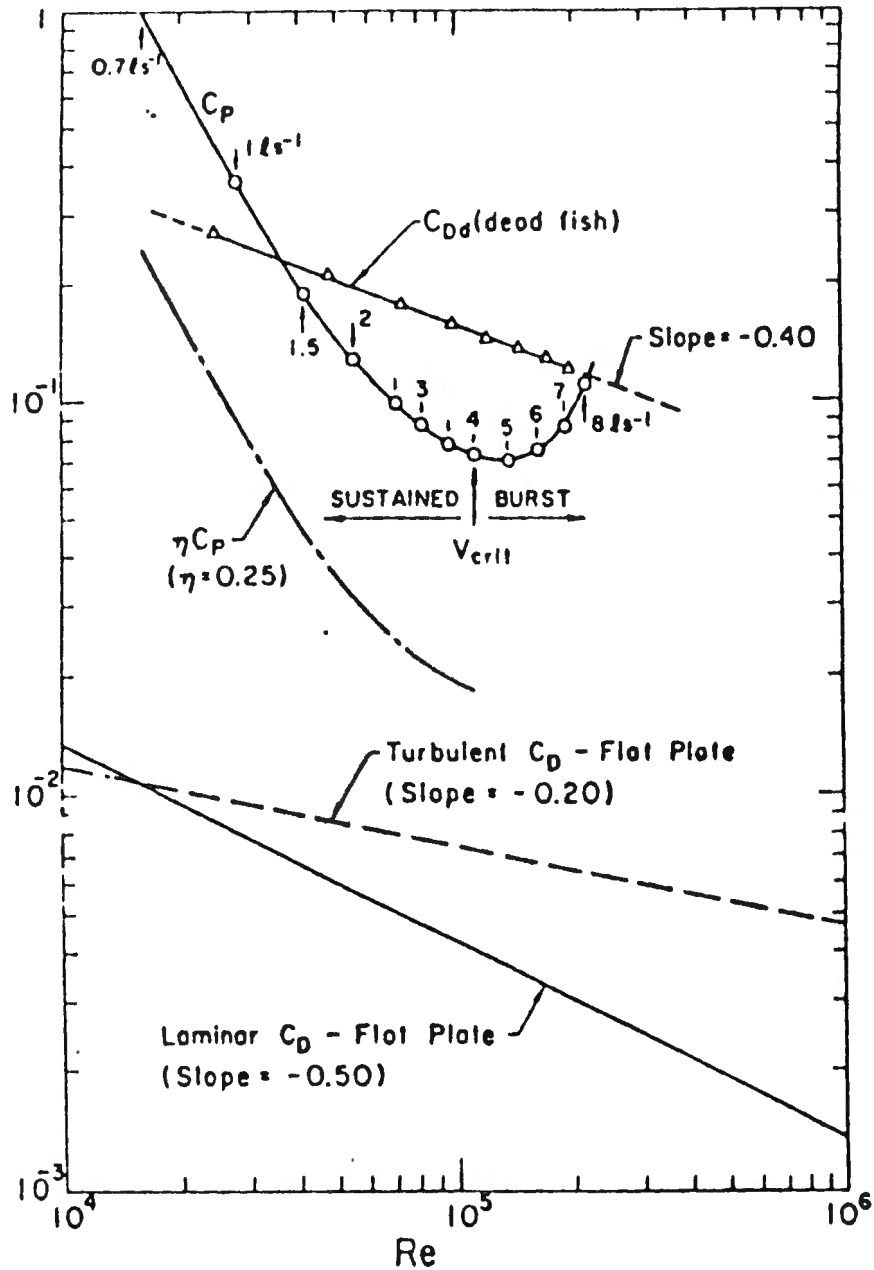
FIG. Variation of the measured metabolic power coefficient, C_p, with the Reynolds number and the variation of the measured dead-drag coefficient, C_{Dd}, of freshly killed salmon (adapted from Brett, 1963). The corresponding values of the specific speed are indicated in $\ell\ s^{-1}$ along the C_p curve. An estimate of the swimming drag coefficient, C_D, is provided by the value of ηC_p, shown with a typical value of the overall efficiency $\eta = 0.25$. The drag coefficients of a flat plate for both laminar and turbulent boundary layers are shown for reference.
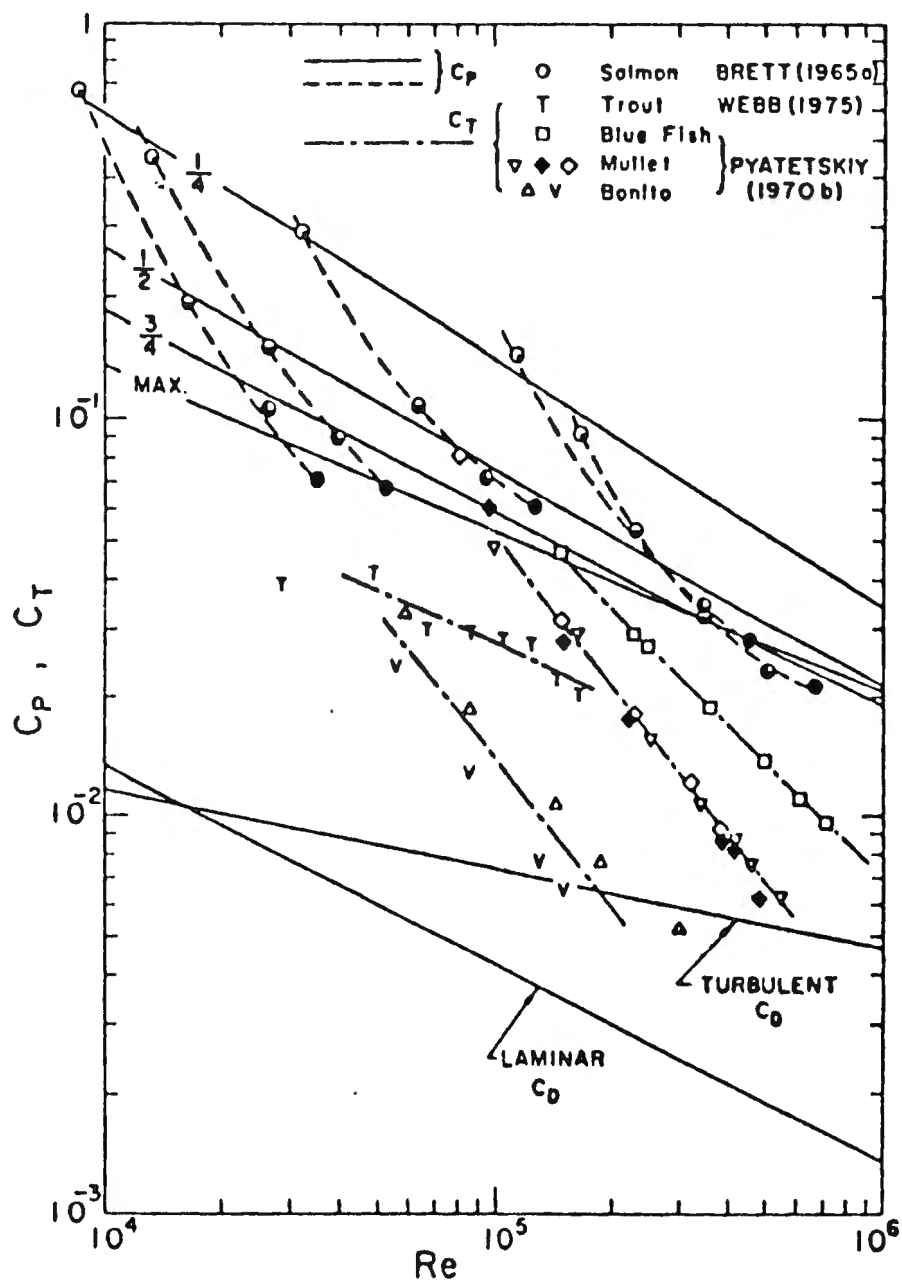
FIG. Scale effects in the variation of the measured metabolic power coefficient (for swimming) with Reynolds number for five different size groups of sockeye salmon (adapted from Brett, 1965a). Solid lines are least-square error fit to C_p at specific activity levels. Dashed lines show variation of C_p with various activity levels for each size group. Dash-dot lines illustrate theoretical thrust coefficient, C_T, computed from eq. 30 for the data of Pyatetskiy (1970b) and Webb (1975).
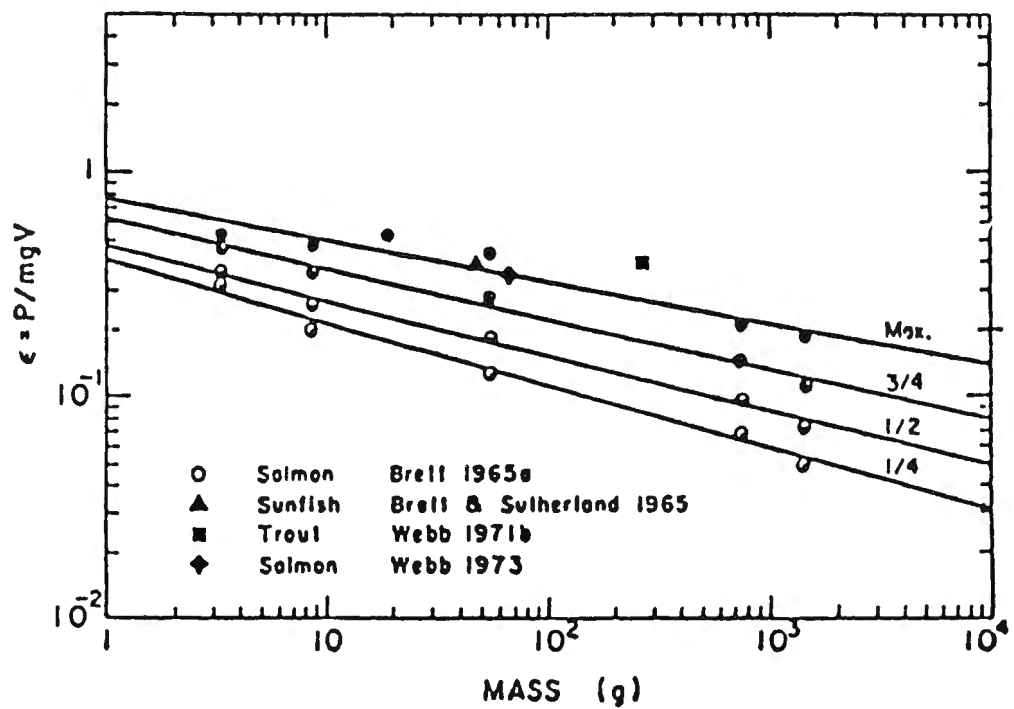
FIG. 5. Relation between specific energy cost for swimming, ε, and body mass for fish swimming at different levels of activity. Solid lines are regression lines obtained from data of Brett (1965a) for salmon at 15°C.
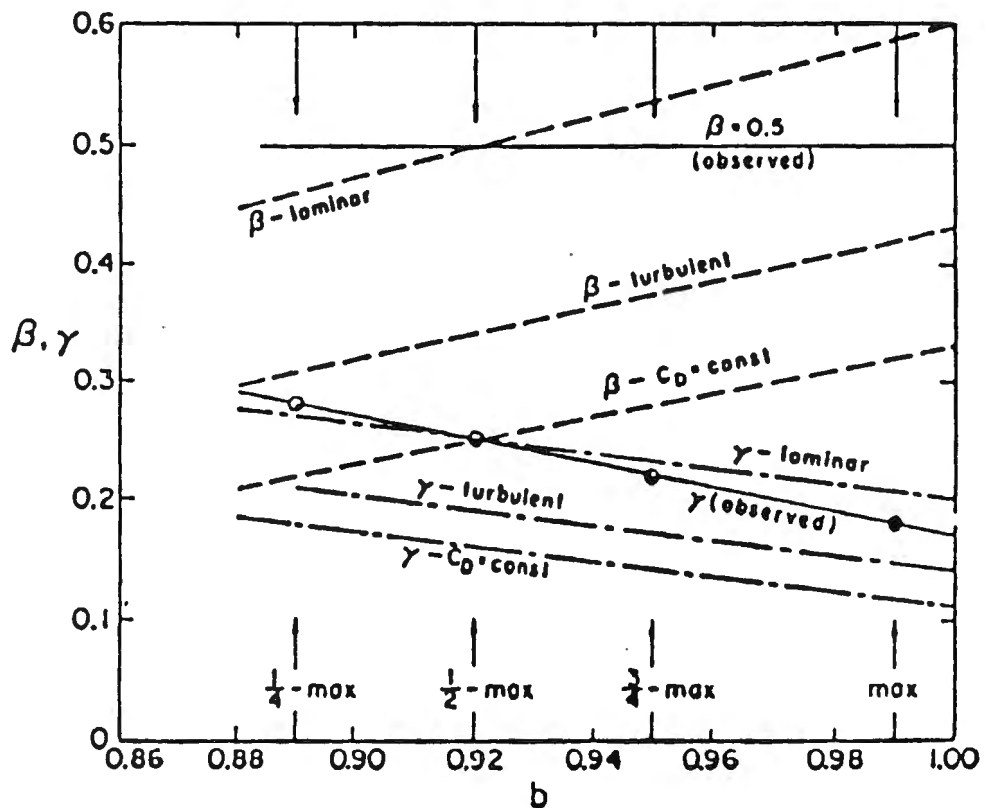
FIG. 6. Comparison of the observed values of β (Brett, 1965a,b) and γ (see Fig. 5 and Table II) with the similarity predictions (eqs. 8,11) based on the three distinct reference states characterized by a laminar boundary layer, a turbulent boundary layer, and C_D = const. (for the case of separated cross flows).
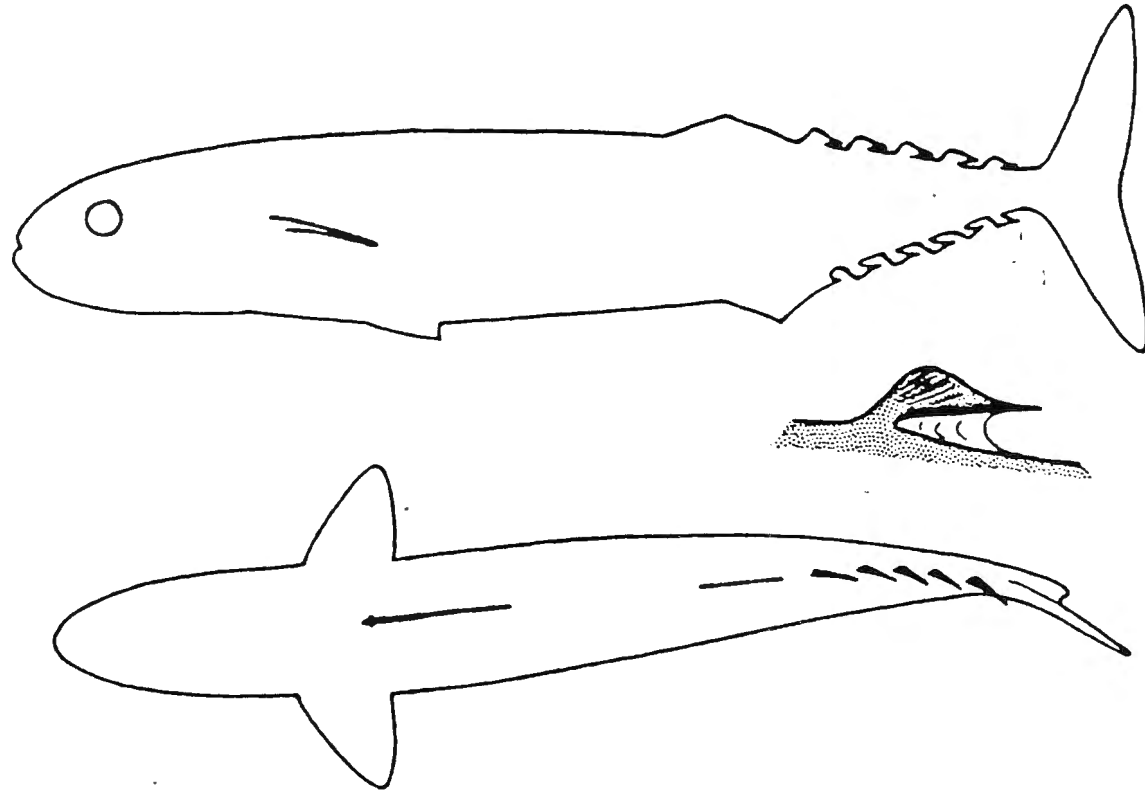
Figure 13. Dorsal and lateral views of mackerel (Scomber scomber) showing caudal finlets, one of which is enlarged to show manner in which a layer of epithelium attaches the finlet along most of its length.
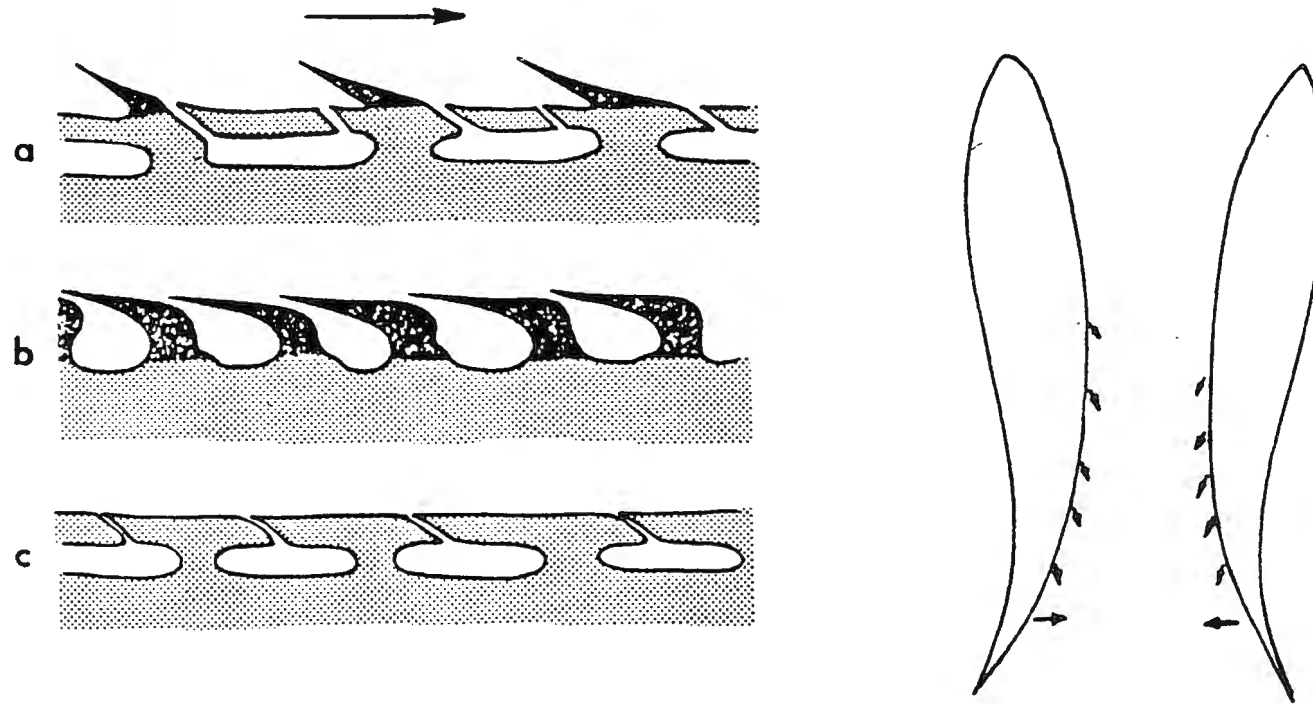
Figure 12.   Diagrammatic section through integument of three
fishes which have subdermal canals and associated pores directed
obliquely rearwards.   Ctenoid scales where present darkly shaded.
Direction of movement of the fish indicated by arrow. a.   Ruvettus.
b.   Tetragonous (an aberrant stromateoid where the scales form
underlying channels).   c.   Schedolphilous.   Ctenoid scales absent.
The diagram at right indicates the manner in which the convex
leading surface of the fish is supposed to eject sea water during
the swimming cycle.

Modes of micro-organism movement

Flagellar motion

1. Planar
2. Helical
3. variations

   mastigonemes

   spirochetes

   spirilla (volutins)

   others

Ciliary motion
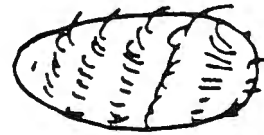
Metachronal waves

1. Ciliates

   Paramecium

   Tetrahymena

   Opalina

2. muco-ciliary system
   in duct (Lardner, Shack, Blake)

   Oviduct

   Cochlea

Amoebic movement

Intracellar flow

Cytoplasmic streaming.

Fundamental Singularities

The Stokes equations

$$\nabla \cdot \underline{u} = 0$$

$$\nabla p = \mu \nabla^2 \underline{u} + \underline{f}$$

(i) Stokeslet (Oseen 1927; Burgers 1928; Hancock 1955)

$$\underline{f} = 8\pi\mu \, \underline{\alpha}(t) \, \delta(\underline{x})$$

$$\underline{U}_S(\underline{x}; \underline{\alpha}) = \frac{\underline{\alpha}}{r} + \frac{\underline{\alpha} \cdot \underline{x} \, \underline{x}}{r^3}$$

$$P_S(\underline{x}; \underline{\alpha}) = -2\mu \, \nabla \cdot \frac{\underline{\alpha}}{r}$$
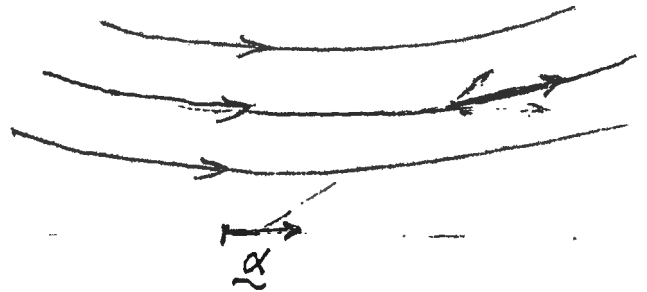
$$\underline{F}_S = 8\pi\mu \, \underline{\alpha}(t)$$

(ii) Rotlet (or couplet – Batchelor 1970; Chwang–Wu 1974)

$$\underline{f} = 4\pi\mu \, \nabla \times \underline{\gamma}(t) \, \delta(\underline{x})$$

$$\underline{U}_R = \nabla \times \frac{\underline{\gamma}}{r}, \qquad P_R = 0$$

$$\underline{\omega} = \underline{\gamma}/a^3$$
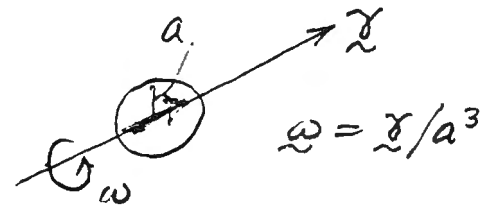
$$\underline{M}_R = 8\pi\mu \, \underline{\gamma}(t)$$

(iii) stresslet (Batchelor 1970)

Stokes force dipole

$$\underline{U}_{SD}(\underline{x}; \underline{\alpha}, \underline{\beta}) = -\underline{\beta} \cdot \nabla \underline{U}_S(\underline{x}; \underline{\alpha}) = \underline{U}_R + \underline{U}_{SS}$$

$$\underline{U}_R(\underline{x}; \underline{\beta} \times \underline{\alpha}), \qquad \underline{U}_{SS} = -\frac{\underline{\alpha} \cdot \underline{\beta} \, \underline{x}}{r^3} + \frac{3(\underline{\alpha} \cdot \underline{x})(\underline{\beta} \cdot \underline{x}) \underline{x}}{r^5}$$

rotlet   stresslet
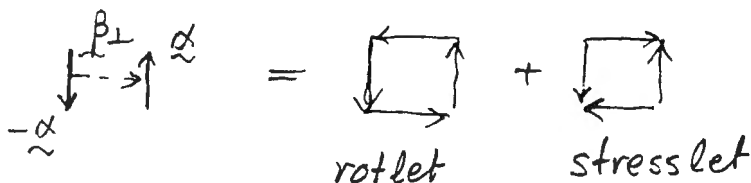
Stokes doublet $(\beta \parallel)$

(iv) mass doublet

$$\underset{\sim}{U}_D(x;\underset{\sim}{\xi}) = \nabla\nabla\cdot\frac{\underset{\sim}{\xi}}{r} = -\frac{1}{2}\nabla^2\underset{\sim}{U}_S(x;\underset{\sim}{\xi})$$

$$P_D(x;\underset{\sim}{\xi}) = -\frac{1}{2}\nabla^2 P_S(x;\underset{\sim}{\xi}) = 0.$$

$\underset{\sim}{\xi}(t)$

(v) higher-order singularities

$$\underset{\sim}{U}_Q(x;\underset{\sim}{\alpha},\underset{\sim}{\beta},\underset{\sim}{\gamma}) = (\underset{\sim}{\alpha}\cdot\nabla)(\underset{\sim}{\beta}\cdot\nabla)\underset{\sim}{U}_S(x;\underset{\sim}{\gamma})$$

Fig. 11. The streamlines (in the laboratory frame) of a self-propelling prolate spheroid of eccentricity 0.9 (upper) and of an externally-driven spheroid of the same shape (lower figure, with $V_s = V_n = 0$).

Fig. 12. Streak photographs of a freely swimming specimen of Paramecium caudatum (upper) and of a dead one sedimenting (towards right) under gravity (lower figure).

Hydromechanics of swimming propulsion.
Part 1. Swimming of a two-dimensional flexible plate at variable forward speeds in an inviscid fluid

By T. YAO-TSU WU

California Institute of Technology,
Pasadena, California

The most effective movements of swimming aquatic animals of almost all sizes appear to have the form of a transverse wave progressing along the body from head to tail. The main features of this undulatory mode of propulsion are discussed for the case of large Reynolds number, based on the principle of energy conservation. The general problem of a two-dimensional flexible plate, swimming at arbitrary, unsteady forward speeds, is solved by applying the linearized inviscid flow theory. The large-time asymptotic behaviour of an initial-value harmonic motion shows the decay of the transient terms. For a flexible plate starting with a constant acceleration from at rest, the small-time solution is evaluated and the initial optimum shape is determined for the maximum thrust under conditions of fixed power and negligible body recoil.

1. Introduction

Aquatic animals propelling themselves in water, or in other liquid media, span a wide range in their sizes and speeds. Large cetaceans, such as porpoises and whales, may have lengths from 2 to 30 m, and can swim at cruising speeds of from 6 to 10 m/s (Lang & Pryor 1966). Microscopic organisms such as paramecia and spermatozoa, ranging from $300\,\mu$m down to $50\,\mu$m in length with length–diameter ratio from 20 to 100, can swim at speeds from 1000 to $80\,\mu$m/s. In between these two extremities there are many species of fishes and aquatic animals of various sizes. Based on the characteristic length l of a body moving at velocity U in a liquid of kinematic viscosity ν, the Reynolds number, $R = Ul/\nu$, measures the relative magnitude of the time average of inertial stress to viscous stress. The value of R is of order 10^8 for the most rapid cetaceans, 10^6 for migrating fishes, 10^5–10^3 for a great variety of fishes, about 10^2 for tadpoles, down to about 1 for *Turbatrix*, 10^{-3} or less for paramecia and spermatozoa (Gray 1968, p. 437), and to the extreme of 10^{-6} or less for bacteria. Thus, the Reynolds number R covers practically the entire range of interest known to hydrodynamicists. Lighthill (1969) has given an excellent survey of the hydromechanics of aquatic animal propulsion, which has elucidated both the zoological and hydromechanical aspects of the subject.

Although R may vary greatly from case to case, the most effective movements of swimming propulsion employed by a large number of aquatic animals of drastically different sizes have been observed to differ very little from an undulatory motion of the body, in the form of a transverse wave propagating along the body from head to tail. A great majority of many species of fishes can be singled out as a pre-eminent class of this mode of propulsion. The remarkable performance of some cetaceans (dolphin, porpoises, whales, etc.) and some well-known game fish families (tuna, wahoo, marlin, swordfish, etc.), using strong tails of large aspect ratio, is only a variation of this basic undulatory mode. In the world of micro-organisms, an enormous variety of creatures, ranging from minute bacteria, larger but still primitive protozoa, to higher level spermatozoa, have been observed to employ either uniformly propagating transverse waves, or whip-like waves, or helical waves along slender flagella as principal means of propulsion. The basic transverse wave mode thus seems to be little affected by the Reynolds number over such a wide range. However, the fundamental principles underlying the hydromechanics of swimming propulsion do become very different for large or small values of the Reynolds number.

For Reynolds number large, the swimming propulsion depends primarily on the inertial effect, since the flow outside a thin boundary layer next to the body surface is irrotational. Viscosity of the fluid is unimportant except in its role of generating the vorticity shed into the wake, and of producing a thin boundary layer, and hence a skin fri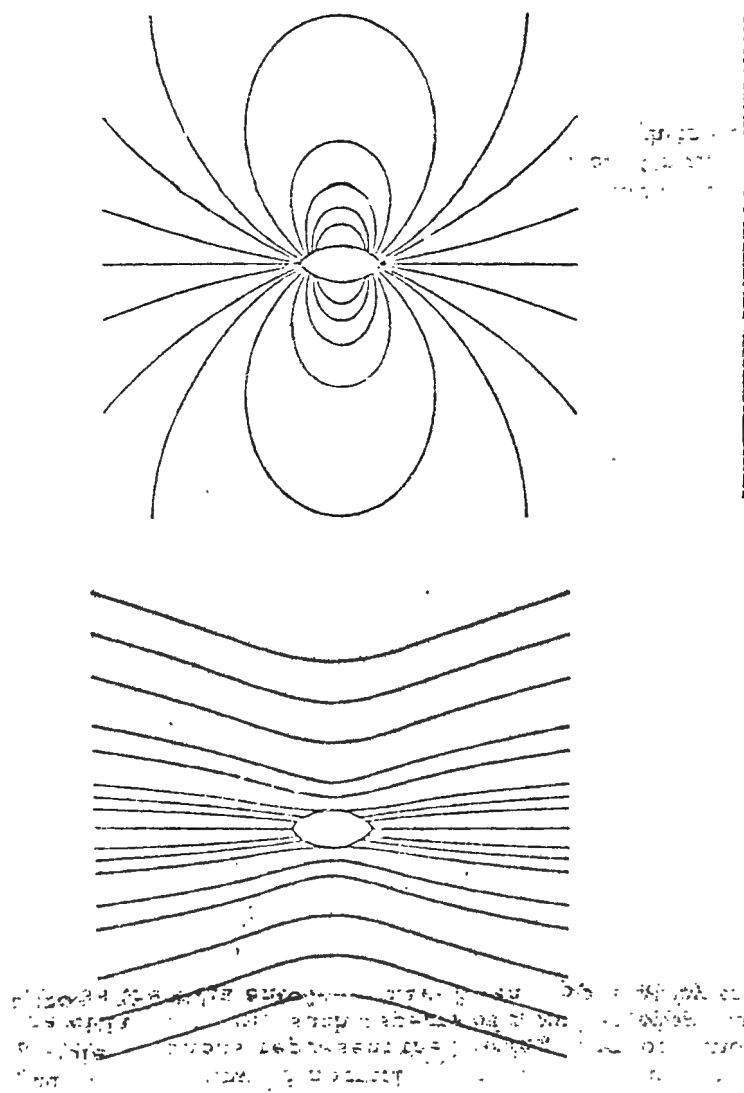ction at the body surface. As the body performs an undulatory wave motion and attains a forward momentum, the propulsive force pushes the fluid backward with a net total momentum equal and opposite to that of the action, while the frictional resistance of the body gives rise to a forward momentum of the fluid by entraining some of the fluid surrounding the body. The momentum of reaction to the inertial forces is concentrated in the vortex wake due to the small thickness and amplitude of the undulatory trailing vortex sheet; this backward jet of fluid expelled from the body can, however, be counterbalanced by the momentum in response to the viscous drag. When a self-propelled body is cruising at a constant speed, the forward and backward momenta exactly balance; they can nevertheless be evaluated separately. This mechanism of swimming motion at large Reynolds numbers has been elucidated by von Kármán & Burgers (1943) for the simple case of a rigid plate in transverse oscillation. Swimming of slender fish has been treated by Lighthill (1960); and the waving motion of a two-dimensional flexible plate has been calculated by Wu (1961).

In the other extremity, movements of microscopic bodies always correspond to small Reynolds numbers. The propulsion in this range depends almost entirely on the viscous stresses, since the inertial forces are then extremely small, except possibly for the motions at very high frequencies. Oscillatory motions in a viscous fluid were discussed as early as 1851 by Stokes. Various studies of the swimming of microscopic organisms have been led by Taylor (1951, 1952a, b), who discussed the propulsion of a propagating, monochromatic, transverse wave along a sheet immersed in a very viscous fluid, and later evaluated the action of waving cylindrical tails of microscopic organisms. Further studies in this field have been contributed by Hancock (1953), Gray & Hancock (1955), Reynolds (1965) and Tuck (1968).

Hydromechanics of swimming propulsion. Part 2. Some optimum shape problems

By T. YAO-TSU WU

California Institute of Technology
Pasadena, California

The optimum shape problems considered in this part are for those profiles of a two-dimensional flexible plate in time-harmonic motion that will minimize the energy loss under the condition of fixed thrust and possibly also under other isoperimetric constraints. First, the optimum movement of a rigid plate is completely determined; it is necessary first to reduce the original singular quadratic form representing the energy loss to a regular one of a lower order, which is then tractable by usual variational methods. A favourable range of the reduced frequency is found in which the thrust contribution coming from the leading-edge suction is as small as possible under the prescribed conditions, outside of which this contribution becomes so large as to be hard to realize in practice without stalling. This optimum solution is compared with the recent theory of Lighthill (1970); these independently arrived-at conclusions are found to be virtually in agreement.

The present theory is further applied to predict the movement of a porpoise tail of large aspect-ratio and is found in satisfactory agreement with the experimental measurements. A qualitative discussion of the wing movement in flapping flight of birds is also given on the basis of optimum efficiency.

The optimum shape of a flexible plate is analysed for the most general case of infinite degrees of freedom. It is shown that the solution can be determined to a certain extent, but the exact shape is not always uniquely determinate.

1. Introduction

One of the most inspiring questions concerning the phenomena of aquatic animal propulsion and of flapping flights of birds and insects is invariably connected with the highest possible hydrodynamic efficiency. This problem has been brought up from time to time by various observers who have noted the impressive capabilitity of these animals in generating fast movements at low energy cost. According to the first principle of energy balance or momentum consideration, as has been explained in part 1 of this paper (Wu 1971), much can already be said about the desirable shapes of body movement: that at large Reynolds numbers, a thin two-dimensional plate gains thrust by sending a transverse wave from head to tail, with amplitude slightly increasing towards the rear, thereby achieving a forward swimming velocity somewhat less than the phase velocity of the body wave form. As for the tail of large aspect-ratio

of some high-performance fish, the tail should move nearly tangentially to the path traversed in the space by the body wave form. These basic features have been elegantly elucidated, with perhaps more physical reasoning, in an excellent review by Lighthill (1969). However, it would still be of great interest to resolve a quantitative determination of the optimum shape under some appropriate constraints.

The problem of the optimum shape is interesting in its own right from the mathematical point of view, since the effective methods of solution do not seem to fall into the known categories of the calculus of variation. The special case of a two-dimensional waving plate in harmonic motion has been treated by Wang (1966), who adopted a discretized Fourier representation of the body motion, and found that his solutions exist only for a set of eigenvalues. However, it is found in the present study that this optimum shape problem is basically not an eigenvalue problem, and therefore merits a new discussion. On physical grounds, it would be indeed difficult to see the significance of the idea that the shape function can have eigensolutions.

In this part we shall consider the optimum shape problem only for the case of two-dimensional flexible plate, of negligible thickness, in harmonic motion. (Some three-dimensional problems will be treated in part 3 of this paper.) The two-dimensional theory is reckoned to have utility in problems of lifting surfaces of large aspect-ratio, such as the tails of some cetaceans and high-performance game fish (the lunate tails: swordfish, tuna, albacore, porpoises, etc.), and even the wings of most birds and some insects. The optimum shape problem is concerned with those profiles or movements that will minimize the energy loss under the condition of fixed thrust (required to overcome the viscous drag), and possibly also under other isoperimetric constraints. First, the optimum movement of a rigid plate is determined by reducing the original singular problem to a regular one of a lower rank. This optimum solution is found to depend on two variables: one being the reduced frequency and the other a 'proportional-loading parameter', defined as the prescribed thrust coefficient divided by the dimensionless heaving amplitude squared. For given loading parameter, a favourable range of the reduced frequency is found in which the thrust contribution coming from the leading edge suction is as small as possible under the prescribed conditions. This consideration seems to provide the optimum range of the reduced frequency utilized in practice.

These theoretical results are further applied to predict the movement of a porpoise tail, and comparisons made with the experimental investigation of Lang & Daybell (1963). As a related problem of interest, the optimum movement of a flapping wing of some birds or flatfish is discussed qualitatively.

The general problem of optimum shape of a flexible surface having an infinite degree of freedom is finally analysed and discussed. It is found that the solution can be determined to a certain extent, and, with the additional degrees of freedom, the optimum efficiency can be further improved from the rigid-plate value, but the exact shape is not uniquely determinate.

1.3-35

Hydromechanics of swimming propulsion.
Part 3. Swimming and optimum movements of slender fish with side fins

By T. YAO-TSU WU

California Institute of Technology,
Pasadena, California

This paper seeks to evaluate the swimming flow around a typical slender fish whose transverse cross-section to the rear of its maximum span section is of a lenticular shape with pointed edges, such as those of spiny fins, so that these side edges are sharp trailing edges, from which an oscillating vortex sheet is shed to trail the body in swimming. The additional feature of shedding of vortex sheet makes this problem a moderate generalization of the paper on the swimming of slender fish treated by Lighthill (1960a). It is found here that the propulsive thrust depends not only on the virtual mass of the tail-end section, but also on an integral effect of variations of the virtual mass along the entire body segment containing the trailing side edges, and that this latter effect can greatly enhance the thrust-making.

The optimum shape problem considered here is to determine the transverse oscillatory movements a slender fish can make which will produce a prescribed thrust, so as to overcome the frictional drag, at the expense of the minimum work done in maintaining the motion. The solution is for the fish to send a wave down its body at a phase velocity c somewhat greater than the desired swimming speed U, with an amplitude nearly uniform from the maximum span section to the tail. Both the ratio U/c and the optimum efficiency are found to depend upon two parameters: the reduced wave frequency and a 'proportional-loading parameter', the latter being proportional to the thrust coefficient and to the inverse square of the wave amplitude. The basic mechanism of swimming is examined in the light of the principle of action and reaction by studying the vortex wake generated by the optimum movement.

1. Introduction

Lighthill (1960a) investigated the inviscid flow around a slender fish which makes swimming movements in a direction transverse to its direction of locomotion, while its cross-section varies along it only gradually. Based on the slender-body theory, Lighthill obtained the result of thrust produced by the fish, time-rate of work done by it, and the rate of shedding of energy, showing that the mean values of these quantities all depend on the movement and body shape at the tail-end section only, and that they will vanish with the virtual mass of the tail. What has primarily been implied here is that the body cross-section varies so gradually, and its shape is so smooth (no sharp edges), that the cross-flow remains attached to body, leaving no vortex sheet until the tail-end section is reached. This situation may represent, quite accurately, several wide classes of aquatic animals, such as the eel *Anguilla vulgaris*, eel-like fishes of the order Heteromi, ribbon fishes of the order Allotriognathi, members of the order Anacanthini like cod and similar fishes, as have been discussed in an interesting review article by Lighthill (1969).

There exist, however, other classes of fishes of more advanced orders which are known as strong, active swimmers, capable of putting on impressive performances. This group of fish orders contains members of the order Isospondyli (such as salmon, trout, etc.) and those of the large order Ostariophysi, to which belong most of the successful freshwater fishes. As an indicative measure of the over-all performance, the swimming speed U is usually expressed by biologists in units of body-length/sec, or $n = U/l$. For instance, pike (*Esox lucius*), salmon (*Salmo salar*), trout (*Salmo gairdneri*), dace (*Leuciscus leuciscus*), and herring (*Clupea harengus*) have been observed to range from $n = 6$/sec to 12/sec (see Hertel 1963, chap. G; Gray 1968, chap. 3). Speeds considerably greater than 10/sec, as high as 20/sec, have also been recorded by Walters & Fierstein (1964) for tunny (*Thunnus albacores*) and wahoo in open water. By and large, the slenderness parameter, δ, defined as the ratio of maximum depth (or height, or called span as in the wing theory) to body length, of this general group of fishes is moderate to small (about from 0·4 down to 0·18 based on body depth including dorsal and ventral fins extended, the smallest δ being represented by the fast-swimming Pacific saury, *Cololabis saira*). Their thickness in the third dimension is yet smaller than their span; the ratio of minor to major axis of cross-section of some slightly compressed species may be as much as 0·6 all the way back to the caudal peduncle (point of minimum depth). As a general feature, the transverse cross-sections of these fishes have rather rounded edges anterior to the section of maximum depth, turning to a more or less lenticular shape with fairly pointed edges to the rear part of body in which may be found a great variety of dorsal, ventral, pectoral, anal, and possibly other smaller fins, to be followed by the caudal fin.

As for the detailed fin shapes and locations, there are perhaps as many different configurations as the number of species. However, as a crude classification, the dorsal and ventral fins may be arranged for hydromechanical reasons into two main types: the elongated 'ribbon fin' and the triangular or trapezoidal 'sail-shaped fin'. Some pre-eminent families of fast fishes equipped with conspicuous ribbon-fins are dolphin fish *Coryphaena hippurus*, which has a dorsal ribbon-fin all the way from head to caudal peduncle and a shorter ventro-anal one, yellow-tail *Seriola quinqueradiata*, atka mackerel *Pleurogrammus azonus*, porgies and breams (e.g. *Pagrus major*, *Dentex tumifrons*). Examples of fast fishes having sail-shaped dorsal and ventral fins are mullet *Mugil cephalus*, which is very fast and migrates widely, barracuda *Sphyraena pinguis*, trout, salmon, and herring. Also, many families of fishes have both types of fins, notably bluefin tuna *Thunnus thynnus*, skipjack, and some mackerels. Furthermore, several fishes (wahoo, tuna, skipjack, mackerel and saury) have behind the main fins a series

OPTIMIZATION PROBLEMS IN HYDROFOIL PROPULSION[*]

Th. Yao-tsu Wu, Allen T. Chwang
California Institute of Technology, Pasadena, California
and Paul K. C. Wang
University of California at Los Angeles

This paper attempts to apply the principle of control theory to investigate the possibility of extracting flow energy from a fluid medium by a flexible hydrofoil moving through a gravity wave in water, or by an airfoil in gust. The present optimization consideration has led to the finding that although the flexible hydrofoil may have an infinite number of degrees of freedom, the optimum shape problem is nevertheless a finite-dimensional one. The optimum shape sought here is the one which minimizes the required power subject to the constraint of fixed thrust. A primary step towards the solution is to reduce the problem to one of minimizing a finite quadratic form; after this reduction the solution is determined by the method of variational calculation of parameters. It is found that energy extraction is impossible if the incident flow is uniform, and may be possible when the primary flow contains a wave component having a longitudinal distribution of the velocity component normal to both the mean direction of flight and the wing span. When such waves of sufficiently large amplitude are present, not only flow energy but also a net mechanical power can be extracted from the surrounding flow.

I. Introduction

Some previous observations on fish swimming and bird flight seem to suggest that some species may have learned, through experience, to acquire the key to high performance by executing the optimum movement that may be of great interest to control theory related to fluid mechanics. An especially intriguing aspect of the optimization problem concerns with the possibility of extracting energy from surrounding flow by an oscillating lifting surface (such as the fish body and fins, bird wings, and artificial wings like airfoil and hydrofoil) and its associated effect on the control of motion.

This general problem has been explored to various degrees of generality. Based on the approximation of potential flow with small amplitude, it has been found by Lighthill (1960) for slender bodies, and by Wu (1961) for two-dimensional plates, that if the basic flow is uniform, energy is always imparted by an oscillating wing to the surrounding fluid, and an extraneous mechanical work must therefore be continuously supplied to maintain the motion. Even though it is impossible in this case to extract energy from the flow field, the highest possible hydromechanical efficiency that can be attained by a wing, subject to delivering a given forward thrust, can be very high, as found by Wu (1971 b, c) for the two-dimensional plate and a slender lifting surface.

As was subsequently pointed out by Wu (1972), the situation becomes drastically different when the basic flow is no longer uniform, but contains a wave component, such as gravity waves in water, or wavy gust in air. The contention that the wave energy stored in a fluid medium can be utilized to assist propulsion has been suggested by intuitive observations. Sea gulls and pelicans have been observed to skim ocean waves over a long distance without making noticeable flapping motions (save some gentle twisting) of their wings. In an extensive study of the migrating salmon, Osborne (1960) found that the increased flow rate in a swollen river did not slow the salmon down (for known biochemical energy expended during the travel) by that much a margin as would be predicted by the law of resistance in proportion to the square of their velocity relative to the flowing water. Several possible explanations were conjectured by Osborne, including the prospect that the flow energy associated with the eddies in river could be converted to generate thrust. To explore this possibility Wu (1972) introduced an energy consideration to an earlier study of Weinblum (1954) on the problem of heaving and pitching of a rigid hydrofoil in regular water waves. It was found that the greatest possible rate of energy extraction is provided by the optimum mode of heaving and pitching. When waves of sufficiently large amplitude are present, not only flow energy but also a net mechanical power can be extracted from the wave field.

A BIDIRECTIONAL LONG-WAVE MODEL

Theodore Yao-tsu Wu

ABSTRACT. For modeling weakly nonlinear and weakly dispersive long gravity waves of typical amplitude a and typical length λ, propagating in both directions in a straight, gradually varying channel of breath $b(x)$ and mean water depth $h(x)$, the Boussinesq equations provide a versatile model, with its validity based on the assumptions that $\alpha = a/h \ll 1$, $\epsilon = (h/\lambda)^2 = O(\alpha)$ and $(d/dx)\log(bh^{1/2}) = O(\epsilon^{3/2})$. On this same basis, a new bidirectional long-wave model is derived to evaluate the cross-sectional mean surface elevation $\zeta(x,t) = \zeta_+ + \zeta_- + \zeta_1$, where ζ_+ and ζ_- denote, respectively, right-going and left-going waves, both of $O(\epsilon)$, and ζ_1 is a term of $O(\epsilon^2)$ representing the interaction between ζ_+ and ζ_-. The evolution equations obtained for ζ_+ and ζ_- exhibit extensions of the Korteweg–de Vries equation to comprise the additional effects of slow variations in the admittance, $(bh^{1/2})$, of varying channels on evolving waves. Main features of this model include: (i) For wave-and-channel-wall interactions, this model accounts for reflection and transmission of long waves in varying channels while maintaining both mass and energy conserved adiabatically. (ii) For wave-wave interactions, head-on collisions between right- and left-going solitary waves are shown to gain a total phase shift which is an algebraic function of the amplitudes of the colliding waves. (iii) For forced generation of nonlinear waves in varying channels, this model admits weakly resonant disturbances with both right-going and left-going components.

1. Introduction

The general subject of nonlinear and dispersive waves evolving in non-uniform media has been of strong interest and active development, the thrust being motivated by attempts for the ultimate generality. For nonlinear long gravity waves, of typical amplitude a and length λ, propagating in a straight, gradually varying channel of breadth $b(x)$ and cross-sectional mean-water-depth $h(x)$, the various models of the Boussinesq family are based on the assumptions that

$$\alpha = a/h \ll 1, \quad \epsilon = (h/\lambda)^2 = O(\alpha), \quad (d/dx)\log(b\,h^{\frac{1}{2}}) = O(\epsilon^{3/2}), \tag{1}$$

(see, e.g. Peregrine [12]; Whitham [22]; Miles [9, 10, 11]; Wu [19, 20, 21]). The models in this class have been found by Teng and Wu [17, 18] to be in broad agreement with existing experiment.

Along a different approach, the additional assumption of unidirectional wave motion in varying channels has been applied to derive the Korteweg–de Vries (KdV) class of equations by Shuto [15], Miles [11], Teng and Wu [17, 18] and others. Similarly, variable-depth form of the Kadomtsev-Petviashvili (K-P) equation has been given by Liu et al. [7]. Whilst Shuto's equation and similar models are known to be adiabatic in conserving energy, they have, however, a crucial deficiency in not conserving mass, with an error which is first order and has a cumulative effect. This effect has been

In regard to Gray's paradox,

"~~From~~ our mechanophysiological study, we have obtained a set of data for the power and thrust coefficients, C_P and C_T versus the Reynolds number Re (over $10^4 < Re < 10^6$). These relations show that (i) C_P measured over the entire range of swimming speed is less than C_D of a dead fish, C_{Dd}; (ii) the C_T estimate from $C_T = \eta\, C_P$, with $\eta = 0.25$ for the muscle + hydro efficiency is considerably less than C_{Dd}; and (iii) these experimentally inferred C_T values are quite consistent with the theoretical evaluations of C_T based on the data of Pyatetskiy and Webb. These findings thereby imply that the fluid resistance a swimming fish experiences at cruise is not only possible, but quite likely to be appreciably smaller than the drag acting on their artificial models. The underlying mechanism that renders this assertion physically possible is thought to lie with the outstanding feature of the unsteadiness of the motion. Further research will be required to bring this mechanism to full comprehension."

1.4 Control of the Turbulent Boundary Layer

John L. Lumley
Cornell University

CONTROL OF THE TURBULENT BOUNDARY LAYER

Professor John L. Lumley

CORNELL UNIVERSITY

The construction of the low-dimensional models of Aubrey et al. is briefly outlined. Motivated by a desire to control the turbulent boundary layer via feedback, we examine the effect on a naturally occurring streamwise vortex pair, of a perturbing pair produced by an actuator. We show how the resulting velocity field modifies coefficients in the above low-dimensional models and sketch a control strategy which reduces the bursting rate and hence the turbulent drag in the model problem.

Thursday, the 9th June 1994
* * NOTE NEW VENUE: Conference Room, Bldg. 1171 * *
Time: 10:30 AM

POC: Dr. Promode R. Bandyopadhyay (Code: 8233; Bldg. 108/2nd) NPT x2588

The seminar by Professor Lumley was canceled at the last minute due to the sudden illness of his wife.

Part 2:

Theoretical Turbulence

2.1 Vortex Interactions with Wall

J. David Walker
Lehigh University

SEMINAR NOTICE

VORTEX INTERACTIONS WITH WALLS

Professor J. D. A. Walker

LEHIGH UNIVERSITY
Bethlehem, PA

Situations where an effectively irrotational freestream contains regions of concentrated vorticity are common in external aerodynamics. Vortices may arise as a consequence of shedding from some upstream surface (e. g. dynamic stall) or near certain three-dimensional boundary geometries which act to promote vortex formation. Geometry-induced creation can occur in any situation where a flow along a wall approaches a surface-mounted obstacle, such as at wing/body junctions and near computer chips mounted on electrical circuit boards. Similar geometries are encountered in a variety of internal flows, such as branching pipes, and in turbine and compressor passages. The cited examples involve macroscopic large-scale motions, but important vortex motions are also prevalent at much smaller scale. Concentrated small vortices of the hairpin type are known to be an important influence in a boundary layer undergoing transition and appear to be the dominant feature in the production of turbulence near solid surfaces.

In this presentation, recent experimental and theoretical work on the influence of vortex motion close to a solid surface will be discussed, with particular reference to the dynamics of turbulent boundary layers. When the flow is at high Reynolds numbers, boundary layers near a surface are found to respond in a generic way to the motion of the vortices above; in this process an abrupt and sharply focused eruption of the near-wall fluid invariably develops. Such an event may be characterized as an unsteady separation of the surface layer; it leads to a strong viscous-inviscid interaction with the external flow and culminates in the violent ejection of concentrated near-wall vorticity away from the surface. Generally, it is not possible to calculate the evolution of these ejections at high Reynolds number using conventional numerical approaches. Recent progress utilizing Lagrangian methods will be discussed.

Thursday, the 14th April 1994
* * NOTE NEW VENUE: Conference Room, Bldg. 1171 * *
Time: 10:30 AM

POC: Dr. Promode R. Bandyopadhyay (Code: 8233; Bldg. 108/2) NPT x2588

VORTEX INTERACTIONS WITH WALLS AND

DYNAMICS OF TURBULENT BOUNDARY LAYERS

J. D. A. WALKER
DEPARTMENT OF MECHANICAL
ENGINEERING AND MECHANICS
LEHIGH UNIVERSITY

SOME APPLICATIONS

1. VORTICES CREATED FROM SHREDDING FROM AN UPSTREAM SURFACE

   - AIRCRAFT TRAILING VORTICES

   - DYNAMIC STALL ON AIRFOILS AND HELICOPTER BLADES

   - TURBINES

2. GEOMETRY-INDUCED VORTEX CREATION

   - WING/BODY INTERSECTIONS

   - END-WALL BOUNDARY LAYERS IN TURBINES

   - COMPONENTS ON CIRCUIT BOARDS

3. TURBULENCE AND TRANSITION

$\rightarrow |\Delta z^+ = 100| \leftarrow$

104 mm

outer layer

$y^+ = \dfrac{u_\tau y}{\nu} \approx 120$

wall layer

bubble wire

LOW u   HIGH u

END-ON

TURBULENT BOUNDARY LAYERS

OBJECTIVES

1. DETERMINE CAUSE AND EFFECT RELATIONSHIPS

   - RELATION OF FLOW STRUCTURE TO OBSERVED EVENTS
     (PRIMARILY NEAR THE SURFACE)

   - ORIGIN OF THE "LOW-SPEED" STREAKS

   - CAUSE OF WALL-LAYER BURSTING
     (LOCAL WALL LAYER BREAKDOWN, INTERACTION)

2. ESTABLISH DYNAMICAL PICTURE

   - CONTROL ISSUES?

APPROACH

- UNDERSTAND RELEVANT BASIC PHYSICAL PROCESSES

- IDENTIFY MOST BASIC ELEMENT OF TURBULENCE NEAR A SURFACE

- ANALYSIS IS ASYMPTOTIC FOR LARGE RE

(a) Symmetric   (b) Asymmetric

HAIRPIN VORTEX

UNDERSTAND INTERACTIONS WITH

    (1) THE SURFACE FLOW

    (2) THE BACKGROUND SHEAR FLOW

    (3) EACH OTHER

THEN IT IS POSSIBLE TO INTERPRET OBSERVED BEHAVIOR IN TRANSITION AND THE TURBULENT WALL LAYER.

TURBULENT BOUNDARY LAYERS

OBJECTIVES

1. DETERMINE CAUSE AND EFFECT RELATIONSHIPS

    - RELATION OF FLOW STRUCTURE TO OBSERVED EVENTS
      (PRIMARILY NEAR THE SURFACE)

    - ORIGIN OF THE "LOW-SPEED" STREAKS

    - CAUSE OF WALL-LAYER BURSTING
      (LOCAL WALL LAYER BREAKDOWN, INTERACTION)

2. ESTABLISH DYNAMICAL PICTURE

    - CONTROL ISSUES?

APPROACH

- UNDERSTAND RELEVANT BASIC PHYSICAL PROCESSES

- IDENTIFY MOST BASIC ELEMENT OF TURBULENCE NEAR A SURFACE

- ANALYSIS IS ASYMPTOTIC FOR LARGE RE

(a) Symmetric   (b) Asymmetric

<u>HAIRPIN VORTEX</u>

UNDERSTAND INTERACTIONS WITH

     (1) THE SURFACE FLOW

     (2) THE BACKGROUND SHEAR FLOW

     (3) EACH OTHER

THEN IT IS POSSIBLE TO INTERPRET OBSERVED BEHAVIOR IN TRANSITION
AND THE TURBULENT WALL LAYER.

REGENERATION

- THE PRODUCTION OF NEW TURBULENCE

- RELEVANT EVENTS IN TRANSITION AND TURBULENT BOUNDARY LAYERS ARE UNSTEADY SEPARATION OF THE SURFACE LAYER

VORTEX MOTION <u>PROVOKES</u> SURFACE LAYER ERUPTIONS $\Rightarrow$ NEW HAIRPIN VORTICES

BENEFITS

1. MEAN-FLOW PREDICTION (WALL LAYER)

   ATTACHED FLOW ON EXTENDED SURFACES

   $\Rightarrow$ ALGORITHMS FOR   (A) HEAT TRANSFER
                                       (B) SUPERSONIC BOUNDARY LAYERS
                                       (C) 3-D BOUNDARY LAYERS

2. CONTROL

   - ENHANCEMENT (HEAT TRANSFER, MIXING)

   - SUPPRESSION (DRAG AND NOISE REDUCTION)

SUMMARY

1. GENERIC ERUPTIVE PHENOMENON
   (VORTEX-INDUCED SURFACE-LAYER ERUPTIONS)

   $\Rightarrow$ VORTICITY CONCENTRATIONS NEAR SURFACE

   $\Rightarrow$ AN ABRUPT, DISCRETE ERUPTION

2. VORTICITY FIELD ABOVE THE SURFACE

   $\Rightarrow$ GROWTH TO LARGER SCALE

3. WALL-LAYER STREAKS

4. REGENERATION OF HAIRPIN VORTICES NEAR THE SURFACE

VORTEX INTERACTIONS WITH WALLS

- ALL VORTICES NEAR A SURFACE INDUCE AN ADVERSE
  PRESSURE GRADIENT IN THE NEAR-WALL FLOW

- AT HIGH RE, THIS PROVOKES SEPARATION OF THE SURFACE
  LAYER

$\Rightarrow$ A GENERIC EVENT IN TWO (OR THREE) DIMENSIONS

VORTICITY NEAR THE SURFACE IS ABRUPTLY COMPRESSED
ALONG A NARROW STREAMWISE BAND AND LEAVES THE SURFACE
IN A SHARPLY-FOCUSED SPIKE (DOUBLE-SIDED SHEAR LAYER)

$\Rightarrow$ A VISCOUS-INVISCID INTERACTION IN WHICH "PARCELS" OF
VORTICITY ARE EJECTED INTO THE EXTERNAL FLOW

General Sequence of Events

Stage 1 - Triggering Phase

An adverse pressure gradient leads to the evolution of recirculation in surface flow (1st MRS condition)

$\Rightarrow$ zero vorticity line (2-D)
zero vorticity surface (3-D)
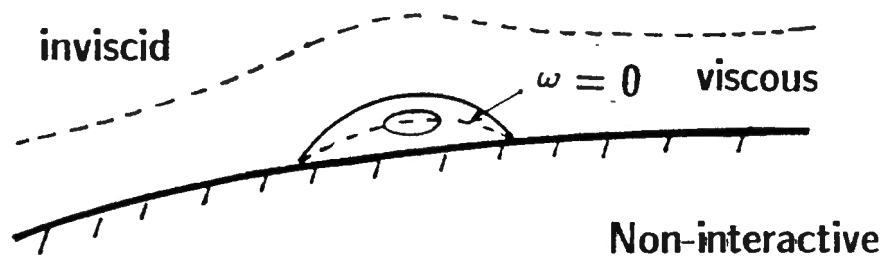
Stage 2 - Separation

Focussing and concentration of surface layer vorticity

$\Rightarrow$ outward moving spike
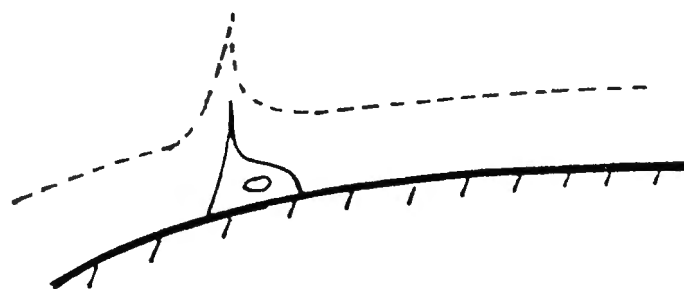
Onset of Interaction

- sharp local pressure changes

developing narrow-band eruption (localized)

Stage 3 - Strong Interaction

Double-sided vorticity layer leaves the surface; a window opens in boundary layer

eruptive layer
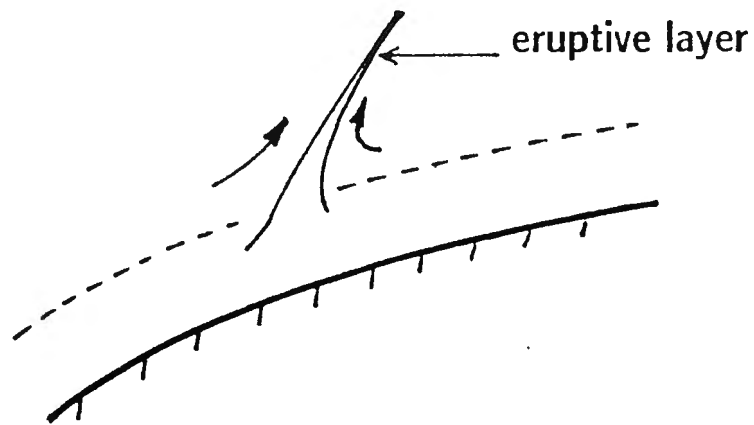
Stage 4 - Inviscid Interaction

Roll-Up
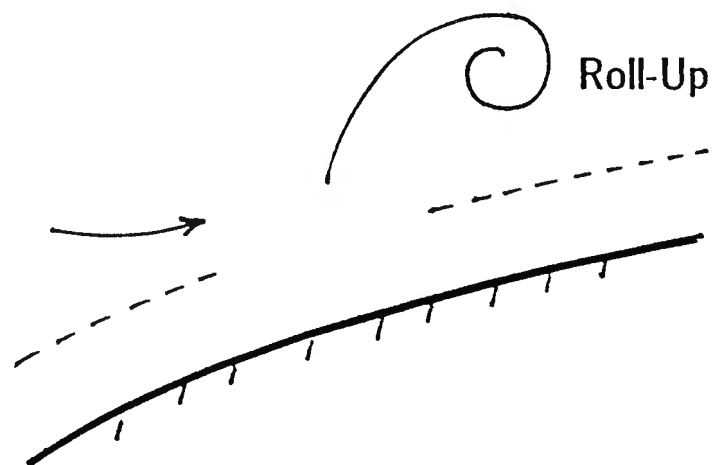
Last three stages involve moving
fronts of concentrated vorticity
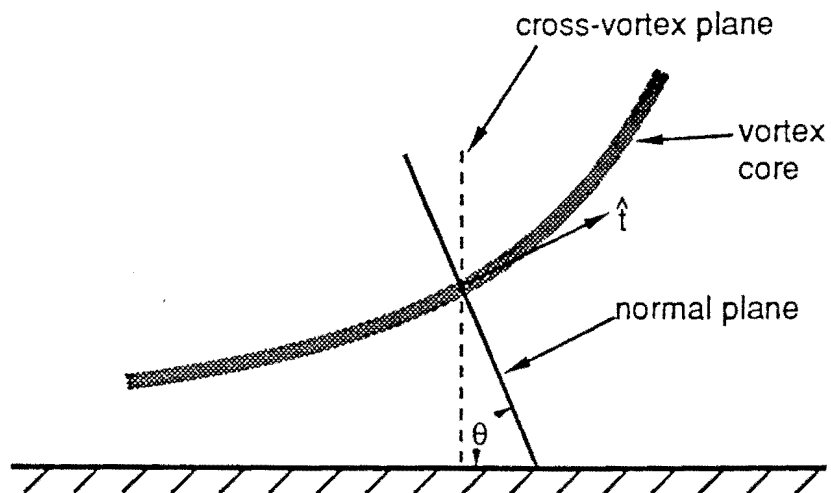
Figure 2. Instantaneous flow induced by a vortex near a wall in a frame of reference moving with the vortex core and in the cross-vortex plane: (a) instantaneous streamline patterns (... possible spiral motion), (b) flow speed, pressure, and pressure gradient induced near the surface, (c) the cross-vortex plane.

2(a)

2(b)

$$\longleftarrow U_\infty(s) , \quad \frac{dP_\infty}{ds} > 0$$

$$\longleftarrow U_\infty(s) , \quad \frac{dP_\infty}{ds} > 0$$

(a) The evolution of recirculation near the surface

(b) Eddy growth

(c) Focussing and compression; solid lines denote the equi-vorticity contours in the surface layer; arrows indicate compression of the erupting spike
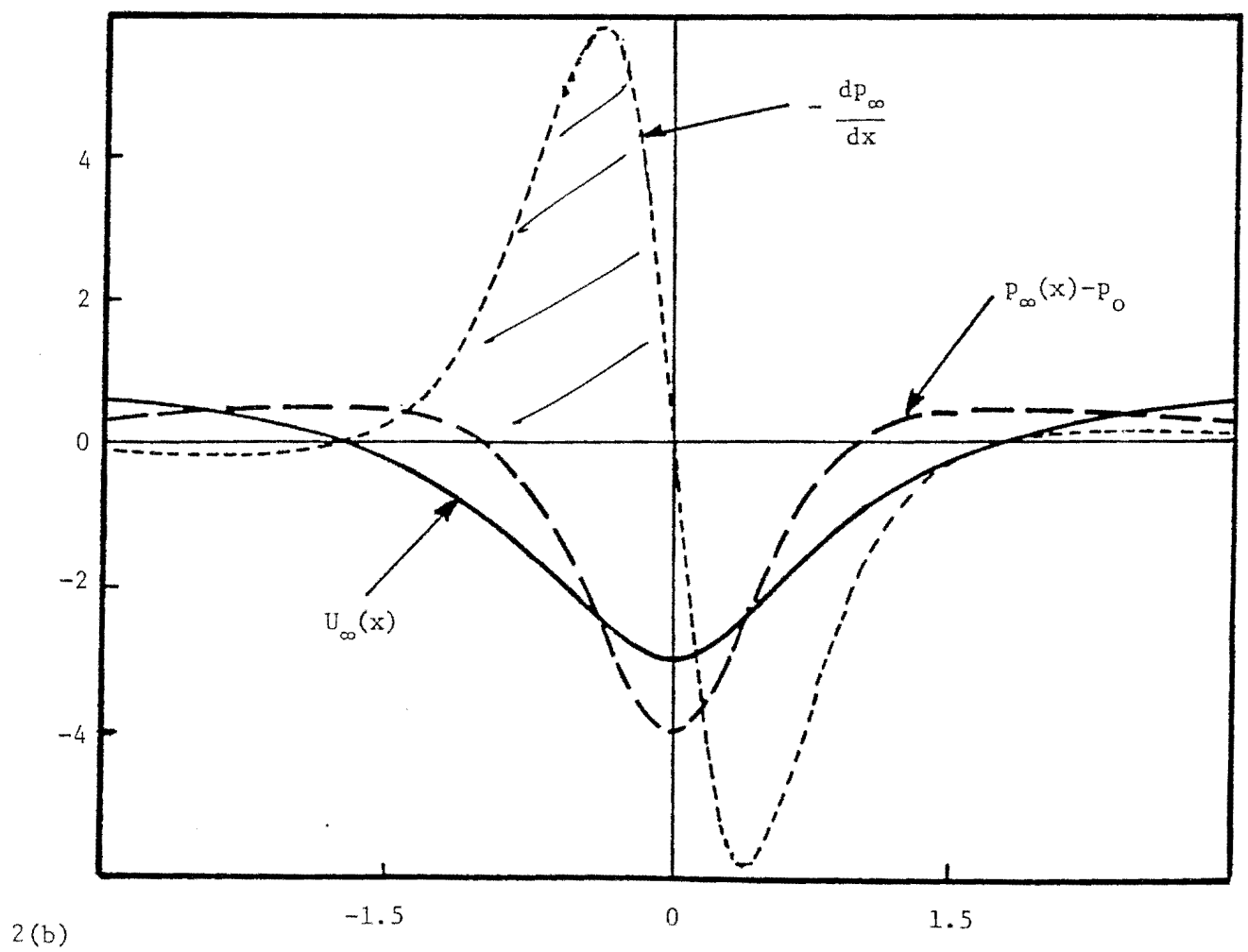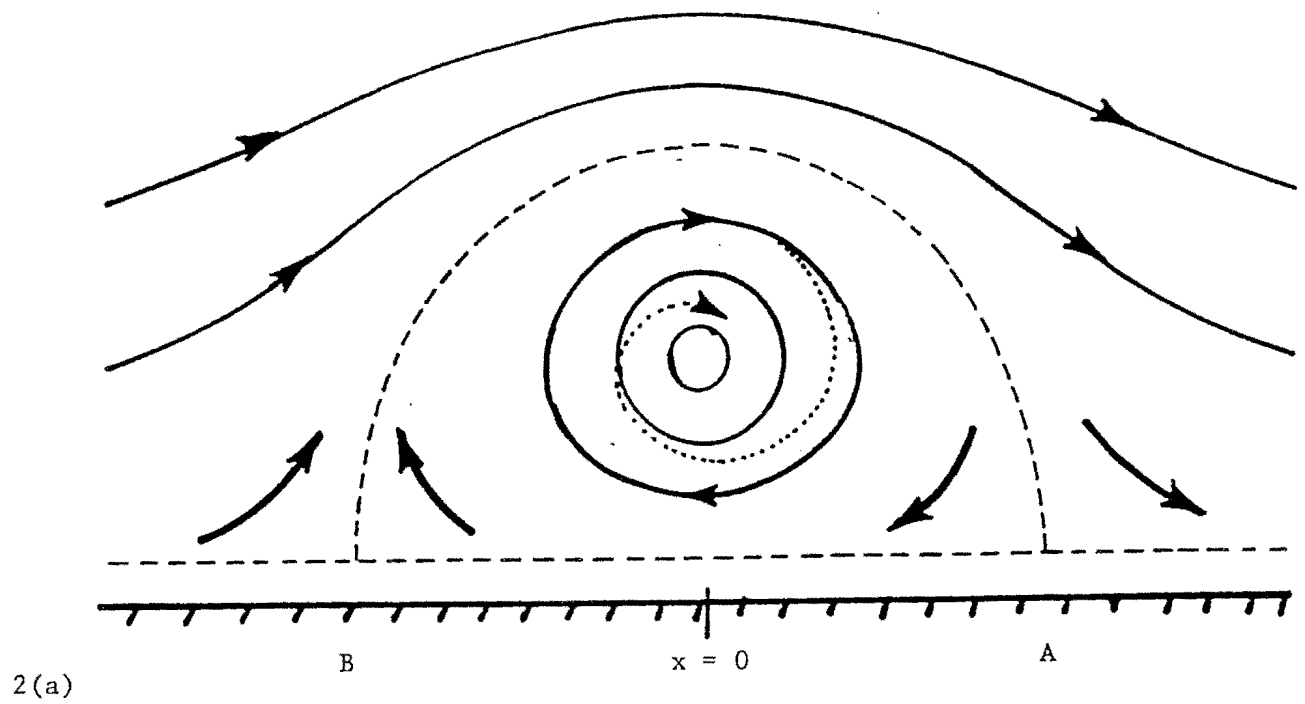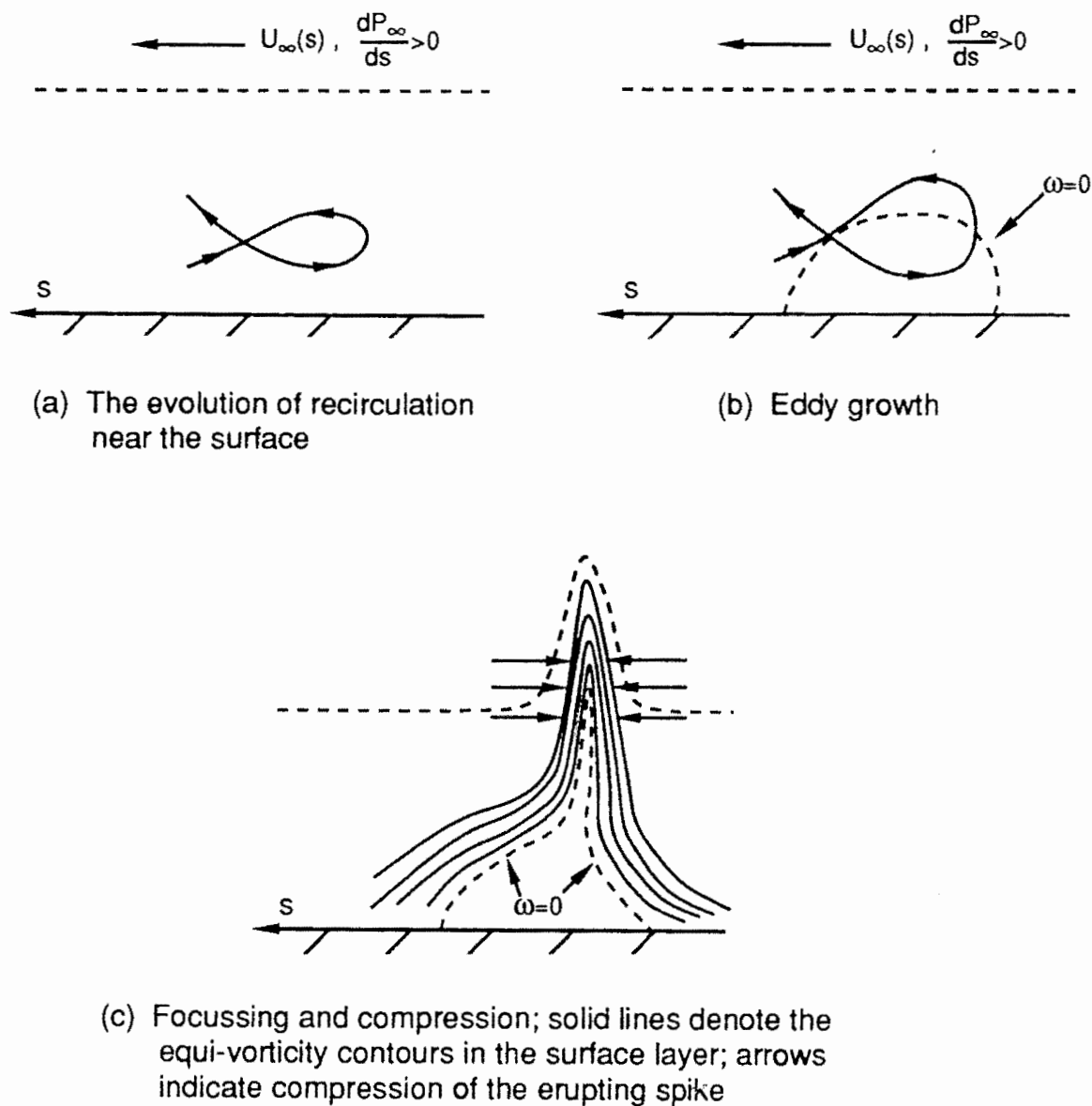
Figure 3. Schematic diagram of the stages in the separation of a two-dimensional surface layer (not to scale).

(a)

$t = 0.25$

(b)

$t = 0.45$

(d)

$t = 0.989$

2.1-20
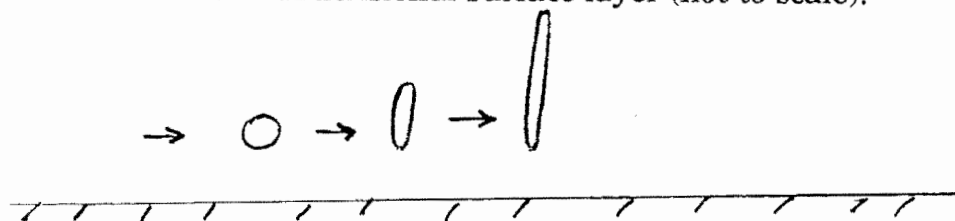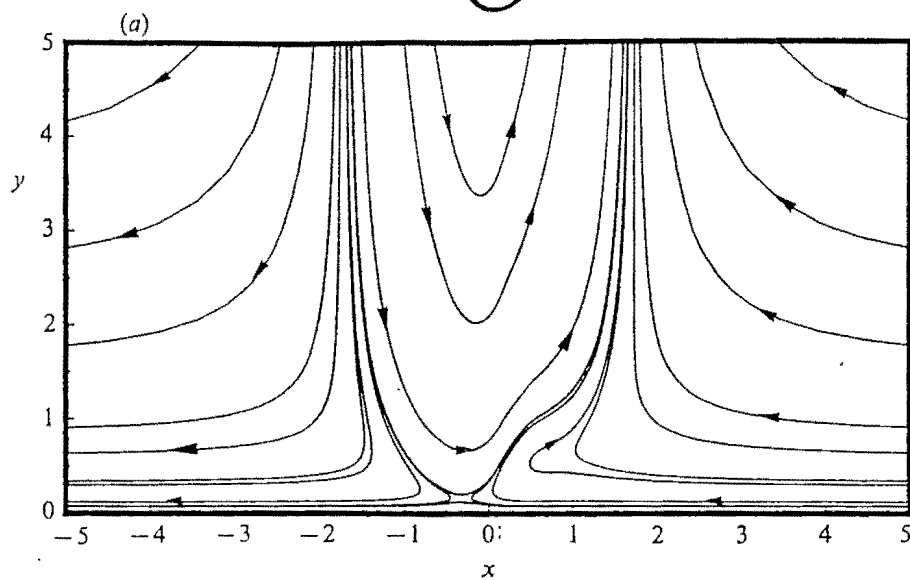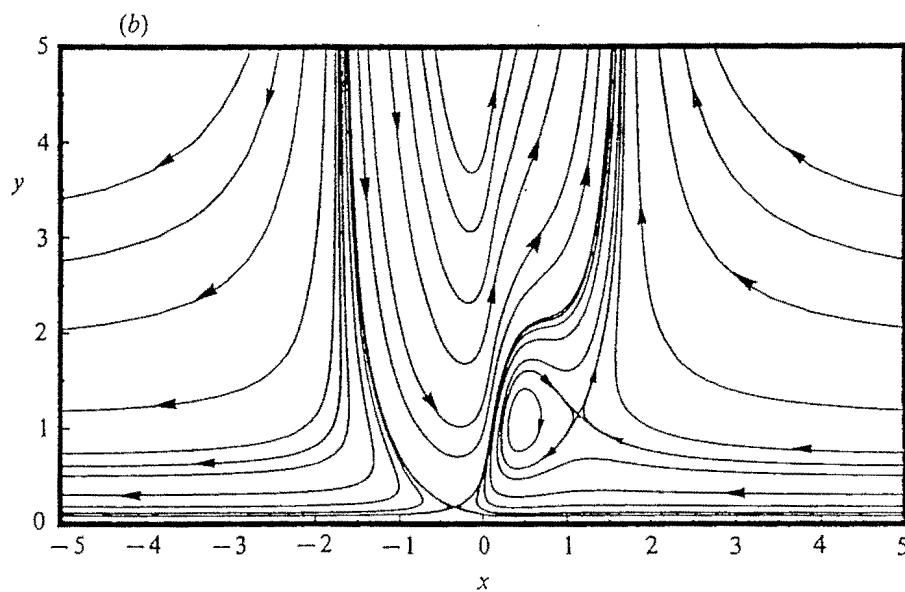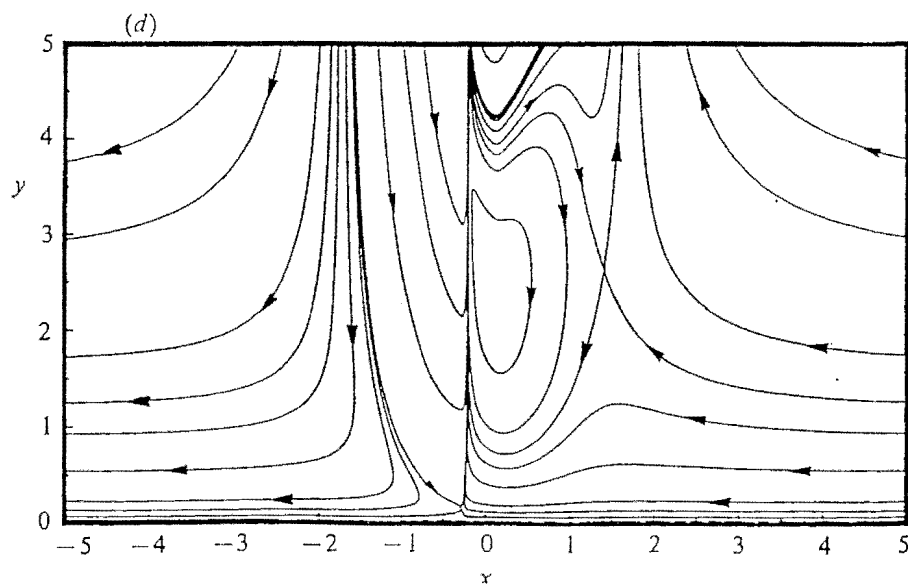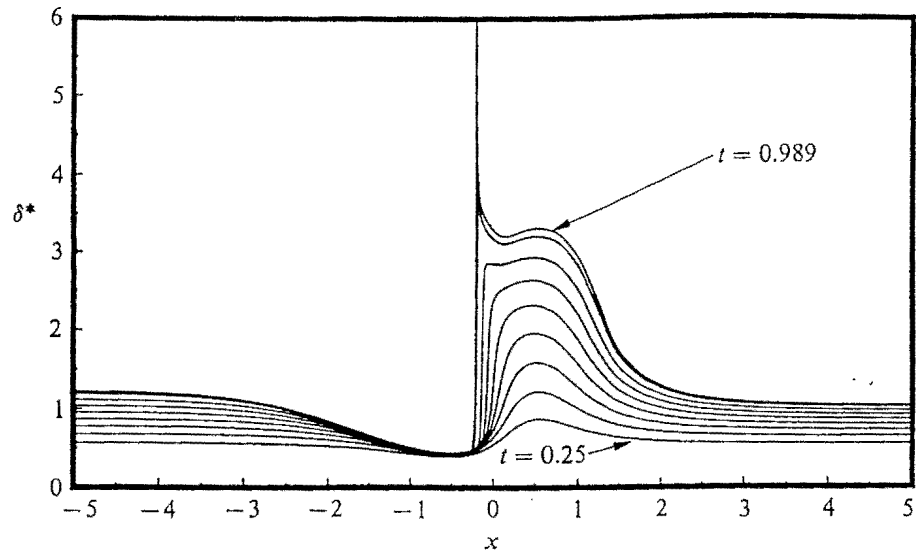
FIGURE 4. Temporal development of the displacement thickness; plotted curves are at $t = 0.25$ (0.10) 0.95 and $t_s = 0.989$.
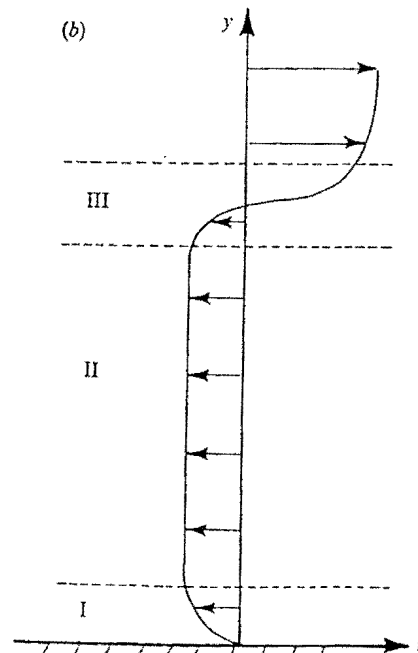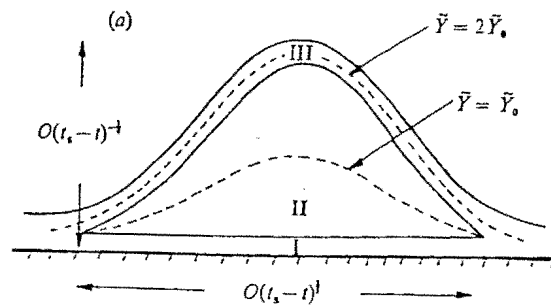
FIGURE 5. Schematic of boundary-layer structure near a point of eruption. (a) Structure near x_s (not to scale); (b) a typical velocity profile near $x = x_s$ (for a stationary wall).
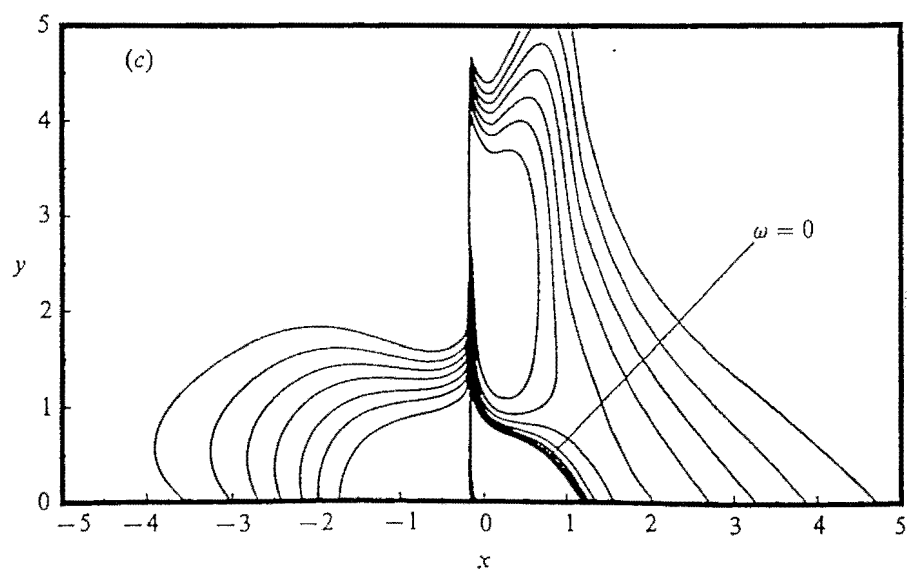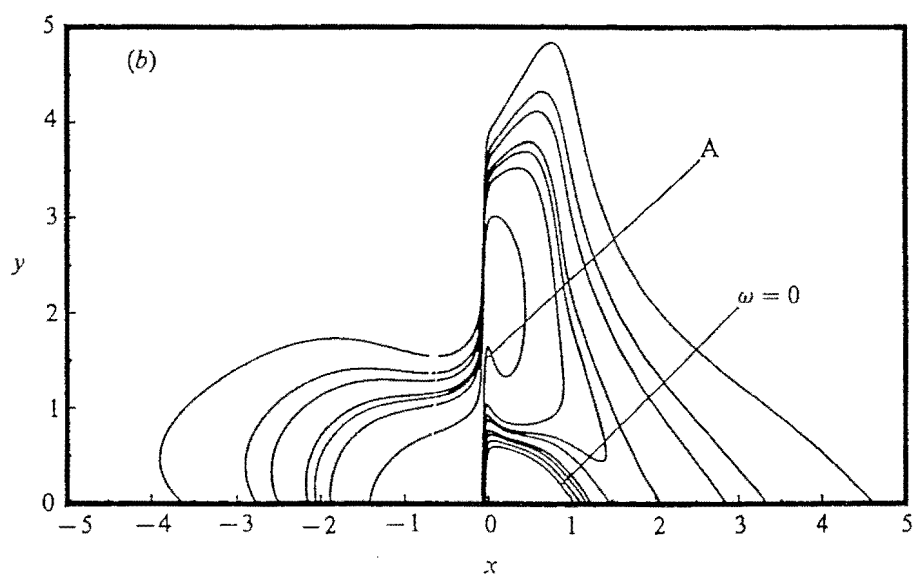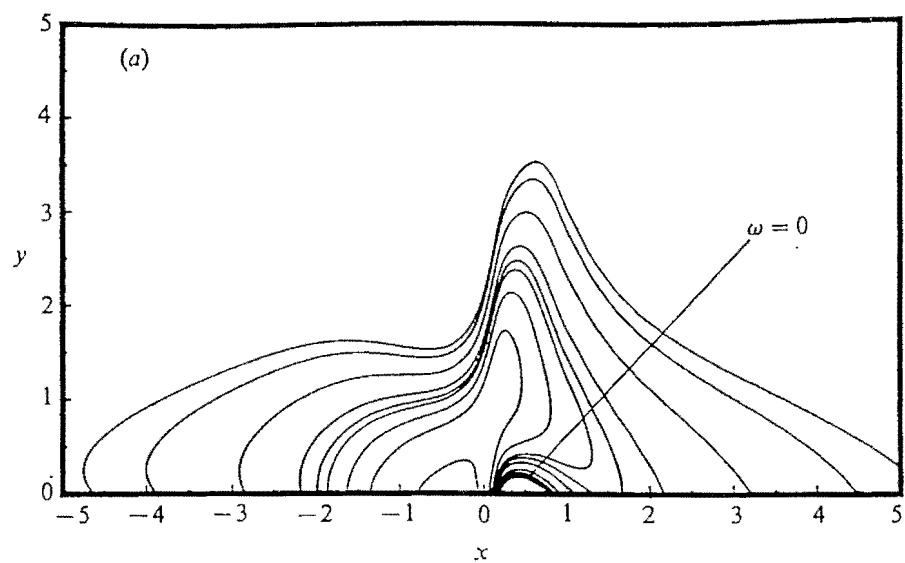
FIGURE 6. Evolution of the constant-vorticity contours. (a) $t = 0.45$; (b) $t = 0.75$; (c) $t = 0.95$.

(a)

(b)

lateral motion of
streamwise vortices

streamwise vortices

cylinder

vortex-induced surface eruptions

(c)

(d)

(e)

(f)
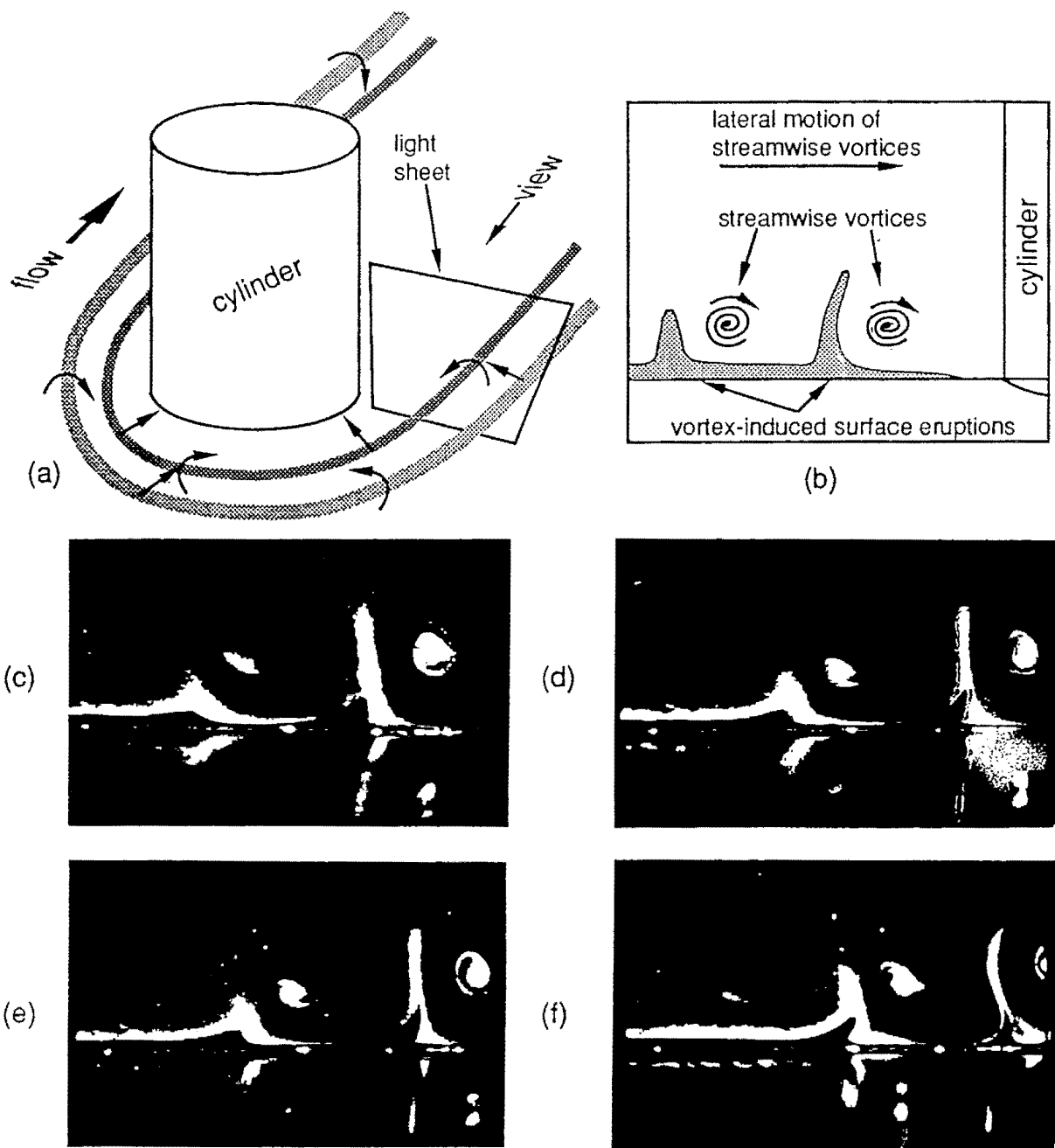
A temporal sequence of end-view photographs illustrating
streamwise necklace vortex legs and associated surface eruptions

Figure 5. End-view of necklace vortex legs and induced surface eruptions.
Visualization using hydrogen bubbles and light-sheet illumination.
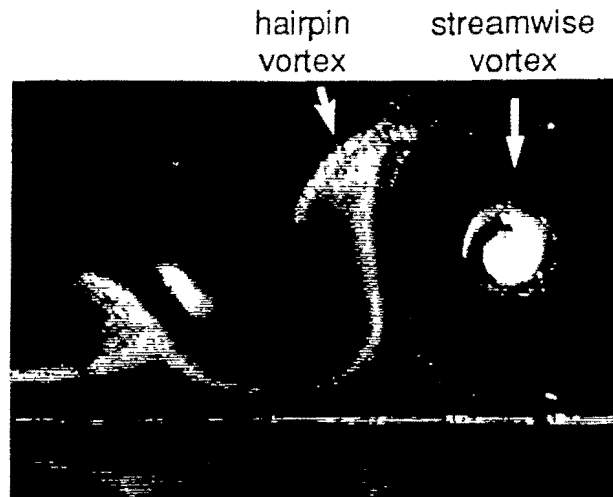
a) End-view, light-sheet photograph showing the breakdown of an eruptive spire (low-speed ridge) induced by a streamwise necklace vortex leg.
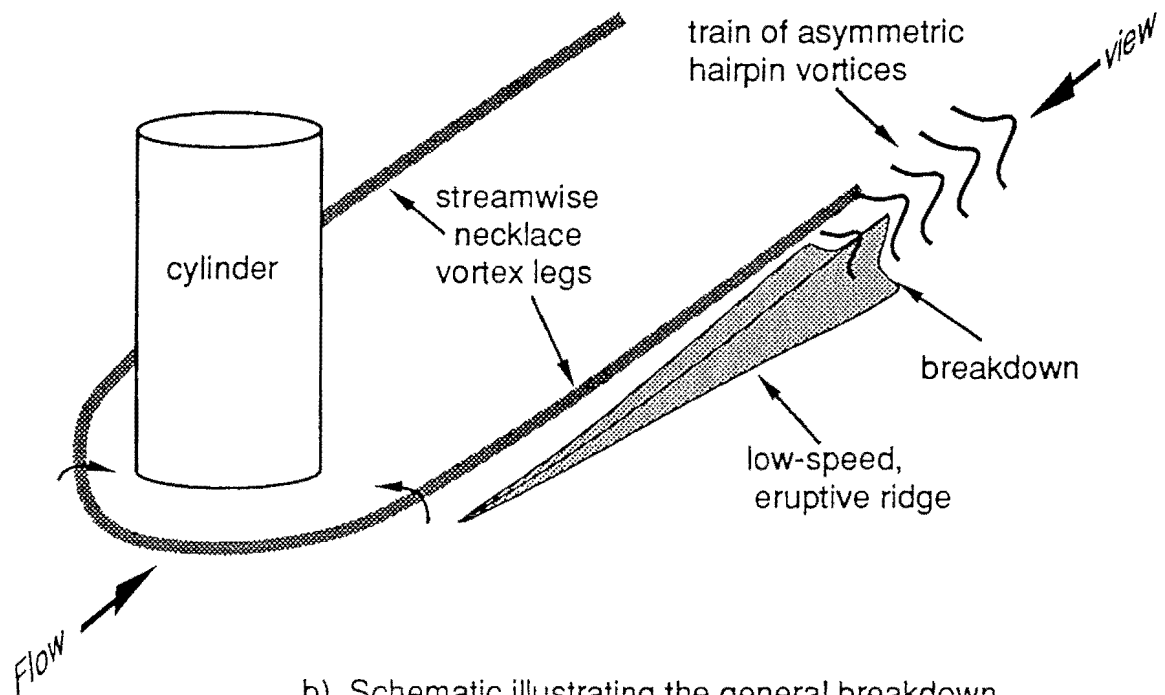
b) Schematic illustrating the general breakdown process for the low-speed, eruptive ridge.

Figure 20.   Characteristics of the breakdown of the eruptive spires induced by streamwise necklace vortex legs.

BIOT - SAVART

$$\frac{\partial \vec{X}_i}{\partial t} = - \sum_{i=1}^{N} \epsilon_i \int_{C_i} \frac{(\vec{X}_i - \vec{x}) \wedge d\vec{x}}{\{|\vec{X}_i - \vec{x}|^2 + \mu^2\}^{3/2}} + U_{ext}(y)\hat{j}$$

$$+ \sum_{i=1}^{N} \epsilon_i \int_{\overline{C}_i} \frac{(\vec{X}_i - \vec{x}) \wedge d\vec{x}}{|\vec{X}_i - \vec{x}|^3}$$

$$\epsilon = \frac{\Gamma}{4\pi L U_0} = \frac{1}{2} sgn(\Gamma) \frac{Re_v}{Re}$$

$$Re_v = K/\nu \quad , \quad Re = \frac{U_0 L}{\nu}$$

Algorithms

Moore (1972), Hon & Walker (1987)

Callegari & Ting (1978), Liu et al (1985)

Hama (1962), Aref & Flinchem (1984)
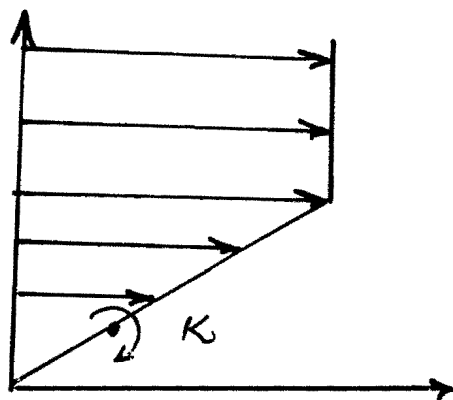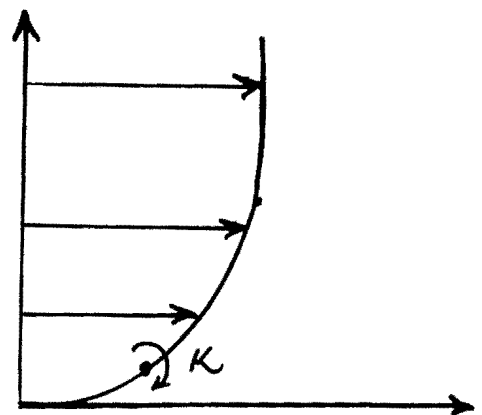
Linear Shear   Turbulent Profile
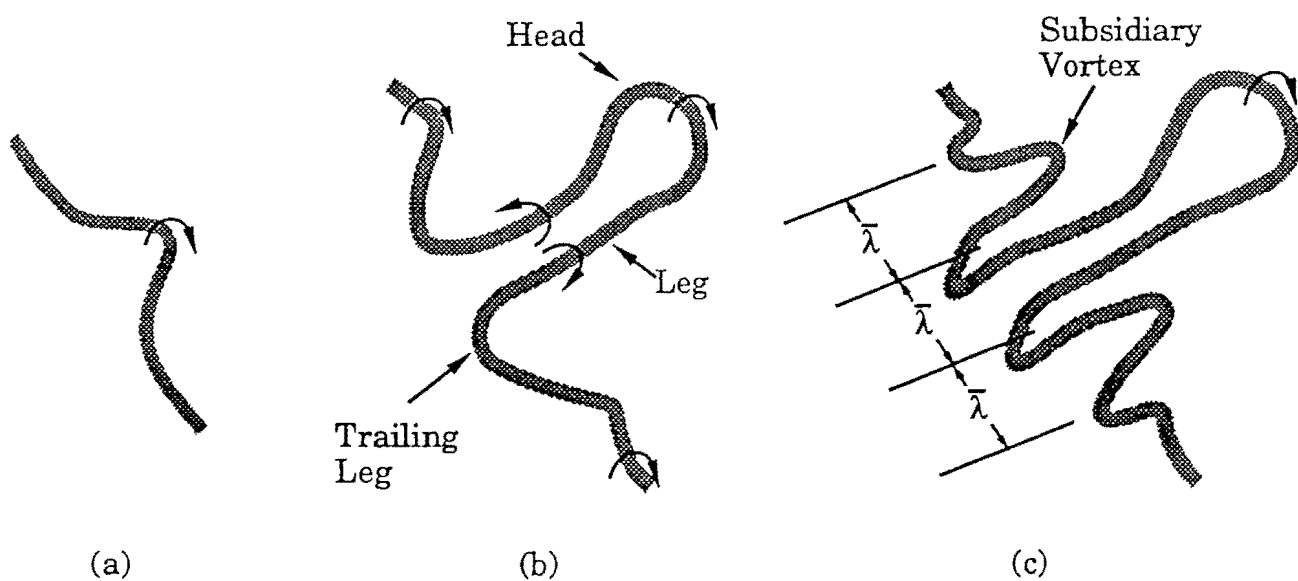
Figure 6. Evolution of a symmetric hairpin vortex in a shear flow.
(a) initial distortion, (b) development of vortex legs and head,
(c) evolution of subsidiary vortices and penetration toward the
surface.
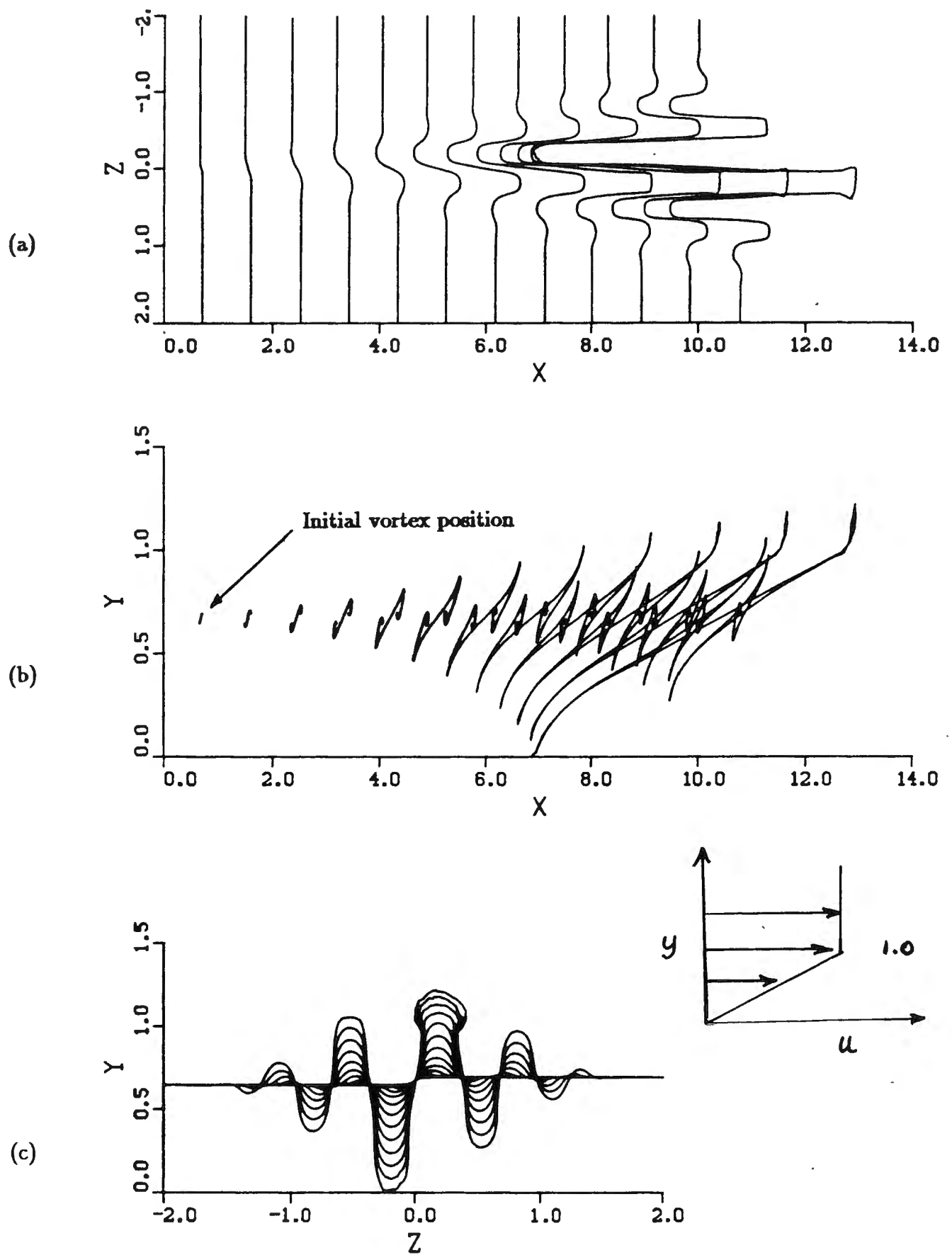
Figure 8. Evolution of a small "step" in a two-dimensional vortex convected in a uniform shear flow: (a) top view, (b) side view, (c) end view; $\epsilon = 0.00267$, 440 time steps with $\Delta t = 0.034$. The vortex position is plotted every 40 time steps.

(a)

(b)

Initial vortex position

(c)
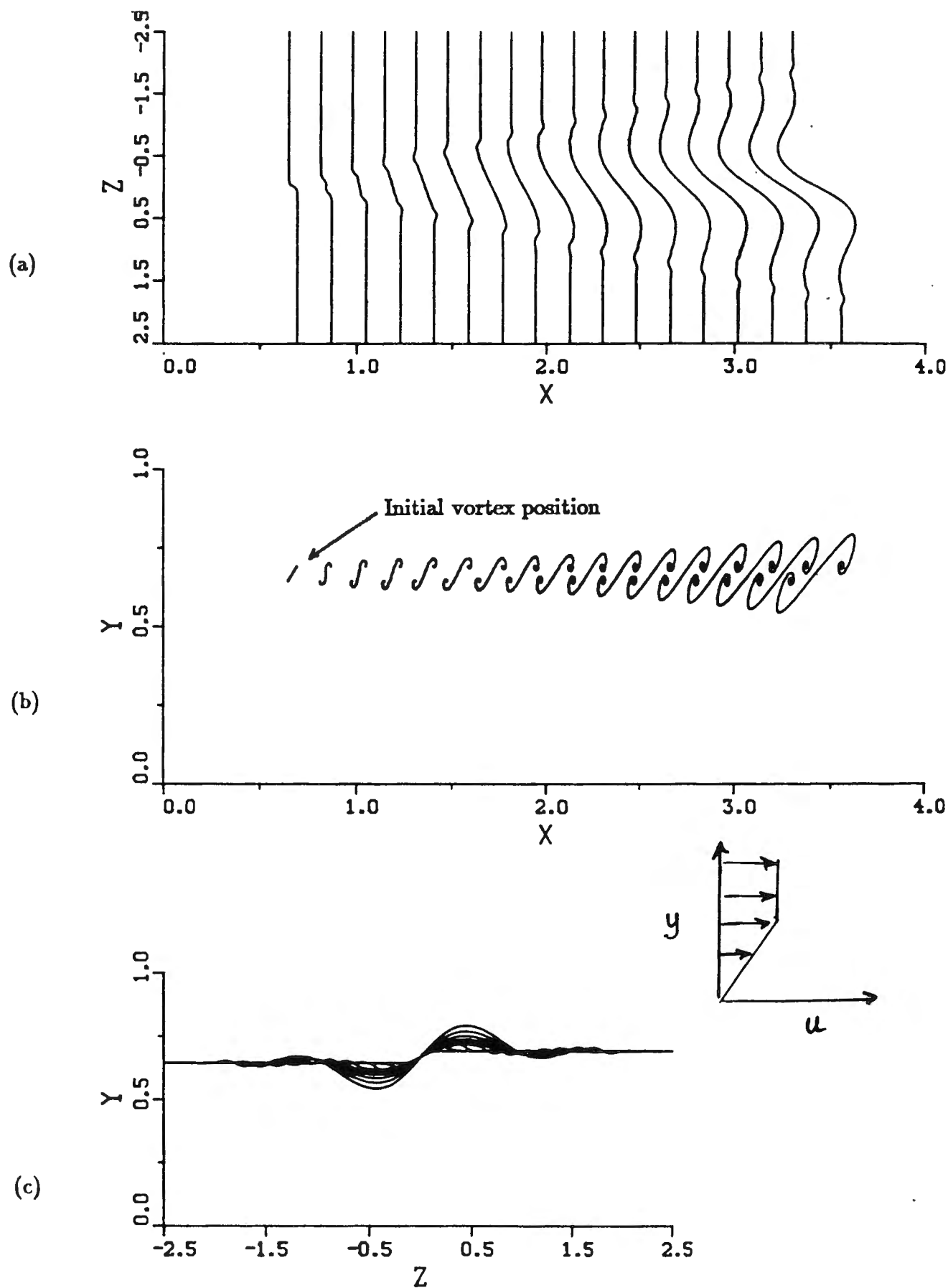
Figure 9. Evolution of an asymmetric hairpin for a reduced level of uniform shear: (a) top view, (b) side view, (c) end view; $\epsilon = 0.00134$, 640 time steps with $\Delta t = 0.0067$. The vortex position is plotted every 40 time steps.

2.1-28
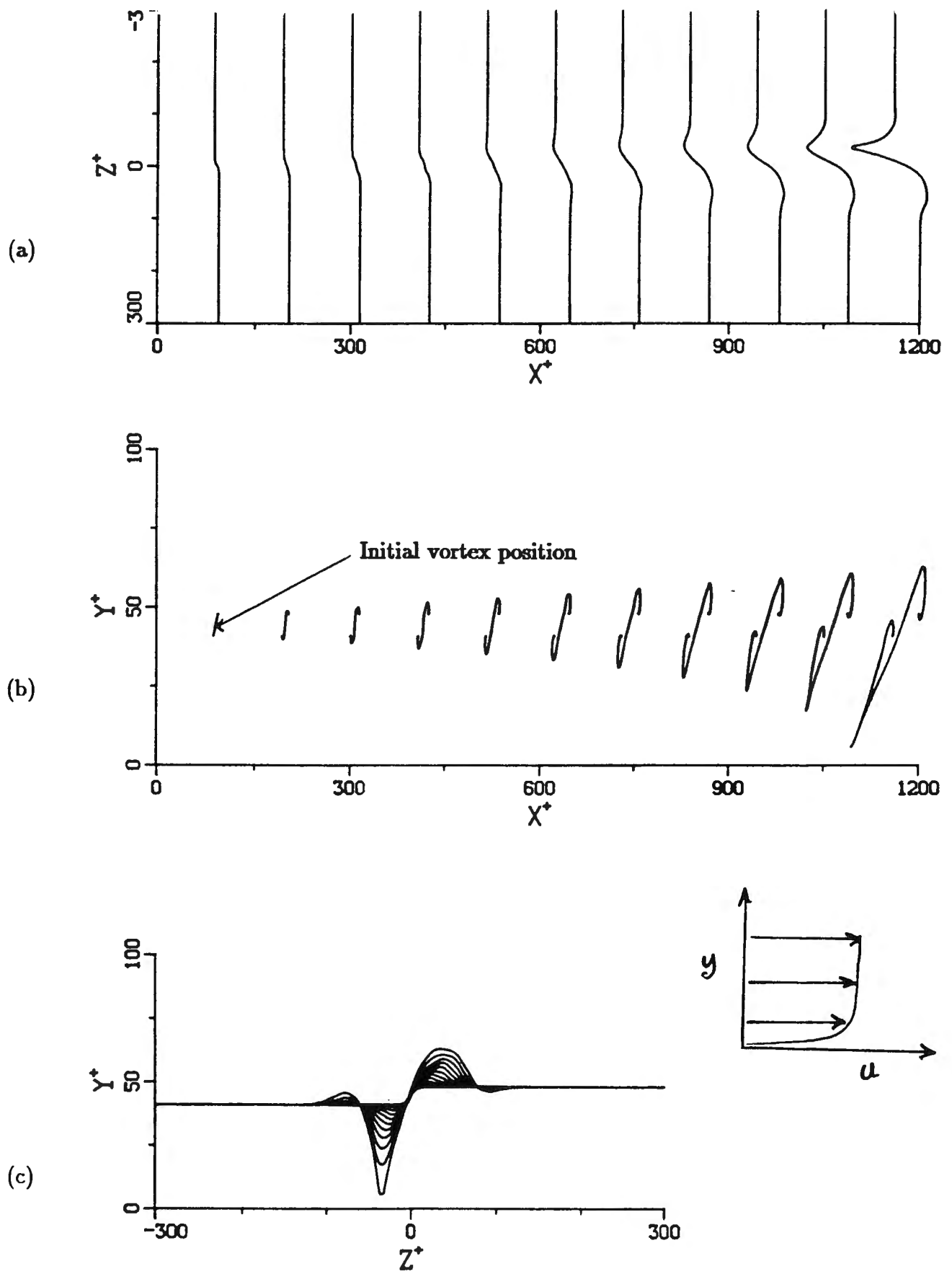
Figure 10. Evolution of an asymmetric hairpin vortex in a turbulent mean profile: (a) top view, (b) side view, (c) end view; $\epsilon = 0.0013$, 400 time steps with $\Delta t = 0.016$. The vortex position is plotted every 40 time steps.
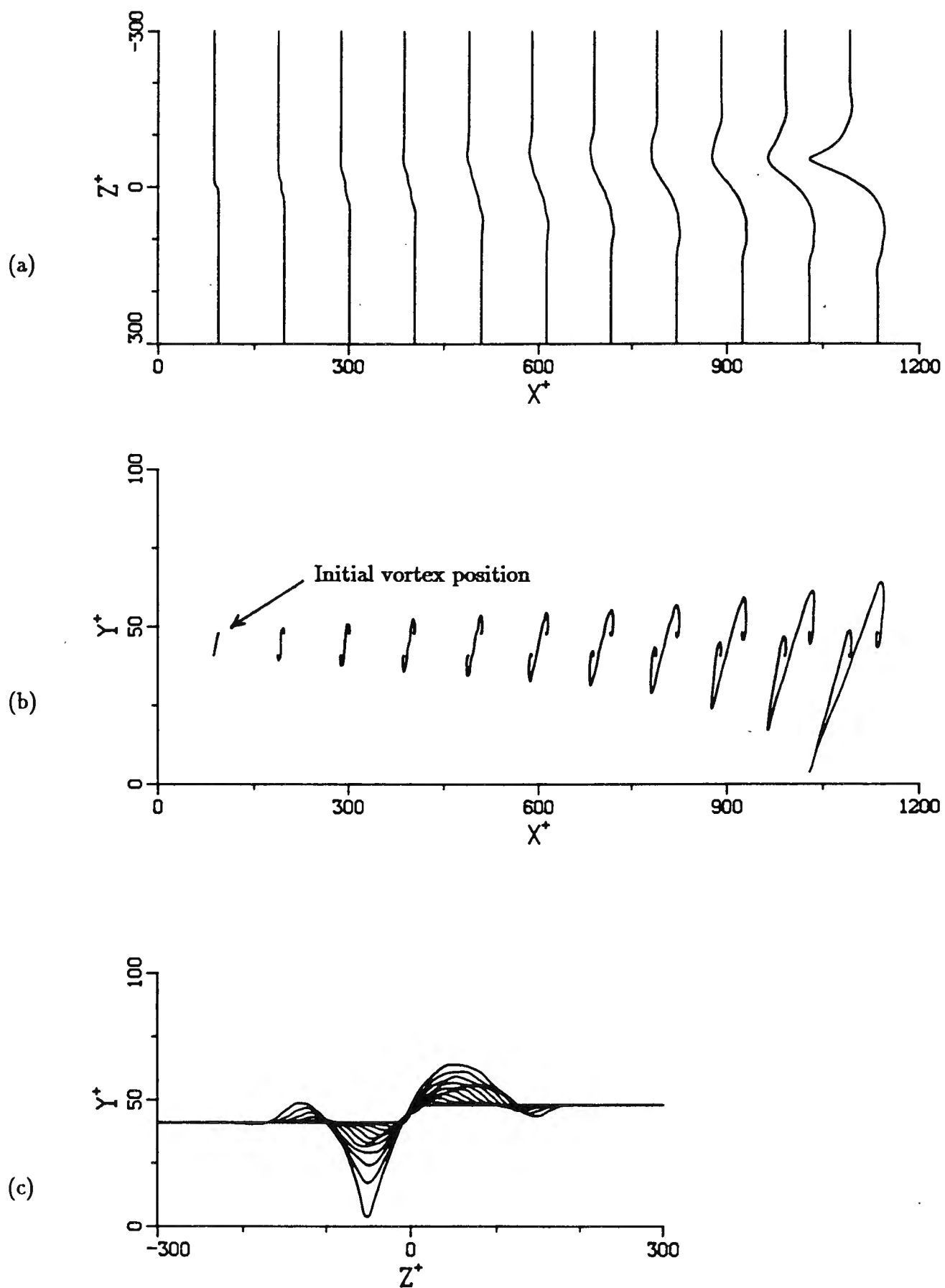
Figure 11. Evolution of an asymmetric hairpin vortex in a turbulent mean profile: (a) top view, (b) side view, (c) end view; $\epsilon = 0.0025$, 380 time steps with $\Delta t = 0.016$. The vortex position is plotted every 38 time steps.
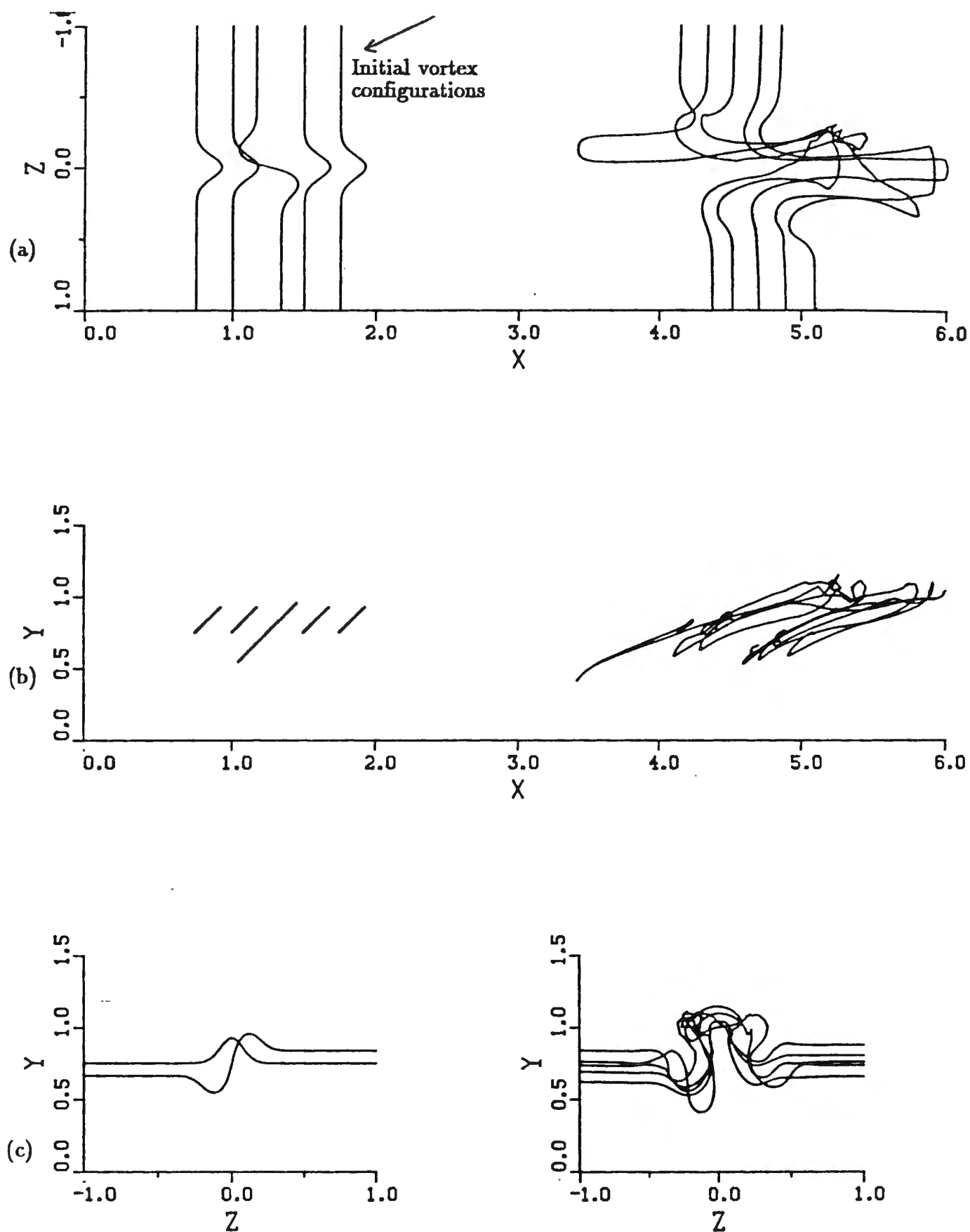
Figure 12. Evolution of multiple hairpin vortices in a uniform shear: (a) top view, (b) side view, (c) end view; all three coordinates are plotted on the same scale.
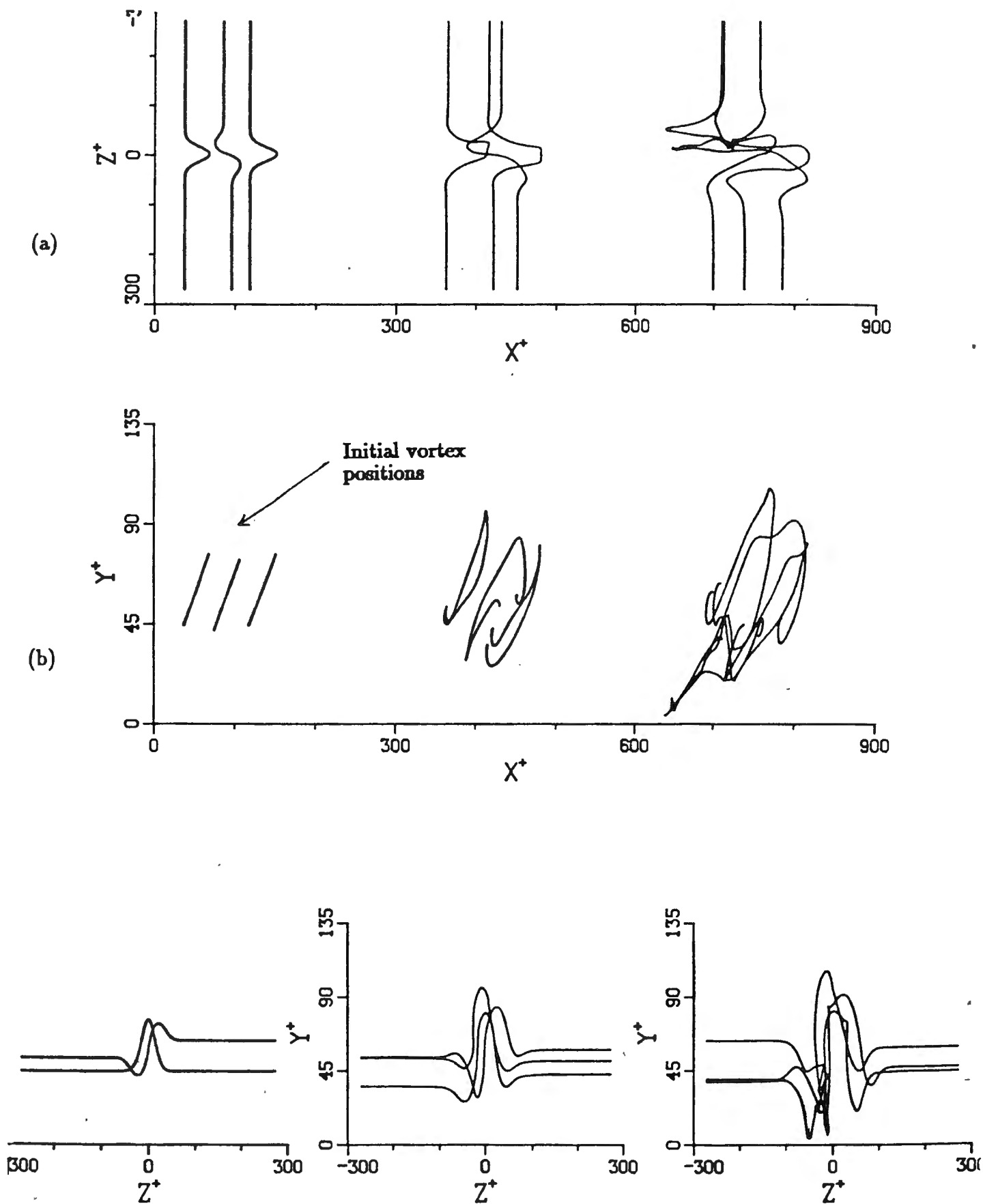
Figure 13. Evolution of three vortices in a turbulent mean profile: (a) top view, (b) side view, (c) end view; $\epsilon = 0.0013$, vortices shown after 120 and 240 time steps with $\Delta t = 0.016$.
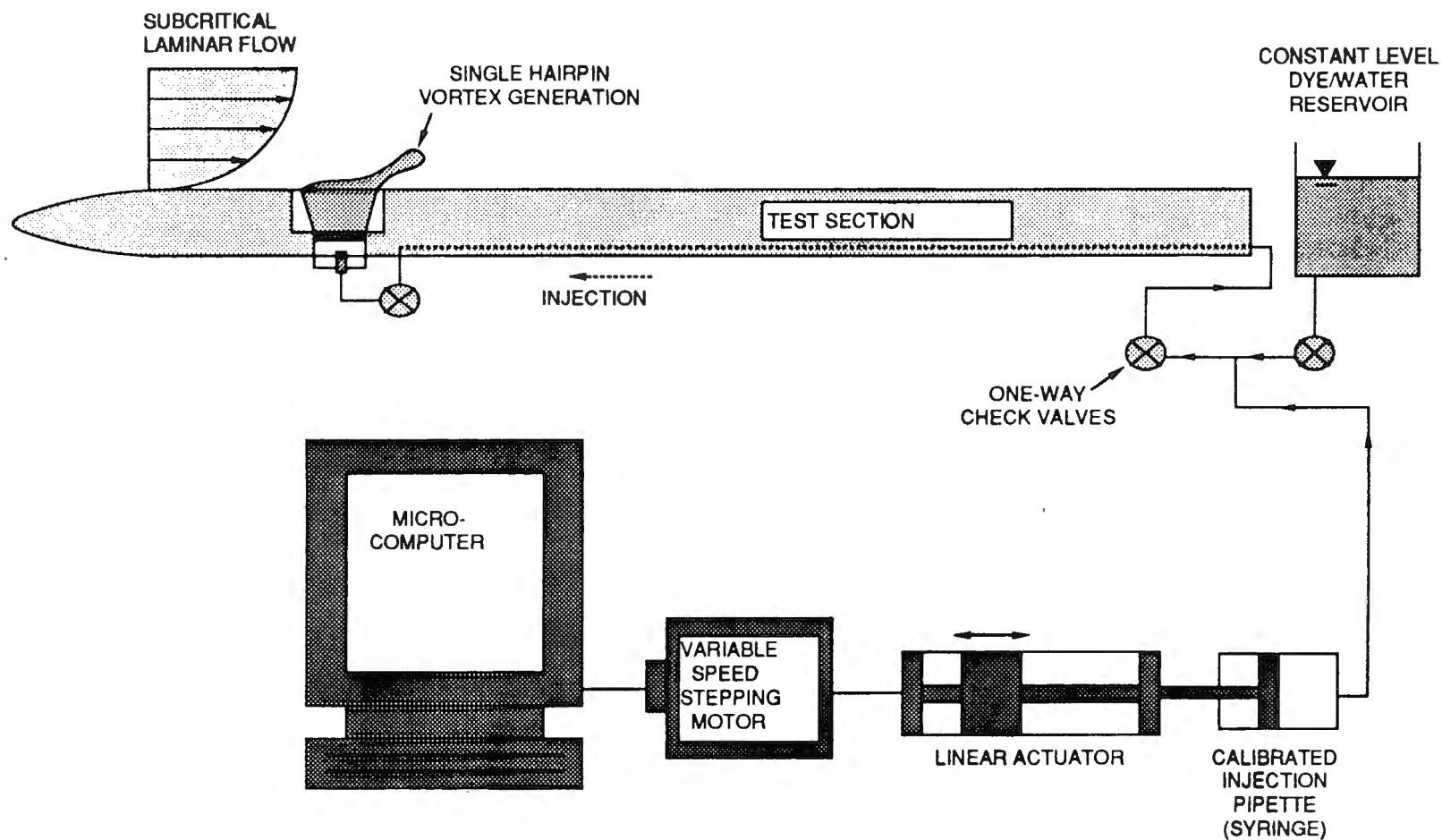
Figure 14. Experimental system for generating single hairpin vortices using controlled injection through a narrow streamwise slot into a subcritical laminar boundary layer.

LEGS

FLOW ▸▸

PLAN-VIEW

HEAD

SIDE-VIEW

(a)

Leg

Head

Leg

FLOW ↗
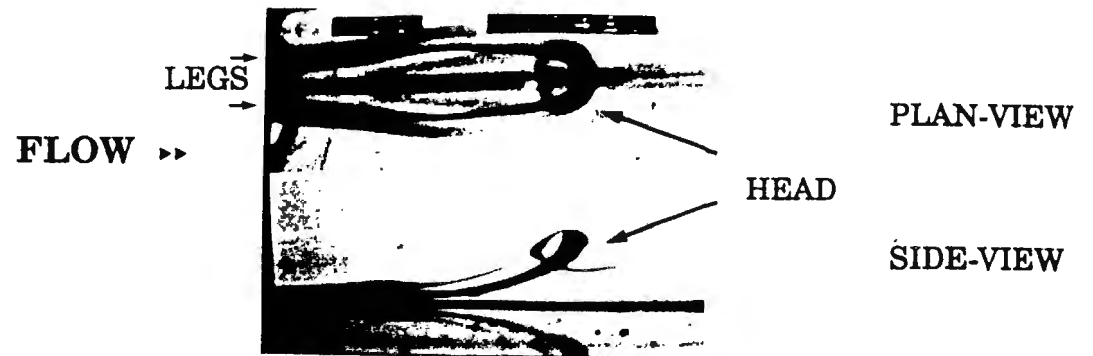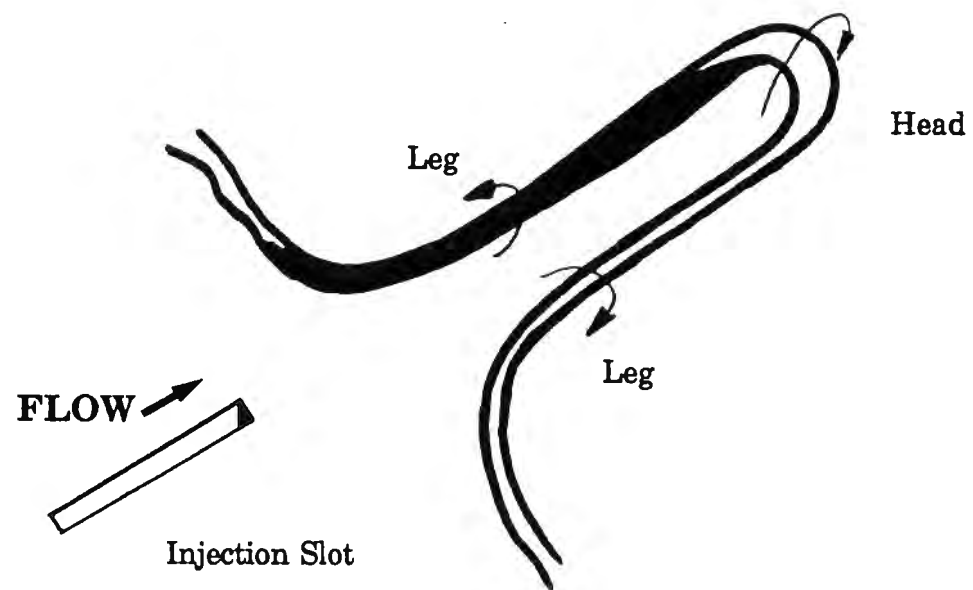
Injection Slot

(b)

Figure 15. Illustration of experimental generation of a single hairpin vortex by surface injection using system shown in figure 14. (a) Dual-view picture of dye-marked single hairpin vortex. (b) Isometric schematic of single hairpin after generation.
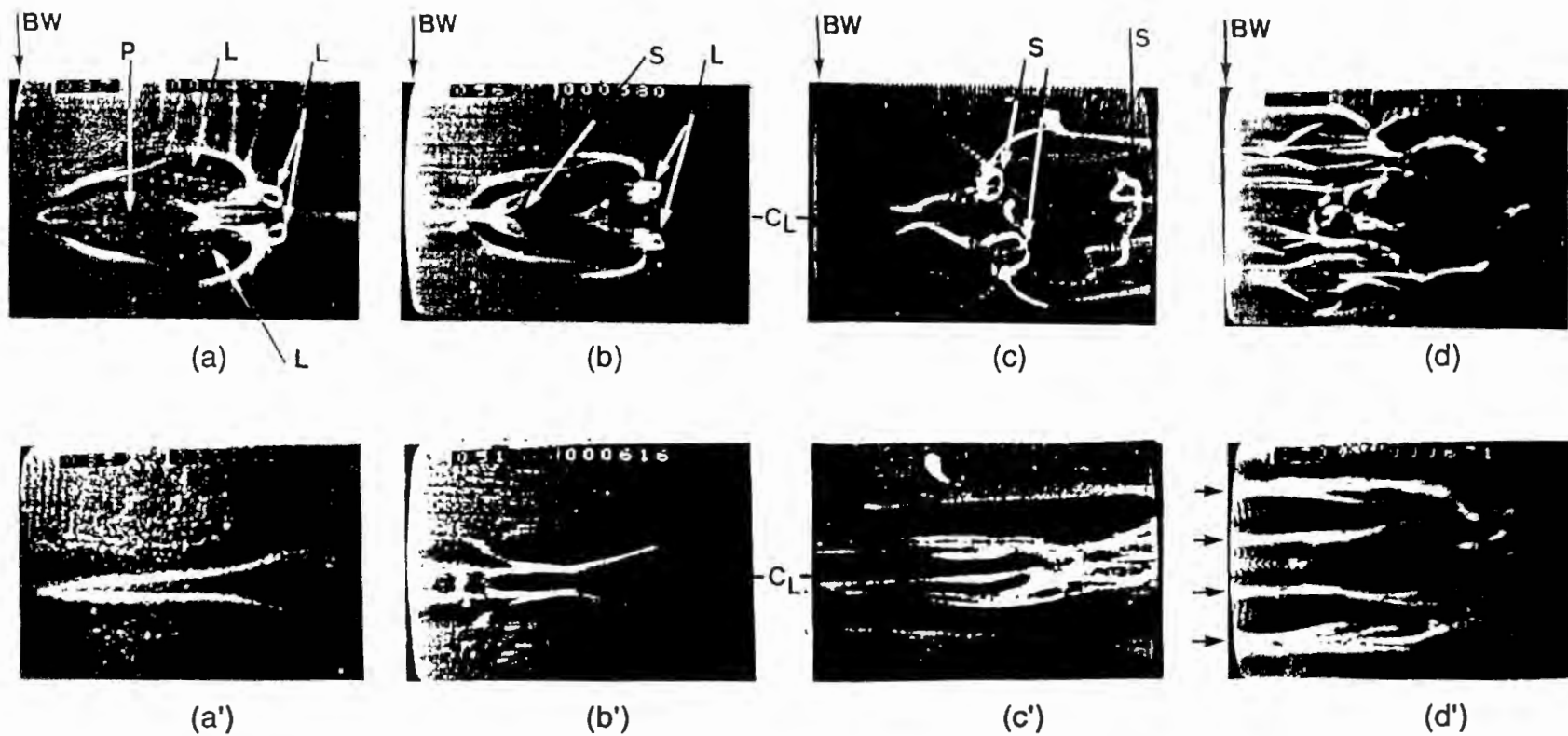
Figure 17. Dual-level, plan-view visualization of hydrogen bubble patterns generated by left-to-right passage of developing hairpin vortex (c.f. figure 16). BW denotes the position of the bubble wire, P the location of an initial "pocket" formation (Falco, 1991), L the location of the vortex legs, S the evolution of secondary hairpin vortices (see §5), and C_L the plane of symmetry. Bubbles are generated at $y/\delta=0.4$ for upper row visualizations, and $y/\delta=0.1$ for lower row visualizations.

deformation of time lines
indicating low-speed streak

cylinder

view

cylinder

flow

streamwise vortex leg

Flow
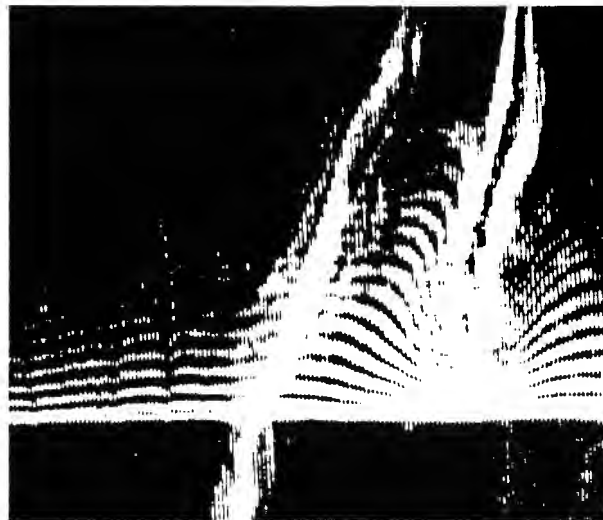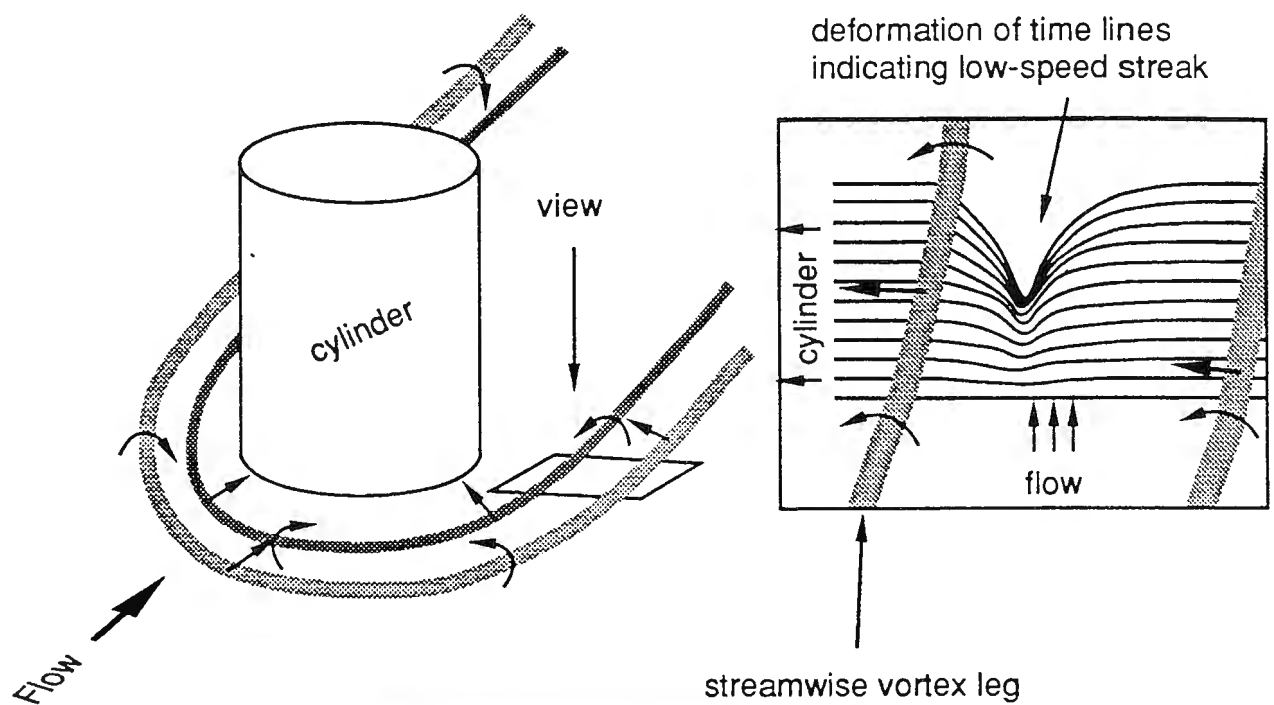
Plan-view photograph showing a streamwise necklace vortex
leg (visualized by upstream hydrogen bubble wire) interacting
with surface fluid (visualized by bubble wire near surface) to
create low-speed streak at surface.

Figure 18 Plan-view of necklace vortex leg interaction to create low-speed streak

Primary Hairpin

Interaction with Legs

Trailing Low-Speed Streak Regions

(a) Symmetric case with wide separation of legs

Interaction with Legs

Trailing Low-Speed Streak Region

(b) Symmetric case with legs closer together; the two streaks merge

Single-Leg Hairpin

Interaction with Leg

Trailing Low-Speed Streak Region

(c) Asymmetric case
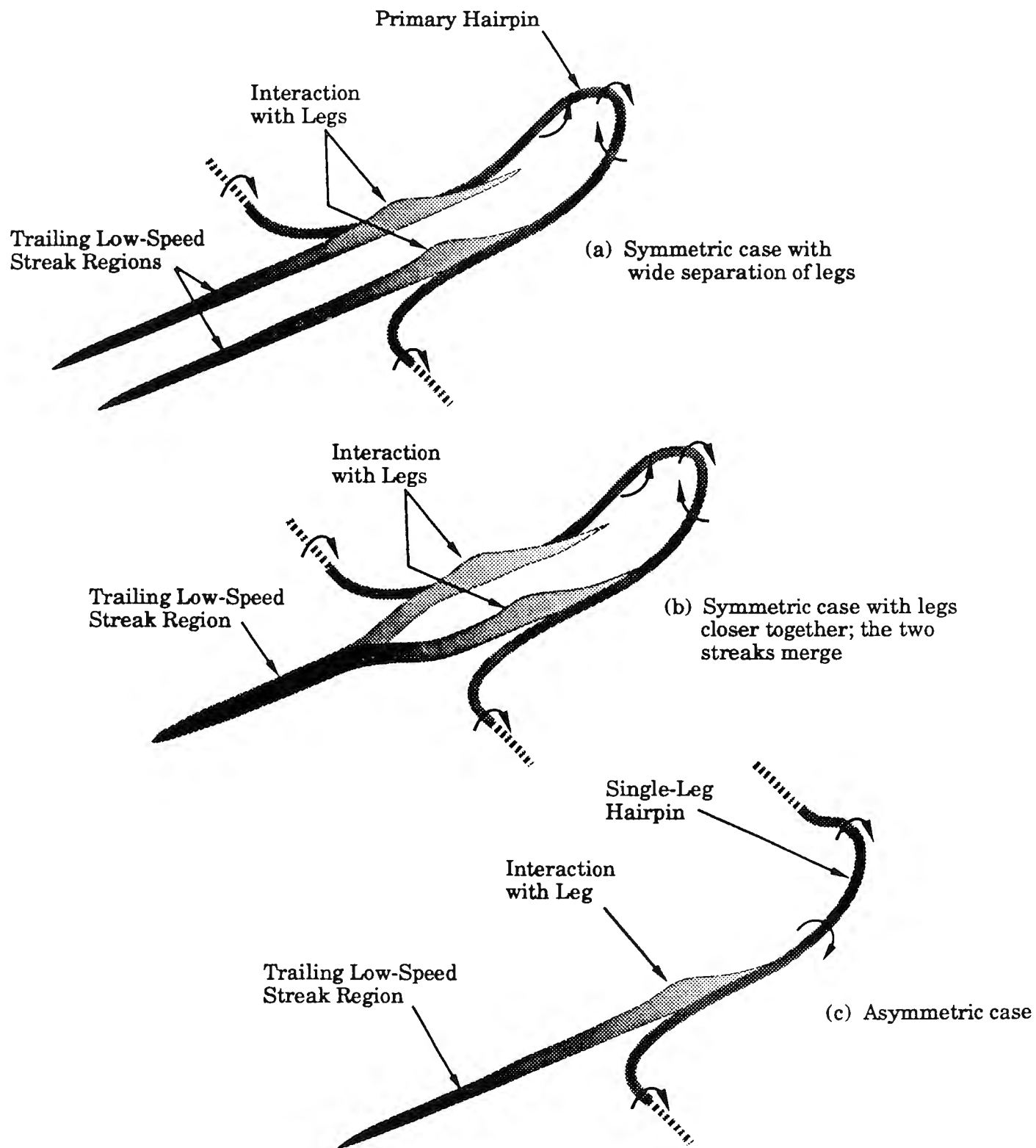
Figure 19. Schematic diagram of the processes whereby moving hairpin vortices induce low-speed streaks.

2.1-37
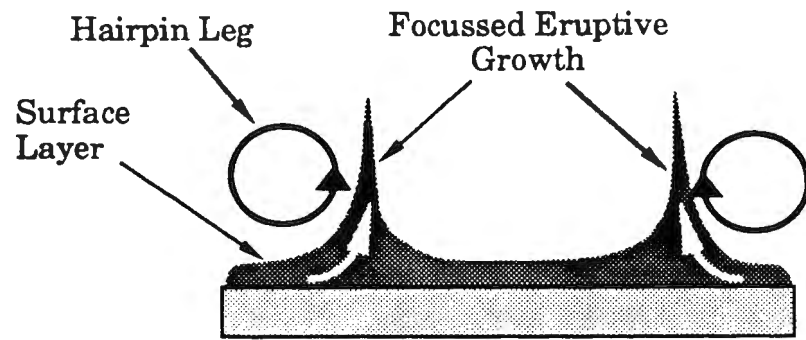
(a) Symmetric hairpin legs
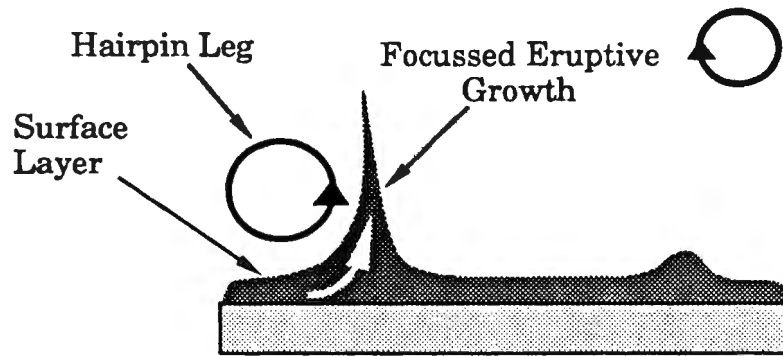
(b) Asymmetric hairpin legs

Figure 21. Schematic diagram of location of vortex-induced separation of the surface layer for symmetric and asymmetric hairpin vortex legs.
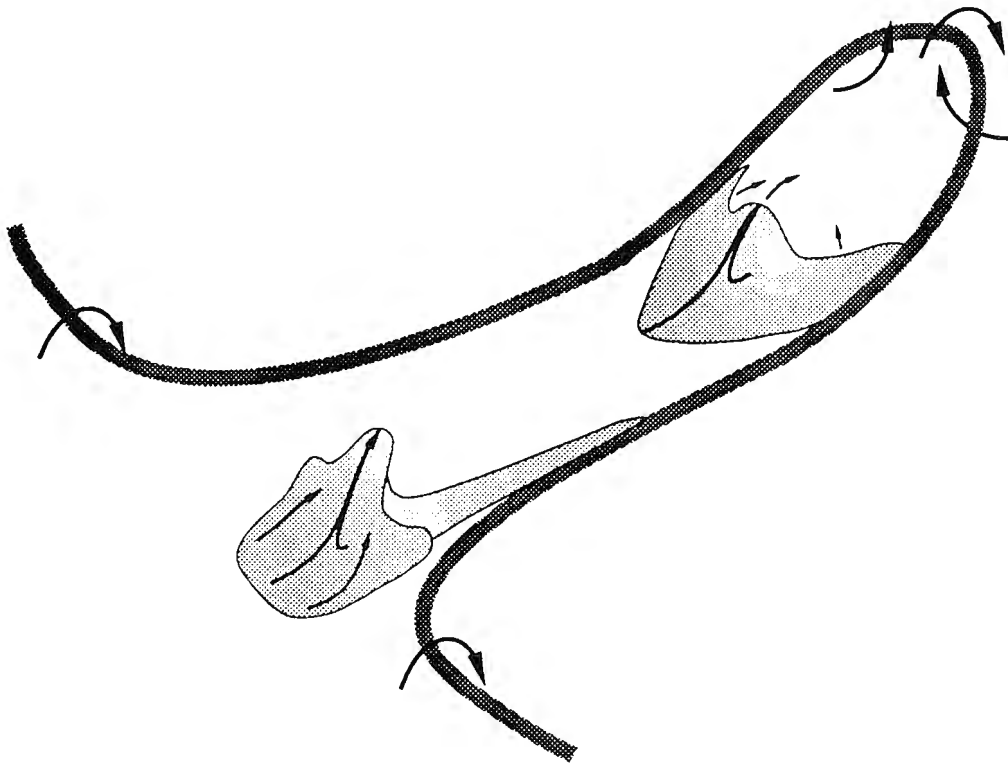
b) Rapid Outward Movement of the Erupting
   Ridge Which Contains Concentrated Vorticity.
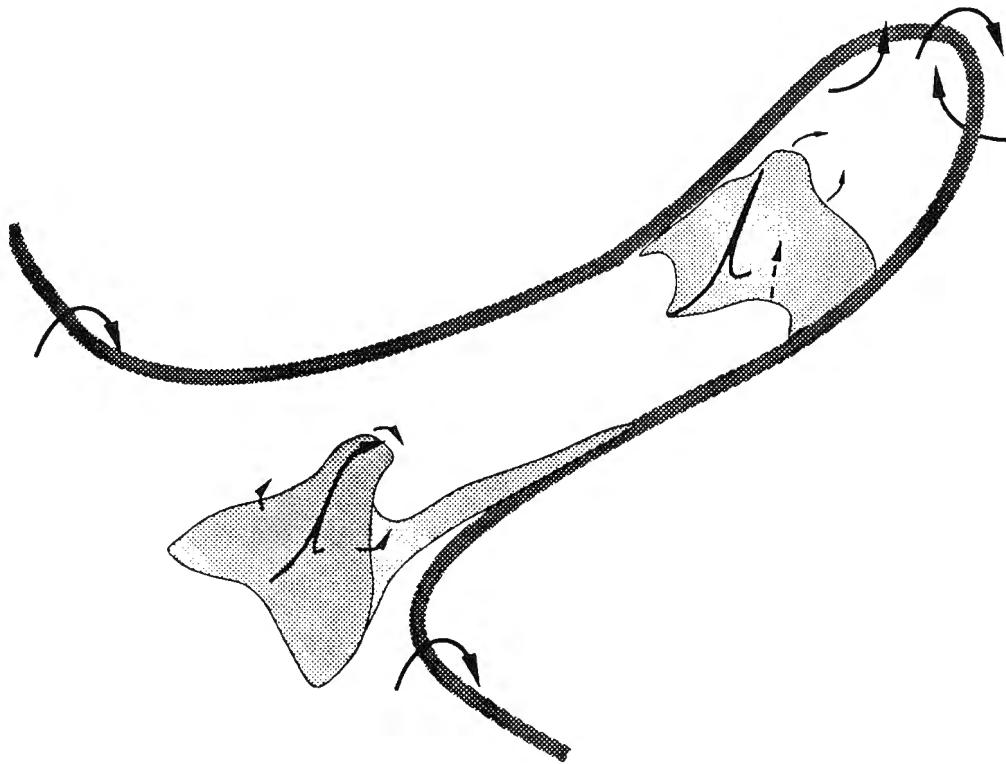
c) The Erupting Sheet Starts to Roll Over
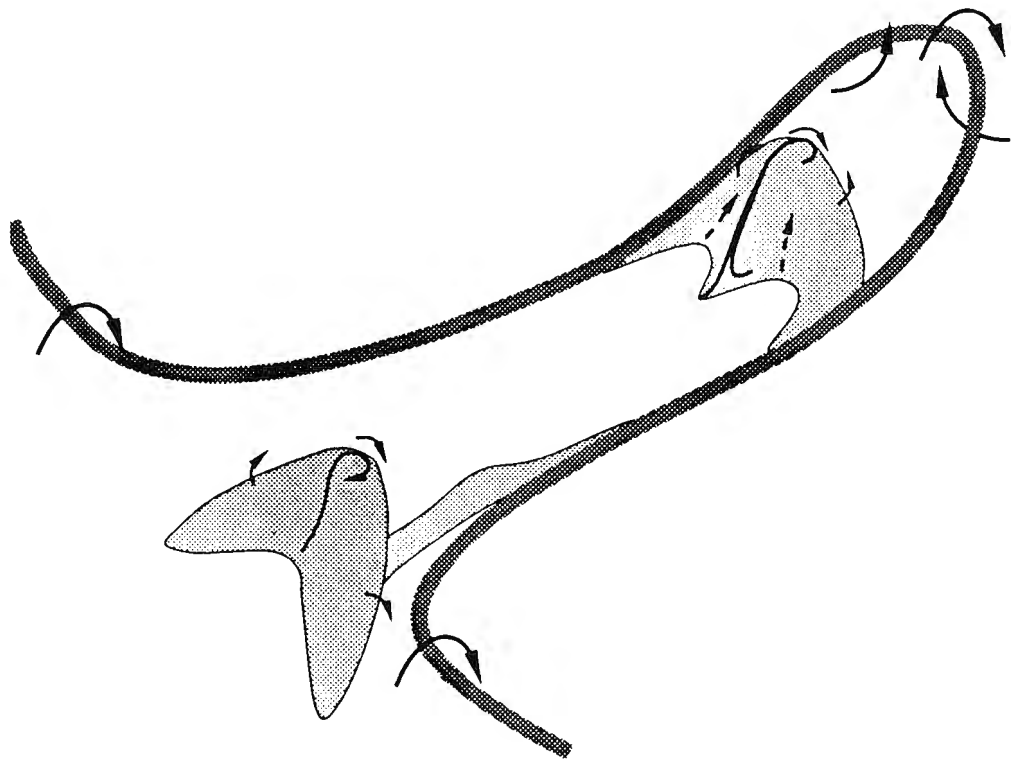
d) Partial Roll-over Reached
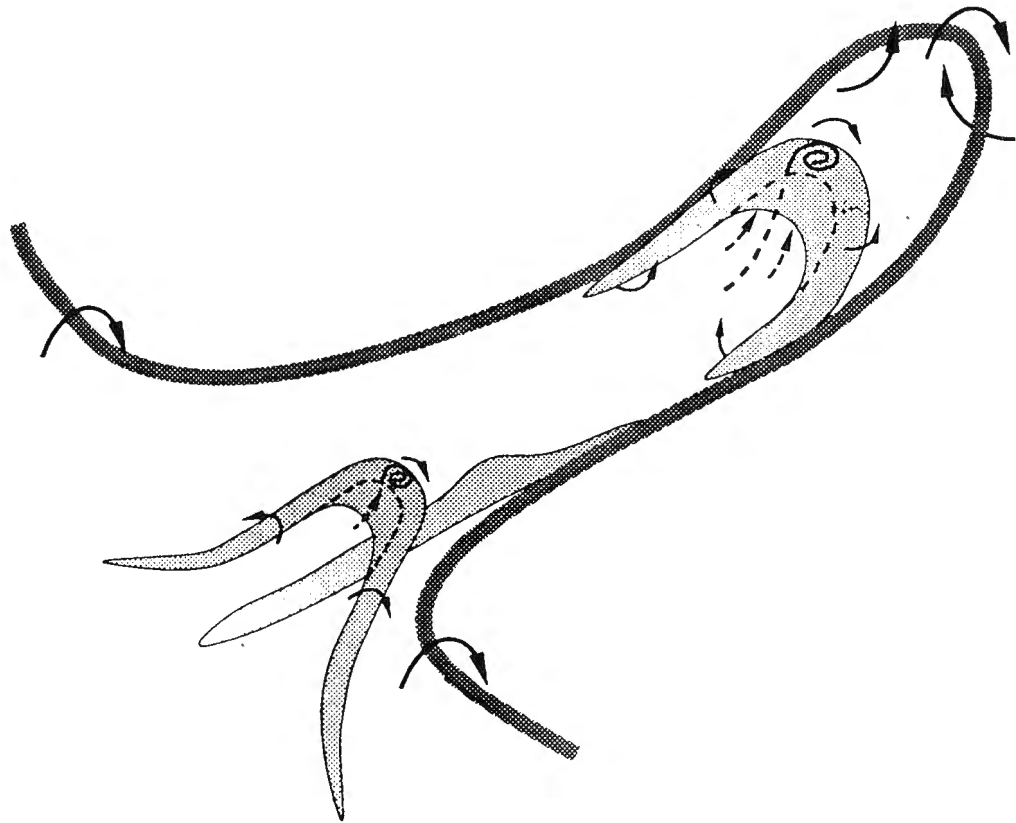
e) Complete Generation of
   Secondary Hairpin Vortices
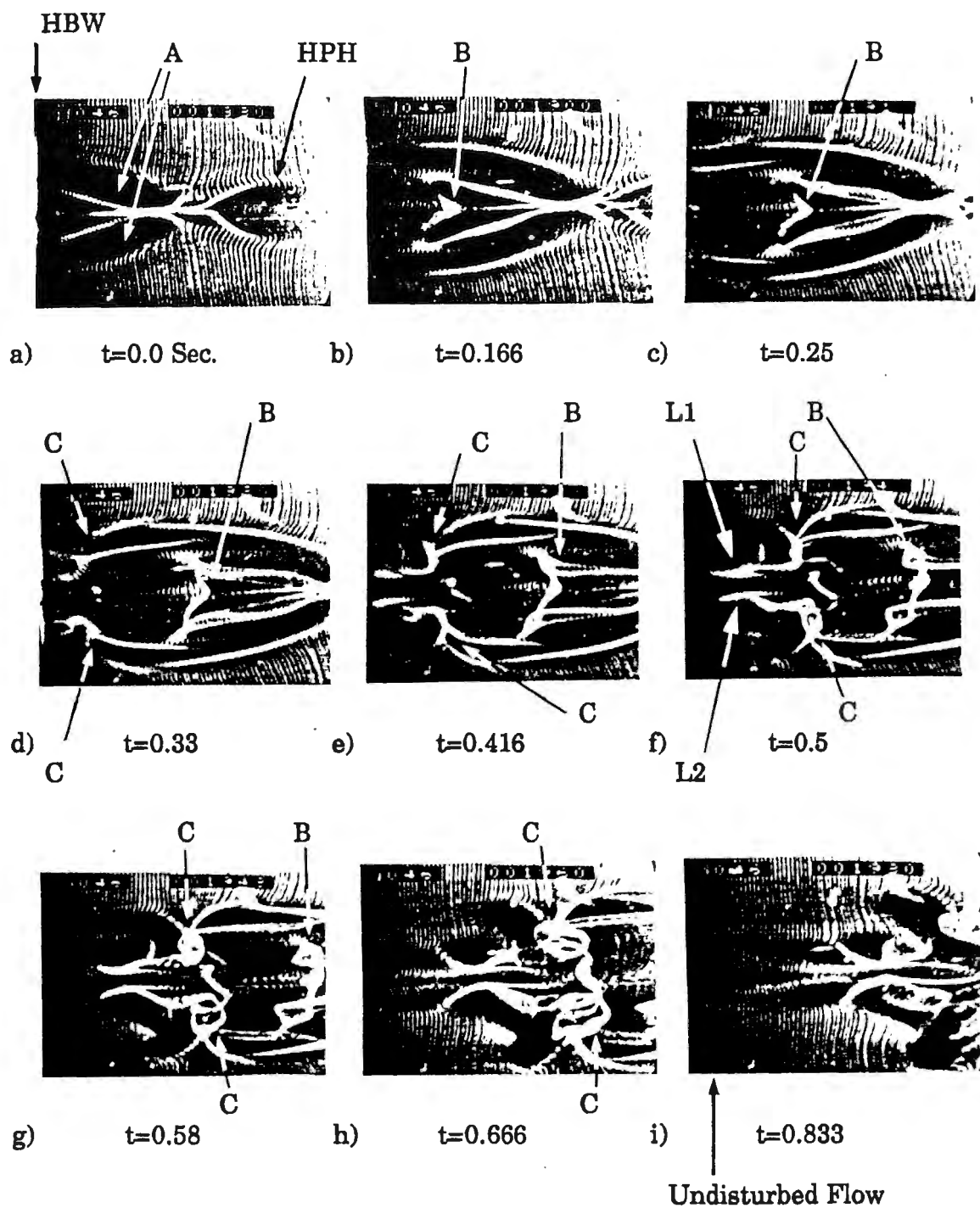
Figure 23. Plan-view hydrogen bubble wire visualization sequence illustrating the development of secondary vortices near the surface as a primary hairpin vortex passes a fixed streamwise location. HBW denotes the position of the hydrogen bubble wire, HPH is the location of head of primary vortex, A the location of the trailing legs of primary vortex, B the development of a secondary vortex behind head of primary, C the development of secondary vortices adjacent to the legs of the primary vortex, and L1,L2 the legs nearest the symmetry plane for the secondary vortices indicated by C.

a) The Onset of Interaction -- Sharp, Crescent-shaped Ridge Develops in the Surface Flow Where the Induced Pressure Gradient Near the Surface is Adverse.

b) Rapid Outward Movement of the Erupting Ridge Which Contains Concentrated Vorticity.

c) The Erupting Sheet Starts to Roll Over

d) Partial Roll-over Reached

e) Complete Generation of Secondary Hairpin Vortex
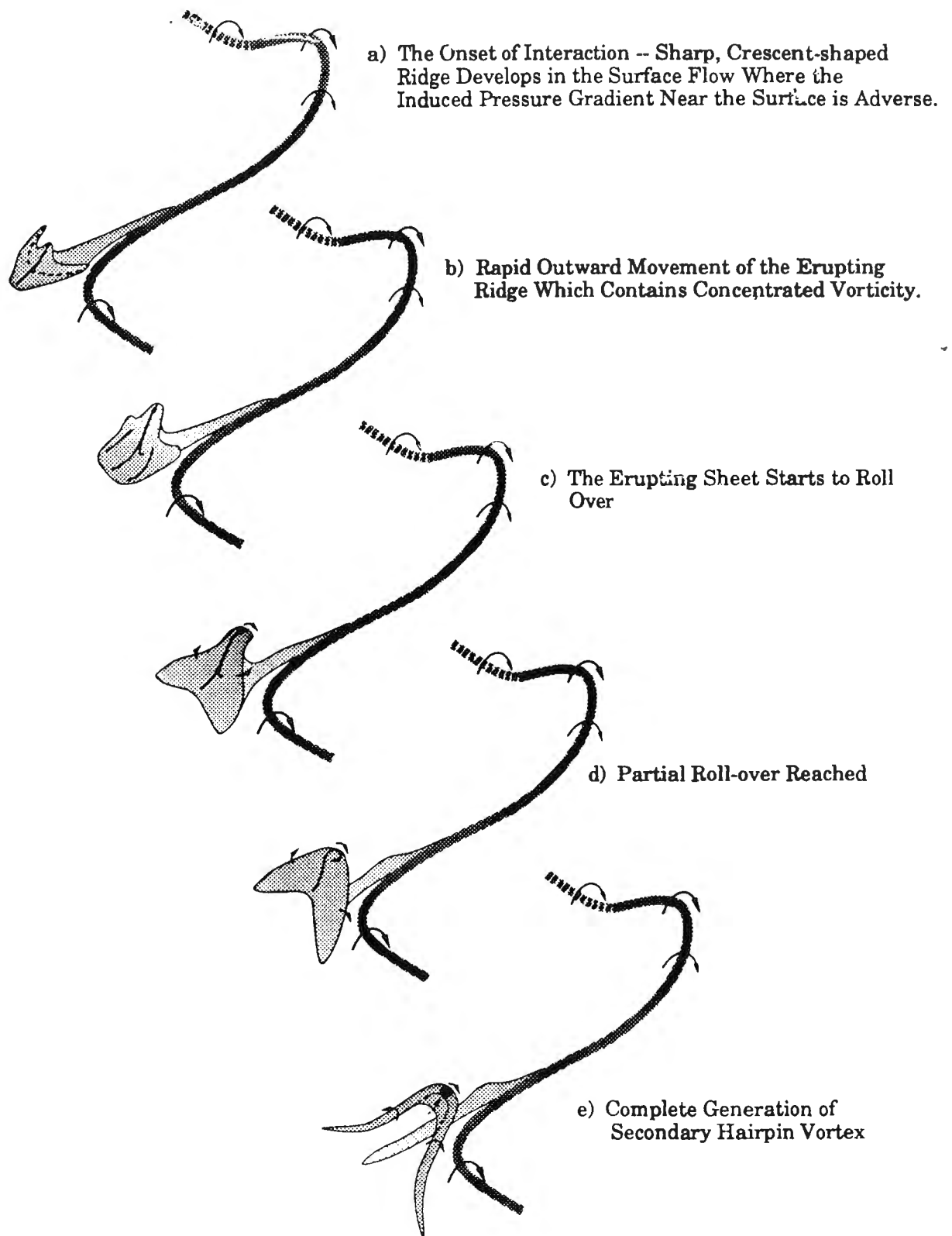
Figure 24. The generation of secondary vortex via surface interaction for an asymmetric hairpin vortex
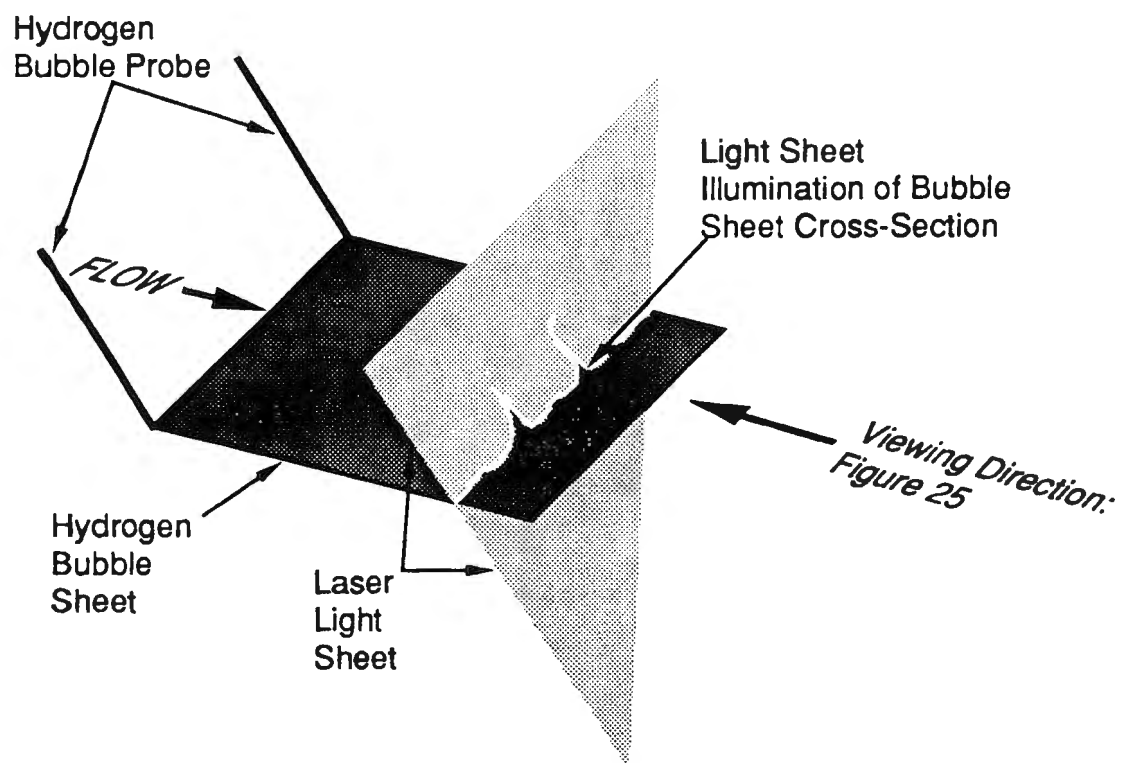
Figure 25. Schematic diagram of laser sheet visualization technique employed to visualize eruptive events in a turbulent boundary layer.

(a) tip penetration, y^+=92

(b) tip penetration, y^+=105

Figure 26. End-view visualization, using a horizontal hydrogen bubble wire and laser light-sheet
illumination (see figure 25), showing eruptive spires emanating from near-wall region of a
turbulent boundary layer ($Re_\theta \approx 1150$). Lateral field of view $\approx$ 250 wall units, wire located y^+ =7
from surface, and $x^+ \approx$ 150 upstream of light sheet. Compare with eruptions induced by
streamwise vortex as shown in figure 5.

2.2 Synthetic Turbulence

Katepalli R. Sreenivasan
Yale University

SEMINAR NOTICE

SYNTHETIC TURBULENCE

Professor K. R. Sreenivasan

YALE UNIVERSITY

We discuss schemes for generating stochastic signals that possess many properties of high-Reynolds-number turbulence. The use of such signals, designated "synthetic turbulence", in providing initial conditions for direct numerical simulations and in the development of turbulence models will be discussed briefly.

Thursday, the 12th May 1994
* * NOTE NEW VENUE: Conference Room, Bldg. 1171 * *
Time: 10:30 AM

POC: Dr. Promode R. Bandyopadhyay (Code: 8233; Bldg. 108/2) NPT x2588

2.2-3/2.2-4
Reverse Blank

SYNTHETIC TURBULENCE

References

"Synthetic turbulence" by *A. Juneja, D.P. Lathrop, K.R. Sreenivasan and G. Stolovitzky,* Phys. Rev. E. May 1994

"A scheme for generating initial fields for the direct numerical simulation of box-turbulence", by *A. Juneja, G. Erlebacher, and K.R. Sreenivasan,* preprint, April 1994

Synthetic turbulence (ST) = turbulence-like stochastic signals constructed from some simple rational "rules"

Among other things: ST has the same energy spectrum, dissipation rate, single-point PDFs for velocities and velocity increments, intermittency characteristics, structure functions up to some high order, fractal dimension, etc. as high-Reynolds-number turbulence

Two practical goals

Construct ST to provide efficient intial conditions for DNS

Obtain subgrid-scale viscosity and a few other modeling constants (e.g., Kolmogorov constant, turbulent Prandtl number, some constants in the K-ε model)

IF THIS IS POSSIBLE, THE "RULES" MAY BE THOUGHT TO CONTAIN THE RIGHT PHYSICS

FOCUS ON PRINCIPLES BY CONCENTRATING ON ONE-DIMENSIONAL TRACE OF VELOCITY

Generally, initial conditions are chosen to:
(a) Satisfy continuity equation
(b) Possess the desired energy spectrum
(in particular, kinetic energy and energy dissipation rate)

Shortcomings
a. For homogeneous and isotropic turbulence, the decay history is set largely by the initial state

b. Slow convergence of high-order statistics and large-scale properties

For 128^3 box, random initial conditions take about 2500 iterations for convergence
(each step taking about 3 sec on Cray-YMP).

cf: about 300 iterations if started with ST
(comparison)

c. Total vorticity increases initially before decaying

$\frac{1}{3} \mathrm{Tr}(Fl_{ij})$ vs t — 96^3 simulation

$\frac{1}{3} Tr(FL_{ij})$ vs t, with $M_0=0.6$, $M_0=0.4$, $M_0=0.1$
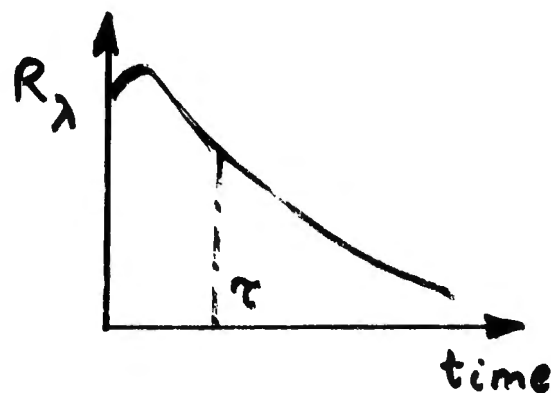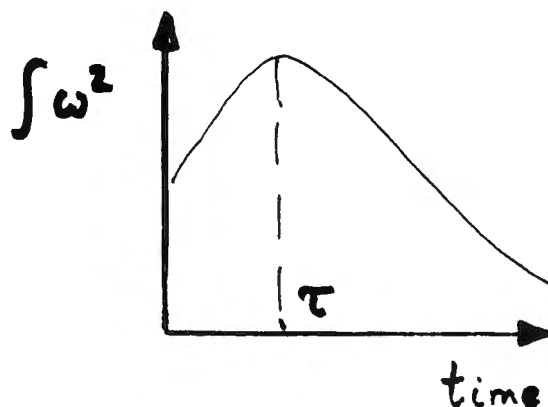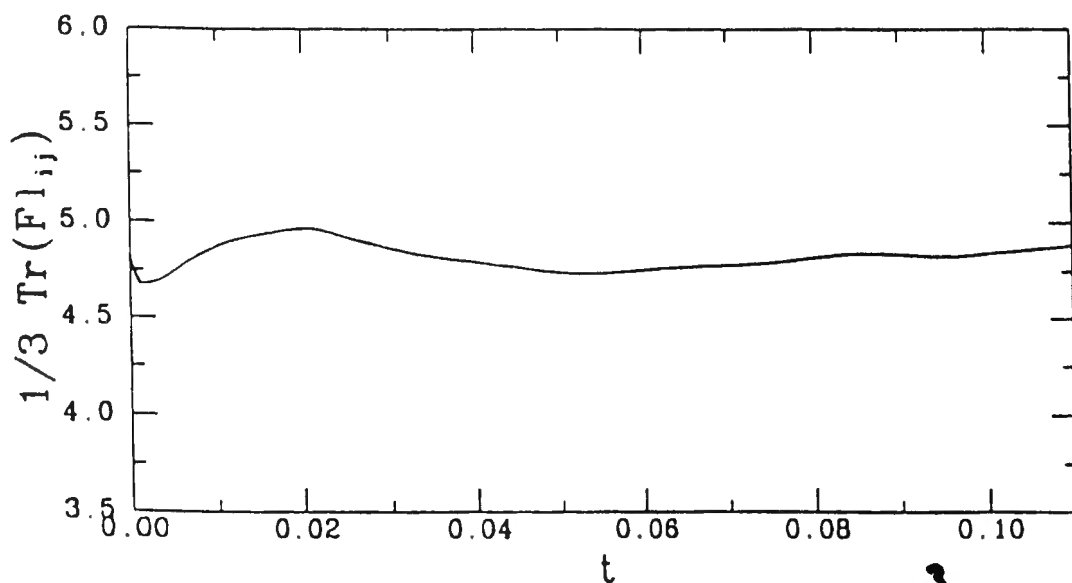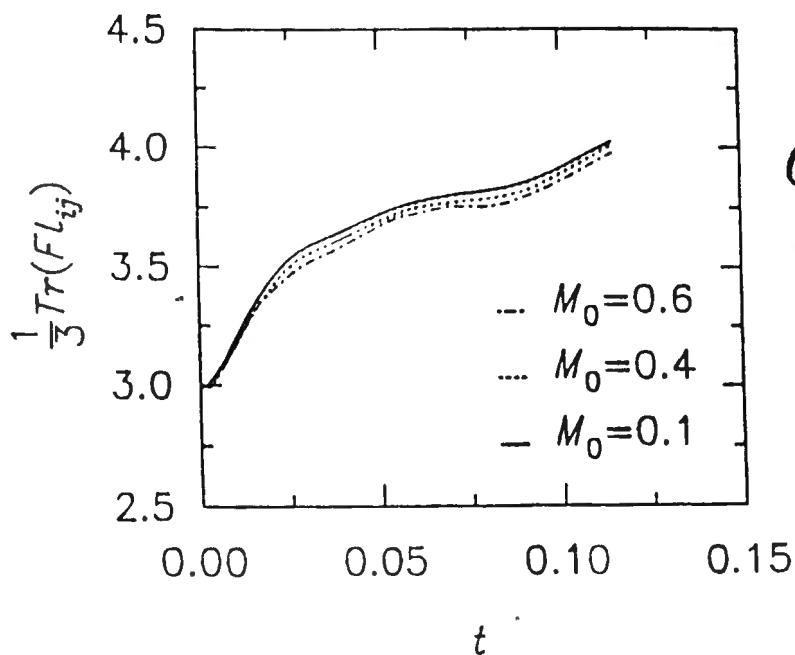
G. Erlebacher et al. J.F.M. 238, 155 (1992)

2.2-7

Non-universal and quasi-universal aspects
(a schematic)

source of
turbulence,
scale: O(L)

non-universal
Large

quasi-universal
"small"

$log \, \phi$

inertial
range

dissipative
range,
scale: O(η)

energy cascade without
dissipation

$log \, f \, (or \, log \, k) \longrightarrow$

(to heat)
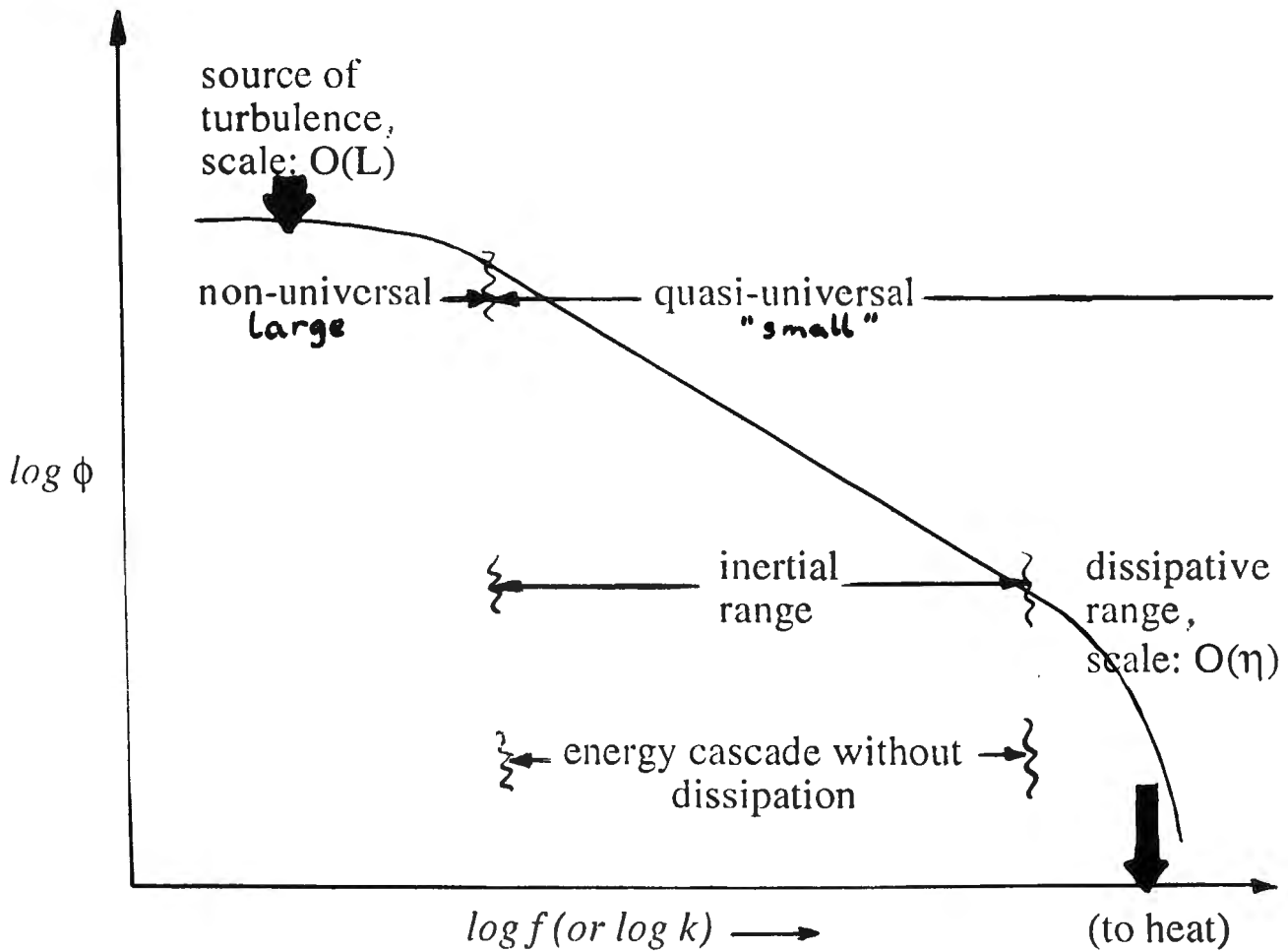
vortex-stretching

≈

successive break-up of eddies

NOTATION

ε: energy dissipation rate per unit mass

ε_r: average of ε over a box of size r

$$\Delta u_r = \Delta u(r) = u(x+r) - u(x)$$

turbulent energy dissipation rate displaying spatial intermittency

6 m above ground

time (or x) $\longrightarrow$

$\langle \mathcal{E} \rangle / \mathcal{E}$

200

100

0

$$\mathcal{E} \sim \left(\frac{\partial u}{\partial x}\right)^2 \sim \left(\frac{\partial u}{\partial e}\right)^2 \sim \left(\frac{\partial u}{\partial t}\right)^2$$
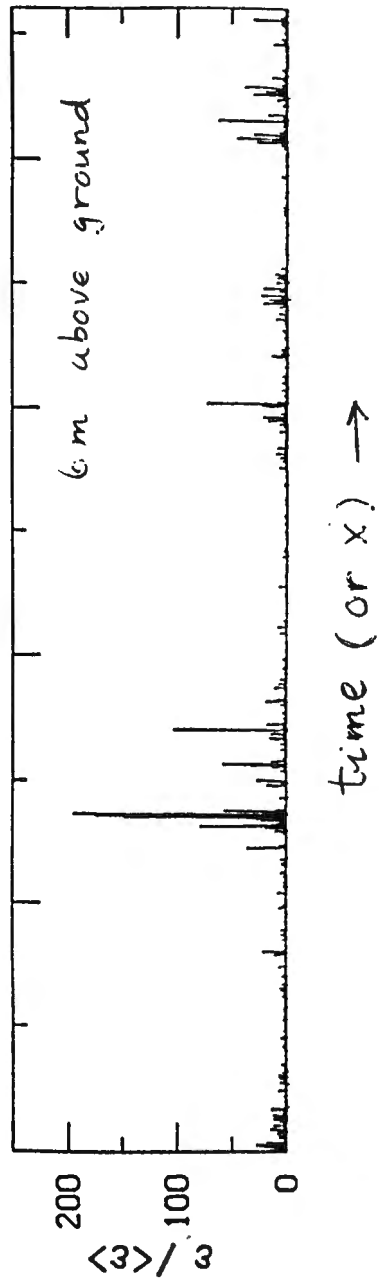
Rate of turbulence strain $\sim \sqrt{\frac{\langle \mathcal{E} \rangle}{\nu}}$

$$r \mathcal{E}_r = \int\limits_{x}^{x+r} \mathcal{E} \, dx \qquad \frac{r}{(r \mathcal{E}_r)^{\frac{1}{3}}}$$

Multiplicative Process

Basis for the multifractal behavior discussed in: C. Meneveau &
K.R. Sreenivasan, J. Fluid Mech. 224, 429-484 (1991)

$$r\varepsilon_r = L\langle\varepsilon\rangle \quad \frac{(L/2)\varepsilon_{L/2}}{L\langle\varepsilon\rangle} \cdot \frac{(L/4)\varepsilon_{L/4}}{(L/2)\varepsilon_{L/2}} \cdots \frac{2r\varepsilon_{2r}}{4r\varepsilon_{4r}} \cdot \frac{r\varepsilon_r}{2r\varepsilon_{2r}}$$

$$r/L = 2^{-n}$$

$$= L\langle\varepsilon\rangle \qquad M_1 \quad \cdot \quad M_2 \quad \cdots \quad M_{n-1} \cdot M_n$$

┌───┐
│ **Identically distributed independent random variables** │
└───┘

Not quite, but its influence is benign:

K·R· Sreenivasan & G· Stolovitzky

J· Stat· Phys· (in print, 1994)

total
measure = 1

$M_{1,1}$ $M_{2,1}$

$M_{2,1}$ $M_{2,2}$ $M_{3,2}$ $M_{4,2}$
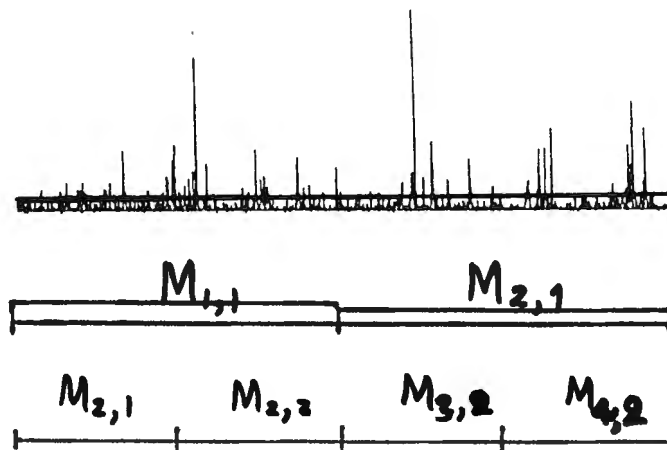
$M_{1,1} + M_{2,1} = 1$

$M_{1,1}$ = measure on left piece / total measure

$M_{2,1}$ = measure on left piece at level 2 / $M_{1,1}$,
          etc

$M_{i,j}$
$M_{i,j+1}$

SCALE   SIMILARITY

each piece = O(L)

$M_{i,j+n}$

each piece = O(η)
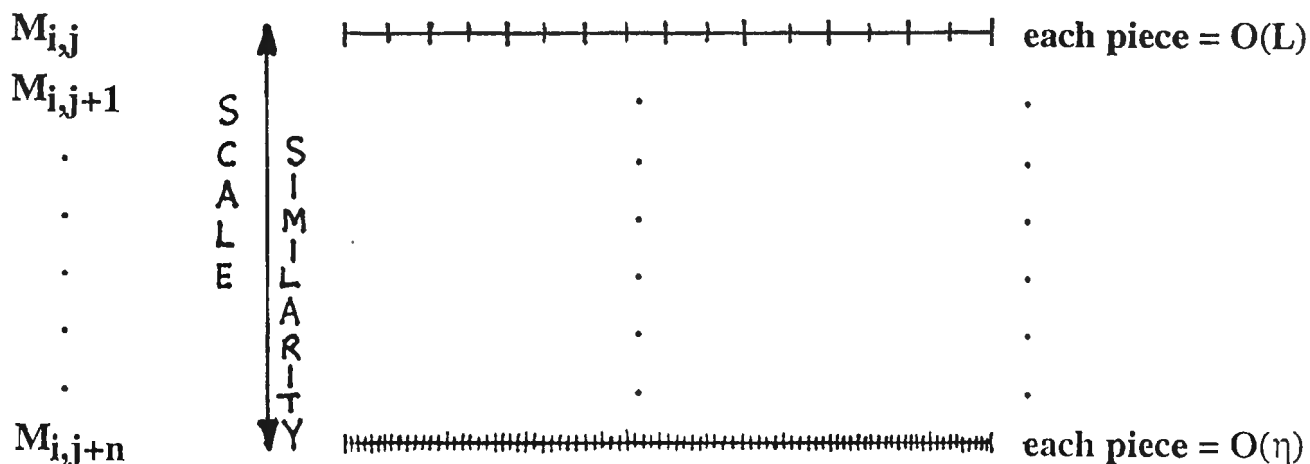
get $p(M_{i,j})$ for each level j

Construction of multiplier distributions

Data from atmospheric
surface layer ($z = 6m$)
$R_\lambda \approx 1800$

$a = 5$

$a = 3$

$a = 2$
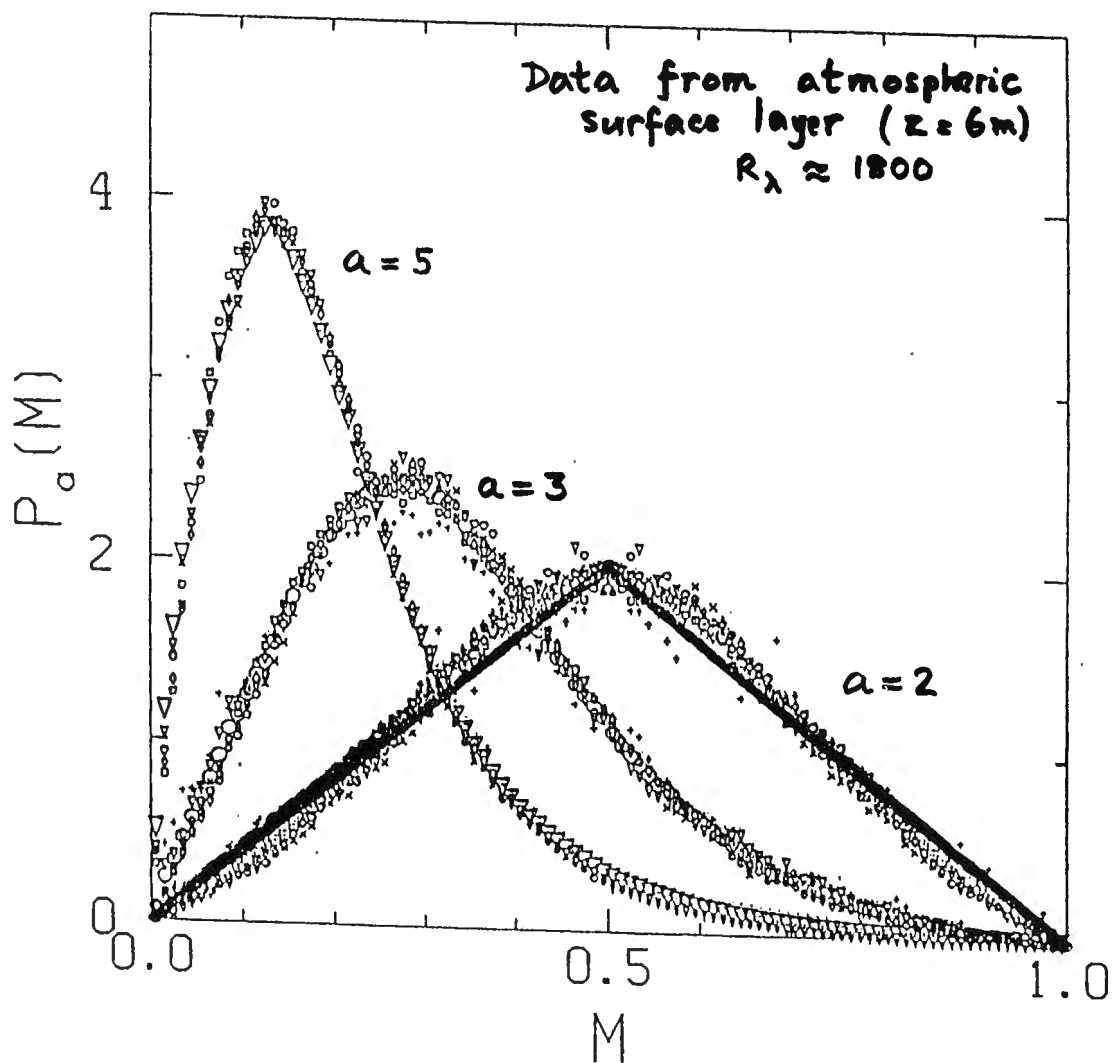
The multiplier distributions

Figure 3   2.2-12

A Quasi-deterministic Model

choose

$$p(M) = 0.5\delta[M-M_O] + 0.5\delta[M-(1-M_O)]$$

and determine M_O by requiring that

$$\langle M^q \rangle_{model} = \langle M^q \rangle_{exp} \qquad (1)$$

for some values of q.

q = 0: normalization condition

q = 1: distribution average = 0.5

$$q = 2: \langle M^2 \rangle_{model} = 0.5\left[M_O^2 + (1-M_O^2)\right]$$

Computing $\langle M^2 \rangle_{exp}$ from previous figure,
we get, using (1), the result that

$$M_O = 0.7$$

Derivation of the p-model from multiplier distribution

$$<(r\varepsilon_r)^q> = (L<\varepsilon>)^q(r/L)^{\xi_q}$$

comparison between experiment and models
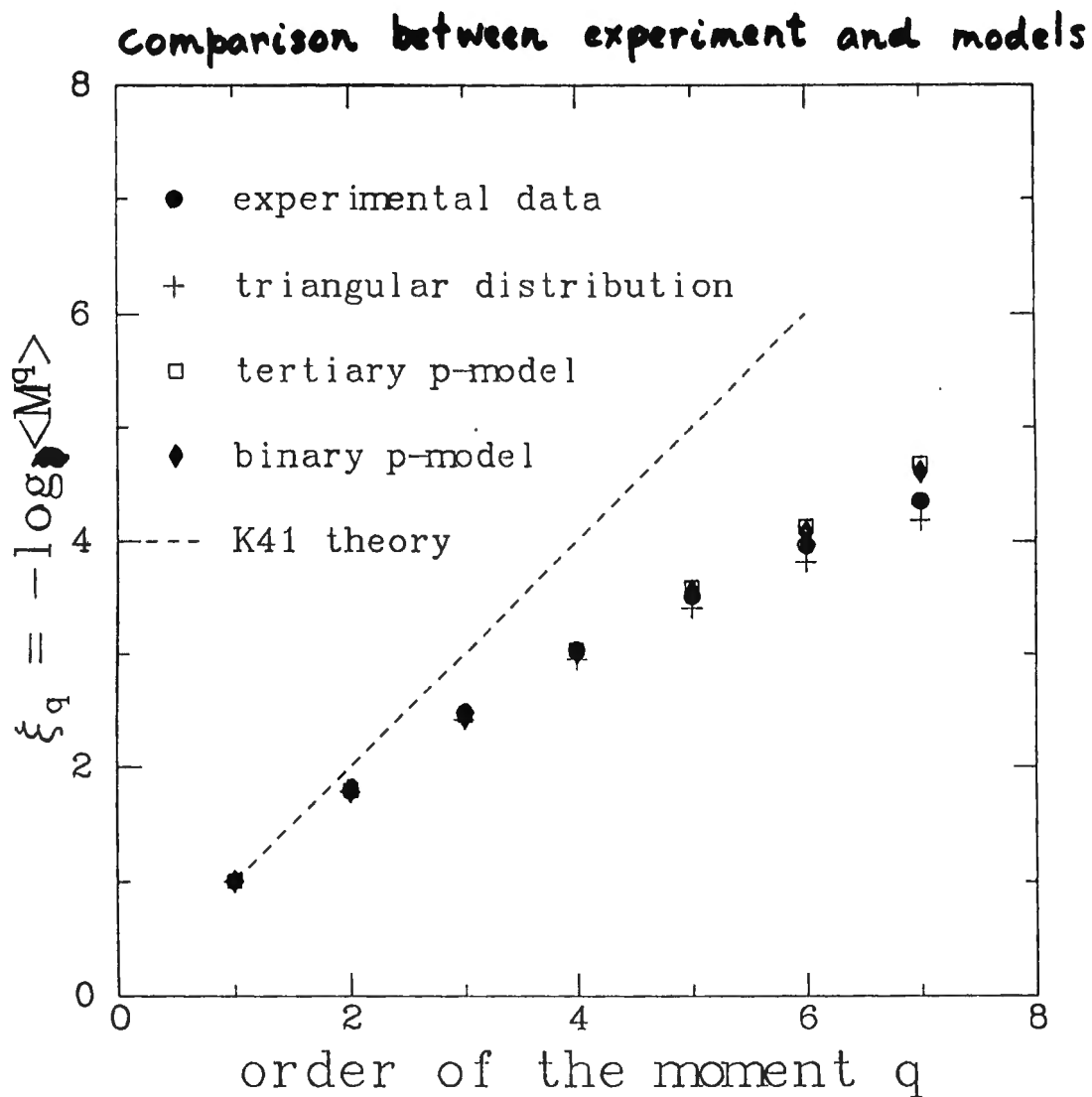
Figure 3: A comparison between moments computed from the measured multiplier distributions and those computed for the different models considered in the text. Experimental data were obtained from a record length of 810,000 data points. The convergence of moments was reasonable; for example, in the last half decade of the record length, the variations observed were smaller (in the log scale) than the symbol size.

Step 1: Generate ε_r by a multiplicative model

C. Meneveau and K.R. Sreenivasan, Phys. Rev. Lett. 59, 1424, 1987
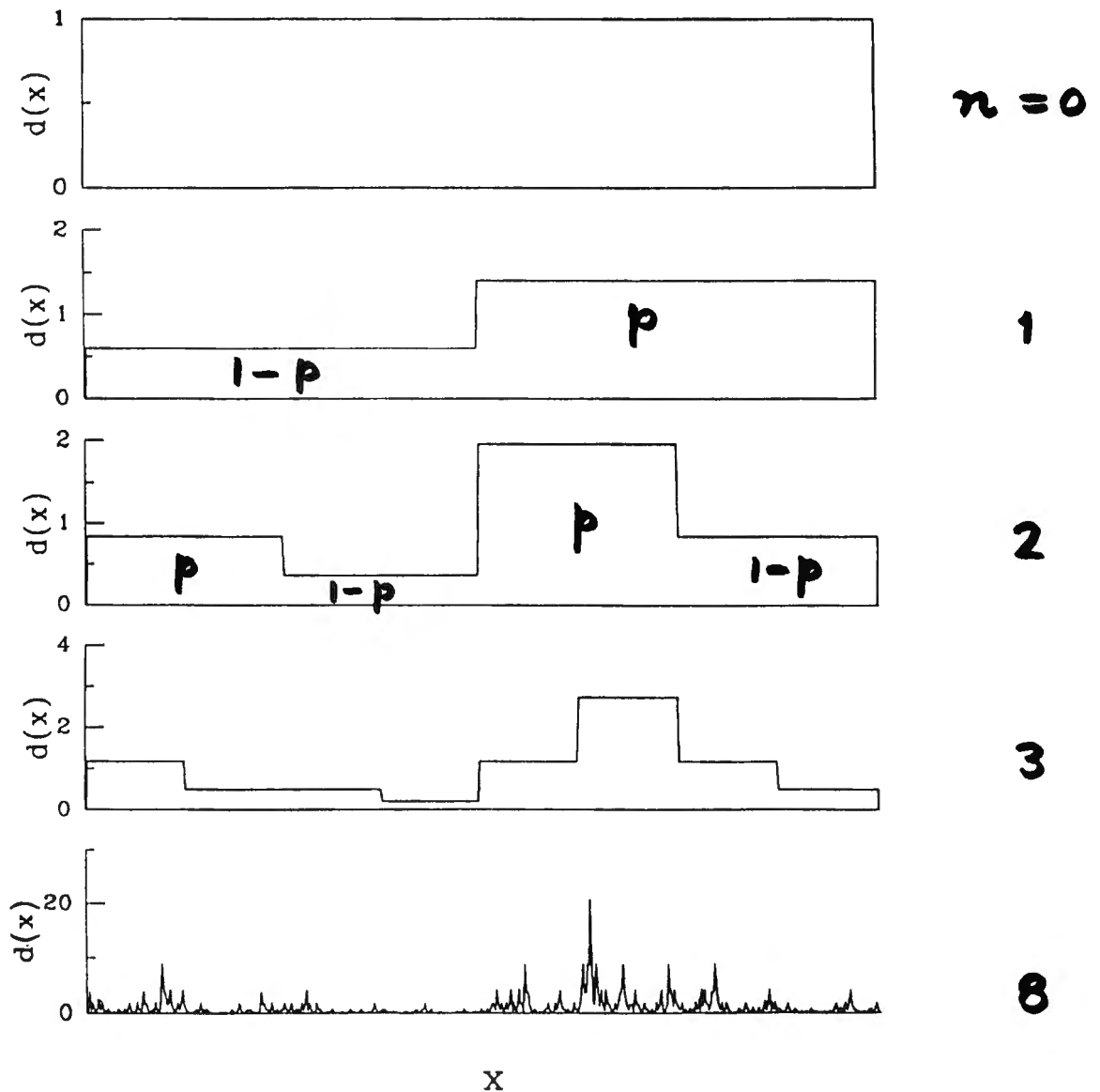
Step 2: Obtain Δu_r from ε_r using KRSH
A.N. Kolmogorov, J. Fluid Mech., 12, 82

$$\Delta u_r = V \, (r\varepsilon_r)^{1/3}$$

↟

already discussed

V is a stochastic variable independent of r and $r\varepsilon_r$ and is hence 'universal'

1. Is V indeed universal?

Appears to be so.

G. Stolovitzky, P. Kailasnath and K.R. Sreenivasan, Phys. Rev. Lett. 69, 1178 (1992)

A. Praskovsky, Phys. Fluids A, 4, 2589 (1992)

S. Chen, G. Doolen, R. Kraichnan and Z.-S. She, Phys. Fluids A, 5, 458 (1993)

I. Hosokawa, J. Phys. Soc. Japan, 62, 10 (1993)

S. Grossmann and D. Lohse, Phys. Fluids A, 6, 611 (1994)

2. Why is V universal, and what are its properties?

G. Stolovitzky and K.R. Sreenivasan, Rev. Mod. Phys. 66, 229-240 (1994)

True for all processes resembling "anti-persistent" fractional Brownian motion; "conditioning" weakens the connection to the specificity of the process

FIG. 3

G. Stolovitzky and K.R. Sreenivasan, Phys. Rev. Lett. 69, 1178, 1992

Atmospheric data, 6 m above ground, R_λ between 1800 and 2500
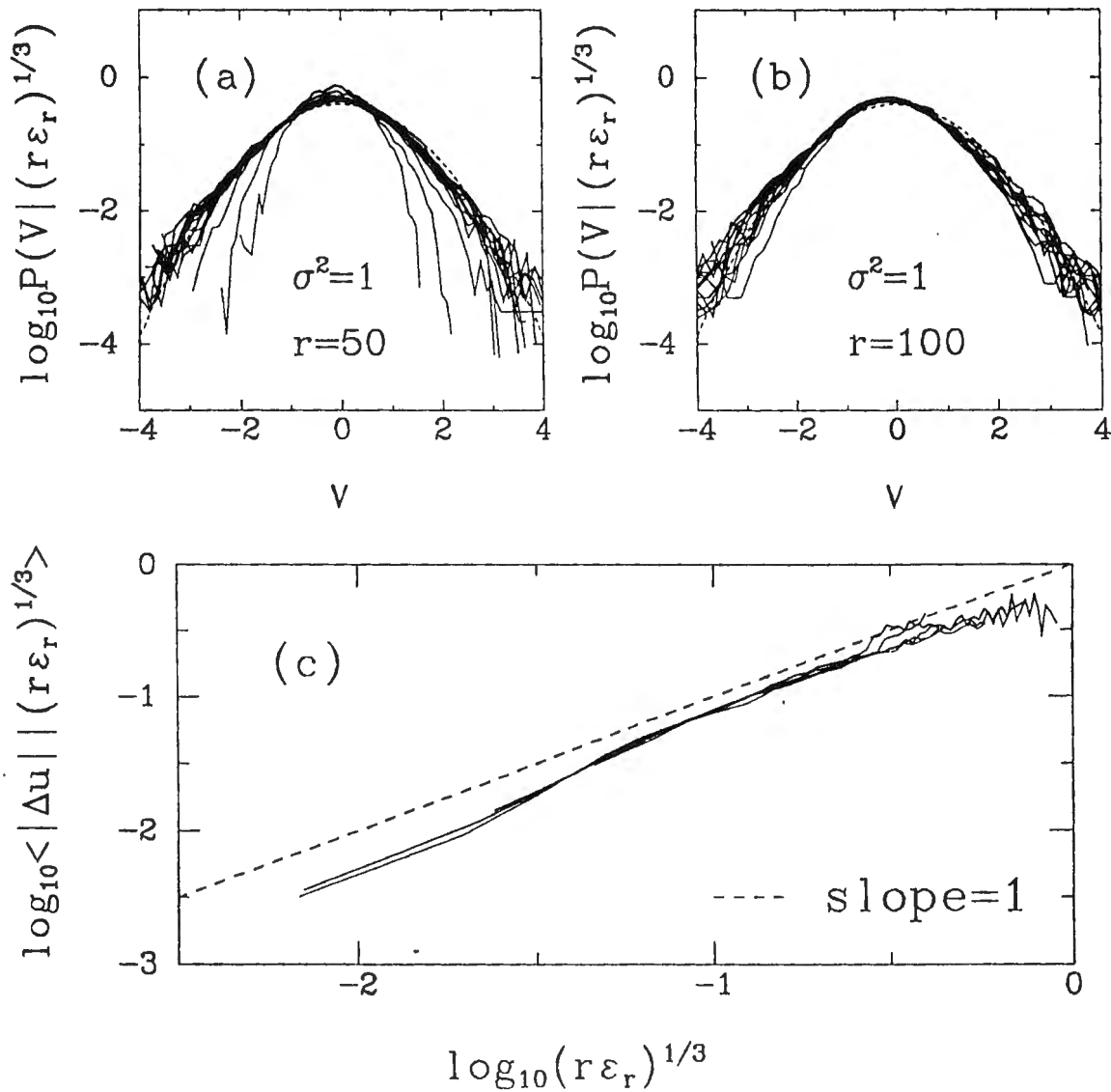
$$\langle (\Delta u_r)^n \rangle \sim r^{\zeta_n}$$
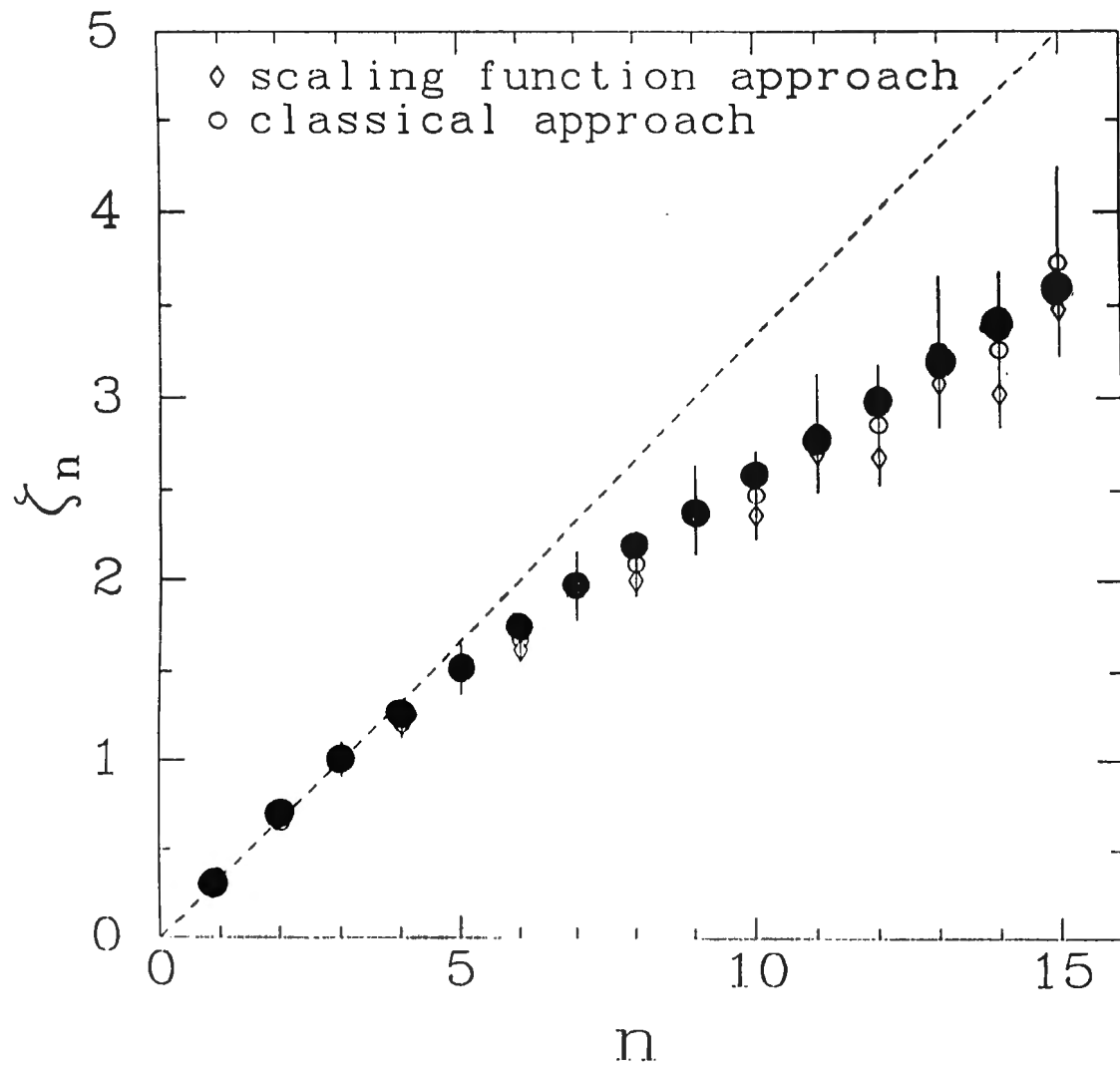
Step 3

The construction of the velocity signal

I step

$$\Delta u_1 = V_1 (r\varepsilon_r)_1^{1/3}$$

u_0 $u_1 = u_0 + \Delta u_1$

II step

$$\Delta u_1 = V_1 (r\varepsilon_r)_1^{1/3} \qquad \Delta u_2 = V_2 (r\varepsilon_r)_2^{1/3}$$

u_0 u_1

$\longrightarrow \quad \frac{1}{2} \quad \longleftarrow$
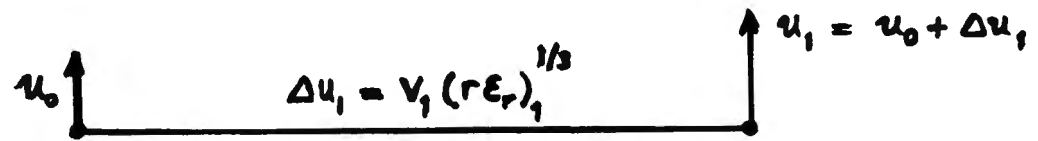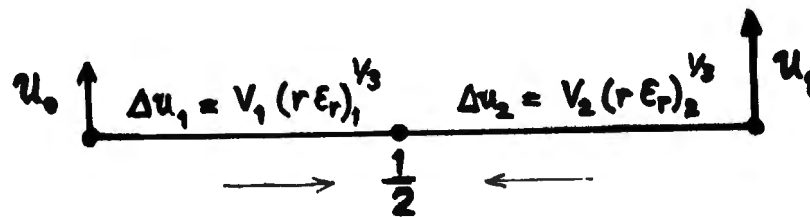
(IN GENERAL)

mismatch at 1/2

$$u_{1/2} = \alpha(u_0 + \Delta u_1) + (1-\alpha)(u_1 - \Delta u_2)$$

$\alpha = 1/2$: random additive process

(by mid-point displacement method)

For all α, can show that:

$$\langle (\Delta u_r)^k \rangle \sim \begin{cases} 0 \text{ if } p = 2m+1 \\ r^{\zeta_m} \text{ if } p = 2m \end{cases}$$

Need "structure" somehow

Tertiary cascades provide such a structure

Mid-point displacement method

$n = 1$

(a)

$n = 2$

(b)

$n = 3$

(c)

sum

(d)
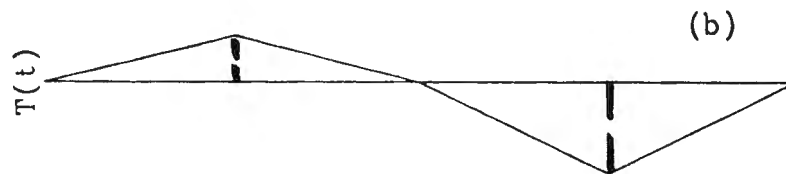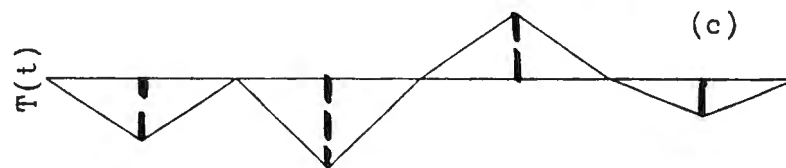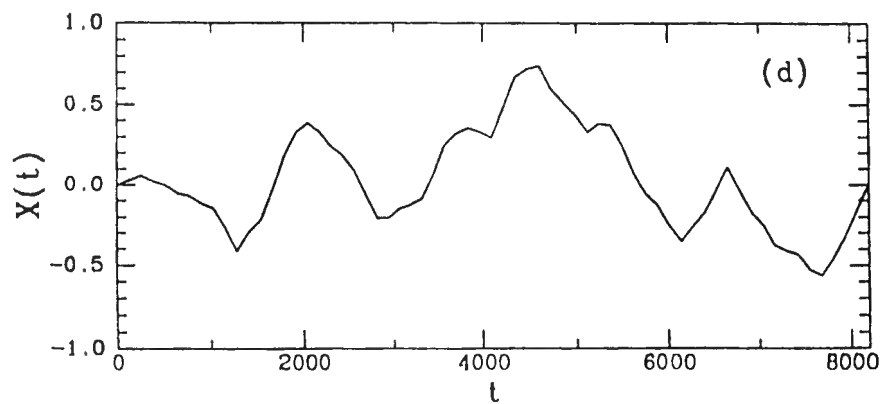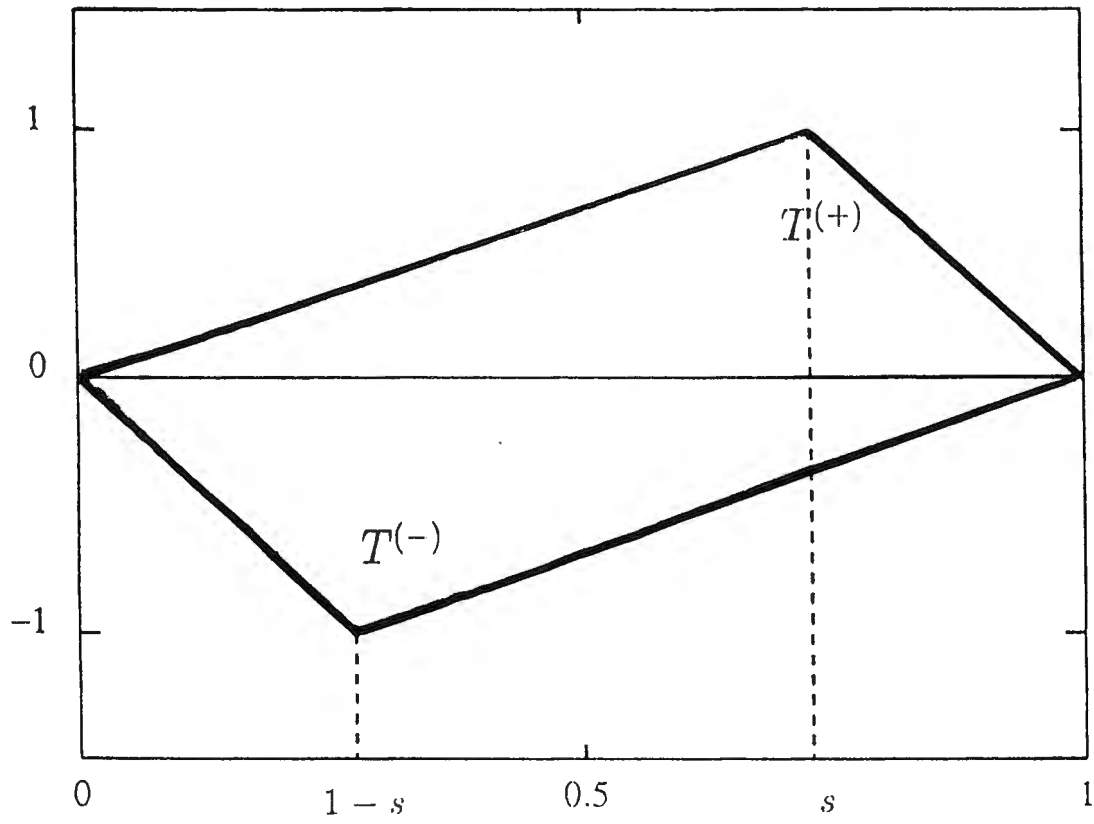
Figure 6: Basic tent functions $T^{(+)}$ and $T^{(-)}$ used in the synthetic turbulence models.
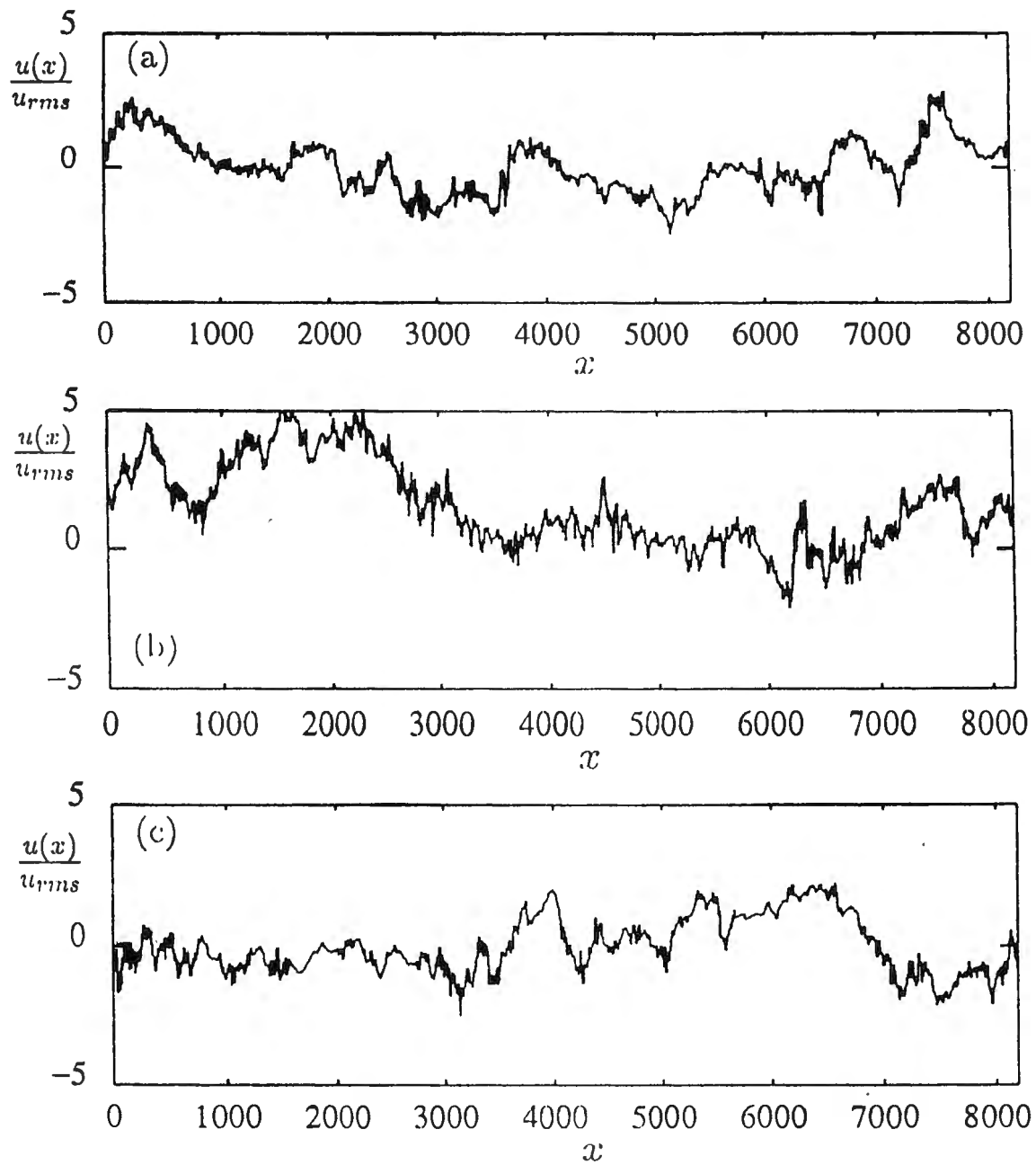
Figure 7: Example velocity sections from (a) atmospheric turbulence, (b) synthetic turbulence based on the p-model, (c) synthetic turbulence based on the l-model.

slope
−1·71

energy density

k

wave number
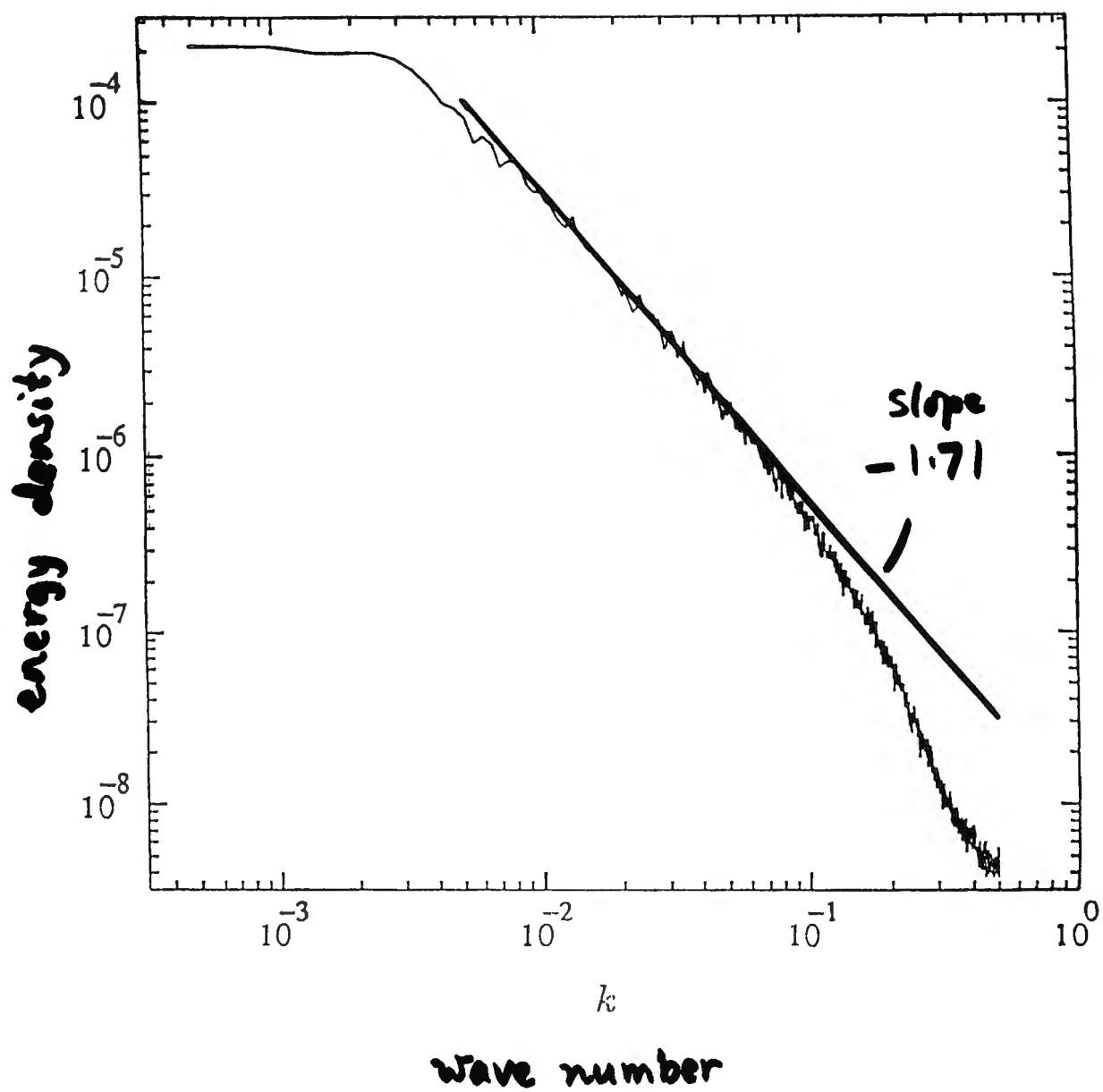
How did the large scale behavior appear?

Simply by allowing several largest inertial-range scales to co-exist

Why does this simple scheme "work"?

Because of the existing balance between the large and small scales set by the right dissipation rate

Would it work in other flows as well?

Probably not – certainly not where the large and small scales are not in equilibrium

Synthetic Turbulence Model in 3-Dimensions
Generating a divergence-free artificial velocity field

Generate 3 scalar fields u', v' and w'

Define $\mathbf{u}^{\mathsf{F}} = (u', v', w')$.

$\mathbf{u}^{\mathsf{F}}$ can be decomposed as

$$\mathbf{u}^{\mathsf{F}}(\mathbf{x}) = \mathbf{u}(\mathbf{x}) + \mathbf{u}^{\mathsf{C}}(\mathbf{x})$$

where

$$\nabla \cdot \mathbf{u} = 0 , \qquad \nabla \times \mathbf{u}^{\mathsf{C}} = 0 .$$

This decomposition can be accomplished in Fourier space according to

$$\hat{\mathbf{u}} = \hat{\mathbf{u}}^{\mathsf{F}} - \frac{\mathbf{k} \cdot \hat{\mathbf{u}}^{\mathsf{F}}}{k^2} \mathbf{k} , \qquad \hat{\mathbf{u}}^{\mathsf{C}} = \hat{\mathbf{u}}^{\mathsf{F}} - \hat{\mathbf{u}} .$$

Transform $\hat{\mathbf{u}}$ back to physical space to define a divergence-free artificial velocity field.

Effect of Projection ?

PDFs of the velocity components

log P(x)

(a)

Homogeneous, isotropic

X = u, v, w
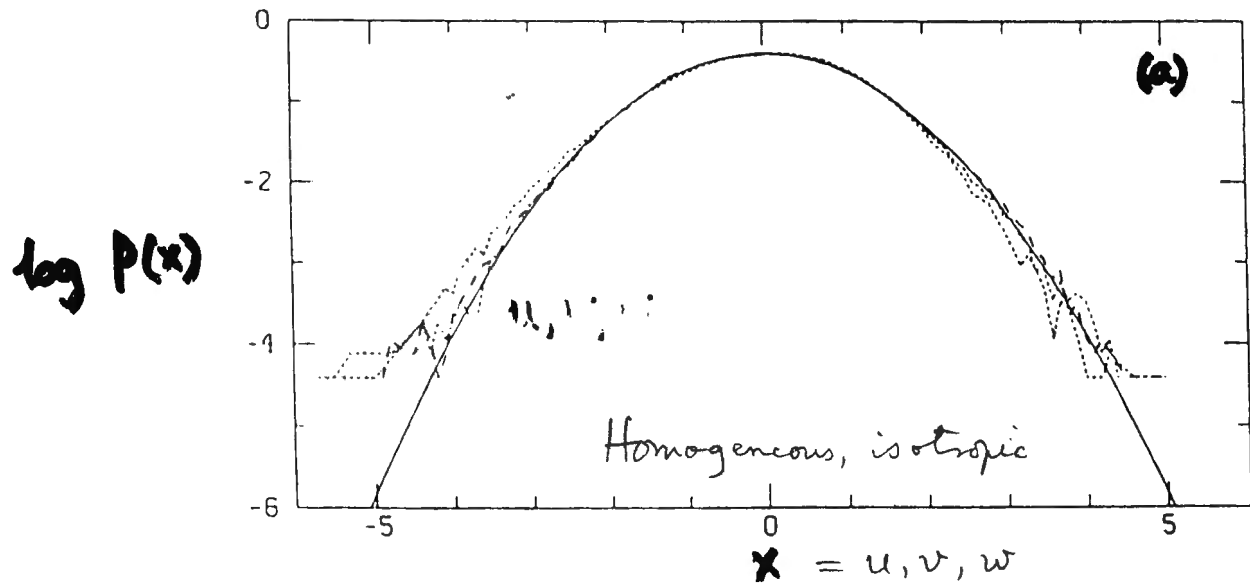
The Kolmogorov constant and the intermittency exponent

$$\phi_u(k) = C_k <\varepsilon>^{2/3} k^{-5/3} (kL)^{-\mu}$$

Kolmogorov constant   Intermittency correction

$$\Delta u(r) = u(x+r) - u(x)$$

known from analysis and construction

can therefore obtain the quantity $\phi_u(k)$, thus C_k and μ

$$C_k = (2/\pi) \, \Gamma(1+\zeta_2) \, \sin(\pi \zeta_2/2)$$
$$= 0.51$$

(cf: best experimental estimate ~ 0.5)

$$\mu = \zeta_2 - 2/3$$
$$= 0.027$$

(cf: best experimental estimate 0.025 ± 0.005)

For the p-model,
$$\zeta_2 = \log_2\{[0.7^{2/3} + 0.3^{2/3}]/2\}$$

Large-eddy simulations and subgrid scale viscosity

1. Typical scale ratio
$$L/\eta = Re^{3/4}$$
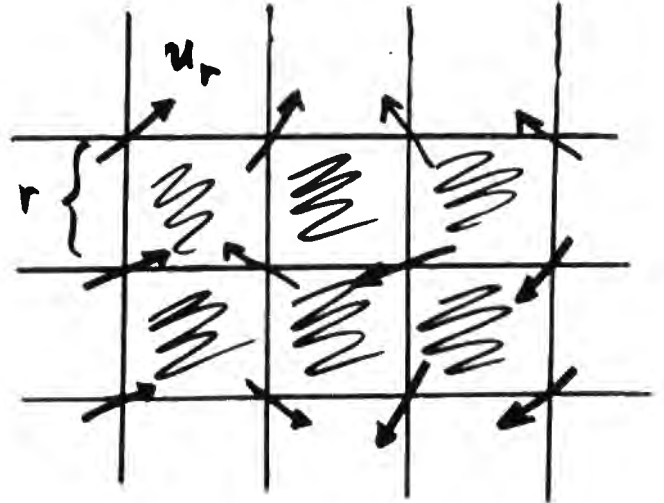
2. Subgrid scale models for large-eddy simulations

    a. Resolve only scales r and above

    b. Incorporate effects of unresolved scales as an effective viscosity

    c. Rewrite NS=0 in terms of u_r, and the additional terms as $<\nu_e(r)>\nabla^2 u_r$

3. Computation of $<\nu_e(r)>$

    a. Write $<\nu_e(r)> = \alpha <|\Delta u_r|> r$

    b. Use $\Delta u_r = V(r\varepsilon_r)^{1/3}$

    c. Use p-model or alternatives

    d. Impose the requirement that

$<\nu_e(r)> \rightarrow \nu$ as $r \rightarrow$ viscous scale

Some results

1. Subgrid scale viscosity

$$\langle \nu_e(r)\rangle = 0.039 \langle\varepsilon\rangle^{1/3} r^{4/3} (r/L)^{\mu_1-1/3}$$

$$\langle[\nu_e(r)]^q\rangle/\langle\nu_e(r)\rangle = \langle|V|^q\rangle/\langle|V|\rangle^q Re^q (r/L)^{\mu_q+q},$$

where the exponents μ_q are known exactly:

$$\mu_q = -\log_b\langle\mu^{q/3}\rangle$$

----

2. The constant C_μ in the K-ε model

As r approaches the large scale, $\nu_e(r) \rightarrow \nu_T$

where $\nu_T = 0.084 K^2/\langle\varepsilon\rangle$

----

3. Others

a. Corrsin-Obukhov constant, $C_\theta = 2.2/C_k$
(turbulent Prandtl number $= 0.9$)

b. Intermittency correction for the scalar, $\mu_\theta = 0.039$

c. For uniformly sheared flows
$$C_\mu = 0.084/(1+bS^2),$$
where b can be computed.

d. Log-law velocity profile can be generated for channel flows

Concluding remarks

1. Analysis of high-Reynolds-number turbulence data reveals much statistical order.

2. This order can be codified into some very simple "rules".

3. The "rules" can in turn be implemented to generate synthetic turbulence, which resembles real turbulence to a remarkable degree.

(Suggests that the abstraction of the "rules"and their implementation for creating ST are substantially correct at the level considered.)

4. ST can be used for prescribing efficient initial conditions for DNS, leading to much saving in convergence time.

5. ST can also be used to evaluate some turbulence modeling constants.

6. Extension to scalars is quite straightforward.

Appendix

Biographical Information on Seminar Speakers

CURRICULUM VITAE

SERGEI KASHIN

Research Experience:

1993 to present - Adjunct Professor of Biology, Department of Biology and Marine Science Center, Northeastern University and East Point, Nahant, Massachusetts. Investigating the motor behavior and physiology of motor systems in lower animals. Teaching graduate course "Biology of Fishes".

1991-1992 - Research Fellow, Environmental Group, ARCO Oil and Gas Company. Investigated toxicity of industrial effluents on aquatic ecosystems.

1989-1991 - Visiting Researcher, Scripps Institution of Oceanography. *In vivo* study of fish sarcomeres.

1971-1989 - Senior Researcher, Institute of Oceanology, Moscow, USSR. Short term changes in ocean ecosystems.

1979-1989 - Director, Laboratory of Ecology and Modelling, Institute of Oceanology, Academy of Sciences of USSR.

1985 - Chief Scientist, Amazon River Expedition. Fish adaptations to the low oxygen conditions.

1988 - Chief Scientist, Expedition to Benguella Upwelling Area, Southeast Atlantic. Productivity in upwelling ecosystems.

EDUCATION: BA (Diploma of Zoology), Department of Biology, Moscow State University, Moscow, USSR, 1962.

Dissertation: *Biology of Siberian Sturgeon, Acipenser baeri.*

Ph.D. (Candidate of Biological Sciences). Institute of Oceanology, Academy of Sciences of USSR, Moscow.

Title: *Organization of Fish Locomotion and Geometry of Musculature.*

RESEARCH GRANTS AND FELLOWSHIPS:

Karolinska Institute of Neurophysiology, Stockholm, Sweden, Postdoctoral Fellow. 1975-1976,

British-Soviet Exchange of Scientists, Bristol, United Kingdom. 1977.

U.S. Geological Survey/University of California at Los Angeles, Department of Biology, Visiting Scientist. 1979-1980.

CURRICULUM VITAE

NEWMAN, Barry George

CURRENT APPOINTMENT: Canadair Professor of Aerodynamics, McGill University

EDUCATION:

St. John's College, Cambridge, Strathcona Open Major Scholarship in Mathematics	1944
Part I Mechanical Sciences Tripos, Cambridge; 1st Class	1946
Part II (Aeronautics); 1st Class; B.A. and M.A.	1947
Ph.D., Sydney University, Australia	1951

PROFESSIONAL APPOINTMENTS:

Scientific Officer, Flight Research Projects	1951-1953	R.A.A.F.
Assistant Research Officer: Flight Research	1953-1955	N.R.C., Canada
University Lecturer	1955-1958	Cambridge University
Visiting Lecturer	1957	Miss. State University
Canadair Visiting Professor in Fluid Mechanics	1958	Université Laval
Canadair Professor of Aerodynamics	1959-present	McGill University
Chairman, Dept. of Mechanical Engineering	1969-1972	McGill University
Visiting Research Officer	1982	N.R.C.

ACADEMIC ACTIVITIES

COURSES TAUGHT

305-331A-B	Fluid Mechanics
305-533A	Subsonic Aerodynamics
305-610A	Fundamentals of Fluid Mechanics
305-612A	Viscous Flow and Boundary-Layer Theory

CONTRIBUTIONS TO UNIVERSITY, FACULTY, AND DEPARTMENTAL GOVERNANCE.

1961-1964	Secretary of Graduate Faculty.
1968-1972	Member of Committee on Research.
1973-1975	Member, Planning Committee of Graduate Faculty.
1974-present	Pro Dean, Graduate Faculty.
1975-1979	Member, Tenure Committee, Faculty of Engineering.
1977-1979	Member, Nominating Committee for Graduate Faculty.
1978-1979	Member, McGill Athletics Review Board.
1979-1982	Member, Senate.
1980-present	Member, Nominating Committee of Senate.

| 1989-present | Member, Council, Faculty Club: Vice President 1991-93; President 1993-95. |
| 1989-present | Chairman, Liaison Committee for the M.Eng. in Aerospace Engineering. |

CONSULTING AND OTHER PROFESSIONAL ACTIVITIES

Consultant, Canadair Ltd.	Aircraft and aerodynamic design	1959-1970
Consultant, Expo Corporation	Wind effects on buildings	1966
Consultant, Boeing Scientific Research Laboratories	Jets and wall jets	1967
Consultant, Dept. of Transport	Licensing of light aircraft	1971
Consultant, Asbestos Corp.	Wind effects on the roof of a German building	1973
Consultant, Pratt & Whitney Canada Inc.	Flow and heat transfer behind impeller disks, and internal aerodynamics, jet flap and Coanda jet flap cascades.	1973-1991
Consultant, S.O.D.E.M. Quebec	Wind turbines	1975
Consultant, Pulp & Paper Research Institute	Disk refining of wood pulp	1975-1977 1980-present
Consultant, Midland Ross	Analysis of web stability in a wood-pulp dryer	1977-1980

AWARDS AND HONOURS

1961	Edward Busk Memorial Prize - Royal Aeronautical Society.
1964	Tour of British Universities and Research Establishments under the auspices of the British Council.
1966	Invited paper General Motors Conference on 'Fluid Mechanics of Internal Flow'.
1967	N.R.C. Senior Travelling Fellowship - Sabbatical leave in Cambridge University, Dept. of Theoretical Physics and Applied Mathematics.
1969	Turnbull Lecturer, Canadian Aeronautics and Space Institute.

1975-1976	N.R.C. Senior Travelling Fellowship - Sabbatical leave in Cambridge University Engineering Dept.
1975-1976	Visiting Scholar, Corpus Christi College, Cambridge.
1981	Invited lecturer CANCAM '81, Moncton.
1982	Visiting Research Officer, National Aeronautical Establishment, N.R.C.
1987	Honorary Chairman CANCAM, 1987, Edmonton.

MEMBERSHIP ON NATIONAL AND INTERNATIONAL BODIES

1964	Fellow, Royal Aeronautical Society.
1964	Fellow, Canadian Aeronautics and Space Institute.
1965-present	Member, Order of Engineers, Québec.
1961-64, 1967-69 1978	Member and Chairman, N.R.C. Associate Committee on Aerodynamics.
1967-1975	Member and latterly Chairman, D.R.B. Advisory Committee for Plasma and Fluid Dynamics.
1968	Chairman, Technical Programme Committee, C.A.S.I. International Aerospace Exposition.
1970-1975	McGill Member, Canadian Research Management Association.
1971-1973	Member, National Committee for International Union of Theoretical and Applied Mechanics.
1974-1976 1984-1987	Member, Council Canadian Aeronautics and Space Institute.
1978-1979	Coordinator and chief reviewer in Fluid Mechanics, CANCAM '79.
1979-1984	Member, Aeronautics Advisory Board, Dept. of Transport.
1981	Member, A.S.M.E.
1982	Fellow, Royal Society of Canada.
1983-present	Member, Academy of Science of the Royal Society of Canada.
1983-1985	Member, Advisory Committee on Aerodynamics for the N.A.E.
1984-1987	Member, Council of the Royal Society of Canada.
1985-1987	Vice-President, Academy of Science of the Royal Society of Canada.
1987	Founding Fellow, Canadian Academy of Engineering.
1993-1995	Director, Division of Applied Science and Engineering, Academy of Science of the Royal Society of Canada.

Curriculum Vitae
Theodore Yao-tsu Wu

California Institute of Technology, Pasadena, CA 91125 U.S.A.
Telephone:(818) 395-4230   Fax: (818)795-9839
e-mail: tywu@romeo.caltech.edu

Personal

Education

B.S. (Aeronautics) Chaio-Tung University, Shanghai, China 1946
M.S. (Aeronautics) Iowa State College, Ames, Iowa 1948
Ph.D. (Aeronautics) California Institute of Technology 1952

Professional Experience

Faculty member, Division of Engineering and Applied Science, California Institute of Technology, Pasadena, CA, U.S.A., 1952-
Research Fellow, 1952-55;
Assistant Professor of Applied Mechanics, 1955-57;
Associate Professor of Engineering Science, 1957-61;
Professor of Engineering Science, 1961-

Awards and Honors

Guggenheim Fellow, 1964
Elected member, National Academy of Engineering, 1982-
Elected member, Academia Sinica, 1984-
Visiting Professor, Hamburg Univ., West Germany, 1964-65
Achievement Award, Chinese Engineers and Scientists Assoc. So. CA, 1971
C.S.I.R.O. Fellow, Australian Universities and C.S.I.R.O. Fellowship, 1976
Adjunct Professor, Shanghai Jiao Tong Univ., Shanghai, China, 1979-
Honorary Professor, Northwestern Polytechnical Univ., Xian, China, 1979-
Russell Severance Springer Visiting Professor, UC, Berkeley, 1980
JSPS Fellow, Japan Society for the Promotion of Science Fellowship, 1982
Honorary Professor, Harbin Shipbuilding Eng. Institute, China, 1987-
Honorary Fellow, Institute of Mechanics, Academia Sinica, 1988-
Distinguished Lecturer, Hong Kong Univ. of Science and Technology, 1992
Invited Visiting Professor, Hong Kong Univ., Hong Kong, April 1992
1993 CAFA Achievement Award - Chinese-American Faculty Assoc., So. CA.
1993 Fluid Dynamics Prize Award - American Physical Society

Reviewer and Referee Service

Journal of Fluid Mechanics; Physics of Fluids; Mathematical Reviews; Publications of ASME, ASCE, AIAA, SNAME, and other scientific journals in addition to those journals charged with editorship. Reviewer of proposals for the National Science Foundation, USARO(D) and other agencies.

Publications

Author or coauthor of over 100 professional papers, books and reports.

Affiliations

Sigma Xi; Phi Tau Phi; Pi Mu Epsilon
Member, U.S. National Academy of Engineering, Special Fields and Interdisciplinary Engineering Peer Committee, 1992-
Member, Ges. Angew. Math. u. Mech. (W. Germany & Austria), 1965-
Fellow, American Physical Society, 1967-
Vice-Chairman, Division of Fluid Dynamics, American Physical Society, 1990-91; Member, Executive Committee, Division of Fluid Dynamics, 1991-
Member, Society of Naval Architects and Marine Engineers, 1972-
Member, Society for Industrial and Applied Mathematics, 1987-
Member, Intern. Towing Tank Conference, Wave Resistance Committee, 1967-78; Chairman, 1977-78
American Towing Tank Conference, 1956-; Chairman, 1972-74
Hydrodynamics H-5 and H-8 Panels of Soc. Nav. Arch. Mar. Eng., 1963
Member, AIAA, Fluid Mechanics Committee, 1949-58
National Research Council, Committee on Recommendation for U.S. Army Basic Scientific Research, 1975-78
Program Review Counselor for the College of Engineering, University of Iowa, 1976
Promotion Review Committee, Institute of Applied Mechanics, National Taiwan University, 1990

Consulting Experience

Aerojet General, Bendix Corporation, Chevron Corporation, CONVAIR General Dynamics, Douglas Aircraft Company, General Electric, Lockheed Aircraft Company, North American Aviation, TRW Systems and other industrial companies.
Consultant for NRAC, Dept. of the Navy, 1982-83
Consultant for David Taylor Research Center, Dept of the Navy, 1985

Editorship

Co—editor, Advances in Applied Mechanics, 1982-
Editorial Board, Advances in Applied Mechanics, 1971-
Editorial Committee, Journal of Ship Research, 1972-
Editorial Board, The Physics of Fluids, 1979-82
Editorial Board, Wave Motion, 1978-
Editorial Committee, Annual Review of Fluid Mechanics, 1980-84; 1991-
Editorial Committee, Applied Mathematics and Mechanics, 1979-
Editorial Committee, Newton – Graphic Science Magazine, 1986-
Editorial Committee, Advances in Hydrodynamics, 1988-
Advisory Board, Journal of Acta Mechanics Sinica, 1990-

John L. Lumley

B.A. - Harvard College, 1952, Engineering Sciences and Applied Physics

M.S.E. - The Johns Hopkins University, 1954, Mechanical Engineering

Ph.D. - The Johns Hopkins University, 1957, Aeronautics. Particular emphasis on turbulence and stochastic processes.

Haute Distinction Honoris Causa - Ecole Central de Lyon, 1987.
Fellow, American Academy of Arts and Sciences.
Member, National Academy of Engineering.
Timoshenko Medal, American Society of Mechanical Engineers, 1993
AIAA Fluid and Plasmadynamics Award, 1982.
APS Fluid Dynamics Prize, 1990.

Post-doctoral fellow, J.H.U., 1957-1959. The Pennsylvania State University at University Park, 1957-1977; Professor of Aerospace Engineering, 1963-74; Evan Pugh Professor of Aerospace Engineering, 1974-1977. Cornell University (Sibley School of Mechanical and Aerospace Engineering), Willis H. Carrier Professor of Engineering, 1977-present. Fulbright Senior Lecturer, Belgium; Guggenheim Fellow, France, 1973-74; Author, *Stochastic Tools in Turbulence* (1970); co-author, *Structure of Atmospheric Turbulence* (with H.A. Panofsky; 1964); *A First Course in Turbulence* (with H. Tennekes; 1971). Principal, *Deformation of Continuous Media* (1963), *Eulerian vs. Lagrangian Frames in Fluid Mechanics* (1968) (Motion Picture Films). Technical Editor, *Statistical Fluid Mechanics* (by A.S. Monin and A.M. Yaglom) (1971, 1975); *Variability of the Oceans* (by A.S. Monin, V.M. Kamenkovich and V.G. Kort) (1977). Member, Johns Hopkins Society of Scholars, Sigma Xi, New York Academy of Sciences, Society for Natural Philosophy, American Association for the Advancement of Science; Associate Fellow, American Institute of Aeronautics and Astronautics; Fellow, American Physical Society (Division of Fluid Dynamics), American Academy of Mechanics.

Research papers (Last Five Years)

124. Shih, T.-H. & Lumley, J. L. 1986. Second order modeling of particle dispersion in a turbulent flow. *J. Fluid Mech.* 163: 349-363

126. Shih, T.-H. & Lumley, J. L. 1986. A general form of the equations for turbulent flows with a passive scalar. *Mathematical Modeling.* 7: 353-370.

128. Shih, T.-H., Lumley, J. L. & Janicka, J. 1987. *Second order modeling of a variable density mixing layer. J. Fluid Mech.* 180: 93-116.

133. Lumley, J.L. 1986. Evolution of a non-self-preserving thermal mixing layer. *Phys. Fluids* 29 (12): 3976-3981.

134. Leibovich, S. & Lumley, J.L. 1986. Complex fluid motions: Models and metaphors. *Cornell Engineering Quarterly* 20: 27-35.

135. Lumley, J.L. 1987. Turbulence modeling. In *Proceedings of the Tenth U.S. National Congress of Applied Mechanics*, ed. J.P. Laub. pp. 33-39. New York: ASME.

136. Aubry, N., Holmes, P., Lumley, J.L. and Stone, E. 1987. The dynamics of coherent structures in the wall region of a turbulent boundary layer. *J. Fluid Mech.* In press.

137. Aubry, N., Holmes, P., Lumley, J.L. and Stone, E. 1987. Models for coherent structures in the wall layer. In: *Advances in Turbulence,* eds. G. Comte-Bellot, J. Mathieu, pp. 346-356. Berlin/Heidelberg: Springer.

138. *Turbulent Shear Flows 5,* eds. F. Durst, B.E. Launder, J.L. Lumley. F.W. Schmidt, J.H. Whitelaw. Heidelberg: Springer.

139. Sarkar, S. & Lumley, J.L. 1987. Angular dispersion of material lines in isotropic turbulence. *Phys. Fluids.* 30 (5): 1269-1271.

140. Lumley, J. L. 1987 The state of turbulence research. In *Advances in Turbulence,* eds. W. K. George & R. E. A. Arndt, pp. 1-10. New York: Hemisphere.

141. Aubrey, N. Holmes, P.H., Lumley, J.L. and Stone, E. 1990. The behavior of coherent structures in the wall region by dynamical systems theory. In *Near-Wall Turbulence* eds. S.J. Kline & N. H. Afgan, pp. 672-691. Washington, DC: Hemisphere.

142. Aubry, N., Holmes, P., Lumley, J.L. and Stone, E. 1989. A simple model for the wall region of a turbulent boundary layer. In *International Symposium on Flow-Induced Vibration and Noise* . (ed. M.M. Reischman, M.P. Paidoussis, R.H. Hansen). New York: ASME 53-62: Vol. 7.

143. Aubry, N., Holmes, P. & Lumley, J. L. 1990. The effect of modeled drag reduction on the wall region. *Theoretical and Computational Fluid Dynamics,* 1: 229-248.

144. Berkooz, G. Guckenheimer, J., Holmes, P., Lumley, J.L., Marsden, J., Aubry, N. & Stone, E. 1990 Dynamical-systems-theory approach to the wall region. AIAA Paper No. 90-1639.

145. Lumley, J. L. 1989. Low Dimensional Models of the Wall Region of a Turbulent Boundary Layer, and the Possibility of Control. In *Proceedings, 10th Australasian Fluid Mechanics Conference,* ed. A. E. Perry. pp. K54.1-K54.6 Melbourne, Aus.: University of Melbourne.

146. Lumley, J. L. 1989. Order and Disorder in Turbulent Flows. In *Proceedings, 1989 Newport Conference on Turbulence,* ed. L. Sirovich. Heidelberg: Springer. In press.

147. Ettestad, D.J. & Lumley, J.L. 1989. A Correction Term for the Swirling Jet. In *Mathl. Comput. Modelling.* Vol. 12 No. 12, pp. 1583-1588.

148. Ettestad, D.J. & Lumley, J.L. 1989. Modelling the Dissipation Transport Term. In *Math. Comput. Modelling.* Vol. 12 No. 7, pp. 865-869.

149. Lumley, J. L. 1990. Opening remarks. In *Whither Turbulence? Turbulence at the crossroads.* Lecture Notes in Physics Vol. 357 ed. J. L. Lumley. pp. 1-4. Berlin etc.: Springer.

150. Lumley, J. L. 1990. The utility and drawbacks of traditional approaches. Comment 1. In *Whither Turbulence? Turbulence at the crossroads*. Lecture Notes in Physics Vol. 357 ed. J. L. Lumley. pp. 49-58 Berlin etc.: Springer.

151. Lumley, J. L. ed. 1990. *Whither Turbulence? Turbulence at the crossroads*. Lecture Notes in Physics Vol. 357. Berlin etc.: Springer.

152. Berkooz, G., Holmes, P. & Lumley, J. L. 1990. Control of the boundary layer and dynamical systems theory: an update. In *The Global Geometry of Turbulence, Impact of Nonlinear Dynamics*, ed. Javier Jiménez. pp. 211-220. New York/London: Plenum.

153. Berkooz, G., Holmes, P. & Lumley, J. L. 1991. Intermittent dynamics in simple models of the turbulent wall layer. *J. Fluid Mech.* 230: 75-95.

154. Lumley, J. L. 1992. Some comments on turbulence. *The Physics of Fluids.* A 4(2): 203-211.

155. Panchapakesan, N. R. & Lumley, J. L. 1990. Turbulence measurements in an axisymmetric jet of air. *J. Fluid Mech.* Accepted for publication.

156. Panchapakesan, N. R. & Lumley, J. L. 1990. Turbulence measurements in an axisymmetric jet of helium. *J. Fluid Mech.* Accepted for publication.

157. Ristorcelli, J. R., Jr. & Lumley, J. L. 1990. Turbulence in the Czochralski crystal melt. *Proceedings, ICHMT XX Materials Processing Symposium, Dubrovnik, Yugoslavia.* Berlin, etc.: Springer. To appear.

158. Lumley, J. L. 1991. Some comments on research support. *Nonlinear Science Today* 1(2): 5-6.

159. Review of: Acheson, D. J. 1990. *Elementary Fluid Dynamics.* Oxford, UK: Clarendon. 397 pp. and Chorin, A. J. & Marsden, J. E. 1990 *A Mathematical Introduction to Fluid Mechanics.* (Second Edition). Heidelberg: Springer. 168 pp. for *Physics Today*, November 1991.

160. Review of McComb, W. D. 1990 *The Physics of Fluid Turbulence.* Oxford, UK: Clarendon. 572 pp. for *Science*, August 1991.

161. Shih, T.-H. & Lumley, J. L. 1993. A Critical Comparison of Second Order Closures with Direct Numerical Simulations of Homogeneous Turbulence. *AIAA Journal*, 31(4): 663-670.

162. Berkooz. G., Holmes, P. & Lumley, J. L. 1993. The Proper Orthogonal Decomposition in the Analysis of Turbulent Flows. *Annual Review of Fluid Mechanics*, 25: 539-575.

163. Berkooz, G., Holmes, P. & Lumley, J. L. 1992. Low dimensional models of the wall region in a turbulent boundary layer: new results. Proceedings of IUTAM Symposium and NATO Advanced Research Workshop on the Interpretation of Time Series from Nonlinear Mechanical Systems, Coventry, UK. *Physica D*, in press.

164. Berkooz, G., Holmes, P., Aubry, N. & Lumley, J. L. 1992. Observations regarding "Coherence and chaos in a model of the turbulent boundary layer"(by X. Zhou & L. Sirovich). *Physics of Fluids*, submitted.

165. Berkooz, G., Holmes, P. & Lumley, J. L. 1992. On the relation between low dimensional models and the dynamics of coherent structures in the turbulent wall layer. *Theoretical and Computational Fluid Dynamics*, in press.

166. Ristorcelli, J. R. & Lumley, J. L. 1992. A second order turbulence simulation of the Czochralski crystal growth melt: the buoyantly driven flow. *Journal of Crystal Growth*, under review.

167. Ristorcelli, J. R. & Lumley, J. L. 1991. Turbulence simulations of the Czochralski melt, part 1: the buoyantly driven flow. Report No. FDA-91-04. Sibley School of Mechanical and Aerospace Engineering. Ithaca, NY: Cornell.

168. Holmes, P., Berkooz, G. and Lumley, J. L. 1991. Turbulence, dynamical systems and the unreasonable effectiveness of empirical eigenfunctions. In *Proceedings of the International Congress of Mathematicians, Kyoto 1990*. pp. 1607-1617. Hong Kong: Springer.

169. Berkooz, G., Holmes, P., & Lumley, J. 1992. Dynamics and control of coherent structures in the turbulent wall layer - an overview. In *Stability in Aerospace Systems*, Report No. 789. Neuilly sur Siene, France: AGARD.

170. Berkooz, G., Carlson, H., Holmes, P. & Lumley, J. L. 1993. Progress in understanding the dynamics of coherent structures in the wall layer, control and simulation. In *Near-Wall Turbulent Flows*, R. M. C. So, C. G. Speziale & B. E. Launder, eds. pp. 3-21. Amsterdam: Elsevier.

171. Shih, T.-H., & Lumley, J. L. 1993. *Remarks on turbulent constitutive relations.* NASA Technical Memorandum 106116, ICOMP-93-12, CMOTT-93-6. Cleveland: Lewis Research Center.

172. Ristorcelli, J. R. & Lumley, J. L. 1992. A second order turbulence simulation of the Czochralski melt flow. *J. Materials Processing & Manufacturing Science*, 1(7): 69-82.

173. Ristorcelli, J. R. & Lumley, J. L. 1992. Instabilities, transition and turbulence in the Czochralski crystal melt. *J. Crystal Growth.*, 116: 447-460.

Dr. J. David A. Walker
Professor of Mechanical Engineering and Mechanics
354 Packard Laboratory #19
Lehigh University
Bethlehem, Pennsylvania 18015-3085
215-758-3789

Education

B.A., Honours Applied Mathematics, University of Western Ontario, Canada, 1967

M.Sc., Applied Mathematics, University of Western Ontario, Canada, 1968

Ph.D., Applied Mathematics, University of Western Ontario, Canada, 1971

Professional Experience

Honorary Research Fellow (with K. Stewartson, F.R.S.) University College London, England, 1971-73

Visiting Assistant Professor, Mechanical Engineering, Purdue University, 1973-74

Assistant Professor, Mechanical Engineering, Purdue University, 1974-78

Associate Professor, Mechanical Engineering, Lehigh University, 1978-83

Professor, Mechanical Engineering and Mechanics, Chairman, Thermo-Fluids Division, Department of Mechanical Engineering and Mechanics, 1989-present.

Honors

Dillon Gold Medal in Applied Mathematics, 1967

Pi Tau Sigma Teaching Award, "Professor of the Year", 1991

Eleanor and Joseph Libsch Research Award, Lehigh University, 1991

Fellow of American Physical Society, 1991

Chairman of Fluid Dynamics Technical Committee, AIAA, 1992-1996.

Associate Fellow of AIAA, 1993

A. v. Humboldt Senior Scientist Award 1994

Graduate Student Supervision

- Fourteen Ph.D. students (F. P. Yau, R. K. Scharnhorst, A. T. Conlisk, G. G. Weigand, T. L. Doligalski, M. C. Ece, E. A. Bogucz, S. Ersoy, T. L. Hon, H. D. Kim, V. Peridier, A. T. Degani, J. He, K. W. Cassel)
- Fifteen M. S. students (A. J. Crisalli, T. L. Doligalski, M. C. Ece, L. J. Yuhas, W. V. Lee, U. Sobrun, K. Brinckman, S. He, K. Cassel, T.-W. Lou, R. Epstein, J. Geosits, B. Freed, L. Iannone, M. Demir)
- Currently supervising six Ph.D. candidates, four M.S. students

Biographical Sketch

Dr. Walker is a Professor of Mechanical Engineering and Mechanics at Lehigh University, Bethlehem, Pennsylvania and is nationally recognized for his research in fluid mechanics and the thermal sciences. His principal research interests are associated with (1) the development of theoretical and computational models of physical systems and processes involving fluid motion, as well as heat and mass transfer and (2) the application and development of modern numerical and mathematical methods to predict such processes. His major research contributions have been in the areas of computational fluid dynamics, boundary-layer turbulence, unsteady viscous flows, heat and mass transfer, gas centrifuge theory, electroplating processes and numerical methods.

Dr. Walker received his undergraduate and graduate degrees at the University of Western Ontario in London, Ontario, Canada. As an undergraduate he received the A. O. Jeffrey Award for the highest standing in third year Honors Mathematics and the Dillon Gold Medal in 1967 for the highest standing in Honors Applied Mathematics. During the summer of 1967, he was employed as a research assistant at the National Aeronautical Establishment in Ottawa, Canada, and was involved with compressible boundary-layer research in connection with the supersonic wind tunnel there. His studies toward the Master of Science and Ph.D. degrees were supported by fellowships from the National Research Council of Canada. The research was supervised by Professor S. C. R. Dennis and concerned the development of calculation methods for the viscous steady and unsteady flow past spheres.

Upon completion of his Ph.D. studies in 1971, Dr. Walker won a National Research Council of Canada Postdoctoral Fellowship (the equivalent of a NATO Postdoctoral Fellowship) to work with the late Professor K. Stewartson, F.R.S. at University College London in the University of London, England. During the period from 1971 - 1973, he carried out research related to compressible unsteady boundary-layer flows in shock tubes, flow separation in rotating and magnetohydrodynamic flows, and heat transfer processes for low Reynolds number flows past spheres.

In 1973, he joined the School of Mechanical Engineering at Purdue University as an Assistant Professor. During this period, he carried out research in the modeling of turbulence and heat transfer processes in boundary layers, in unsteady laminar flows and in the evaluation of the heat and mass transfer processes that take place in rapidly-rotating gas centrifuges.

Dr. Walker joined Lehigh University in 1978 as an Associate Professor and was subsequently promoted to Professor of Mechanical Engineering and Mechanics in 1983. His research at Lehigh has been associated with turbulence modeling, heat and mass transfer processes in turbulent boundary layers and in rapidly rotating gas centrifuges, unsteady viscous boundary-layer flows, numerical methods, the prediction of electroplating rates on metal surfaces, and hypersonic boundary-layer separation. He is nationally recognized for his research in unsteady flows and turbulence and over the past several years has given several invited presentations at various international meetings, workshops, and national scientific meetings.

Over the years, Dr. Walker has been the principal or co-principal investigator on thirty-one research grants and contracts totaling approximately $6,500,000. These include several grants and contracts from NASA, AFOSR, United Technologies and AMP Incorporated. Dr. Walker has served as the Project Director of a combined Industry/University NSF grant with United Technologies Research Center to study heat transfer effects on gas turbine blades and as a Principal Investigator on a recent AFOSR URI entitled "Computational and Analytical Methods in Nonlinear Fluid Mechanics". He is the author of over eighty refereed technical journal publications, conference proceedings and other publications in the areas of fluid mechanics, heat and mass transfer, and numerical methods. Twenty-nine graduate students (fourteen Ph.D.'s) have graduated with Dr. Walker as their major professor. He currently advises six Ph.D. candidates and four Master's students.

He is a member of AIAA, the American Physical Society, Sigma Xi and ASME and was selected to the AIAA Fluid Dynamics Technical Committee in 1989. He is a Fellow of the American Physical Society and an Associate Fellow of AIAA. He was elected Chairman of the Fluid Dynamics Technical Committee in 1992 for the term 1993-1996. Dr. Walker is currently Chairman of the Thermo-Fluids Division in the Department of Mechanical Engineering and Mechanics at Lehigh University.

Recent Representative Publications (Total Publications - 85)

1. Doligalski, T. L., Smith, C. R. and Walker, J. D. A. 1994 "Vortex interactions with walls", *Ann. Rev. Fluid Mechs.* 26, pp. 573-616.

2. Kerimbekov, R. M., Ruban, A. I. and Walker, J. D. A. 1994 "Hypersonic boundary-layer separation on a cold wall", *J. Fluid Mech.* (in press).

3. Degani, A. T., Smith, F. T. and Walker, J. D. A., "Asymptotic structure of three-dimensional turbulent boundary layers", *J. Fluid Mech.* 250, pp. 43-68, 1993.

4. Smith, C. R., Walker, J. D. A., Haidari, A. H. & Sobrun, U., "On the dynamics of near-wall turbulence", *Phil. Trans. Roy. Soc. Lond. A* 336, pp. 131-175, 1991.

5. He, J., Kazakia, J. Y., Ruban, A. I. & Walker, J. D. A., "An algebraic model for dissipation in supersonic turbulent boundary layers", AIAA Paper 92-0311.

6. Degani, A. T. & Walker, J. D. A., "Computation of three-dimensional turbulent boundary layers using embedded functions", AIAA Paper 91-0440, submitted to *AIAA J.*

7. Degani, A. T., Walker, J. D. A., Power, G. & Ersoy, S. "On the application of algebraic turbulence models to high Mach number flows", AIAA-91-0616.

8. Degani, A. T., Smith, F. T. & Walker, J. D. A., "The three-dimensional turbulent boundary layer near a plane of symmetry", *J. Fluid Mech.* 234, pp. 329-360, 1991.

9. Peridier, V. J., Smith, F. T. & Walker, J. D. A., "Vortex-induced boundary-layer separation, Part I: The limit problem Re $\to \infty$", *J. Fluid Mech.*" 232, pp. 99-131, 1991.

10. Peridier, V. J., Smith, F. T. & Walker, J. D. A., "Vortex induced boundary-layer separation. Part II - Unsteady interaction boundary-layer theory", *J. Fluid Mech.* 232, pp. 133-165, 1991.

11. Hoyle, J. M., Smith, F. T. & Walker, J. D. A., "On sublayer eruption and vortex formation", *Comp. Phys. Commun.* 65, pp. 151-157, 1991.

12. Walker, J. D. A., Ece, M. C. & Werle, M. J., "An embedded function method for turbulent flow prediction", AIAA Paper 87-1464, 19th Fluid Dynamics, Plasma Dynamics and Lasers Conference, Honolulu, Hawaii, June 1987; *AIAA J.* 29, pp. 1810-1818, November, 1991.

13. Hon, T.-L. & Walker, J. D.A., "Evolution of hairpin vortices in a shear flow", NASA Technical Memorandum 100858, ICOMP-88-9, NASA Lewis Research Center, Cleveland, Ohio, 1988; *Comp. & Fluids* 20, pp. 343-358, 1991.

14. Walker, J. D. A., "Models based on dynamical features of the wall layer", *Appl. Mech. Rev.* 43, No. 5, Part 2, pp. 5232-5239, 1991.

15. He, J., Kazakia, J. Y. & Walker, J. D. A., "Embedded function methods for supersonic turbulent boundary layers", AIAA Paper 90-0306, January 1990.

Curriculum Vitae: KATEPALLI R. SREENIVASAN
Mason Laboratory, Yale University, New Haven, CT 06520-2159

Tel: (203) 432-4345, Fax: (203) 432-1054
e-mail: krs@kolmogorov.eng.yale.edu

Personal Information: ███████████████████████████████████

Academic Degrees:
> B.E. (Mech. Engg.) Bangalore University (I Rank), 1968; M.E. (Aero. Engg.) Indian Institute of Science (1 Rank), 1970; Ph.D. (Aero. Engg.) Indian Institute of Science (gold medal), 1975; M.A. (Privatim) Yale University, 1986

Current Position
> Harold W. Cheel Professor of Mechanical Engineering (concurrent appointments in the Departments of Physics and Applied Physics)

Professional Society Membership:
> American Academy of Mechanics; American Institute of Astronautics and Aeronautics; American Mathematical Society; American Physical Society; American Society of Mechanical Engineers; Society for Natural Philosophy; Sigma Xi

Awards and Honors:
> Sir M. Visvesvaraya Memorial Prize, 1968; Indumati Lalbai Memorial Gold Medal, 1968; Institution of Engineers Prize and Honorary Graduate Membership, 1968; J. R. D. Tata Fellow, 1973; P. S. Narayana Gold Medal for the best Ph.D. thesis in Mechanical Sciences, 1975; Humboldt Fellow, 1983; Fellow, American Physical Society, 1985; Elected to the Connecticut Academy of Science and Engineering, 1988; Guggenheim Fellow, 1989; Induction to Society of Scholars, Johns Hopkins University, 1991; Distinguished Alumni Award of the Aerospace Department, Indian Institute of Science, 1992; Fellow, American Society of Mechanical Engineers, 1993.

A summary of professional and administrative activities:
> Publications relating to turbulent flows, sonic booms, nucleation of droplets in condensation, chaos, fractals, and so forth, about 100.
>
> At various times, associate editor or a member of the editorial board of: Journal of Applied Mechanics (ASME); Proceedings of the Indian Academy of Science, series C (Sadhana); American Scientist; Journal of Nonlinear Science; Springer Book Series on Interdisciplinary Applied Mathematics; Journal of Theoretical and Computational Fluid Dynamics; Physical Review Letters
>
> Delivered numerous invited lectures (including mini-courses) in Universities, Institutes, and Government Laboratories in the U.S., Germany, Great Britain, France, Australia, India, Poland, Norway, the Netherlands, Italy, etc. Among them: Emerging Scholar Lecture, University of Notre Dame; the First Stanley Corrsin Memorial Lecture, Johns Hopkins University; Phillips Lecture, Haverford College; Sabita Choudhury Memorial Lecture, Indian Institute of Science
>
> Invited speaker in many international meetings and workshops on fluid dynamics and physics, turbulence, nonlinear dynamical and fractals

Organized several scientific workshops, meetings and discussion sessions in meetings such as IUTAM, SIAM, APS, 3rd World Conference on Experimental Heat Transfer, Fluid Mechanics and Thermodynamics, etc.

At various times: Representative of the Division of Fluid Dynamics of the American Physical Society for the Committee on the International Freedom of Scientists; member of the Executive Committee of the Division; member of the Fluid Dynamics Prize Committee; member of the Frenkiel Award Committee; Chairman (and the Past Chairman) of the Fluid Dynamics Division of the American Physical Society; member of the publications committee of the APS (DFD); member of the Fluids Engineering Division of the American Society of Mechanical Engineers, etc.

Participated in collaborative atmospheric and oceanic measurement expeditions in Australia, as well as in field experiments on sonic booms in India

At Yale: as Chairman of the Mechanical Engineering Department, for five and one-half years generally responsible for its administration; specifically, for appointments and promotions and for renewing the ABET-accreditation of the Mechanical Engineering Curriculum; as acting Chairman of the Council of Engineering (Applied Physics, Chemical Engineering, Electrical Engineering and Mechanical Engineering) for half-a-year, responsible for the management of the Council Administration; member of the Advisory Committee for Physical Sciences and Engineering

Miscellaneous:

Mentioned in "American Men and Women of Science", "Who is Who in the East," "Who is Who in the World", etc.

Visiting positions held:

Visiting Professor, Aerospace Department, University of Tucson, Arizona; Visiting Scientist, Center for Atmospheric Sciences, Indian Institute of Science; Visiting Scientist, DFVLR, Goettingen, West Germany; Visiting Professor of Aeronautics, California Institute of Technology; Visiting Professor of Physics, Rockefeller University; Visiting Professor, Jawaharlal Nehru Center for Advanced Scientific research, Bangalore, India.

Graduate students supervised, and post-doctoral fellows and visitors:

Fourteen Ph.D.'s completed; about a dozen post-doctoral fellows and visitors to-date

DISTRIBUTION LIST

Internal

Codes   02244 (routing copy)
0251 (Conforti)
0261
0262 (2)
10 (Nadolink)
10B (Griffin)
102 (Lima)
103 (Dickinson)
104
20
213 (Schloemer, Snarski, Payne)
214 (Bakewell, Keith, Hurdis, Chen, Abraham)
2211 (Graham, Nguyen)
23132 (Keefer)
38
382
383
411 (Kalinowski, Wagner)
60
72
80 (Dence, Myers)
801 (Meng)
814
82 (White)
8211 (Aaron)
8212 (Shonting)
8222 (Nugent)
8213 (Impagliazzo)
8214 (Kemp)
8231 (Khoury)
8232 (Hendricks, Hrubes)
8233 (Bandyopadhyay (30), Beauchamp, Dick, Grant, Henoch, Huyer,
        Philips, Rice, Uhlman, Varghese)
8234 (Corriveau, Harari)
83
832
8322 (Jordan)
833

Total: 87